# Cellular mechanisms of antigen-specific immunotherapy of autoimmune disease

**Dissertation**

Zur Erlangung des Grades

"Doktor der Naturwissenschaften"

Am Fachbereich Biologie

der Johannes Gutenberg-Universität Mainz

von

**Anja Wegner**

geboren am 09.02.1981 in Halberstadt

Mainz, 2016

Die vorliegende Arbeit wurde in der Zeit von November 2013 bis October 2016 an der Universität Bristol unter der Leitung von Professor David C. Wraith angefertigt und wird am Fachbereich Biologie der Johannes Gutenberg Universität (D77) eingereicht.

## ABSTRACT

The ideal treatment of autoimmune diseases, such as Multiple Sclerosis, would be to specifically target the disease-causing immune cells without compromising the broader function of the immune system. This could be achieved by either deleting these cells or transform them into regulatory cells able to ameliorate disease. In the TCR-transgenic TG4 mouse model, where CD4$^+$ T cells are specific for the myelin basic protein (MBP) Ac1-9 peptide, immunotherapy based on the administration of cognate peptide in escalating dose immunotherapy (EDI), induces tolerance in these myelin-specific CD4$^+$ T cells and protects the animals from experimental autoimmune encephalomyelitis (EAE). In this thesis, three aspects of this method of tolerance induction are addressed.

First, we demonstrate that antigen-specific peptide immunotherapy leads to an increase in the number of CD4$^+$ Foxp3$^+$ Treg cells and IL-10-secreting CD4$^+$ T cells not just in secondary lymphoid structures, but in organs throughout the whole body. In addition to an increase in the number of CD4$^+$ T cells with regulatory properties, effector T cells were prevented from entering the central nervous system (CNS). Analysis of changes to the phenotype of CD4$^+$ T cells during EDI demonstrated that the inhibitory receptors TIM-3, TIGIT and PD-1 were significantly upregulated on both IL-10-secreting cells and Foxp3$^+$ cells but no single receptor or a combination could be regarded as a biomarker for tolerised CD4$^+$ T cells.

In the second part, we demonstrate the important principle that tolerised CD4$^+$ T cells can mediate regulation of not only T cells specific for the treatment peptide, but also CD4$^+$ T cells that recognise immunodominant peptides from related proteins. We found that tolerised MBP-specific CD4$^+$ T cells were able to exert linked bystander suppression of MOG$_{35-55}$-reactive T cells *in vivo*, most successfully so when both peptides where presented by the same antigen-presenting cell.

Finally, we reveal a previously unknown role for a subset of antigen-presenting cells with regulatory properties, known as polymorphonuclear myeloid-derived suppressor cells (PMN-MDSCs) in limiting immune responses after EDI. Although best known for their detrimental role as immunosuppressors in cancer, PMN-MDSCs could play a beneficial role in the treatment of autoimmune disease. We discovered that the number of PMN-MDSCs increases over the course of EDI. *In vitro*, these PMN-MDSCs inhibited CD4$^+$ T cell

proliferation in a cell contact-dependent manner, mediated by arginase-1. Upon adoptive transfer into untreated mice, PMN-MDSCs suppressed CD4$^+$ T cell activation. The spleen might be a particularly important site for the function of PMN-MDSCs as the removal of the spleen abrogated not only the increase of PMN-MDSCs in other organs, but also reneged tolerance induction.

Overall, this body of work not only contributes new insights into the changes in CD4$^+$ T cell phenotype during EDI, it also reveals a new aspect of bystander suppression in autoimmune disease and, most importantly, unveils the discovery of an as-yet undescribed role for PMN-MDSCs in antigen-specific tolerance induction.

## ZUSAMMENFASSUNG

Die ideale Behandlung von Autoimmunerkrankungen, wie die multiple Sklerose (MS), wäre die krankheitserzeugende Immunzelle anzusteuern ohne die generelle Funktion des Immunsystem zu beeinflussen. Dies könnte erreicht werden durch entweder die Beseitigung der pathogenen Zellen oder die Transformation dieser Zellen in krankheitsregulierende Immunzellen, die in der Lage sind die Krankheit zu mildern. In dem T-Zell-Antigenrezeptor transgenen Mausmodel Tg4, in dem die CD4$^+$ T-Zellen spezifisch das Myelin-Basische-Proteinpeptid (MBP) Ac1-9 erkennen, Immuntherapie basierend auf der Verabreichung des Peptids MBP$_{Ac1-9}$ in steigenden Dosen (EDI) induziert Toleranz in diesen myelinspezifischen T-Zellen und verhindert die Entwicklung von experimenteller autoimmune Enzephalomyelitis (EAE), dem Tiermodell für MS. In dieser Dissertation werden drei Aspekte dieser Methode, Toleranz zu erreichen, addressiert.

Als Erstes zeigten wir, dass antigen-spezifische Peptideimmuntherapie zu einem Anstieg in der Anzahl der CD4$^+$ Foxp3$^+$ regulatorischen T-Zellen und der Interleukin 10 (IL-10)-produzierenden CD4$^+$ T-Zellen nicht nur in sekundären lymphoiden Strukturen führt sondern auch in Organen im ganzen Körper. Zusätzlich zu dem Anstieg von CD4$^+$ T-Zellen mit regulierenden Eigenschaften, verhinderte die Behandlung die Migration von Effektor-T-Zellen in das zentrale Nervensystem (CNS). Die genauere Analyse des CD4$^+$ T-Zellphänotyps während EDI zeigte, dass die Zelloberflächenrezeptoren TIM-3, TIGIT und PD-1 signifikant hochreguliert wurden in beiden IL-10-produzierenden Zellen und Foxp3$^+$ T-Zellen aber das keiner der Rezeptoren oder eine Kombination der Rezeptoren als Biomarker für tolerisierte CD4$^+$ T-Zellen fungieren kann.

Im zweiten Teil weisen wir das wichtige Prinzip nach, dass tolerisierte CD4$^+$ T-Zellen nicht nur T-Zellen regulieren, die spezifisch sind für das Peptid welches für die Behandlung gebraucht wurde, sondern auch CD4$^+$ T-Zellen regulieren, die immundominante Peptide von verwandten Proteinen erkennen. Wir beobachteten, dass tolerisierte MBP-spezifische CD4$^+$ T-Zellen in der Lage waren Bystander-Unterdrückung von MOG$_{35-55}$-spezifischen CD4$^+$ T-Zellen *in vivo* auszuüben, zumeist besser wenn beide Peptide von der gleichen antigenpräsentierenden Zelle präsentiert wurden.

Zum Schluss deckten wir eine bisher noch nicht bekannte Rolle von einer Subpopulation von antigenpräsentierenden Zellen mit regulierenden Eigenschaften auf, bekannt als polymorphonukleare myeloide Unterdrückerzellen (PMN-MDSCs), die Immunantworten nach EDI hemmen. Obwohl bestens bekannt für ihre nachteilige Rolle als Immununterdrücker in Krebs, diese PMN-MDSCs könnten eine förderliche Rolle in der Behandlung von Autoimmunerkrankungen spielen. Wir stellten fest, dass die Anzahl von PMN-MDSCs steigt im Verlauf von EDI. *In vitro* Experimente zeigten, dass diese PMN-MDSCs zellkontaktabhängige CD4$^+$ T-Zellenproliferation inhibieren, vermittelt durch das Enzym Arginase 1. PMN-MDSCs verhinderten T-Zellenaktivierung nach adoptiven Transfer in unbehandelte Mäuse. Die Milz könnte ein wichtiger Ort sein für die Funktion von PMN-MDSCs, weil die Entfernung der Milz nicht nur die Expansion der PMN-MDSCs in anderen Organen verhindert, sondern auch Toleranzinduzierung.

Insgesamt liefert diese Dissertation nicht nur neue Einblicke in die Veränderungen des CD4$^+$ T-Zellphänotyps im Verlauf von EDI, sondern zeigt auch einen neuen Aspekt von Bystander-Unterdrückung in Autoimmunerkrankungen auf. Aber noch viel bedeutender ist die Entdeckung einer noch nicht beschriebenen Rolle für PMN-MDSCs in antigenspezifischer Toleranzinduzierung.

**CONTENTS**

## LIST OF FIGURES

## LIST OF TABLES

## LIST OF ABBREVIATIONS

| | |
|---|---|
| APC | antigen-presenting cell |
| BLN | brachial lymph nodes |
| BM | bone marrow |
| BMDC | bone marrow-derived dendritic cell |
| CD | cluster of differentiation |
| CFA | complete Freund's adjuvant |
| CNS | central nervous sytem |
| CTLA-4 | cytotoxic T lymphocyte associated antigen 4 |
| DC | dendritic cell |
| DTH | delayed-type hypersensitivity |
| EAE | experimental autoimmune encephalomyelitis |
| EDTA | ethylenediaminetetraacetic acid |
| FACS | flow cytometry |
| FCS | foetal calf serum |
| FITC | fuorescein isothiocyanate |
| Foxp3 | forkhead box P3 |
| FSC | forward scatter |
| GFP | green fluorescent protein |
| IDO | indoleamine 2,3-dioxygenase |
| IFN-γ | Interferon gamma |
| IL | interleukin |
| ILN | inguinal lymph nodes |
| Ig | immunoglobulin |
| iNOS | inducible nitric oxide synthase |
| i.p. | intraperitoneally |
| IRES | internal ribosome entry site |
| ITIM | immunoreceptor tyrosine-based inhibition motif |
| L-NMMA | NG-monomethyl-L-arginine |
| LPS | lipopolysaccharide |
| MBP | myelin basic protein |
| MDSCs | myeloid-derived suppressor cells |
| MHC | major histocomptability complex |

| | |
|---|---|
| MLN | mediastinal lymph nodes |
| M-MDSCs | monocytic myeloid-derived suppressor cells |
| MOG | myelin oligodendrocyte glycoprotein |
| MS | multiple sclerosis |
| 1-MT | 1-methyl analogue of tryptophan |
| NO | nitric oxide |
| OVA | ovalbumin |
| PBS | phosphate buffered saline |
| PD-1 | Programmed Death Receptor -1 |
| PD-L1 | programmed death-ligand 1 |
| PE | phycoerythrin |
| PFA | paraformaldehyde |
| PLP | proteolipid protein |
| PMA | phorbol 12-myristate 13-acetate |
| PMN-MDSCs | polymorphonuclear myeloid-derived suppressor cells |
| ROS | reactive oxygen species |
| s.c. | subcutaneous |
| SSC | sideward scatter |
| STAT | signal transducer and activator of transcription |
| TCR | T cell receptor |
| Tg4 | TCR-transgenic mouse specific for the epitope of MBP, Ac1–9 (acetylated N-terminal nonamer) |
| Tg4$^{IL-10/GFP}$ | IL-10 reporter strain in which IRES-GFP was introduced into the 3' untranslated region of the IL-10 gene. |
| Tg4IL10$^{-/-}$ | Tg4 IL-10KO mouse |
| Th1 | T helper cells (Type 1) |
| Th2 | T helper cells (Type 2) |
| Th17 | T helper cells (Type 17) |
| TIGIT | T-cell immunoreceptor with Ig and ITIM Domains |
| TIM-3 | T-cell immunoglobulin and mucin-domain containing-3 |
| Treg | regulatory T cell |
| WT | wild type |

# 1    INTRODUCTION

## 1.1    The human immune system

The immune system is a highly balanced and tightly regulated arrangement with multiple checkpoints, committed to attack and destroy invading pathogens as well as rogue endogenous cells (i.e. cancerous). The activation of the innate immune system gives a rapid response, and involves the interaction of different innate leukocytes e.g. natural killer cells, macrophages or neutrophils (1). In contrast, adaptive immunity is a process, represented by thymus-derived T-lymphocytes and bone-marrow-derived B-lymphocytes, which can take days to weeks and is most often linked with the acquisition of specific memory (2). The primary link between the innate and adaptive immune system is provided by professional antigen-presenting cells (APC), namely dendritic cells (3).

## 1.2    Thymic development of lymphocytes

The thymus is required for the generation of functional CD4$^+$ and CD8$^+$ T cells from T-lymphocyte precursors (4). During the process of thymic selection, T cells are selected against self-reactivity ensuring that they do not react against host tissue antigens allowing cells specific for foreign antigens to emerge. The maturation process is characterized by both positive and negative thymocyte selection and T cell receptor (TCR) gene rearrangement (5, 6). In the first step, developing T cells are selected for their compatibility with self-major histocompatibility complex molecules (MHC). In the thymus, MHC molecules are expressed on thymic epithelial cells and resident antigen-presenting cells (7). MHC molecules are specialised molecules that bind peptide fragments and display them on the cell surface for recognition by T cells. Developing T cells that do not interact with the MHC molecules with sufficient affinity die by neglect. At this beginning of this stage, T cells express two co-receptors that stabilise the interaction with MHC, CD4 and CD8. T cells with TCRs that interact well with class 1 MHC (MHC-I) molecules retain only the expression of CD8, whereas T cells that bind MHC class 2 (MHC-II) will only continue to express CD4. In the next step, developing T cells are selected against the ability of their TCRs to recognise self-antigens. The transcription factor Autoimmune Regulator (AIRE) regulates the expression and thus presentation of a wide range of tissue-specific antigens in the thymus (8). The T cell receptor

only recognises peptides that are displayed on MHC molecules.  Developing T cells are exposed to antigen-presenting cells with self-peptide-MHC complexes on their surface, during their migration through the thymus (9, 10). T cells with TCRs of high affinity to the peptide-MHC complex will be destroyed (negative selection), thus eliminating potentially self-reactive cells (11). Cells that survive this step further differentiate into mature CD4+ and CD8+ T cells. These will mostly progress as conventional T cells into the periphery, although some with T-cell receptor signalling at the higher end of the affinity scale but not strong enough to induce deletion will upregulated the transcription factor Foxp3 and adopt regulatory properties. These cells are known as thymic regulatory T cells (tTreg).

## 1.3    Differentiation of effector CD4+ T lymphocytes

After maturation in the thymus into conventional CD4+ T cells and CD4+ regulatory T cells (12), they differentiate further into distinct effector types in the peripheral lymphoid organs upon encounter of their specific antigen presented by professional APCs. The initial classification of CD4 T cells revealed a dichotomy mainly distinguished by cytokine secretion profile (13), which also reflects functional differences (Figure 1.1).

CD4+ T-helper 1 (Th1) cells produce IL-2, IFN-γ and TNF-α, mediating cellular immunity, whereas CD4+ T-helper 2 (Th2) cells secrete IL-4, IL-5, and IL-13, which in turn regulate humoral immunity (14). T-helper cell fate determination and their respective cytokine production are controlled by their expression levels of master transcription factor and signalling transducer and activator of transcription (STAT) proteins. The activities of STATs are regulated by posttranslational modifications mediated by cytokines. The first transcription factor that was identified was the Th2 master regulator GATA3 (15, 16) and Th2 differentiation requires a strong STAT5 signal (17). Th2 cells promote the clearance of extracellular parasites by upregulating the numbers of eosinophils and inducing an antibody response (18).

The Th1 master regulator is T-bet which induces IFN-γ production in T cells (19). IFN-γ in turn is important for the activation of STAT1 and for the induction of T-bet (20). Th1 cells are responsible for the elimination of intracellular pathogens by activating cells with phagocytic capacities including macrophages and microglia (18).

Besides the classical Th1 and Th2 cells, further investigation has led to the discovery of new subsets of CD4$^+$ T cells including Th17 cells (18).

Th17 cells express high levels of the transcription factor RORγt (21) and their differentiation is controlled by the cytokines IL-6, IL-21, and IL-23 (22, 23) which activates STAT3. The deletion of *Stat3* results in the loss of IL-17-producing CD4 T cells in mice (24). The main physiological function of Th17 cells is the protection of the host from infectious diseases (25).
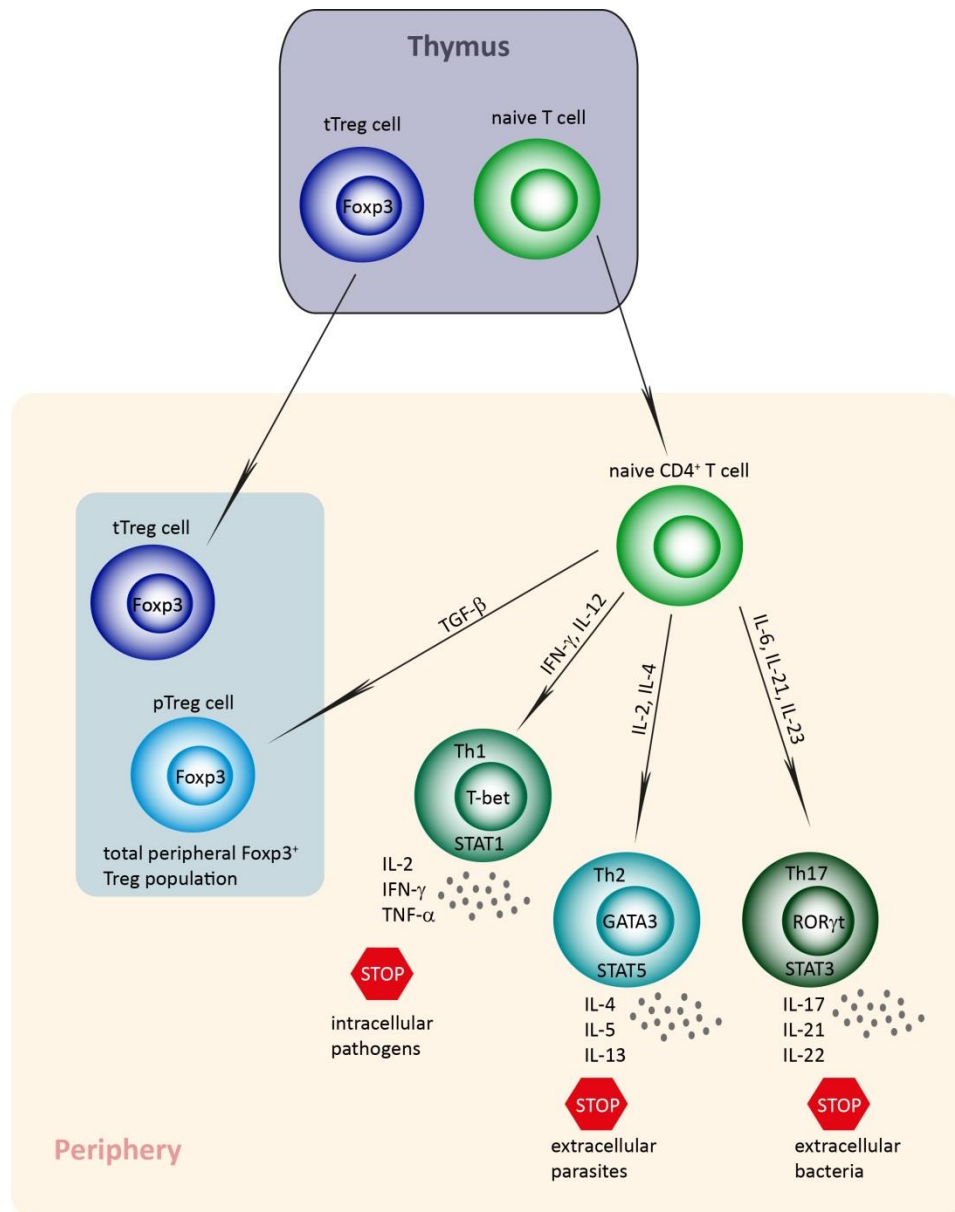
**Figure 1.1. CD4⁺ T cell differentiation.** Naïve CD4⁺ T cells from the thymus differentiate into Tregs and three main subsets of effector CD4⁺ T cells in the periphery, Th1, Th2 and Th17. The differentiation of the CD4⁺ T cell subsets is largely dependent on the cytokine milieu at the time of activation. This controls the expression of different transcription factors and signalling transducer and activator of transcription (STAT) proteins. The CD4⁺ Foxp3⁺ Treg population in the periphery consists of thymus-derived Tregs (tTreg) and peripherally induced Tregs (pTreg).

If T helper cells get aberrantly activated, the undesirable responses of Th1 and Th2 cells can contribute to the pathology in allergy and autoimmunity. Airway hyperresponsiveness in patients with asthma is mediated by CD4$^+$ Th2 lymphocytes, which can be isolated from the lungs of those patients (26). In most cases the development of organ-specific autoimmune diseases is facilitated by Th1 T cells. For example, CD4$^+$ T cells isolated from spinal cord lesions of EAE mice secrete IFN-γ and IL-2 after stimulation (27, 28). Interestingly, these IFN-γ-producing CD4$^+$ T cells are ex-Th17 cells, whose conversion was IL-23 mediated, that started to produce IFN-γ to a great extent during the development of EAE as revealed by fate mapping (29, 30). Moreover, it was shown that IL-17 producing CD4$^+$ T cells do not have a major impact on the development of EAE because the specific overexpression of IL-17A exclusively in CD4$^+$ T cells did not resulted in exacerbation of MOG-induced disease while the ubiquitous overexpression of IL-17 led to skin inflammation in mice very early on (31).

## 1.4 Multiple sclerosis (MS)

MS is a chronic inflammatory disorder of the central nervous system where immune cells attack myelinated axons of the brain (32). It is a putative T cell mediated disease, induced by T cells specific for the proteins that make up the myelin sheath, namely myelin-basic protein (MBP), myelin-oligodendrocyte glycoprotein (MOG) and proteolipid protein (PLP).

The axonal myelin sheath formed by glial oligodendrocytes in the CNS and Schwann cells in the peripheral nervous system (PNS) secures rapid action potential conduction (33) and provide trophic support for the axons (34) . The two most abundant protein components in myelin are MBP with 30% (35) and PLP with 50% (36), whereas MOG is a relatively minor component with 0.05% (37).

In MS patients, MBP-reactive T cells are more frequent than PLP-reactive T cells among mononuclear cells isolated from the cerebrospinal fluid (38). The pathological picture of MS also comprised hallmarks of neurodegeneration (39). In some MS patients the thalamic grey matter exhibited a substantial neuronal loss of up to 30%-35% (40). Another study showed that disease progression and disability is associated with metabolic dysfunction in neurons using MR spectroscopy (41).

## 1.5    EAE as a model for MS

Experimental autoimmune encephalomyelitis (EAE) is the murine model of MS and focusses on demyelination as it is the most salient feature common in both EAE and MS. It can be induced by immunization with whole spinal cord homogenates or myelin proteins/peptides in adjuvant, or by passive transfer of activated, myelin-specific CD4$^+$ T cells into hosts. The pathogenesis and course of the disease vary substantially, depending on the mouse model and the encephalitogenic peptide used (42). One major difference between EAE and MS is that the human disease develops spontaneously, while EAE is mostly induced, although some spontaneous mouse models have been developed (43). But even these models mostly do not represent the human situation perfectly, as they are TCR transgenic animals with a very limited T cell repertoire (44, 45). Another disadvantage is the use of genetically homogenous inbred mouse strains, since genetic heterogeneity underlies the complex diversity in pathology of MS (46). However, for the investigation of the mechanism behind the pathology a homogeneous genetic background facilitates a more accurate analysis. Despite the variety of models developed at the moment there is no highly relevant murine model available for primary progressive MS (46), which occurs in about 10% of people with MS (47). But despite the stated disadvantages, the EAE model is a very powerful tool to study the immune response observed in MS patients.

## 1.6    Treatment options of MS

There is no cure for MS, but a wide spectrum of therapies are available, which are most often based on a broad immune suppression such as the use of  steroids given at high doses (48). Therapies that have been successfully translated into clinical daily routine use glatiramer acetate (49) and mitoxantrone (50). The former drug is a random polymer of four amino acids found in myelin basic protein, namely glutamic acid, lysine, alanine and tyrosine, and it has been suggested to inhibit the binding of self-peptides to MHC class II antigens (49) and to modulate DC inducing anti-inflammatory Th cells producing IL-10 (51). The latter drug exerts its immunosuppressive activity by inhibiting DNA synthesis (50). Other therapies use IFN-β (52), which limits T cell migration across the blood-brain-barrier (BBB), decreases the

production of the pro-inflammatory cytokine IL-17 and increases anti-inflammatory IL-10-production.

In addition, monoclonal antibodies are used as therapeutics. The use of the humanized monoclonal antibody to α4 integrin, natalizumab, inhibits the migration of T cells towards the CNS (53). α4 integrin is a cell-surface adhesion molecule mainly expressed on lymphocytes (54) that can interact with the vascular cell adhesion molecule (VCAM)-1 on endothelial cells and enables the transmigration of the lymphocyte.

Other therapies focus on the depletion of B cells by using rituximab, a chimeric monoclonal antibody that depletes CD20$^+$ B cells (55) which in turn affects antibody production and the activation of macrophages and T cells (56). Most of these available therapies suppress the immune system non-specifically, work only in a subset of patients, and/or have serious adverse effects. Thus, to find a treatment, that provides a cure and is well tolerated with minimal adverse effects is the principal aim of our research.

## 1.7 Peptide immunotherapy

A promising approach to the treatment of MS relies on the use of soluble, synthetic peptides, based on the sequence of known disease-associated antigens, to promote tolerance induction. Peptide immunotherapy is already used successfully in the treatment of allergy. For example, in cat-allergic asthmatic subjects peptide immunotherapy resulted in a reduced proliferative response of cultured PBMCs to the cat allergen (57).  In line with this, production of the Th2 cytokine, IL-4 and IL-13, was reduced in response to the allergen. In the corresponding mouse model reduction of allergic lung inflammation was accompanied by a considerable increase in the production of IL-10 in T cells after tolerance induction. So it seems that the mechanism, by which tolerance induction exerts its immunoregulatory activity, can at least in part be explained by the production of IL-10. The success of peptide immunotherapy in allergy has now been extended to the field of autoimmune disease. In an EAE mouse model (Tg4), where T cells express a TCR specific for the immunodominant epitope of MBP$_{Ac1-9}$, the induction of EAE can be prevented by repetitive application of the cognate peptide (58). By exchanging the lysine residue in position 4 with a tyrosine [Ac1–9(4Y)], the beneficial effect of tolerance induction was further increased (59). The treatment could significantly delay the onset and ameliorate the severity of the disease. This results

from the induction of anergy in CD4$^+$ T cells and a switch in serum cytokines towards IL-10. These IL-10-secreting T cells originate from Th1 cells and inhibit IL-12 secretion by dendritic cells, which is linked to reduced DC maturation and interaction with T cells. The application of the peptide has proven to be safe, reliable and effective for the induction of tolerance in the animal model. Based on the findings in the animal model, other short immunodominant peptides which can directly bind to MHCII without the need for antigen processing (known commercially as apitopes) have now successfully completed two Phase I clinical trials to go forward to Phase II clinical trials in the treatment of MS (60).

## 1.8    Dose escalation protocol

To further reduce the risk of adverse effects in response to the given peptide, a dose escalation protocol was applied for subcutaneous delivery of the high self-antigen doses, required for effective tolerance induction in an autoimmune setting (61, 62). Autoimmune diseases and allergies share a common link in that the body wrongly attacks self-antigens in case of MS or the body responds inappropriate to normally harmless antigens from the environment. Lessons for the safe and efficient induction of tolerance in MS can be learned from the wider experience in allergy. In the latter, the first step for developing a dose escalation protocol is to determine an elevated tolerated dose. This dose then is gradually increased to a high maintenance dose. By gradually escalating the dose, a much higher allergen dose can be tolerated than at the beginning. This dose escalation protocol was proven to be effective and successful in the treatment of various allergies. The underlying immunological mechanism was provided by the examination of beekeepers (63). In the beginning of the season, the keepers show signs of inflammation in response to stings on their skin. Within several days, with regular exposure to large doses of venoms, the immune response disappeared. The mechanism that helped to dampen the immune response is the switch from a classical T cell into an IL-10-producing regulatory T cell. A comparable pattern of immune regulation can thus be observed in the treatment of allergies and EAE with a dose escalation protocol.

## 1.9 Regulatory T cells and their role in autoimmunity

The immune system selectively kills infiltrating pathogens, but at the same time it can also damage host tissues. It is essential to keep the balance between beneficial and detrimental signals, maintaining immune homeostasis by suppressing autoreactive T and B cells. Regulatory T cells are now regarded as one of the key population that attenuate inflammation and prevent autoimmunity by promoting and controlling tolerance (64). Tregs are characterized by the expression of the forkhead transcription factor Foxp3 (65). As mentioned above, one major subset of Treg cells develop in the thymus as a separate lineage from conventional T cells and Foxp3 is their master transcriptional regulator (tTreg) (66). Critical for tTreg development is the activation of STAT5 by IL-2 (67).

Foxp3 is induced during thymic seletion but this master regulator can also be induced in the periphery by the cytokine TGF-β at the time of antigen encounter (pTregs). Foxp3 is essential for the development and function of Tregs (68) and the constitutive expression of Foxp3 in Tregs is also essential for maintaining their suppressive activity (69). The importance of Foxp3 in man and mouse is shown in cases where Foxp3 is lost. This results in the development of an autoimmune-like disease with hyper-responsive CD4^{+} lymphocytes in human immune dysregulation, polyendocrinopathy, enteropathy, X-linked syndrome (IPEX) (70) and the murine scurfy model (71). However, merely inducing the expression of Foxp3 in a conventional T cell does not necessarily convey a regulatory phenotype (72).

Another crucial constitutively expressed marker for Tregs is CD25, the alpha chain of the IL-2 receptor that augments the affinity of the receptor (73). Tregs are dependent on IL-2 for their development, function and survival in the periphery. High expression levels of CD25 have also been shown to be essential in maintaining the stability of regulatory T cells and their suppressive phenotype. In a murine inflammatory model of autoimmune arthritis, CD4^{+}CD25^{lo} expressing Foxp3^{+} Treg cells lost their expression of Foxp3 and their ability to suppress inflammation, while their CD25^{hi} counterparts retained their Foxp3 expression. Not only did these ex-Foxp3^{+} Treg cells lose their suppressive function, they switched to an activated pathogenic Th17 phenotype and aggravated bone destruction.

A second subset of peripherally induced regulatory T cells called [IL-10]Treg cells is characterized by the production of IL-10 but the lack of the transcription factor Foxp3 (74). The natural role of [IL-10]Treg was first shown in a study where CD4^{+} T cells specific for food

and aeroallergens in healthy individuals were found to contain a greater frequency of IL-10-secreting than interferon-γ-secreting or IL-4-secreting CD4$^+$ T cells, in contrast to allergy sufferers. In addition, with increasing doses of allergen the frequency of $_{IL-10}$Treg cells is further increased in healthy individuals (75).

The therapeutic potential of Treg cell subsets was soon realized and several studies have looked into the therapeutic benefit of transferring Treg cells derived from conventional T cells. The production of Foxp3$^+$ Tregs from naïve CD4$^+$ T cells *in vitro* (iTregs) (68) was used for adoptive transfer to try to restore immune imbalance. Additionally, adoptive transfer of Foxp3$^+$ iTregs has been shown to suppress the development of various autoimmune conditions including colitis (76) and CNS autoimmune disease (77). The adoptive transfer of $_{IL-10}$Tregs was shown to be protective e.g. in rheumatoid arthritis (78) and CNS autoimmune disease (79).

Regulatory T cells exert their suppressive activity through a variety of different mechanisms. These include the release of inhibitory cytokines, such as TGF-β (80) and Interleukin-10 (IL-10) (81). Others include cell-contact dependent mechanisms like the expression of inhibitory receptors such as cytotoxic T lymphocyte-associated antigen-4 (CTLA-4) (74), programmed death-1 (PD-1) (74) and inducible T-cell costimulator (ICOS) (82). Another control mechanism of peripheral tolerance to further limit self-reactivity and the development of autoimmune diseases is the induction of T cell anergy (83). This inability of a T cell to mount a complete response to its target antigen occurs, when steady-state dendritic cells present the antigen without the necessary co-stimulatory molecules required for priming a naïve T cell.

**1.10 Co-stimulatory and co-inhibitory molecules involved in T cell regulation**

T cell activation is tightly regulated by signalling of co-stimulatory and co-inhibitory molecules through their respective receptors. These molecules modulate the effect of the interaction between the TCR and it cognate peptide-MHC complex and fine-tune the T cell response. Whereas co-stimulatory molecules, such as CD28, augment the strength of TCR signalling, co-inhibitory molecules have a negative regulatory effect on T cell activation. A wide range of co-inhibitory molecules have been described, including CTLA-4, lymphocyte-activation gene-3 (LAG-3), T cell Ig- and mucin domain–containing molecule 3 (TIM-3,) programed death-1 (PD-1), and T cell immunoreceptor with Ig and ITIM domains (TIGIT) (84). For the purpose of this thesis we will mainly focus on the latter three molecules.

CD28 was identified as a co-stimulatory receptor, augmenting the proliferation of CD4^{+} T cells and their IL-2 production (85). CD28 binds to two ligands, namely B7-1 (CD80) (86) and B7-2 (CD86) (87) expressed on antigen-presenting cells which provide signals for T cell growth and their survival (88). CD86 is constitutively expressed on APCs at low levels and is rapidly upregulated in response to activation of the APC while CD80 is upregulated at later time points (89, 90). Interestingly the B7 ligands CD80 and CD86 (91) bind to the co-inhibitory receptor CTLA-4 as well. While CD28 is constitutively expressed on the surface of T cells (92), CTLA-4 expression is rapidly upregulated after T-cell activation (93). CD28 signalling reduces the threshold of T cell activation by reducing the number of needed TCR interactions to fully activate a T cell (94). Furthermore, by promoting T cell survival and their production of cytokines, CD28-signalling initiates T cell differentiation (95). The inhibitory molecule CTLA-4 competes with CD28 for their shared ligands and has a higher binding affinity for them (96) although when competing with each other it is more likely that CD86 binds to CD28 while CD80 binds strongly to CTLA-4 (97). The importance of negative T cell regulation became apparent in CTLA-4-deficient mice where the loss of CTLA-4 led to vast lymphoproliferation, multiorgan destruction and early death of those mice (98, 99) caused by unrestricted CD80/CD86-co-stimulation (100). Furthermore, CTLA-4-signalling is essential in the establishment of peripheral T cell tolerance (101, 102).

### 1.10.1    The co-inhibitory molecule TIM-3

The gene coding for TIM-3 encodes both a membrane-bound form of this protein and a soluble form (103). TIM-3 is widely expressed on $CD4^+$ Th1 lymphocytes, resulting in the suppression of T cell responses, but not on Th2 lymphocytes (104). TIM-3 expressed on phagocytes can bind to phosphatidylserine which is exhibited on the surface of apoptotic cells and can mediate their uptake by those phagocytosing cells (105). The interaction of the alarmin protein high-mobility group box 1 (HMGB1) with TIM-3 expressed on tumour-associated DCs suppressed innate immune responses elicited by pattern-recognition receptors to nucleic acids (106). TIM-3 can also be co-expressed with its ligand carcinoembryonic antigen cell adhesion molecule 1 (CEACAM1) on activated T cells during tolerance induction and both form a heterodimer which is important for the promotion of TIM-3 expression on the surface of the T cell (107). Signalling through the TIM-3 pathway is also prerequisite for the generation of regulatory T cells but it is not essential for their immunosuppressive effector function (108). How Tim-3 exerts its immunoregulatory function and through which receptor-ligand interaction is debated. An initial study showed Galectin-9 as the inhibitory ligand for TIM-3 on murine T cells (109). The engagement of the ligand with its receptor induced cell death in Th1 lymphocytes although the cell death in TIM-3 deficient Th1 lymphocytes was not completely abolished, indicating that Galectin-9 might signal through a different receptor. Intraperitoneally administered recombinant Galectin-9 eluted in PBS containing 80 mM alpha-lactose and 0.5 mM dithiothreitol *in vivo* resulted in the reduced production of IFN-γ in antigen-specific Th1 cells in an *in vitro* recall response. Furthermore, intravenous injection of small interfering RNA (siRNA) against Galectin-9 into mice resulted in a reduced disease severity and mortality in an EAE experiment. It should be mentioned that the actual interaction between Galectin-9 with its putative receptor was not analysed. Follow-up studies which focussed on the physical proof of TIM-3–Galectin-9 interactions did not find any evidence of their interaction. Fully differentiated Th1 cells from WT and TIM-3 KO mice were both susceptible to apoptosis to the same degree induced by Galectin-9 (110) . In a similar vein, Galectin-9 does not act as a ligand for TIM-3 during the activation of human T cells (111). Human T cells were activated with stimulator cells expressing high levels of human Galectin-9 but the presence of Galectin-9 did not reduced the T cell proliferation.  In patients with chronic infections, TIM-3

expressing CD4$^+$ T cells seem to be dysfunctional in response to TCR-mediated stimulation *in vitro* and the addition of a TIM-3 antibody was able to reverse the functional impairment (112-114). TIM-3 expression seemed to be a marker for activated CD8$^+$ T cells in infection and its expression seems to impede CD8$^+$ T cell responses to acute infections (115). The soluble form of TIM-3 was found to promote the development of tumours by suppressing the generation of tumour-specific T cells (116). In contrast to the detrimental impact in a tumour rejection model mentioned before, the membrane-bound form of TIM-3 has a beneficial effect in immune-mediated disease. Blockade of Tim-3 through the administration of an anti-TIM3-antibody resulted in a more severe EAE with more ample demyelinating lesions filled with activated macrophages and increased mortality compared with the IgG control (31). Moreover, the administration of the fusion protein Tim-3–Ig *in vivo* in already tolerised mice abrogated the hypoproliferation of T cells in an *in vitro* recall response to cognate antigen and left the production of the Th1 cytokines IL-2 and IFN-γ unaffected. Furthermore, the immunisation of TIM-3-deficient mice with ovalbumin (OVA) and a single high dose of the soluble OVA peptide to induce tolerance did not impede the proliferative response of whole splenocytes in response to antigen (32).

### 1.10.2   The co-inhibitory molecule PD-1

The first description of the transmembrane PD-1 receptor was as a 'death-inducing' gene activated in a murine T cell hybridomas undergoing programmed cell death (117). Cells that undergo programmed cell death will switch on a range of genes, including that encoding for PD-1, leading to *de novo* synthesis of RNA and proteins that mediate a controlled death. The increase of mRNA expression of PD-1 in the thymus could also be seen after i.p. injection of an anti-CD3 mAb into mice, indicating that PD-1 plays a role in thymic selection. That PD-1 has an important role as a negative regulator of immune responses became clear when the disruption of the PD-1 gene in mice lead to the spontaneous development of lupus-like glomerulonephritis and arthritis (118). The stimulation of T cells with anti-CD3+antiCD28 initiates a series of intracellular signals that increases glucose uptake, cellular metabolism and cell cycle progression (119). PD-1 engagement during the stimulation of CD4$^+$ T cells with anti-CD3-, anti-CD28-, and anti-MHC II-coated beads resulted in a decrease of glucose uptake

and glycolytic rate which in turns inhibits lymphocyte proliferation (120). Furthermore PD-1 engagement during the stimulation of human CD4$^+$ T cells with antiCD3+antiCD28 inhibited the upregulation of Bcl-xL mRNA (121). Bcl-xL is a CD28-induced cell survival factor which prevents the cell from undergoing apoptosis (122).

PD-1 is expressed by a wide range of cells including activated monocytes, natural killer (NK) T cells , DCs, B cells and T cells (123). Whilst the receptor is not constitutively expressed on resting conventional T cells, its expression is induced after activation of T cells (124). PD-1 can bind to several ligands, including PD-L1 (B7-H1) (125) and PD-L2 (B7-DC) (126) (127). The expression pattern of the two PD-1 ligands varies between different cell types (128). PD-L1 is constitutively expressed by naive CD4$^+$ T cells and further upregulated by CD3 stimulation while PD-L2 is not expressed on naive CD4$^+$ T cells and only marginally increased after stimulation. The same expression pattern is evident in B cells as PD-L1 is expressed by freshly isolated B cells and further upregulated by stimulation, whereas the expression of PD-L2 could not be detected on B cells even after stimulation. Similar results were obtained for peritoneal macrophages. PD-L1 is expressed by macrophages to a high degree and further upregulated when stimulated, while PD-L2 could only be detected on activated macrophages. Both PD-1 ligands are expressed on CD11c$^+$ bone marrow derived dendritic cells (BMDC) during culture. Isolated CD11c$^+$ splenic DCs express PD-L1 and further upregulate the expression after stimulation. PD-L2 could not be found on freshly isolated CD11c$^+$ DC but was considerably increased upon stimulation.

PD-1: PD-L1 signalling inhibits T cell function by engagement of the PD-1 receptor on the T cell with PD-L1 (129). PD-L1 expression in the APC compartment seems to be more important than in the T cell population for the protection against CNS autoimmune disease because the transfer of wild type MOG$_{35-55}$-specific T cells into PD-L1$^{-/-}$ recipients induced more severe clinical disease compared to PD-L1$^{-/-}$ T cells transferred  into wild type recipients. PD-1 has also been shown to be critical in the establishment and maintenance of tolerance in a type-1 diabetes model. Administration of anti-PD-1 or anti-PD-L1, but not anti-PD-L2, after tolerisation of NOD mice with insulin-coupled fixed splenocytes (INS-SP) (130) resulted in the break of already established tolerance and the rapid development of diabetes marked by T cell expansion and the production of inflammatory cytokines in the pancreas.

Moreover, the treatment with anti-PD-1 before the administration of INS-SP abrogated the induction of tolerance altogether.

### 1.10.3   The co-inhibitory molecule TIGIT

TIGIT is a protein with a single extracellular immunoglobulin domain, a type 1 transmembrane region and a single intracellular immunoreceptor tyrosine-based inhibitory motif (ITIM) (131). TIGIT is expressed on T cells, including Tregs and memory subsets, as well as on NK cells. It is absent on naïve T cells but is induced after the activation with anti-CD3/CD28. In the presence of a blocking anti-TIGIT antibody, T cells cultured with anti-CD3 plus autologous CD11c$^+$ DCs showed hyperproliferation and increased IFN-γ production, thus indicating the function of TIGIT as a co-inhibitory receptor. Radioligand binding assays showed that TIGIT is able to bind two ligands with different affinities expressed on APCs. TIGIT binds with high affinity to CD155 (PVR), while the interaction with CD112 (PVRL2) is of low affinity. The interaction of TIGIT with CD155 expressed on DCs modifies their function. The receptor-ligand interaction inhibits the production of IL-12p40 by DCs and increases the production of the pro-inflammatory cytokine IL-10. Later on, it was shown that TIGIT has a T cell–intrinsic inhibitory function as well (132). Restimulation of T cells from TIGIT$^{-/-}$ mice *in vitro* showed augmented proliferation and production of proinflammatory cytokines by T cells, including IL-6, IFN-γ, and IL-17 compared to wild type mice. Although TIGIT engagement inhibits T cell activation it simultaneously upregulates the expression of cytokine receptors like IL-2R, IL-7R, and IL-15R and increases the expression of the antiapoptotic molecule Bcl-xL, thus promoting T cell survival.

The administration of an anti-TIGIT blocking antibody into mice resulted in a more rapid disease onset in a collagen-induced arthritis model and in exacerbation of EAE induced with MOG peptide, driven by the production of pro-inflammatory cytokines IL-17A and TNF-α (133). Furthermore, TIGIT-deficient mice developed more severe MOG peptide-induced EAE. The same finding was apparent in a model of graft-versus-host disease (GVHD) where TIGIT-deficient or wild type T cells were transferred into irradiated mice and mice receiving TIGIT-deficient cells developed accelerated disease. Maintaining peripheral tolerance by dampening T cell activation is one of the main functions of TIGIT signalling. Furthermore,

TIGIT promotes Treg cell function and is a target gene of Foxp3 (134). Methylation limits access of Foxp3 to its DNA targets. Increased expression of TIGIT in Tregs was associated with hypomethylation of the TIGIT locus, which facilitates Foxp3 binding. *In vitro*, TIGIT was shown to be important for Foxp3$^+$ iTreg cell differentiation because TIGIT-deficient T cells did not expand to the same extent as their wild type counterparts when stimulated with TGF-β (135). In addition, TIGIT$^+$ Treg cells show augmented inhibition of effector T cell proliferation *in vitro* compared to their TIGIT$^-$ counterparts.

## 1.11 Suppressive activity of interleukin 10

It is now more than a quarter of a century ago that IL-10, an anti-inflammatory and immunosuppressive cytokine, was discovered by Mosmann and his colleagues (136). They described a new factor, secreted by murine Th2 clones that inhibited the cytokine production of Interleukin 2 by Th1 clones. This ''cytokine synthesis inhibitory factor'' (CSIF) is now better known as IL-10.

The cellular source of IL-10 is not limited to certain T cell subsets, but it is a hallmark of the majority of leukocytes (137), including monocytes, macrophages and dendritic cells. IL-10-secreting T cells are important in the regulation of undesirable responses to environmental antigens (74) and autoantigens (138). This is evidenced by IL-10-deficient mice, which develop severe inflammation in the intestine leading to chronic enterocolitis and death at 6 weeks of age because the immune system excessively responds to enteric antigens (139). IL-10 plays a pivotal role in the development of EAE as well because immunisation of IL-10 deficient mice with encephalitogenic peptide increased their susceptibility and severity of disease compared to WT mice (140). Also, isolated T cells from those mice exhibit a more proinflammatory profile when stimulated with their cognate antigen. Moreover, IL-10-deficient Tg4 mice, mentioned above, develop spontaneous EAE unlike their IL-10-sufficient counterparts (77). Finally, studies in humans have shown that peripheral blood mononuclear cells (PBMCs) of secondary progressive (SP) MS patients showed a fundamental reduction of IL-10 mRNA levels during disease progression (141) .

## 1.12  IL-10 Reporter mouse models

In order to identify IL-10-producing cells *in vivo,* several IL-10 reporter mouse strains have been developed. Nearly all of the available IL-10 reporter strains are knock-in mice, where a reporter gene was introduced into the *IL10* locus (142). The majority of IL-10 reporter mice were generated by introducing an autofluorescent reporter gene into the *IL10* locus without interfering with regulatory elements like the 5' and 3'-untranslated regions (UTR), influencing gene expression. Those reporter mice include: IL-10$^{eYFP}$ (143), tiger mice (144), IL-10-B-Green mice (145) and ITIG mice (146). IL-10 expression is tightly controlled at the post-transcriptional level by sequences in the 3'UTR that contain messenger RNA-destabilizing motifs. To increase the weak expression of IL-10, some models have been created where those destabilizing motifs were exchanged with an mRNA-stabilizing polyadenylation sequence. Those alternative IL-10 reporter mice include Vert-X mice (147), IL10$^{Venus}$ mice (148) and 10BiT mice (149). A major disadvantage of these models is that they are unable to report IL-10 expression on a protein level. Another approach to decrease the detection limit of IL-10 is the use of enzymatic reporters which leads to signal amplification like in the ITIB mice (146). It uses the enzymatic reporter gene TEM-1-β-lactamase, which allows the substrate coumarin-cephalosporin-fluorescein (4)-acetoxymethyl (CCF4-AM) to be detected. The advantage of the ITIB mouse is that it enables the monitoring of weak IL-10 expression in all lymphoid cell types as well as in cells with high autofluorescence like myeloid cells. We chose the tiger IL-10 reporter strain, in which IRES-GFP was introduced into the 3'UTR of the IL-10 gene because the focus of the laboratory is mainly on T cells with a low autofluorescence and their IL-10 production (98). One disadvantage of the tiger mouse is that the reporter construct does not reflect post-transcriptional regulation. GFP is more stable than IL-10 which means that GFP will remain in cells after IL-10 is already secreted or degraded. On one hand this could lead to false positives, but it could also be considered an advantage when trying to detect which cells produced IL-10 as IL-10 is only secreted for a very short time. Despite this augmented detection of IL-10 in the tiger model, significant eGFP signals can only be detected in T cells and not other immune cells known to produce this cytokine. Homozygous mice were not used experimentally due to a higher percentage of IL10$^-$ GFP$^+$ cells. The crossing of two strains, Tg4 and tiger (Tg4$^{IL-10/GFP}$), allows us to induce tolerance and/or EAE and investigate the spatiotemporal distribution of IL-10-secreting cells

in lymphoid and non-lymphoid tissue during the course of tolerisation and during the progression of EAE.

## 1.13  T cell licensing

Recent data from our group indicate that encephalitogenic T cells in the Tg4$^{IL-10/GFP}$ model are prevented from accessing the brain in a tolerised mouse (AW, personal observations). After the activated CNS-specific T cells enter the bloodstream, they do not immediately invade the brain (150). Rather, they undergo an adjustment process, known as T cell licensing, which allows them to cross the blood-brain barrier and enter the brain. This fine-tuning takes place in peripheral lymphoid organs, like the spleen (151). It remains to be elucidated if the circumvention of T cell entry is mediated by IL-10-producing T cells or other regulatory cell types. Recent studies have brought another organ into play, where T cells could reside during the adjustment process, namely the lung. The lung is an organ not previously linked with T cell trafficking to the CNS (152) but one group demonstrated that encephalitogenic T cells, directly injected into the lung of a rat, can immediately cause disease without a further licensing process in the spleen. Using a passive transfer model of EAE, Odoardi et al. observed that autoreactive T cells did not directly migrate into the CNS. They appeared in the lungs in the preclinical phase of EAE before entering CNS. Notably, when those MBP-specific T cells were extracted from the lung and injected into naïve rats, they accumulated in the CNS within 24 h. Furthermore, when MBP-specific T cells were transferred i.p. into newborns and these animals were then immunised with MBP either subcutaneously or intra-tracheally, memory T cells stimulated in the lung were able to confer EAE to the same extent as their counterparts stimulated in the peripheral lymph nodes. This hypothesis of an unexpected role of the lung in CNS autoimmune disease is further supported by a UK study, where regular smoking was found to be associated with more severe MS and faster progression of disability when compared to people who have never smoked (153). This would suggest that in damaged lungs, the potential for immune regulation of encephalitogenic T cells is impaired. Smoking is considered to be a risk factor for the development of the autoimmune disease rheumatoid arthritis (RA) as well, which leads to

the accumulation of citrullinated proteins in the lung and the development of autoantibodies against these proteins (154).

## 1.14 Bystander suppression

Another very important aspect of tolerance induction in antigen-specific peptide immunotherapy is the induction of bystander suppression. This phenomenon would allow for the treatment of autoimmune disorders characterised by immune responses to multiple antigens without the need to tolerise specifically against each one (155). Bystander suppression is the result of tolerance induction to one specific antigen. If this antigen, to which tolerance is already established, is presented together with a second antigen then the response to the second antigen can be inhibited. Both antigens would generally be derived from the same target structure. For example, bystander suppression was shown in a model of EAE where the treatment with a short MBP peptide inhibited the development of disease induced by whole myelin which comprises of a heterogeneous mixture of autoantigens. In line with this, the administration of the PLP epitope 139-151 was able to suppress T cell responses to both itself and to two epitopes from MBP. Furthermore, this epitope suppressed the development of EAE induced with MBP peptides both prophylactically and therapeutically (156). Foxp3$^+$ regulatory T cells have been shown to have the ability exert bystander suppression (157). CD25$^+$ Tregs induced by vaccination with Salmonella expressing Escherichia coli colonization factor antigen I fimbriae were able to protect against EAE induced with PLP$_{139-151}$ after transfer into naïve SJL mice. This protection was demonstrated to be dependent on TGF-β as the administration of anti-TGF-β after adoptive transfer of Treg cells abrogated protection against EAE and enhanced the production of IL-17.

## 1.15 Myeloid-derived suppressor cells (MDSCs)

As mentioned, escalating dose immunotherapy leads to an upregulation of co-inhibitory molecules like TIM-3 or PD1 on CD4$^+$ T cells (61). Another study found that transgenic overexpression of TIM-3 on T cells results in the increase in a population of CD11b$^+$ Ly6G$^+$ cells (158). These innate cells are known as myeloid-derived suppressor cells and were described more than 30 years ago in cancer patients (159). Since then, the understanding of their detrimental role in cancer has been well described. In cancer patients, as well in tumour-bearing mice these immature myeloid cells accumulate and contribute to tumour escape to a great extent by suppressing antigen-specific T cell responses (160)(161).

### 1.15.1 Phenotype of MDSCs

In mice, MDSCs are broadly defined as CD11b$^+$ Gr1$^+$ cells. Normal mouse bone marrow contains 20–30% of CD11b$^+$ Gr1$^+$ cells , but these cells make up only a small proportion (2–4%) of spleen cells and are very rare in the lymph nodes (161). Anti-Gr1 antibodies recognise two targets, LY6G and LY6C. Based on their differential LY6G and LY6C expression a further distinction in MDSC subsets can be made (162). Polymorphonuclear MDSCs (PMN-MDSCs) have a CD11b$^+$ LY6G$^+$ LY6C$^{low}$ phenotype, whereas MDSCs with monocytic morphology (M-MDSCs) are CD11b$^+$ LY6G$^-$ LY6C$^{hi}$.

### 1.15.2 Differentiation and activation of MDSC

MDSCs are a heterogeneous population of cells which arise from myeloid precursor cells generated from hematopoietic stem cells in the bone marrow. Under steady-state conditions, these immature myeloid cells migrate to secondary lymphoid tissue where they differentiate into macrophages, neutrophils and dendritic cells that lack suppressive features (163). However, in pathological circumstances like infection, inflammation, tumour or autoimmune disease they desist from differentiation and start to accumulate and become suppressive MDSCs. The expansion and activation of MDSCs in cancer can be regulated by multiple factors. Granulocyte-macrophage colony-stimulating factor (GM-CSF) produced by tumour cells leads to striking alterations of haematopoiesis and to an expansion of MDSC

(164). The direct activation of MDSCs is achieved by factors including IFN-γ, produced by activated T cells or tumour stromal cells (165). This was demonstrated by co-culturing CD11b$^+$ cells from tumour bearing mice with responder T cells from IFN-γ$^{-/-}$ or wild type mice in the presence of allogeneic splenocytes. The lack of IFN-γ production by alloantigen-stimulated T cells abolished the suppressive activity of the tumour-induced CD11b$^+$ cells. The suppressive activity of MDSC is not only dependent on IFN-γ but also on IL-10 (166). Huang et al. adoptively transferred MDSC and CD4$^+$ T cells into irradiated tumour-bearing mice. The mice received injections of neutralizing anti-IL-10 or anti-IFN-γ antibodies post transfer. After recovery of the adoptively transferred T cells their proliferative response was evaluated and the antibody treatment with either anti-IL-10 or anti-IFN-γ led to the abrogation of their hypoproliferative response.

### 1.15.3 Suppressive mechanisms of MDSCs

T lymphocytes are dependent on the non-essential amino acid L-arginine for their proliferation. An increased arginase activity in myeloid cells leads to a shortage of this amino acid and to an arrest in the T cell cycle progression (167). L-arginine serves as a substrate for two enzymes: nitric oxide synthase (NOS), which metabolize L-arginine into nitric oxide (NO) and citrulline, and arginase, which converts L-arginine into urea and L-ornithine. Studies indicate that PMN-MDSC and M-MDSC subsets utilize different effector molecules and signalling pathways for their suppressive activity to regulate T cell function (168). Whereas the inhibition of inducible NOS (iNOS) could partly reverse suppression by M-MDSCs, suggesting an NO-dependent mechanism, it did not affect suppression by PMN-MDSCs. Conversely, arginase inhibitor decreased suppression of PMN-MDSCs, while the suppressive activity of M-MDSCs was unaffected. NO, itself, can inhibit T cells e.g. via the inhibition of MHC class II gene expression on antigen presenting cells (169) or the induction of T cell apoptosis (170). Arginase activity in MDSC may result in increased production of superoxide anion ($O_2^-$) (171). Superoxide is very unstable and is converted to $H_2O_2$ and reactive nitrogen species (RNS). $O_2^-$ can react with NO, generating RNS like peroxynitrite (PNT). Subsequently, PNT can induce nitration of the amino acid tyrosine which impairs tyrosine phosphorylation. This, in turn, can inhibit T cell activation and proliferation (172). Myeloid

cells have the potential to produce large amounts of reactive oxygen species (ROS) and PNT during direct cell-cell contact with CD8^{+} T cells (173). This leads to the nitration of the T-cell receptor which impairs the conformational flexibility of the TCR chains. This process, which leads to anergy, was only observed when CD8^{+} T cells were activated with their specific antigen, whereas their responsiveness to non-specific stimuli was maintained. This antigen-specific T cell suppression seems to be dependent on MHC I expression on MDSCs because the blockade of the interaction between the MDSCs and T cells using an MHC class I antibody abrogated the suppression of the CD8^{+} T cell response *in vitro* (174). The same antigen-specific T cell suppression is evident *in vivo* and has been demonstrated in a model of inflammatory bowel disease (175). The co-transfer of MDSCs with clone 4/T-cell receptor (CL4-TCR) hemagglutinin (HA)-specific CD8^{+} T cells, which express a TCR that recognizes an epitope of the HA protein presented by MHC I, into naive VILLIN-HA mice, where HA is specifically expressed in the intestine, ameliorated enterocolitis. These results are in accordance with a study in a model of sporadic immunogenic cancer (176). In mice harbouring large immunogenic tumours an increase in frequency of MDSCs could be seen which do not inhibit responses of CD8^{+} T cell against unrelated antigens. It has been a topic of debate whether MDSCs can promote antigen-specific tolerance in CD4^{+} T cells. However, in recent years it has become apparent that MDSCs exhibit their immunosuppressive activity on CD4^{+} T cells as well and that this interaction is a reciprocal relationship (177). A study showed that splenic PMN-MDSCs reduced the production of IFN-γ by CD4^{+} T-cells in response to an OVA-derived peptide in co-culture. This reduction was dependent on the expression of MHC-II on PMN-MDSC because MHC-II^{-/-} MDSC fail to limit the CD4^{+} T cell response (178). Furthermore, those activated antigen-specific CD4^{+} T cells transformed PMN-MDSC into non-specific suppressors. This was demonstrated in a model where OT-II transgenic CD4^{+} T cells were transferred into C57BL/6 mice followed by the transfer of MDSCs and immunization with the cognate OVA peptide. LN cells were isolated ten days later and restimulated *in vitro* with their specific peptides or anti-CD3/CD28 antibodies and in both cases the cell proliferation, assessed by $^3$H-thymidine uptake, was reduced (178).

In cancer models, the interaction between Tregs and MDSCs is documented in detail (166). Monocytic Gr-1^{+}CD115^{+} MDSCs from tumour-bearing mice were able to induce the expansion of Foxp3^{+} Treg cells *in vitro*. Moreover, the adoptive co-transfer of CD115^{+}Gr-1^{+}

MDSCs and T cells into an irradiated host bearing a tumour revealed an increase in Foxp3 gene expression in conjunction with a reduced T cell proliferative response to peptide stimulation. More importantly, the residual tumour mass was increased in mice receiving Gr-1$^+$CD115$^+$ MDSCs showing that they suppress anti-tumoural T-cell responses. This process was dependent on IL-10 and IFN-γ, as determined by the administration of neutralizing antibodies *in vivo*. A later study from the same group could prove that Treg differentiation is dependent on the expression of the co-stimulatory receptor CD40 on M-MDSC because MDSC from CD40-deficient mice bearing a tumour failed to induce Tregs (179).

### 1.15.4   MDSCs in autoimmunity

In contrast to the role of MDSC in infection and cancer, the role of MDSC in autoimmunity remains controversial. On the one hand, the accumulation of CD11b$^+$Ly6C$^{high}$ M-MDSCs in EAE positively correlated with disease severity and an improvement in pathology was accompanied by the reduction of these cells (180). Moreover, depletion of MDSCs was found to ameliorate myelin injury and decrease the EAE clinical scores and the number of Th17 cells *in vivo* (181).  Both of these studies showed that MDSCs can act as pathological effector cells and contribute to the damage of the CNS. However, in contrast to these studies their beneficial role in autoimmune diseases including diabetes (182) or EAE (183) has become increasingly appreciated in recent years. MDSCs have been shown to be able to limit T cell mediated pathology and tissue injury as a result of their suppressive activity. A protective effect of MDSCs could be shown in a murine model for type-1 diabetes (151), where the transfer of MDSC could significantly delay diabetes onset and inhibited pancreatic lymphocyte infiltration and insulitis.  Furthermore, a beneficial effect in EAE could be seen (152) because CD11b$^+$Ly6C$^{hi}$ cells, which accumulated significantly after the induction of EAE in the spleen and blood, suppressed the proliferation of activated CD4$^+$ T cells by inducing apoptosis through the production of nitric oxide (NO). Most of the published MDSCs studies used murine models but a small number of studies have investigated their role in human patients with autoimmune diseases. In patients with rheumatoid arthritis (RA) MDSC were identified in the synovial fluid (SF) that were able to limit the expansion of joint-infiltrating pathogenic T cells (184).  MDSCs were also found to be significantly increased in the

peripheral blood of patients with active MS (185). *In vitro*, these MDSCs suppressed the activation and proliferation of autologous T cells. Moreover, in patients with type-1 diabetes, MDSCs accumulate in peripheral blood and have been shown to be able to suppress T cell proliferation (186).

## 2    SCOPE OF STUDY

One of the major features of the autoimmune disease MS is that T cell aberrantly recognise self-peptides of the myelin sheath and attack the CNS. Antigen-specific immunotherapy of MS aims to restore immune tolerance while avoiding the use of non-specific immunosuppressive drugs.

To better understand the process of successful tolerance induction, we addressed three major aspects of antigen-specific immunotherapy:

- Analysis of biomarkers of tolerance induction on CD4+ T cells throughout the body during antigen-specific immunotherapy
- Investigation of bystander suppression of myelin-reactive T cells
- Defining the involvement of MDSCs in tolerance induction

Effective tolerance induction of the Tg4 TCR-transgenic murine model for MS, EAE, involves repeated administration of a self-peptide in a dose-escalating manner to re-educate pathogenic T cells to become protective IL-10secreting regulatory T cells. The main focus of the laboratory of Professor David C. Wraith is to understand the underlying mechanisms of tolerance induction. This includes the phenotypic characterisation of IL-10-secreting CD4+ T cells and CD4+ Foxp3+ T cells in lymphoid and non-lymphoid tissue during the course of tolerisation and during the progression of EAE. In this body of work, we expanded upon the current understanding of these phenotypic changes by examining the changes in expression of Foxp3 and co-inihibitory molecules on CD4+ T cells not only in lymphoid organs but also other tissues that have been suggested to play a role in controlling immune homeostasis, in an IL-10-reporter mouse model.

The clinical application of antigen-specific peptide immunotherapy for MS is still challenging due to the complexity of immunological changes required and the involvement of T cells specific for a range of myelin antigens. To address the latter, it would be beneficial if the regulatory T cells induced could inhibit not only effector T cells that recognise the same antigen but also those that recognise epitopes from other myelin proteins. Therefore, we investigated if tolerised CD4+ T cells specific for an MBP peptide were able to exert bystander suppression of MOG-reactive T cells.

While investigating the induction of regulatory CD4$^+$ T cell subsets we made the novel observation that the development of MDSCs was augmented as a result of peptide treatment. MDSCs have been studied intensively in the fields of cancer and autoimmunity, but their involvement in the induction of antigen-specific tolerance was not described previously. Because of their suppressive effect on the immune system in cancer, we hypothesised that PMN-MDSCs and their interactions with CD4$^+$ T cells could be beneficial for antigen-specific immunotherapy. Thus, the phenotypic and functional characteristics of MDSCs during tolerance induction in our EAE model were evaluated.

# 3 MATERIALS & METHODS

## 3.1 Mice

All animal experiments were carried out under the UK Home Office Project Licence number 30/2705 and 30/3195 held by Professor David Cameron Wraith and the study was approved by the University of Bristol ethical review committee. Mice were bred and kept under specific pathogen-free conditions on a 12 hour light/dark cycle at the University of Bristol Animal Services Unit. Food and water was provided ad libitum.

The Tg4 T cell receptor (TCR) transgenic mouse was described previously (187). CD4$^+$ T cells in this model express a Vα4 Vβ8.2 transgenic TCR specific for an acetylated nine-residue peptide of MBP (Ac1-9) in the context of I-Au. This mouse was backcrossed onto the B10.PL (H2u) background.

The crossing of the Tg4 with an IRES-GFP reporter knock in mouse (B6.129S6-Il10tm1Flv/J from The Jackson Laboratory)) allowed the detection of IL-10 *in vivo* (Tg4$^{IL-10/GFP}$).

B.10.PL (B10.PL-H2u H2-T18a/ (73NS)SnJ) mice were purchased from Jackson Laboratory. C57BL/6 (NCrl) mice were purchased from Charles River and crossed with B10.PL mice and the resulting F1 generation was used in experiments of bystander suppression.

Tg4 CD45.1$^+$ mice were a kind gift from Professor Steve Anderton (University of Edinburgh).

Generation of Tg4IL-10$^{-/-}$ mice has been previously described (Gabrysová et al. 2009). Briefly, mice were generated by breeding B10.129P2-Il10tm1Cgn/J (The Jackson Laboratory) with Tg4 mice and bred to provide a homozygous Tg4IL-10$^{-/-}$ line. Tg4$^+$ IL-10$^{+/-}$ were used for the breeding stock because homozygous Tg4IL-10$^{-/-}$ mice develop spontaneous EAE at 6 − 8 weeks.

## 3.2 Peripheral blood phenotyping

Peripheral blood from the tail vein was collected from each mouse into a flow cytometry tube (Sarstedt #55.1579) containing FACS buffer (1xPBS (Lonza #17-516F), 2% FCS (labtech #FCS-SA), 2 μM EDTA (Sigma-Aldrich #E7889). The blood cells were pelleted for five minutes

at 560 x g at 4°C. The supernatant was discarded and the pellet was resuspended in 50 µl of FACS buffer containing flow cytometry antibodies listed in table. After an incubation of 20 minutes in the dark at 4°C the cells were washed with PBS (1xPBS (Lonza #17-516F) and centrifuged for 560 x g at 4°C for five minutes. Each cell pellet was resuspended in 1 ml of diluted 1-step Fix/Lyse solution from eBioscience (#00-5333-57) and incubated for 10 minutes at room temperature in the dark. After washing the cells with PBS the pellet was resuspended in 100 µl of FACS buffer and analysed on the flow cytometer (BD LSRII or BD LSR Fortessa X-20).

**Table 3.1.Peripheral blood phenotyping antibodies.**

| antibody | clone | dilution | company & catalogue number |
| --- | --- | --- | --- |
| anti-mouse CD4 PerCP-Cyanine5.5 | RM4-5 | 1:200 | eBioscience #45-0042 |
| anti-mouse Vβ 8.1/Vβ 8.2 TCR FITC | KJ16-133 | 1:200 | eBioscience #11-5813 |
| anti-mouse CD19 APC | eBio1D3 | 1:200 | eBioscience #17-0193 |
| anti-rat RT1B (MHCII) PE | OX-6 | 1:500 | BioLegend #205308 |

## 3.3   Genotyping

Mouse ear biopsies were processed according to the instructions in the DNeasy® Blood & Tissue Kit from Qiagen (# 69506). Briefly, the tissue was lysed by incubating the ear notches in 180 µl ATL plus 20 µl of proteinase K overnight at 56°C in a water bath. 200 µl buffer AL and 200 µl 96% ethanol were added to the cell suspension and thoroughly mixed by vortexing. The mixture was then pipetted into a DNeasy Mini spin column placed in a 2 ml collection tube. The tube was centrifuged for one minute at 6000 x g. After that the column was washed with the recommended wash buffers AW1 and AW2. The flow-through was always discarded. To elute the DNA from the column 150 µl of water was added to the centre of the spin column, incubated for one minute at room temperature and then centrifuged for one minute at 6000 x g. 2 µl of the DNA solution was used for polymerase chain reaction (PCR) analysis. PCR was used to genotype transgenic GFP reporter knock-in

(Tg4<sup>GFP/IL-10</sup>) mice for the presence of the GFP reporter with the primers listed in table. The reactions were performed in a thermocycler PCR machine. All amplifications were performed in a total volume of 25 µl, containing template DNA, 1 µM of each primer (purchased from Eurofins MWG) and diluted GoTaq®Hot Start Green Master Mix from Promega (#M5122). Standard PCR program started with three minutes of denaturation at 94°C, followed by 35 cycles consisting of denaturation at 94°C for 30 seconds, annealing at 63°C for one minute and elongation at 72°C for one minute and a final elongation step at 72°C for two minutes.

**Table 3.2. Genotyping primer for Tg4<sup>GFP/IL-10</sup> mice.**

| primer | Sequence 5'-3' | T melting (°C) |
|---|---|---|
| oIMR 8625 (common) | GTG TGT ATT GAG TCT GCT GGA C | 54.8 |
| oIMR 8626 (WT reverse) | GTG TGG CCA GCC TTA GAA TAG | 54.4 |
| oIMR 8292 (mutant reverse) | CCA AAA GAC GGC AAT ATG GT | 49.7 |

To genotype Tg4 IL-10 knockout mice, PCR was used as described above with the primers listed in table. The PCR program used started with two min of denaturation at 94°C, followed by 35 cycles consisting of denaturation at 94°C for one minute, annealing at 55°C for two minutes and elongation at 72°C for three minutes and a final elongation step at 72°C for five minutes.

**Table 3.3. Genotyping primer for Tg4 IL-10KO mice.**

| primer | Sequence 5'-3' | T melting (°C) |
|---|---|---|
| oIMR 86 (WT reverse) | GTG GGT GCA GTT ATT GTC TTC CCG | 59.1 |
| oIMR 87 (common) | GCC TTC AGT ATA AAA GGG GGA CC | 57.1 |
| oIMR 88 (mutant reverse) | CCT GCG TGC AAT CCA TCT G | 53.2 |

Afterwards the PCR samples were separated on a 2% agarose gel (1 x TAE (Sigma #T9650), 0.5 µg/ml ethidium bromide (Sigma-Aldrich # 09-0617 SAJ) at 100 mV.

## 3.4 Peptides

The acetylated native N-terminal murine myelin basic protein (MBP) peptide MBP$_{Ac1-9}$(4K) (AcASQKRPSQR), the high affinity analogue of the MBP$_{Ac1-9}$(4Y) peptide (AcASQYRPSQR) with tyrosine substituted for lysine at position four (188), the MOG$_{35-55}$ peptide and the linked peptides were custom-synthesized by GL Biochem Shanghai. Linked peptides were created by introducing the linker sequence HFFK between MBP$_{Ac1-9}$ and MOG$_{35-55}$. The paired phenylalanine residues would represent a potential cleavage motive for cathepsins D and E during antigen processing because those two aspartyl proteases tend to cleave dipeptide bonds that have hydrophobic residues (189).

## 3.5 Flow cytometric analysis (FACS)

Multi-colour flow cytometry has been used to identify cell population expressing a given antigen. These cell populations were isolated from various different organs as described later. All antibodies used were purchased from either eBioscience or Biolegend. In each case, the amount of antibody was used according to the manufacturer's instruction or based on titration experiments to optimise the signal to noise ratio. The cells were evaluated using up to 10-colour combinations. For compensation in multi-colour analysis eBioscience OneComp eBeads (#01-1111-42) were used. One drop of beads were mixed with 1 µl of antibody and incubated for 20 minutes at 4°C in the dark. After washing with 1xPBS the beads were suspended in 200 µl FACS buffer.

## 3.6 Cell isolation and preparation

Mice were sacrificed by cervical dislocation. The spleen, lymph nodes were removed and mashed through a 40 µm cell strainer (Falcon #352340) in a Petri dish (Thermo scientific #101R20). The cell suspension was transferred to a 50 ml falcon tube (Corning #430829) and washed with cold PBS. The tubes were centrifuged at 550 x g for five minutes at 4°C (all centrifugation steps use this setting). The supernatant was discarded and the cell pellet was resuspended in 1 ml lysis buffer (Sigma #R7757) to allow erythrocyte lysis (only for spleen)

and incubated for four minutes at RT. The cells were washed with PBS and immediately centrifuged.

## 3.7 Cell isolation and preparation of liver

The liver was cut with a scalpel blade (Swann-Morton #0101) into smaller 5 mm pieces in a 6-well plate (Corning™Costar™ #3516) containing liver digestion buffer (complete RPMI 1640 (Lonza #BE-12-167F), 20 mM HEPES (Lonza #BE17-737E), 5% FCS (labtech #FCS-SA), 50 U Penicillin/Streptomycin (Lonza #DE17-603E), 2 mM L-Glutamine (Gibco #31350-010), 50 μM β-mercaptoethanol (Gibco #31350-010) + 500 U/ml Collagenase IV (Worthington #LS004188) and 150U/ml DNase I solution (Roche #10104159001) and incubated for 30 minutes at 37°C. The liver was dissociated through a 40 μm cell strainer in a Petri dish. The resulting cell suspension was collected in a 50 ml falcon tube and the cells were pelleted at 400 x g for 10 min at 4°C. The supernatant was discarded and the cell pellet was resuspended to a volume of 15 ml complete RPMI and mixed with 8.5 ml isotonic Percoll (GE Healthcare #17-0891-01), giving a final concentration of 36% isotonic Percoll. This suspension was thoroughly mixed and separation was performed at 500 x g for 10 min at 4°C. The supernatant was removed and the pellet was resuspended in 1 ml lysis buffer to allow erythrocyte lysis and incubated for four minutes at RT. The cells were washed with PBS and immediately centrifuged at 550 x g for five minutes at 4°C.

## 3.8 Cell isolation and preparation of brain and spinal cord

The brain/spinal cord was cut with a scalpel blade into smaller pieces in a 6-well plate containing CNS digestion buffer (complete RPMI + 275 U/ml Collagenase IV and 15 U/ml DNase I solution) and incubated for 20 minutes at 37°C. The tissue was homogenised using a 5 ml syringe (Terumo #SS+05S1) with a 19G needle (Terumo #NN-1950R) and ejected through a 40 μm cell strainer in a 50 ml falcon tube and the cells were pelleted at 280 x g for five minutes at 4°C. The supernatant was discarded and the cell pellet was resuspended to a volume of 7 ml in 70% Percoll. The gradient was prepared by underlaying 4 ml 30% Percoll with 4 ml 37% Percoll with a 5 ml pipette (Corning #4051) in a 15 ml tube (Corning #430791).

The 37% Percoll fraction was underlayed with the 70% Percoll cell suspension and separation was performed at 500 x g for 30 min at RT with no brakes. The myelin layer was removed and the lymphocytes and microglia above the 70% Percoll layer were removed and transferred into a 15 ml falcon tube and filled up with PBS. The cells were pelleted at 280 x g for five minutes at 4°C.

### 3.9   Cell isolation and preparation of lung

The lung was cut with a scalpel blade into smaller pieces in a 6-well plate containing lung digestion buffer (complete RPMI 1640 + 400 U/ml Collagenase IV and 80 U/ml DNase I solution and incubated for 30 minutes at 37°C. The lung was mashed through a 40 μm cell strainer in a Petri dish. The resulting cell suspension was collected in a 50 ml falcon tube and the cells were pelleted at 400 x g for 10 min at 4°C. The supernatant was discarded and the cell pellet was resuspended in complete RPMI.

### 3.10   Cell surface stain

Cells were washed with PBS before adding 0.5 μg anti-mouse CD16/CD32 (eBioscience #14-0161-85) to block unspecific binding of antibodies to Fc receptors, followed by an incubation time of 15 minutes at 4°C. For T cell staining blocking with Fc block was not performed. The surface antibodies were directly added as well as fixable viability stain to exclude dead cells (eFluor® 780 from eBioscience # 65-0865-18 or Zombie Aqua™ dye from BioLegend #423102) in a 1:1000 dilution. After an incubation of 30 minutes at 4°C in the dark, cells were washed with PBS and then 200 μl of FACS buffer was added for the analysis on the flow cytometer.

### 3.11  Flow cytometric analysis of T cells

**Table 3.4. Antibodies used for flow cytometric analysis of T cells.**

| antibody | clone | dilution | company & catalogue number |
|---|---|---|---|
| anti-mouse CD4 PerCP-Cyanine5.5 | RM4-5 | 1:200 | eBioscience #45-0042 |
| anti-mouse CD4 A700 | GK 1.5 | 1:100 | BioLegend #100430 |
| anti-mouse Foxp3 PE | FJK-16s | 1:100 | eBioscience #12-5773-82 |
| anti-mouse Foxp3 eFluor®450 | FJK-16s | 1:100 | eBioscience #48-5773-82 |
| anti-mouse PD1 (CD279) PE/Cy7 | RMP1-30 | 1:200 | BioLegend #109110 |
| anti-mouse Tim-3 (CD366) PE | 8B.2C12 | 1:200 | eBioscience #12-5871-83 |
| anti-mouse Tim-3 (CD366) APC | 8B.2C12 | 1:200 | eBioscience #17-5871-82 |
| anti-mouse TIGIT (Vstm3) APC | 1G8 | 1:200 | BioLegend #142106 |
| anti-mouse CD62L FITC | MEL-14 | 1:200 | BioLegend #104406 |
| anti-mouse CD8 APC | 53-6.7 | 1:200 | eBioscience #17-0081-81 |

### 3.12  Flow Cytometric analysis of MDSCs

**Table 3.5. Antibodies used for flow cytometric analysis of MDSCs.**

| antibody | clone | dilution | company & catalogue no |
|---|---|---|---|
| anti-mouse Ly-6G A700 | 1A8 | 1:200 | BioLegend #127622 |
| anti-mouse Ly-6G FITC | 1A8 | 1:200 | BioLegend #127606 |
| anti-mouse Ly-6C APC/Cy7 | HK1.4 | 1:200 | BioLegend #128025 |
| anti-mouse CD11b PerCP-Cyanine5.5 | M1/70 | 1:200 | BioLegend #101228 |
| anti-mouse CD11b PE/Cy7 | M1/70 | 1:200 | BioLegend #101216 |
| anti-mouse Galectin-9 PE | 108A2 | 1:200 | BioLegend #137903 |
| anti-mouse PD-L1 (B7-H1, CD274) APC | 10F.9G2 | 1:200 | BioLegend #124311 |
| anti-mouse CD80 Brilliant Violet 421™ | 16-10A1 | 1:200 | BioLegend #104725 |
| anti-mouse CD80 APC | 16-10A1 | 1:200 | BioLegend #104713 |
| anti-mouse CD86 Brilliant Violet 605™ | GL-1 | 1:200 | BioLegend #105037 |
| anti-mouse CD40 PE/Cy7 | 3/23 | 1:200 | BioLegend #124621 |
| anti-mouse MHCII(I-A/I-E) APC/Cy7 | M5/114.15.2 | 1:200 | BioLegend #107627 |

### 3.13 Intracellular cytokine staining (ICCS)

Cells were activated with 5 ng/ml PMA (Sigma # P8139) plus 500ng/ml Ionomycin (Sigma # I0634) and Golgi Stop (BD Bioscience # 554724) was added in a 1:1500 dilution. The cells were incubated at 37°C in a $CO^2$ incubator for three hours. Cell surface and viability stain was performed as described elsewhere. Cells were then fixed with 200 µl IC fixation buffer (eBioscience #00-8222-49) for 20 minutes at 4°C in the dark. After washing once with FACS buffer and once with diluted permeabilisation buffer (eBioscience # 00-8333-56) cells were stained with antibodies for intracellular cytokines in diluted permeabilisation buffer for 30 minutes at 4°C in the dark. Before adding 200 µl FACS buffer for the analysis on the flow cytometer, washing with FACS buffer was performed.

**Table 3.6. Antibodies used for intracellular cytokine staining.**

| antibody | clone | dilution | company & catalogue no |
|---|---|---|---|
| anti-mouse IL-2 FITC | JE S6-5H4 | 1:200 | BioLegend #503806 |
| anti-mouse IL-4 PE/Cy7 | BVD6-24G2 | 1:200 | eBioscience #25-7042-82 |
| anti-mouse IL-10 PE | JE S6-16E3 | 1:200 | BioLegend #505008 |
| anti-mouse IL-17A PerCP-Cyanine5.5 | eBio17B7 | 1:200 | eBioscience #45-7177-82 |
| anti-mouse IFNγ APC | XMG 1.2 | 1:200 | eBioscience #17-7311-82 |
| anti-mouse TNFα Brilliant Violet 605™ | MP6-XT22 | 1:200 | BioLegend #506329 |

### 3.14 Transcription factor staining

For transcription factor staining, the Foxp3/Transcription Factor Staining Buffer Set from eBioscience (#00-5523-00) was used according to the manufacturer's instructions. First surface and viability stain was performed as described elsewhere. The Foxp3 fixation solution was prepared by diluting one part concentrate with three parts diluent. After washing with PBS the cells were incubated with Foxp3 fixation solution for 30 minutes at room temperature. In case of the GFP reporter knock-in (Tg4[GFP/IL-10]) mice, samples needed to be prefixed with 0.5% paraformaldehyde (EMS #15710) for 30 minutes at room temperature to prevent losing the GFP signal before the Foxp3 fixation step. Cells were washed afterwards with PBS and the antibody for the transcription factor was added in FACS

buffer and the solution was incubated for 30 minutes at room temperature in the dark. Cells were washed and 200 µl FACS buffer was added.

## 3.15  Proliferation assay

The fluorescent dye is equally distributed among daughter cells with each division. For *in vitro* dye dilution proliferation assays up to 10 x $10^6$/ml splenic CD4$^+$ T cells in 5 ml PBS were labelled with cell proliferation dye eFluor®450 (eBioscience #65-0842) in a dilution of 1:2000. They were incubated for 20 minutes at 37°C in a $CO^2$ incubator. The double amount of RPMI 1640 with 10% FCS was added and the tube was further incubated for 20 minutes at 37°C in a CO2 incubator. After washing the cells with PBS they were co-cultured with different cell types.

## 3.16  Dendritic cell isolation (DC)

For the isolation of mouse dendritic cells (DCs) from spleen the CD11c Microbeads Kit from MACS Miltenyi was used (#130-052-001). Spleens were cut into smaller pieces with a sterile scalpel in a 6-well plate in 5 ml digestion buffer (complete RPMI 1640, 2000 U Collagenase IV, 50 U DNase I) for 15 minutes at room temperature. Afterwards the spleen was mashed through a 40 µm cell strainer. The cell suspension was washed with PBS and red blood lysis was performed by adding 1 ml of Red Blood Cell Lysing Buffer Hybri-Max™ and incubation for four minutes at room temperature. Cells were again washed with PBS and cell number was determined by using a haemocytometer (Improved Neubauer from Hawksley #AC1000). The cell pellet was resuspended in 400 µL MACS buffer (1xPBS (Lonza #17-516F), 10% BSA, 2 µM EDTA (Sigma-Aldrich #E7889) per $10^8$ total cells. Subsequently, 100 µL of CD11c MicroBeads per $10^8$ total cells was added and incubated for 15 minutes at 4°C; the cells were washed by adding 1–2 mL of buffer per $10^7$ cells and centrifuged at 200 × g for 10 minutes. According to the number of total cells and the number of CD11c$^+$ cell the appropriate MACS Column and MACS Separator were chosen. The column was prepared by rinsing with the appropriate amount of MACS buffer. The cell suspension was applied onto the column. The column was washed three times with the appropriate amount of buffer. After this, the

column was removed from the separator and it was placed on a collection tube, the appropriate amount of buffer was pipetted onto the column and the magnetically labelled cells were flushed out by firmly pushing the plunger into the column.

### 3.17  CD4$^+$ T cell or naïve CD4$^+$ T cell isolation

CD4$^+$ T cells were isolated using the MagniSort™ Mouse CD4 T cell Enrichment Kit (#8804-6821-74) or the MagniSort™ Mouse CD4 Naïve T cell Enrichment Kit (#8804-6824-74) from eBioscience according to the instructions. A single-cell suspension of lymphocytes at a concentration of $1 \times 10^7$ cells/100 μL in FACS buffer was prepared. The desired number of cells, but not more than $2 \times 10^8$, was placed in a FACS tube. 20 μL of MagniSort™ Enrichment Antibody Cocktail per 100 μL of cells was added and mixed well by pulse vortexing five times. The cell suspension was incubated at room temperature for 10 minutes. The cells were washed by bringing the volume up to 4 mL with FACS buffer and then centrifuged at 300 x g for five minutes. The supernatant was discarded and the cells were thoroughly resuspended to their original volume with FACS buffer. 20 μL of MagniSort™ Negative Selection Beads per 100 μL of cells were added, mixed well by pulse vortexing five times and incubated at room temperature for five minutes. The volume was brought up to 2.5 mL with FACS buffer. The cells were mixed by pipetting up and down three times with a P1000 pipette set to one millilitre. The FACS tube was inserted into the Magnet until the bottom of the tube was touching the bench top through the hole in the bottom of the magnet. After incubation at room temperature for five minutes the supernatant was poured in a continuous motion into a 15 mL tube containing the untouched, negatively selected T cells.

### 3.18  CD4$^+$ T cell depletion with MicroBeads

This assay is based on the magnetically labelling of the CD4$^+$ T cells which are retained later on a column. The spleen was mashed through a 40 μm cell strainer. The cell suspension was washed with PBS and red blood lysis was performed by adding 1 ml of Red Blood Cell Lysing Buffer Hybri-Max™ and incubation for four minutes at room temperature. Cells were again washed with PBS and cell number was determined by using a haemocytometer. The cell

pellet was resuspended in 90 µL MACS buffer per $10^7$ total cells. Then 10 µL of CD4 MicroBeads (Miltenyi Biotec #130-049-201) per $10^7$ total cells was added and incubated for 15 minutes in the refrigerator, the cells were washed by adding 1–2 mL of buffer per $10^7$ cells and centrifuged at 200 × g for 10 minutes. According to the number of total cells and the number of CD4$^+$ T cells the appropriate MACS Column and MACS Separator were chosen. The column was prepared by rinsing with the appropriate amount of MACS buffer. The cell suspension was applied onto the column and the unlabelled cell fraction was collected into a 15 ml tube. The column was washed three times with the appropriate amount of buffer and the effluent was collected into the same tube. The cell number was determined after a centrifugation step at 200 × g for 10 minutes.

### 3.19 Generation and culture of murine bone-marrow derived dendritic cells (BMDC)

Mice were culled by cervical dislocation and the legs were removed, stripping away as much muscle as possible. Legs were kept in complete RPMI on ice. In tissue culture hood, legs were placed in a petri dish with PBS and residual muscle was removed. The leg was cut in two on the knee joint. Femur and tibia were transferred to a fresh sterile petri dish and the ends of the bones were cut off. A 10 ml syringe with an orange 25 G needle (BD Microlance™ #300400) was filled with RPMI and the needle was inserted into the marrow cavity, flushing the bone-marrow out of the bone. The cell suspension was pipetted through a 40 µm cell strainer into a 15 ml Falcon tube and centrifuged at 500 x g for five minutes. The supernatant was removed and the cell number was assessed. 2 x $10^6$ cells in 5 ml of GM-CSF medium (20 µg/ml GM-CSF from BioLegend #576304 in complete RPMI) were placed in one well of a 6-well plate and incubated for 10 days in a $CO_2$ incubator at 37°C. 2 ml of the media was removed on day three, six and eight and replaced with 2 ml fresh GM-CSF medium. To mature dendritic cells LPS (Sigma #L2654) was added for 20 to 24 hours at a concentration of 1 µg/ml. Cells were harvested with a cell scraper (Corning® #3010).

## 3.20 Fluorescence-activated cell sorting

Flow sorting is able to isolate a unique cell type from a heterogeneous population based on their phenotypic characteristics. G-MDSCs were sorted based on their marker expression profile of CD11b$^+$ Ly6G$^+$. Sorted CD4$^+$ T cells were CD4$^+$ CD8$^-$ B220$^-$. In some experiments the splenocyte cell suspension was depleted of CD4$^+$ T cells before the sort of G-MDSCs using Mouse CD4 (L3T4) MicroBeads from Miltenyi Biotec (#130-049-201). The cell sort was performed using the BD Influx™ cell sorter operated by Dr Andrew Herman (Director of Flow Cytometry).

## 3.21 *In vitro* bystander suppression assay

Immature and mature BMDCs from the F1 generation of B10.PL x C57BL/6 were generated. B10.PL x C57BL/6 were antigen challenged *in vivo* with 100 µg MBP$_{Ac1-9}$ and 100 µg MOG$_{35-55}$ at the base of the tail as described later. TG4 CD45.1$^+$ mice received dose escalation immunotherapy. Splenic CD4$^+$ T cells from both strains were isolated with a magnetic separation kit and labelled with eFluor 450 cell proliferation dye as described before. 1 x 10$^5$ BMDC, 1 x 10$^5$ tolerised Tg4 T cells (T$_{tol}$) and 1 x10$^6$ conventional B10.PL x C57BL/6 T cells (T$_{conv}$) were co-cultured in complete RPMI with 10 µg/ml MBP$_{Ac1-9}$(4K) and/or 10 µg/ml MOG$_{35-55}$ in a 48-well plate (Corning #3548) in a total volume of 1 ml for four days in a CO$_2$ incubator at 37°C.

## 3.22 *In vitro* suppression assay

PMN-MDSC and antigen-experienced CD4$^+$ T cells (T$_{ag}$) from MBP$_{Ac1-9}$(4Y)-treated mice were FACS sorted. Naïve CD4$^+$ T cells and CD11c$^+$ cells were isolated according to their isolation protocol. PMN-MDSCs and CD4$^+$ T cells were either co-cultured at a ratio of 1:3 together with CD11c$^+$ cells as antigen-presenting cell (APC) in a APC:T cell ration of 1:10 and MBP$_{Ac1-9}$(4K)-peptide (10µg/ml) or at a 1:1 ratio in the presence of 1 µg/ml plate-bound anti-CD3 (BioXCell #BE0002) and 2 µg/ml anti-CD28 (BioXCell #BE0015-5). Both CD4$^+$ T cell populations were labelled with cell proliferation dye eFluor®450 before co-culture and the level of proliferation was assessed based on the cell proliferation dye dilution by flow

cytometry. $1 \times 10^6$ CD4$^+$ T cells were used for the co-culture for four days in a 48-well plate or $1 \times 10^5$ T cells in a 96-well plate. After four days the supernatant was used for the analysis of nitric oxide and reactive oxygen species (ROS). Some experiments were performed in the presence of blocking antibodies (Table 3.7). For experiments which examined the effect of NOS, arginase-1 or IDO, 0.5 mM L-NMMA (Merck #399275), 0.5 mM BEC (Santa Cruz Biotechnology #sc-205220) or 0.5 mM 1-MT (Sigma #447439) were added at the beginning of the culture. To investigate if the suppressive effect of PMN-MDSC is contact dependent, PMN-MDSC and CD4$^+$ T cells were separated during the co-culture using the transwell assay (Corning #3381).

**Table 3.7. Blocking antibodies used in PMN-MDSC-T cell co-culture.**

| antibody | clone | dilution | company & catalogue number |
|---|---|---|---|
| LEAF anti-mouse CD274 (PD-L1) | 10F.9G2 | 1:100 | BioLegend #124304 |
| LEAF anti-mouse Galectin 9 | RG9-35 | 1:100 | BioLegend #136106 |
| anti-mouse CD210 (IL-10R) | 1B1.3A | 1:423 | BioXCell #BE0050 |
| LEAF anti-mouse CD40 | HM40-3 | 1:100 | BioLegend # 102907 |
| LEAF anti-mouse CD80 | 16-10A1 | 1:100 | BioLegend # 104710 |
| LEAF anti-mouse CD86 | GL-1 | 1:100 | BioLegend # 105010 |

## 3.23 Nitrite (NO2$^-$) quantification using Griess reagent

In the Griess reaction the nitrites form a diazonium salt with the sulphanilamide. When the azo dye agent (N-alpha-naphthyl-ethylenediamine) is added under acidic conditions a pink colour develops. The nitrite stock solution was prepared by dissolving 69 mg of sodiumnitrite (Sigma-Aldrich #237213-5G) in 100 ml of distilled H2O. The top standard of 10,000 nmol was prepared by diluting the stock solution 1:100 in colourless RPMI (Lonza #BE12-918F). Then a 1:2 dilution series was pipetted with RPMI across the plate. Both standards and unknown samples were pipetted in duplicates in a final volume of 50 µl into a 96 well plate. An equal volume of Griess reagent (Sigma #G4410-10G) containing 0.2% naphthyl-ethylenediamine dihydrochloride, 2% sulphanilamide and 5% phosphoric acid was added to each well and incubated for 10 minutes in the dark at room temperature. The absorbance was read on the SpectraMax 190 plate reader (Molecular Devices) at 540 nm (L1) and 630 nm (L2). After a

subtraction (L1-L2) and a further reduction by the blank value the concentration could be determined by comparison to the standard curve.

### 3.24  ROS quantification using Acridan Lumigen PS-3 assay

Acridan compounds can be oxidized and the oxidation products generate chemiluminescence. Acridan Lumigen PS-3 provided in the Pierce®ECL Plus Western Blotting Substrate (#32134) reacts with $H_2O_2$ and forms acridinium ester intermediates which emit light at 430 nm. To perform the assay 50 µl of supernatant was pipetted into a 96-well plate and 50 µl of PBS was added. Substrate A and Substrate B from the kit were mixed in a ratio of 1:40. 50 µl of this mixture was added to the wells and incubated for 10 minutes in the dark at room temperature. Light intensity was measured at 430 nm using the SpectraMax 190 plate reader.

### 3.25  Immunohistochemistry on paraffin sections with Diaminobenzidine-tetrahydrochloride dehydrate (DAB) (performed at the Center for Brain Research at the Medical University of Vienna)

Organs and tissue were removed and immersion fixed in 4% buffered paraformaldehyde (PFA) for up to one day followed by paraffin embedding (Center for Brain Research at the Medical University of Vienna). Tissue was cut into 5 µm sections and transferred onto a glass slide. The sections were dried overnight at 37°C. The tissue was deparaffinised twice in Xylol (Sigma-Aldrich #95692) for 15 minutes. After washing twice with 96% alcohol endogenous peroxidase was blocked with 0.2% hydrogen peroxide (H2O2) (Merck #1.07210) in methanol (VWR #20847.307). After washing again with 96% alcohol the tissue was rehydrated with descending alcohol concentrations and washed in distilled water. The tissue was pre-treated in a steamer for one hour with either 10 mM citrate buffer  pH 6.0 (Sigma #27488) or EDTA buffer (0.5mM Tris from Applichem #A1379.1000; 0.05mM EDTA from Merck #1.08454) followed by washing four times with Tris-buffered saline (TBS =25 mM TRIS; 150 mM NaCl (Merck #1.06404); 20 mM HCl (Merck #1.09057). Unspecific binding was blocked by incubation with 10% foetal calf serum (FCS) from Lonza #DE14-801F in DAKO buffer (#X0909)

for 15 minutes at room temperature. The primary antibody was diluted in 10% FCS in DAKO buffer and the tissue was incubated overnight in a humidified chamber (anti-mouse CD4 1:250, clone 4SM95, eBioscience #14-9766-80 and anti-mouse GFP 1:5000, Ag Sieghart housemade). The sections were washed with TBS and the biotinylated secondary antibody was diluted in 10% FCS in DAKO buffer and added to the sections for one hour at room temperature (Biotin donkey-anti-rat 1:1500 from Jackson #712-065-153 or Biotin donkey-anti-rabbit 1:2000 from Jackson #711-065-152)). After the slides were rinsed in TBS for three to five times Avidin-Peroxidase (1:100 from Sigma #A3151) in 10% FCS/ DAKO buffer was added and incubated for one hour at room temperature. Before the development with 70 mM 3.3´-Diaminobenzidine-tetrahydrochloride dehydrate (DAB) from Sigma #32750, sections were washed three to five times with TBS. To make sure that the slides were optimally developed they were from time to time examined with a light microscope. The reaction was stopped with water and counterstain with haematoxylin (Merck #1.09249) for 20 sec was performed. After flushing with tap water the slides were differentiated in HCl-ethanol for a few seconds and blued in Scott's solution. The sections were dehydrated with ascending alcohol concentrations and butyl acetate (Sigma #45860) and finally covered with mounting medium (Eukitt® from Sigma-Aldrich #03989) and a coverslip.

## 3.26  Immunohistochemistry on paraffin sections with Fast Blue (performed at the Center for Brain Research at the Medical University of Vienna)

Sections were deparaffinised twice in Xylol (Sigma-Aldrich #95692) for 15 minutes. After washing twice with 96% alcohol the tissue was rehydrated with descending alcohol concentrations and washed in distilled water. The tissue was pre-treated in a steamer for one hour with EDTA buffer (0.5mM Tris from Applichem #A1379.1000; 0.05mM EDTA from Merck #1.08454) followed by washing 4 times with Tris-buffered saline (TBS =25 mM TRIS; 150 mM NaCl (Merck #1.06404); 20 mM HCl (Merck #1.09057). Unspecific binding was blocked by incubation with 10% foetal calf serum (FCS) from Lonza #DE14-801F in DAKO buffer (#X0909) for 20 minutes at room temperature. The primary antibody was diluted in 10% FCS in DAKO buffer and the tissue was incubated overnight in a humidified chamber (anti-mouse GFP 1:5000, Ag Sieghart housemade). The sections were washed with TBS and

the secondary antibody conjugated to alkaline phosphatase was diluted in 10% FCS in DAKO buffer and added to the sections for one hour at room temperature (alkaline phosphatase donkey-anti-rabbit 1:200 from Jackson #711-055-152). After the slides were rinsed in TBS for three to five times they were developed with Fast Blue (0.1 M Tris-HCl-buffer pH 8.5, 1.5 mM Levamisole (Sigma #L9756), 0.025% $NaNO_2$, 336 mM Naphtol AS-Mx phosphate (Sigma # N4875), 0.6 mM Fast Blue BB salt (Sigma #F3378),12.5 mM HCl, 1:160 dimethylformamide (Sigma #40250). To make sure that the slides were optimally developed they were from time to time examined with a light microscope. The reaction was stopped with water and the slides mounted with aqueous mounting medium (Aquatex® from Merck #1.08562.0050)

### 3.27 Double staining on paraffin sections with Fast Blue and DAB (performed at the Center for Brain Research at the Medical University of Vienna)

First GFP Fast Blue staining was performed and the slides were then directly treated for 45 minutes in a steamer with EDTA buffer pH 9. After that the CD4 DAB staining was performed.

### 3.28 Escalating dose immunotherapy (EDI)

For immunotherapeutic tolerance induction, mice were treated subcutaneously (s.c.) every three to four days with 200 µl of $MBP_{Ac1-9}$(4Y) in PBS, the high affinity analogue of $MBP_{Ac1-9}$, in an escalating dose regime: 0.08 µg, 0.8 µg, 8 µg, 80 µg, 80 µg, 80 µg. Two hours after the last dose animals were perfused with PBS, organs isolated and single cell suspension prepared. Cells were analysed by flow cytometry.

### 3.29 *In vivo* antigen challenge

Complete Freund's adjuvant (CFA) (Difco #263810) was supplemented with 8 mg/ml Mycobacterium Tuberculosis H37Ra (Difco #231141). A 1:1 emulsion of neuroantigen (4 mg/ml $MBP_{Ac1-9}$, $MBP_{Ac1-20}$ or $MOG_{35-55}$) and CFA was made and sonicated for 20 minutes. The emulsion was further mixed on ice using an 18G blunt fill needle (BD Bioscience #305180) attached to a 1-ml syringe (Terumo #SS+01T1). After drawing the emulsion into

the 1-ml syringe, the 18G needle was replaced with a 25G needle for immunization. Antigen challenge was performed by s.c. injection of 100 µl of the sonicated emulsion at the base of the tail. After 10 days spleen and lymph nodes were harvested and a $^3$H thymidine proliferation assay was set up. In some experiments splenic PMN-MDSCs (1.5 x 10$^6$ in 200 µl PBS) were transferred intraperitoneally (i.p.) three days before the Ag challenge.

### 3.30  $^3$H-Thymidine proliferation assay

For $^3$H-Thymidine proliferation assays, 1 x 10$^6$ whole splenocytes or 2 x 10$^5$ whole lymph node cells in 200 µl were cultured, in triplicate, in a titration of MBP$_{Ac1-9}$[4K] concentrations in a 96-well round bottom plate (Costar #3799). Cells were cultured for three days at 37°C in a $CO_2$ incubator and 0.5 µCi of $^3$H-Thymidine was then added to wells for 16 h before measurement with a 1450 Micro-β counter (Wallac).

### 3.31  Active induction of EAE with Peptide

The neuroantigen CFA emulsion was prepared as described above. Disease was induced by s.c. injection of 100 µl of the sonicated emulsion at the base of the tail. On days zero and two, 200 ng of Pertussis toxin (Sigma Aldrich #P2980) was administered i.p. in 0.5 ml of PBS. EAE was assessed every 12 hours for up to 30 days using the following scoring system: 0, no signs; 1, flaccid tail; 2; impaired righting reflex and/or partial hind limb paralysis; 3, hind limb paralysis; 4, forelimb and hind limb paralysis; 5, moribund. Mice with disease grade two or above were given easy access to mashed-up, hydrated food pellets and water. Mice with a disease score of three or higher were checked three times daily. Mice with a confirmed grade four disease or grade five were culled humanely by cervical dislocation.

### 3.32 Splenectomy in the mouse

For analgesic treatment Acetaminophen was provided in the drinking water (at least 24 hours in advance of surgical procedure) and 100 µg Carprofen (Pfizer 50 mg/ml) per mouse was subcutaneous administered as well. The analgesic treatment was continued on the day of surgery and one day after the operation. Mice were anaesthetised in a chamber with an isoflurane vaporizer that provides anaesthesia, suitable for minor surgical procedures. The isoflurane was mixed with oxygen at a flow rate of 1.5 L/m. The vaporizer output percentage was set to 2.5%. Once the anaesthetic had induced unconsciousness, the mouse was transferred to a nose cone, shaved and placed onto the heated and sterile operation area. The anaesthetic effect was verified by checking the plantar reflex. Anaesthetised mice were positioned on their side onto sterile drape and 2% chlorhexidine digluconate (Alfa Aesar #41385) was used to disinfect the skin. The mouse was covered with a sterile drape and a small incision (10-15mm) was made with a scalpel above the left kidney. The spleen was identified and carefully manipulated through the incision to sit outside the mouse. The splenic arteries and venous supply were then carefully cauterised (F.S.T. #18010-00), thus effectively removing the spleen. The abdominal muscle wall was then closed using a 4-0 synthetic absorbable suture (Ethicon #W9443). The skin incision was closed using 4-0 silk sutures (Ethicon #W501H). Once awake and mobile, they were returned to their regular caging and holding room. Animals were observed daily for the first seven days. Non-absorbable skin sutures were removed at day seven after surgery.

### 3.33 Statistical analysis

The results from FACS experiments are mostly displayed in percentages. To perform statistical tests on percentages it is necessary to perform a data transformation and arcsine transformation is appropriate for data on proportions. The distribution of percentages is binomial and arcsine transformation of data makes the distribution normal. Normality tests were chosen to test if the data set was well-modelled by a normal distribution or not. To test for normality the Shapiro-Wilk test was chosen because this test can be applied to sample sizes smaller than 20 (Shapiro, SS, Wilk, MB (1965) An analysis of variance test for normality (complete samples). *Biometrika* 52 (3–4): 591–611). If the test resulted in a p-value greater than 0.05, it was

assumed that the data were normal distributed. Hence, the Student's t-test for pairwise comparison or one-way analysis of variance (ANOVA) with Sidak's post hoc test was used for the comparison of more than two groups (190). Otherwise the nonparametric equivalents of the t-test the Mann-Whitney U test or the nonparametric equivalent of ANOVA the Kruskal-Wallice with Dunn's post hoc test was used. For sample sizes of three, a nonparametric test was always chosen for comparison.

# 4   RESULTS

## 4.1   Spatiotemporal distribution of tolerised CD4+ T cells in secondary lymphoid organs and non-lymphoid tissues during the course of tolerisation

### 4.1.1   Reduced frequency of CD4+ T cells after tolerisation

Tg4$^{\text{IL-10/GFP}}$ mice, which express the green fluorescent protein in cells that produce IL-10, were treated with MBP$_{\text{Ac1-9}}$(4Y) peptide or with PBS only as a control. Two hours after each dose animals were perfused with PBS and organs were isolated. After gating on viable single CD4+ T cells, various markers associated with T cell tolerance were investigated during the course of escalating dose immunotherapy. Figure 4.1 **A** shows the general gating strategy and representative FACS density plots for each stain on splenocytes from animals that had received 6 doses of MBP$_{\text{Ac1-9}}$(4Y)-EDI (Figure 4.1. B, C, D).
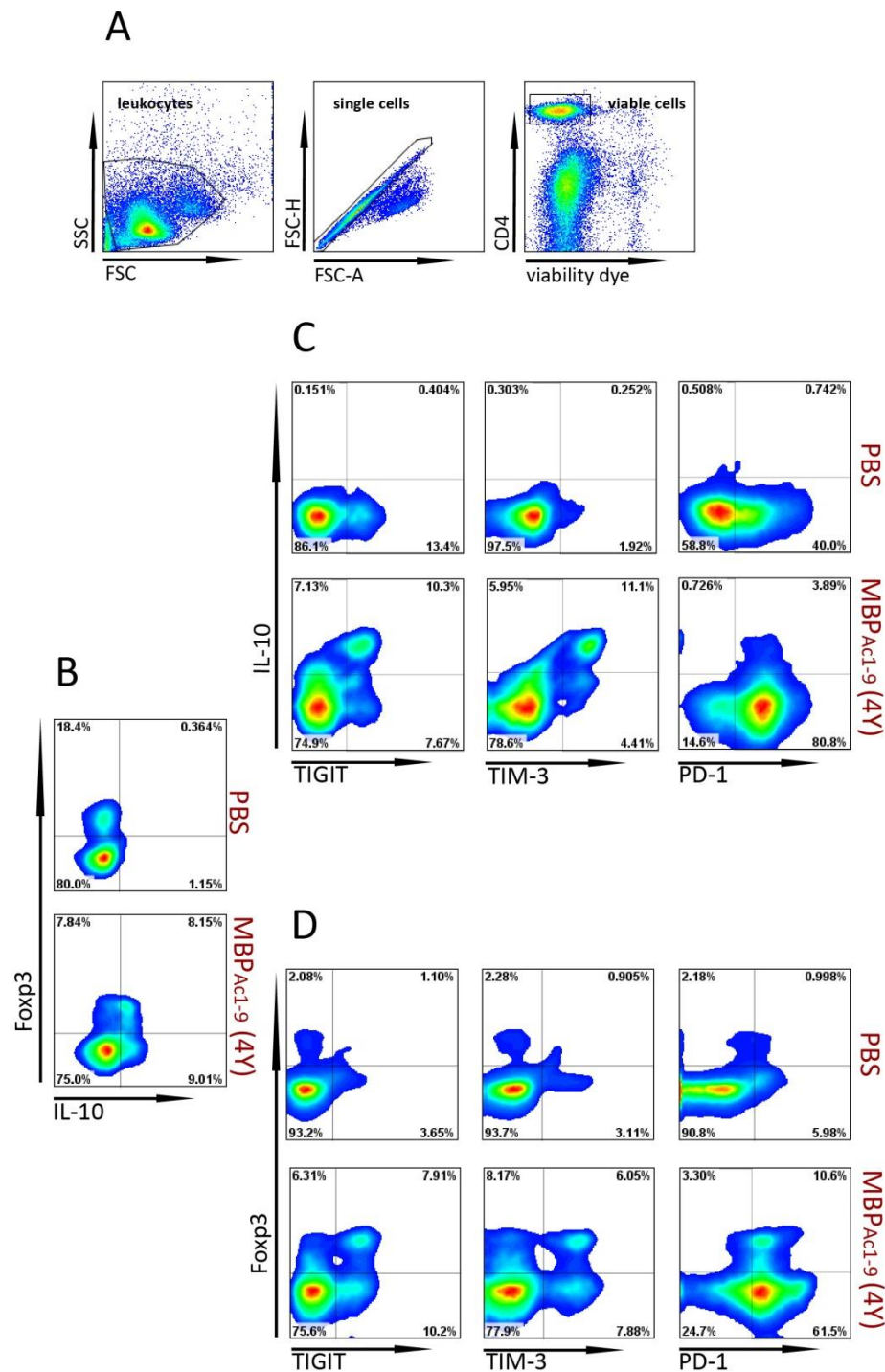
**Figure 4.1. FACS staining of tolerised CD4$^+$ T cells. A)** Gating strategy for CD4$^+$ T cells. Shown are representative FACS density plots from one out of six individuals from the spleen of TG4$^{IL-10/GFP}$ mice treated with control PBS or MBP$_{Ac1-9}$(4Y)-EDI, each receiving 6 doses, gated on single, viable CD4$^+$ T cells. **B)** Foxp3 and IL-10 staining for splenic CD4$^+$ T cells in PBS and MBP$_{Ac1-9}$(4Y)-treated animals **C)** GFP staining in combination with TIGIT, TIM-3 and PD-1 for splenic CD4$^+$ T cells in PBS and MBP$_{Ac1-9}$(4Y)-treated animals **D)** Foxp3 staining in combination with TIGIT, TIM-3 and PD-1 for splenic CD4$^+$ T cells in PBS and MBP$_{Ac1-9}$(4Y)-treated animals.

During the course of tolerisation we noticed a significant decrease in the percentage of CD4$^+$ T cells after the 3$^{rd}$ and 5$^{th}$ doses (Figure 4.2.). In the spleen, only ~10% of splenocytes were CD4$^+$ T cells after MBP$_{Ac1-9}$(4Y)-treatment (p ≤ 0.05), compared to PBS-treated animals. In the inguinal lymph nodes (ILNs) ~60% of cells were CD4$^+$ T cells in the control animals, whereas MBP$_{Ac1-9}$(4Y)-treatment decreased this to ~30%. The same trend was apparent in the mediastinal lymph nodes (lung draining lymph nodes) (MLNs) after the 3$^{rd}$ and 5$^{th}$ dose of MBP$_{Ac1-9}$(4Y)-treatment. Here, we saw a two-fold decrease of CD4$^+$ T cells in the peptide treated animals compared to PBS-treated animals (p ≤0.01). In the lung we observed a small but significant decrease only after the 5$^{th}$ dose of EDI, with around 7% CD4$^+$ T cells on average in MBP$_{Ac1-9}$(4Y)-treated individuals compared to control animals that contained around 9% CD4$^+$ T cells on average (p ≤ 0.05). The brachial lymph nodes (BLNs), liver, brain and spinal cord were only assessed after the 1$^{st}$, 3$^{rd}$ and 5$^{th}$ treatment. The BLNs of MBP$_{Ac1-9}$(4Y)-treated animals showed a significant reduction in the percentage of CD4$^+$ T cells with ~25% CD4$^+$ T cells after the 3rd and 5th dose, compared to PBS treated animals with ~60% CD4$^+$ T cells at both stages (p ≤ 0.0001). In the liver, we again found the same trend with 20% of CD4$^+$ T cells on average in the 3$^{rd}$ dose and 5$^{th}$ dose of MBP$_{Ac1-9}$(4Y)-treatment (p ≤ 0.05), compared to PBS-treated animals with ~45% CD4$^+$ T cell in their livers. In the CNS compartment we did not detect a significant difference as a result of peptide treatment compared to PBS-treated animals.

**Figure 4.2. Distribution of CD4$^+$ T cells during the course of tolerisation.** Tg4$^{IL-10/GFP}$ mice were treated with PBS or MBP$_{Ac1-9}$(4Y)-EDI. Two hours after the indicated dose, animals were perfused with PBS and organs were isolated. Horizontal lines indicate the mean. After the check for normality using the Shapiro-Wilk test either ANOVA followed by Sidak's multiple comparison test was performed for normally distributed data or the Kruskal-Wallice test followed by Dunn's multiple comparison test for data that were not normally distributed (* =

p ≤ 0.05, ** = p ≤ 0.01, *** = p ≤ 0.001, **** = p ≤ 0.0001). In the spleen, ILNs, MLNs, lung and BLNs each dot represents one individual. In the liver in some cases cells from two animals were combined due to low cell numbers while in the CNS compartment each dot represents two animals. Kruskal-Wallice test followed by Dunn's multiple comparison test was applied to spleen, lung, liver, brain and spinal cord data. ANOVA followed by Sidak's multiple comparison test was applied to ILN, MLN and BLN data. N=6-11, from two independent experiments.

## 4.1.2 Expression of co-inhibitory molecules after tolerisation

### 4.1.2.1 Increased frequency of CD4$^+$ TIM-3$^+$ cells after tolerisation

To establish how EDI peptide immunotherapy affects the phenotype of CD4$^+$ T cells, we examined the expression of co-inhibitory molecules. TIM-3 expression on CD4$^+$ T cells in the spleen increased in MBP$_{Ac1-9}$(4Y)-treated animals, most notably between the 3$^{rd}$ and 6$^{th}$ dose (Figure 4.3.). In the spleen, TIM-3 expression was induced in approximately ~10% of CD4$^+$ T cells which represents a statistically significant difference after the 3$^{rd}$ (p ≤0.01) and 5$^{th}$ dose of MBP$_{Ac1-9}$(4Y)-treatment (p ≤ 0.001) compared to PBS-treated animals. TIM-3 expression on CD4$^+$ T cells in the ILNs is on average 5-7% in MBP$_{Ac1-9}$(4Y)-treated animals after the 3$^{rd}$, 5$^{th}$ and 6$^{th}$ dose which represented a significant difference compared to PBS-treated animals (p ≤ 0.0001) (Figure 4.3.). Tim3$^+$ expression on CD4$^+$ T cells reached similar levels in the MLNs, with statistical significance after the 5$^{th}$ (p ≤ 0.001) and 6$^{th}$ dose (p ≤ 0.01).The BLNs, liver, brain and spinal cord were only assessed after the 1$^{st}$, 3$^{rd}$ and 5$^{th}$ treatment. CD4$^+$ T cells isolated from the BLNs significantly upregulated TIM-3 expression with ~5% after the 3$^{rd}$ and 5$^{th}$ doses compared to PBS-treated animals (both p ≤ 0.0001). Interestingly, CD4$^+$ T cells in the lungs, liver and brain of tolerised mice expressed TIM-3 at much higher levels than in the spleen or lymph nodes. In the lung, TIM-3 expression reached up to ~67% after the 6$^{th}$ dose (p ≤ 0.0001) compared to PBS-treated animals. In the liver we observed the same trend of TIM3 expression on CD4$^+$ T cells with a peak of ~22% after the 3$^{rd}$ dose (p ≤ 0.01). In the brain we observed a vast increase of CD4$^+$ TIM-3$^+$ T cells in tolerised animals after the 5$^{th}$ dose of MBP$_{Ac1-9}$(4Y)-treatment (p ≤ 0.05). However, in the spinal cord a significant difference resulting from peptide treatment could not be detected, possibly due to variance in results and a limited number of samples.

**Figure 4.3. TIM-3 expression on CD4$^+$ T cells during the course of tolerisation.** Tg4$^{IL-10/GFP}$ mice were treated with PBS or MBP$_{Ac1-9}$(4Y)-EDI. Two hours after the indicated dose animals were perfused with PBS and organs were isolated. After gating on viable, single CD4$^+$ T cells the marker TIM-3 was investigated during the course of escalating dose immunotherapy. Horizontal lines indicate the mean. After checking for normality using the Shapiro-Wilk test either ANOVA followed by Sidak's multiple comparison test was performed for normally

distributed data or the Kruskal-Wallice test followed by Dunn's multiple comparison test for data that were not normally distributed (* = p ≤ 0.05, ** = p ≤ 0.01, *** = p ≤ 0.001, **** = p ≤ 0.0001). In the spleen, ILNs, MLNs, lung and BLNs each dot represents one individual. In the liver in some cases cells from two animals were combined due to low cell numbers while in the CNS compartment each dot represents two animals. Kruskal-Wallice test followed by Dunn's multiple comparison test was applied to liver, brain and spinal cord data. ANOVA followed by Sidak's multiple comparison test was applied to spleen, ILN, MLN, lung and BLN data. N=6-11, from two independent experiments.

### 4.1.2.2  Increased frequency of CD4$^+$ TIGIT$^+$ cells after tolerisation

Similar to TIM-3, TIGIT expression was found to be increased during the course of peptide immunotherapy. In the spleen, TIGIT expression on CD4$^+$ T cells (up to 12% on average) reached statistically significant differences after the 3$^{rd}$ and 5$^{th}$ doses of MBP$_{Ac1-9}$(4Y)-treatment compared to PBS-treated animals (Figure 4.4). In the lymph nodes, TIGIT expression on CD4$^+$ T cells increased significantly with 5-8% on average in MBP$_{Ac1-9}$(4Y)-treated animals compared to PBS-treated animals (Figure 4.4.). Just as observed for TIM-3, TIGIT expression on CD4$^+$ T cells in the lung and liver was found to be much higher than in the lymphoid organs, with up to ~45% in the lung after the 5$^{th}$ and 6$^{th}$ dose (both p ≤ 0.001) and around 25% in the liver after the 3$^{rd}$ and 5$^{th}$ doses (both p ≤ 0.05) of EDI treatment compared to PBS-treated animals. The BLNs, liver, brain and spinal cord were only assessed after the 1$^{st}$, 3$^{rd}$ and 5$^{th}$ treatment. CD4$^+$ T cells isolated from the BLNs significantly upregulated TIGIT expression with ~8% after the 3$^{rd}$ dose of MBP$_{Ac1-9}$(4Y) (p ≤ 0.0001) compared to PBS-treated animals. In the CNS compartment we did not detect a statistically significant difference after peptide treatment although we did observe a two-fold increase of the mean of CD4$^+$ TIGIT$^+$ in the brain after the 5$^{th}$ dose of MBP$_{Ac1-9}$(4Y)-treatment compared to PBS-treated animals.
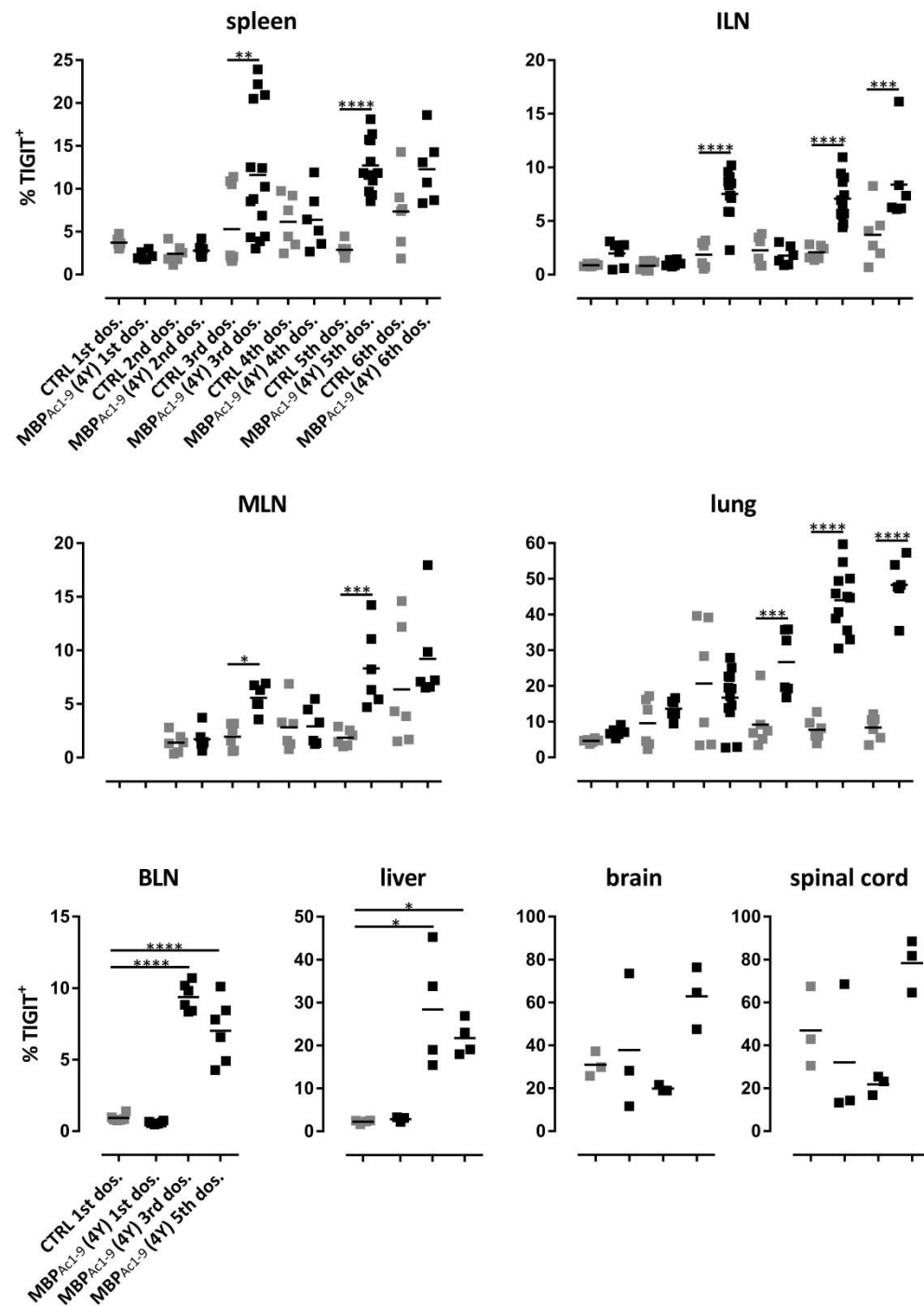
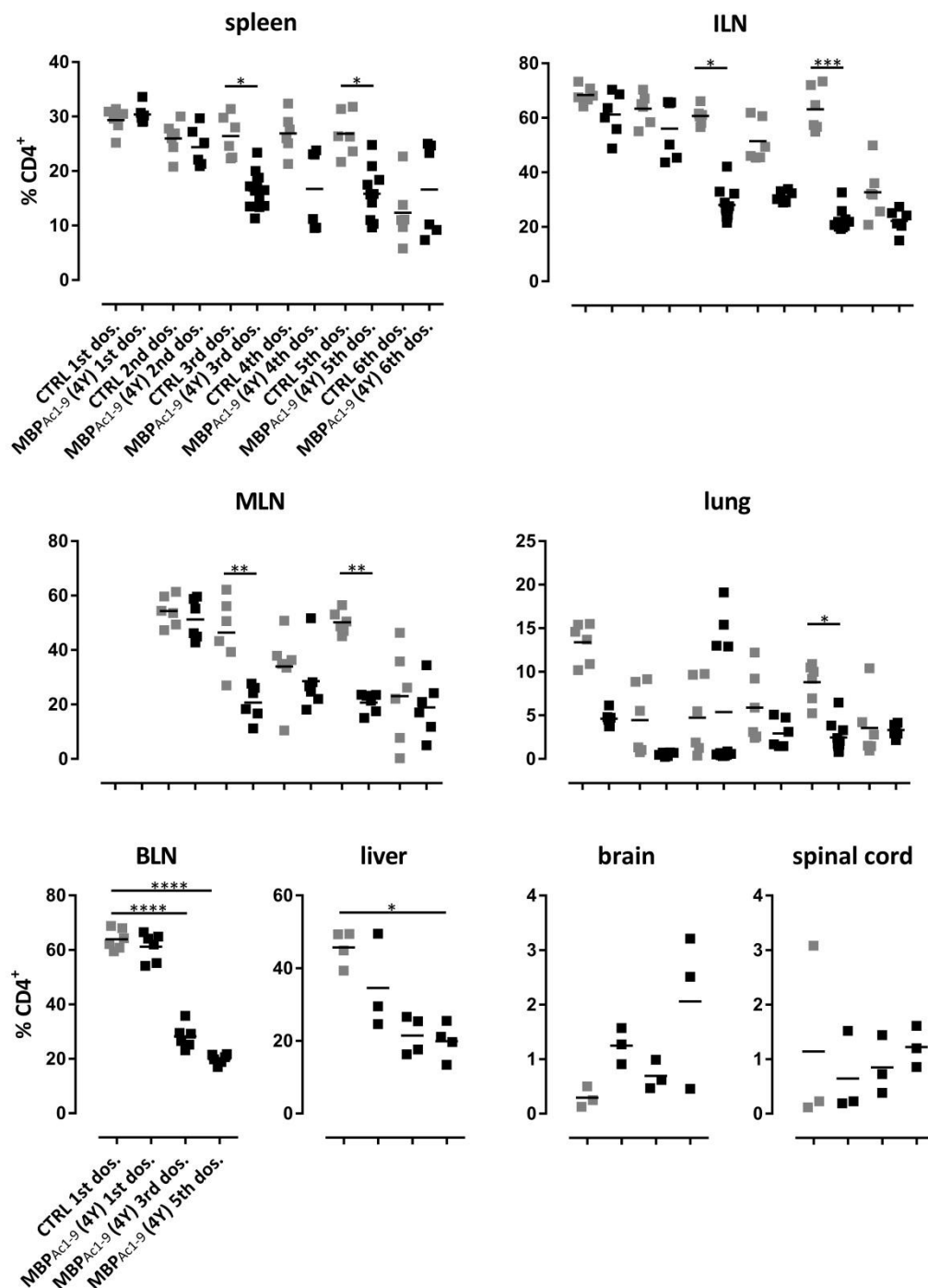**Figure 4.4. TIGIT expression on CD4+ T cells during the course of tolerisation.** Tg4[IL-10/GFP] mice were treated with PBS or MBP$_{Ac1-9}$(4Y)-EDI. Two hours after the indicated dose animals were perfused with PBS and organs were isolated. After gating on viable, single CD4+ T cells, TIGIT expression was investigated during the course of escalating dose immunotherapy. Horizontal lines indicate the mean. After checking for normality using the Shapiro-Wilk test either ANOVA followed by Sidak's multiple comparison test was performed for normally

distributed data or the Kruskal-Wallice test followed by Dunn's multiple comparison test for data that were not normally distributed (* = p ≤ 0.05, ** = p ≤ 0.01, *** = p ≤ 0.001, **** = p ≤ 0.0001). In the spleen, ILNs, MLNs, lung and BLNs each dot represents one individual. In the liver in some cases cells from two animals were combined due to low cell numbers while in the CNS compartment each dot represents two animals. Kruskal-Wallice test followed by Dunn's multiple comparison test was applied to liver, brain and spinal cord data. ANOVA followed by Sidak's multiple comparison test was applied to spleen, ILN, MLN, lung and BLN data. N=6-11, from two independent experiments.

### 4.1.2.3   Increased frequency of CD4$^+$ PD-1$^+$ cells after tolerisation

PD-1 was the third co-inhibitory molecule associated with T cell tolerance of which we examined the expression on CD4$^+$ T cells throughout the body after tolerance induction. Similar to TIM-3 and TIGIT, PD-1 expression was found to be increased during the course of peptide immunotherapy. In the spleen, PD-1 expression on CD4$^+$ T cells of MBP$_{Ac1-9}$(4Y)-treated animals was much higher than found for TIM-3 and TIGIT. PD1 expression reached its peak with ~80% after the 4$^{th}$ dose of EDI (p ≤0.01) compared to PBS-treated animals (Figure 4.5.). A similarly high expression of PD-1 was found in the lymph nodes, with highest mean expression of ~75% after the 4$^{th}$ dose (p ≤ 0.05) in the ILNs and MLNs and ~50% in the BLNs after the 5$^{th}$ dose (p ≤ 0.0001) compared to PBS-treated animals. PD-1 expression on CD4$^+$ T cells in the lung was similarly high with ~80% after the 4$^{th}$ dose (p ≤ 0.05) compared to control animals. In the liver we again observed a major increase of PD-1 expression on CD4$^+$ T cells of tolerised animals with ~80% after the 5$^{th}$ dose (p ≤ 0.01). In the brain PD-1 expression increased significantly with ~60% (p ≤ 0.05), but in the spinal cord a significant difference due to peptide treatment again could not be concluded due to the variance of the results.
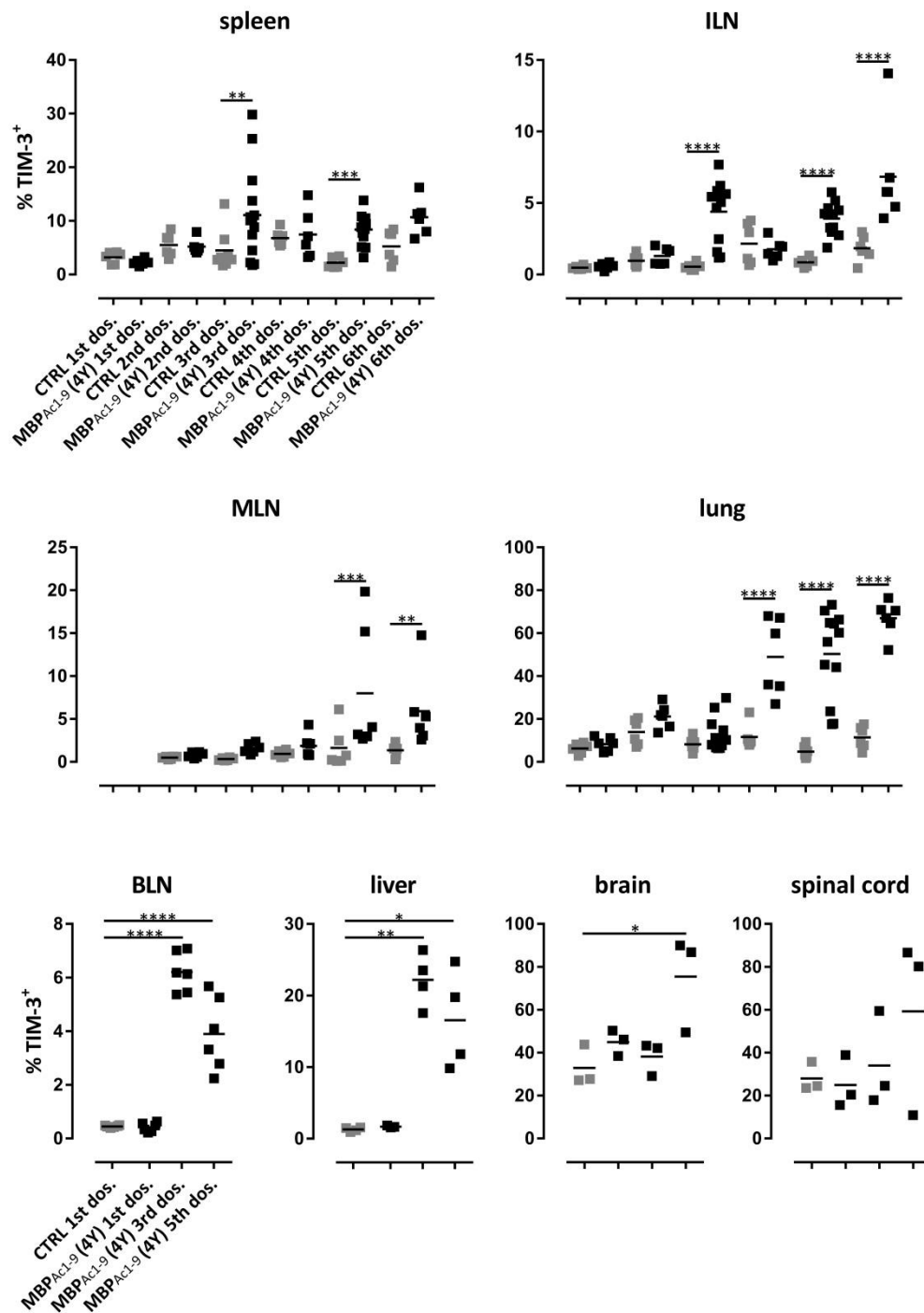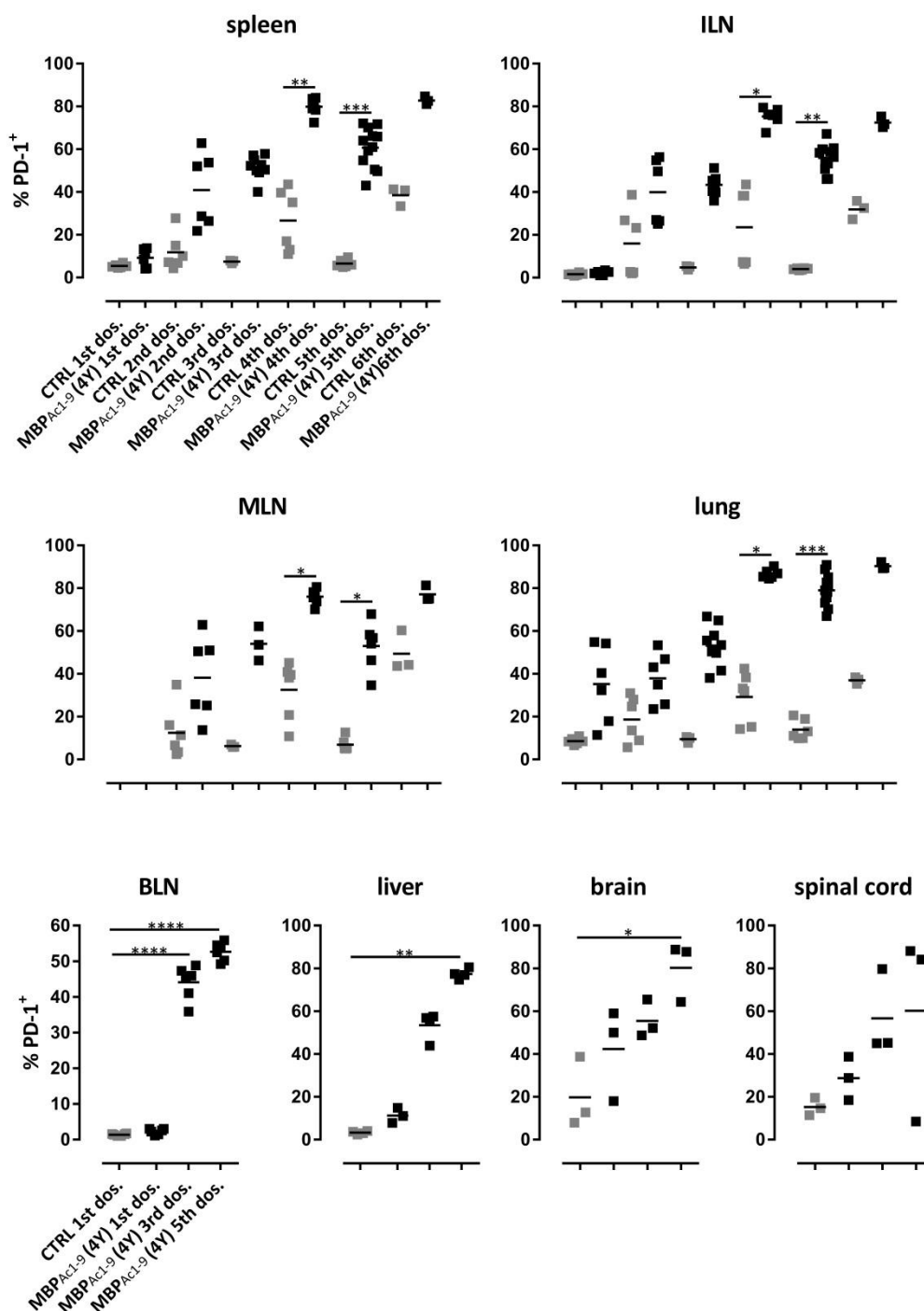
**Figure 4.5. PD-1 expression on CD4+ T cells during the course of tolerisation.** Tg4[IL-10/GFP] mice were treated with PBS or MBP$_{Ac1-9}$(4Y)-EDI. Two hours after the indicated dose animals were perfused with PBS and organs were isolated. After gating on viable, single CD4+ T cells, PD-1 expression was investigated by flow cytometry during the course of escalating dose immunotherapy. Horizontal lines indicate the mean. After checking for normality using the Shapiro-Wilk test either ANOVA followed by Sidak's multiple comparison test was performed

for normally distributed data or the Kruskal-Wallice test followed by Dunn's multiple comparison test for data that were not normally distributed (* = p ≤ 0.05, ** = p ≤ 0.01, *** = p ≤ 0.001, **** = p ≤ 0.0001). In the spleen, ILNs, MLNs, lung and BLNs each dot represents one individual. In the liver in some cases cells from two animals were combined due to low cell numbers while in the CNS compartment each dot represents two animals. Kruskal-Wallice test followed by Dunn's multiple comparison test was applied to liver, brain and spinal cord data. ANOVA followed by Sidak's multiple comparison test was applied to spleen, ILN, MLN, lung and BLN data. N=6-11, from two independent experiments.

### 4.1.3    Changes in Foxp3 expression after MBP$_{Ac1-9}$(4Y)-treatment

In addition to the co-inhibitory molecules described above, we examined the levels of expression of the transcription factor Foxp3, the signature molecule of Treg cells, during the course of EDI because Treg cells are known to play a pivotal role in the maintenance of immune tolerance. The dynamics of CD4$^+$ Foxp3$^+$ regulatory T cells revealed an increase from less than ~5% pre-treatment to ~12% (p ≤ 0.01) in MBP$_{Ac1-9}$(4Y)-treated animals after the 3$^{rd}$ treatment in the spleen (Figure 4.6.). In the lymph nodes, the MBP$_{Ac1-9}$(4Y)-treatment revealed significantly upregulated percentages of CD4$^+$ Foxp3$^+$ T cells to similar levels after the 3$^{rd}$ and 5$^{th}$ dose compared to control animals. In the liver, we observed the same trend of CD4$^+$ Foxp3$^+$ cells with around 15% on average after the 3$^{rd}$ dose (p ≤ 0.05).  On average 30% Foxp3$^+$ T cells were found in the lung of MBP$_{Ac1-9}$(4Y)-treated animals after the 5$^{th}$ dose of treatment but this did not reach statistical significance due to variance. Most notably, in the brain we observed a major increase in the percentage of CD4$^+$ Foxp3$^+$ T cells, up to 50%, after the 5$^{th}$ dose of treatment although this was not statistically significant due to low sample number and variance. Finally, in the spinal cord a significant difference in the percentage of CD4$^+$ Foxp3$^+$ T cells post peptide treatment could be detected as we identified a more than three-fold increase of CD4$^+$ Foxp3$^+$ T cells in the MBP$_{Ac1-9}$(4Y)-group (p ≤ 0.01) compared to PBS-treated animals.

**Figure 4.6. Distribution of CD4+ Foxp3+ regulatory T cells during the course of tolerisation.**
Tg4[IL-10/GFP] mice were treated with PBS or MBP$_{Ac1-9}$(4Y)-EDI. Two hours after the indicated dose animals were perfused with PBS and organs were isolated. After gating on viable, single CD4+ T cells the transcription factor Foxp3 was investigated by flow cytometry during the course of escalating dose immunotherapy. Horizontal lines indicate the mean. After checking for normality using the Shapiro-Wilk test either ANOVA followed by Sidak's multiple

comparison test was performed for normally distributed data or the Kruskal-Wallice test followed by Dunn's multiple comparison test for data that were not normally distributed. (* = p ≤ 0.05, ** = p ≤ 0.01, *** = p ≤ 0.001, **** = p ≤ 0.0001). In the spleen, ILNs, MLNs, lung and BLNs each dot represents one individual. In the liver in some cases cells from two animals were combined due to low cell numbers while in the CNS compartment each dot represents two animals. Kruskal-Wallice test followed by Dunn's multiple comparison test was applied to liver, brain and spinal cord data. ANOVA followed by Sidak's multiple comparison test was applied to spleen, ILN, MLN, lung and BLN data. N=6-11, from two independent experiments.

### 4.1.3.1   Increased frequency of CD4$^+$ Foxp3$^+$ TIM-3$^+$ T cells during dose escalation

After detection of the increase in both co-inhibitory molecules and Foxp3 expression, the question arose as to which population of CD4$^+$ cells expressed both Foxp3 and any of the co-inhibitory molecules analysed. This analysis of co-expression was performed only after the 1$^{st}$, 3$^{rd}$ and 5$^{th}$ dose and not after every dose as in the examination of each individual molecule. In the spleen, up to ~5% CD4$^+$ T cells were Foxp3$^+$ TIM-3$^+$ after the 5$^{th}$ dose (p ≤ 0.0001) (Figure 4.7.). In the lymph nodes Foxp3$^+$ TIM3$^+$ T cells represented around 2 - 3% of CD4$^+$ T cells after MBP$_{Ac1-9}$(4Y)-treatment (p ≤ 0.0001). The percentage of Foxp3$^+$ TIM-3$^+$ cells increased dramatically after the 5$^{th}$ dose in the lung, reaching an average of 30% (p ≤ 0.0001). Differences in the percentage of CD4$^+$ T cells that were Foxp3$^+$ TIM-3$^+$ in liver and the CNS compartment did not reach statistical significance compared to PBS-treated mice.

**Figure 4.7. Distribution of CD4$^+$ Foxp3$^+$ TIM-3$^+$ T cells during the course of tolerisation.** Tg4$^{IL-10/GFP}$ mice were treated with PBS or MBP$_{Ac1-9}$(4Y)-EDI. Two hours after the indicated dose animals were perfused with PBS and organs were isolated. After gating on viable, single CD4$^+$ T cells Foxp3$^+$ TIM-3$^+$ T cells were investigated during the course of escalating dose immunotherapy. Horizontal lines indicate the mean. After checking for normality using the Shapiro-Wilk test either ANOVA followed by Sidak's multiple comparison test was performed for normally distributed data or the Kruskal-Wallice test followed by Dunn's multiple comparison test for data that were not normally distributed (* = p ≤ 0.05, ** = p ≤ 0.01, *** = p ≤ 0.001, **** = p ≤ 0.0001). In the spleen, ILNs, MLNs, lung and BLNs each dot represents one individual. In the liver, in some cases cells from two animals were combined due to low cell numbers while in the CNS compartment each dot represents two individuals. Kruskal-Wallice test followed by Dunn's multiple comparison test was applied to liver, brain and spinal cord data. ANOVA followed by Sidak's multiple comparison test was applied to spleen, ILN, MLN, lung and BLN data. N=6, from two independent experiments.

### 4.1.3.2 Increased frequency of CD4$^+$ Foxp3$^+$ TIGIT$^+$ T cells after tolerisation

CD4$^+$ Foxp3$^+$ TIGIT$^+$ T cells were significantly increased in the spleen and lymph nodes after the 3$^{rd}$ and 5$^{th}$ doses and in the lung after the 5$^{th}$ dose of MBP$_{Ac1-9}$(4Y)-treated animals when compared to PBS-treated animals (Figure 4.8.). In the spleen, CD4$^+$ Foxp3$^+$ TIGIT$^+$ T cells increased from ~3% after the 3$^{rd}$ dose to ~6% after the 5$^{th}$ dose (both p ≤ 0.0001). Lymph

node CD4$^+$ Foxp3$^+$ TIM3$^+$ T cells represented around 2.5% of CD4$^+$ T cells after both the 3$^{rd}$ and 5$^{th}$ doses of MBP$_{Ac1-9}$(4Y). CD4$^+$ Foxp3$^+$ TIGIT$^+$ T cells in the lung reached a statistically significant difference compared to the PBS control group after the 5$^{th}$ dose with ~30% (p ≤ 0.0001). We could not detect a significant difference as a result of peptide treatment in the percentage of Foxp3$^+$ TIGIT$^+$ T cells in the liver and the CNS compartment compared to PBS-treated mice.
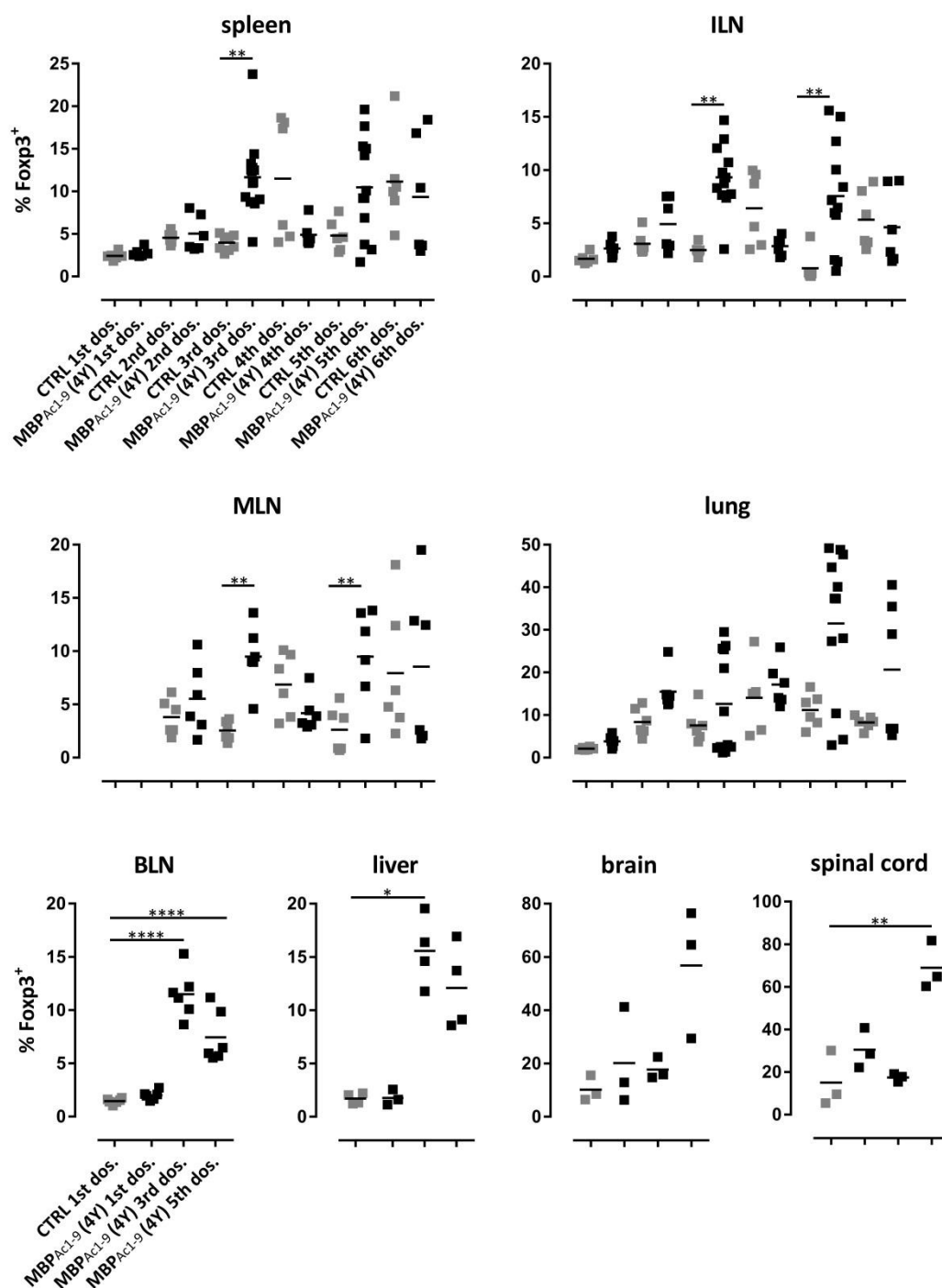


**Figure 4.8. Distribution of CD4$^+$ Foxp3$^+$ TIGIT$^+$ T cells during the course of tolerisation.** Tg4$^{IL-10/GFP}$ mice were treated with PBS or MBP$_{Ac1-9}$(4Y)-EDI. Two hours after the indicated dose animals were perfused with PBS and organs were isolated. After gating on viable, single CD4$^+$ T cells, Foxp3$^+$ TIGIT$^+$ T cells were investigated by flow cytometry during the course of escalating dose immunotherapy. Horizontal lines indicate the mean. After checking for normality using the Shapiro-Wilk test either ANOVA followed by Sidak's multiple comparison test was performed for normally distributed data or the Kruskal-Wallice test followed by Dunn's multiple comparison test for data that were not normally distributed (* = p ≤ 0.05, ** = p ≤ 0.01, *** = p ≤ 0.001, **** = p ≤ 0.0001). In the spleen, ILNs, MLNs, lung and BLNs each dot represents one individual. In the liver, in some cases cells from two animals were combined due to low cell numbers while in the CNS compartment each dot represents two individuals. Kruskal-Wallice test followed by Dunn's multiple comparison test was applied to

liver, brain and spinal cord data. ANOVA followed by Sidak's multiple comparison test was applied to spleen, ILN, MLN, lung and BLN data. N=6, from two independent experiments.

### 4.1.3.3  Increased frequency of CD4+ Foxp3+ PD-1+ T cells during EDI

The percentage of CD4+ Foxp3+ PD-1+ T cells was significantly upregulated in the spleen and lymph nodes after the 3rd and 5th dose and in the lung or liver after the 5th dose of MBP$_{Ac1-9}$(4Y)-treatment compared to PBS-treated animals (Figure 4.9.). Both in the spleen and lymph nodes the percentage reached ~5-8%, but CD4+ Foxp3+ PD1+ T cells in the lung reached ~35% after the 5th dose (p ≤ 0.0001). Hepatic CD4+ Foxp3+ PD-1+ T cells showed a significant increase up to ~10% after the 5th dose of MBP$_{Ac1-9}$(4Y)-treatment (p ≤ 0.05). We could not detect a significant difference as a result of peptide treatment in the percentage of CD4+ Foxp3+ PD-1+ T cells in the CNS compartment compared to PBS-treated mice.
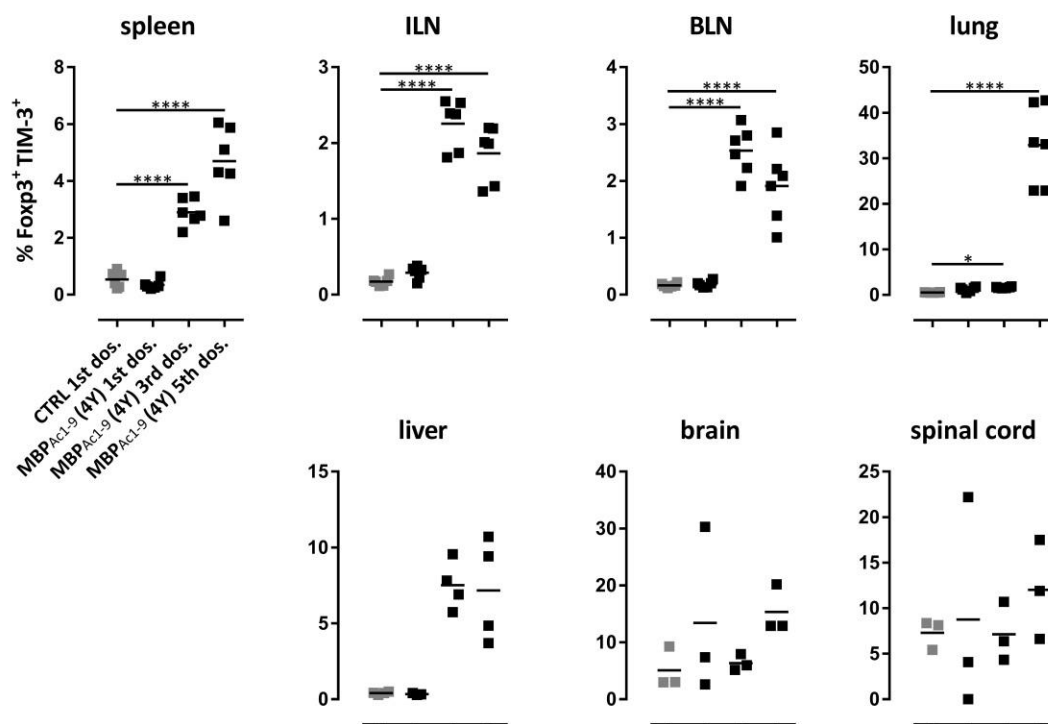


**Figure 4.9. Distribution of CD4+ Foxp3+ PD-1+ T cells during the course of tolerisation.** Tg4$^{IL-10/GFP}$ mice were treated with PBS or MBP$_{Ac1-9}$(4Y)-EDI. Two hours after the indicated dose animals were perfused with PBS and organs were isolated. After gating on viable, single CD4+

T cells, Foxp3$^+$ PD-1$^+$ T cells were investigated by flow cytometry during the course of escalating dose immunotherapy. Horizontal lines indicate the mean. After checking for normality using the Shapiro-Wilk test either ANOVA followed by Sidak's multiple comparison test was performed for normally distributed data or the Kruskal-Wallice test followed by Dunn's multiple comparison test for data that were not normally distributed (* = p ≤ 0.05, ** = p ≤ 0.01, *** = p ≤ 0.001, **** = p ≤ 0.0001). In the spleen, ILNs, MLNs, lung and BLNs each dot represents one individual. In the liver, in some cases cells from two animals were combined due to low cell numbers while in the CNS compartment each dot represents two individuals. Kruskal-Wallice test followed by Dunn's multiple comparison test was applied to liver, brain and spinal cord data. ANOVA followed by Sidak's multiple comparison test was applied to spleen, ILN, MLN, lung and BLN data. N=6, from two independent experiments.

### 4.1.3.4  Increased frequency of CD4$^+$ Foxp3$^+$ GFP$^+$ T cells after tolerisation

Since we know that dose escalation peptide immunotherapy increases IL-10 production in CD4$^+$ T cells we assessed IL-10 production in CD4$^+$ FoxP3$^+$ Treg cells (Figure 4.10.). The percentage of IL-10-producing CD4$^+$ Foxp3$^+$ T cells was significantly increased in the spleen with 2.5% on average after the 3$^{rd}$ and the 5$^{th}$ dose of MBP$_{Ac1-9}$(4Y)-treatment (p ≤ 0.0001). In the ILNs, Foxp3$^+$ T cells produced significantly more IL-10 after the 5$^{th}$ dose (p ≤ 0.01). The 4$^{th}$ dose of MBP$_{Ac1-9}$(4Y) elicited a significant increase of IL-10 production in Foxp3$^+$ T cells in the MLNs (p ≤ 0.05) compared to control animals. 12.5% CD4$^+$ Foxp3$^+$ IL-10$^+$ T cells on average were found in the lung of animals who received the 5$^{th}$ dose of MBP$_{Ac1-9}$(4Y) (p ≤ 0.05). In the BLNs of mice that received 3 doses or 5 doses MBP$_{Ac1-9}$(4Y) the upregulation of IL-10 production was very low but with up to ~0.8% IL-10$^+$ Foxp3$^+$ T cells significant (p ≤ 0.0001). CD4$^+$ Foxp3$^+$ IL-10$^+$ T cells in the liver and spinal cord reached statistical significance after the 5$^{th}$ dose with ~4% in the former and ~12% (both p ≤ 0.05) in the latter.
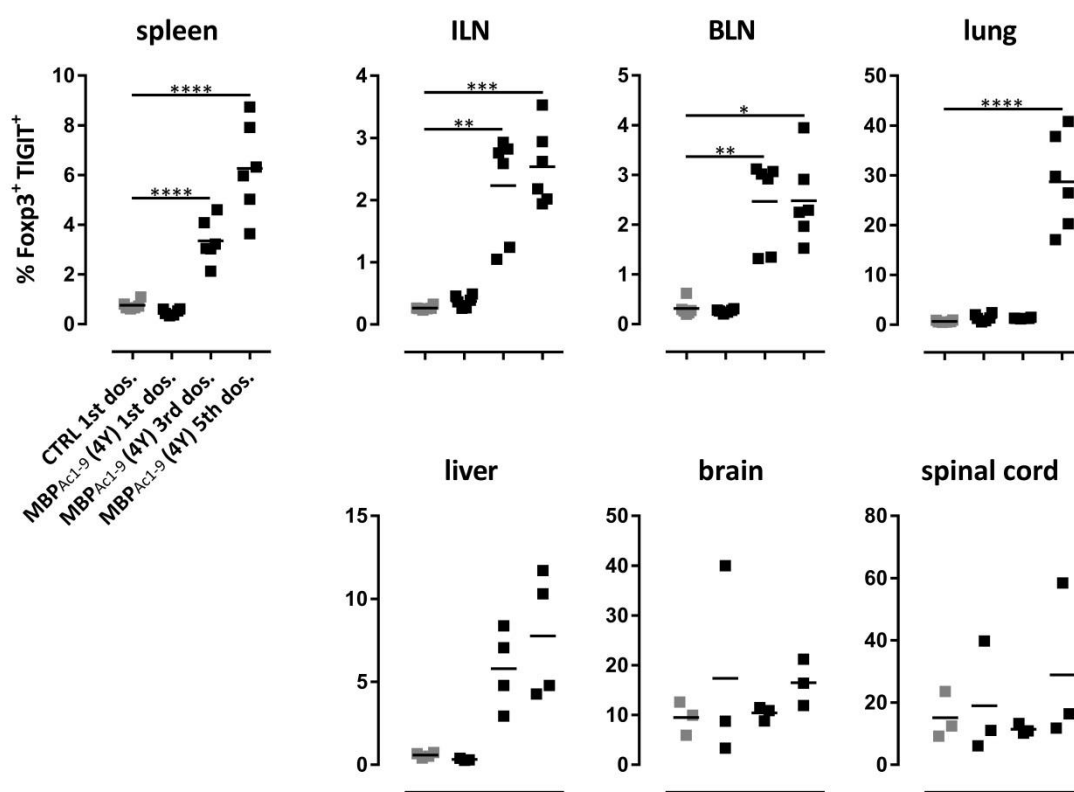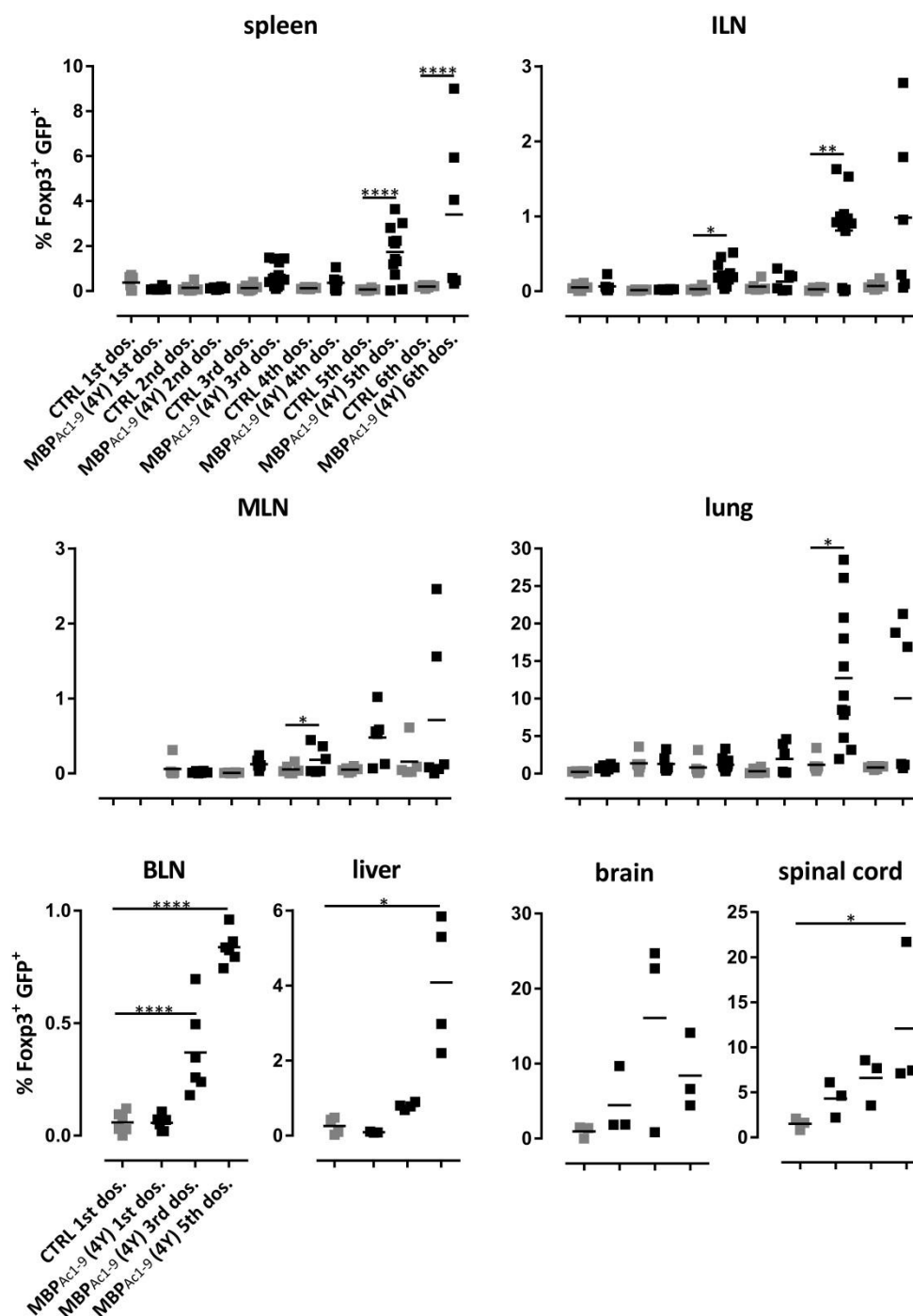
**Figure 4.10. Distribution of CD4⁺ Foxp3⁺ IL-10⁺ T cells during the course of tolerisation.** Tg4$^{IL-10/GFP}$ mice were treated with PBS or MBP$_{Ac1-9}$(4Y)-EDI. Two hours after the indicated dose animals were perfused with PBS and organs were isolated. After gating on viable, single CD4⁺ T cells, Foxp3⁺ IL-10⁺ T cells were investigated by flow cytometry during the course of escalating dose immunotherapy. Horizontal lines indicate the mean. After checking for normality using the Shapiro-Wilk test either ANOVA followed by Sidak's multiple comparison

test was performed for normally distributed data or the Kruskal-Wallice test followed by Dunn's multiple comparison test for data that were not normally distributed (* = p ≤ 0.05, ** = p ≤ 0.01, *** = p ≤ 0.001, **** = p ≤ 0.0001). In the spleen, ILNs, MLNs, lung and BLNs each dot represents one individual. In the liver, in some cases cells from two animals were combined due to low cell numbers while in the CNS compartment each dot represents two individuals. Kruskal-Wallice test followed by Dunn's multiple comparison test was applied to ILN, MLN, lung, liver, brain and spinal cord data. ANOVA followed by Sidak's multiple comparison test was applied to spleen and BLN data. N=6-11, from two independent experiments.

### 4.1.4 Pronounced increase of IL-10 production in CD4$^+$ Foxp3$^-$ T cells

Considering that we know that IL-10-producing CD4$^+$ Foxp3$^-$ T cells can have comparable regulatory functions to CD4$^+$ Foxp3$^+$ Treg cells (191), we investigated IL-10 production in CD4$^+$ Foxp3$^-$ T cells by flow cytometry during dose escalation. A much more pronounced increase of IL-10 production was seen in CD4$^+$ Foxp3$^-$ T cells than in CD4$^+$ Foxp3$^+$ cells (Figure 4.11.). Both in the spleen and lymph nodes, the percentage of IL-10-producing CD4$^+$ Foxp3$^-$ T cells was significantly upregulated with up to ~5-7.5% (p ≤ 0.0001) after the 6$^{th}$ dose of MBP$_{Ac1-9}$(4Y)-treatment compared to PBS-treated animals. The percentage of CD4$^+$ Foxp3-GFP$^+$ cells increased dramatically in the lung after the 6$^{th}$ dose, where it reached an average of 30% (p ≤ 0.001). In the BLNs, liver and brain of EDI-treated animals we detected a significant increase of CD4$^+$ Foxp3$^-$ GFP$^+$ T cells after the 5$^{th}$ dose of MBP$_{Ac1-9}$(4Y)-treatment with ~5-12% on average compared to PBS-treated animals.
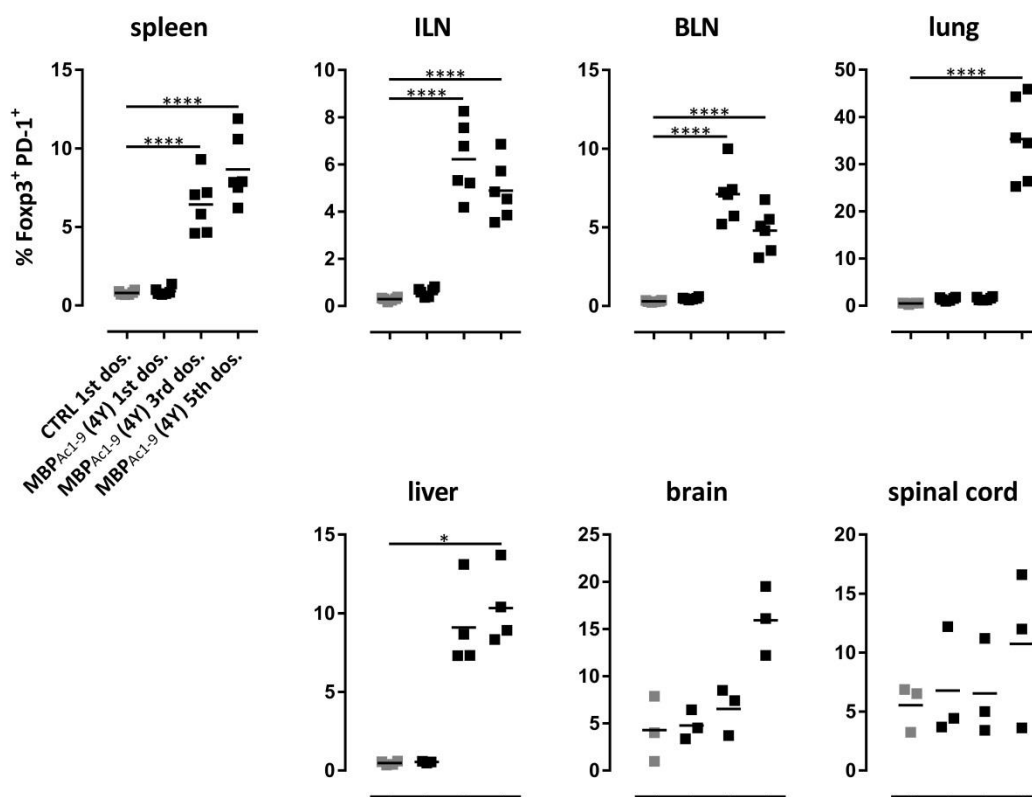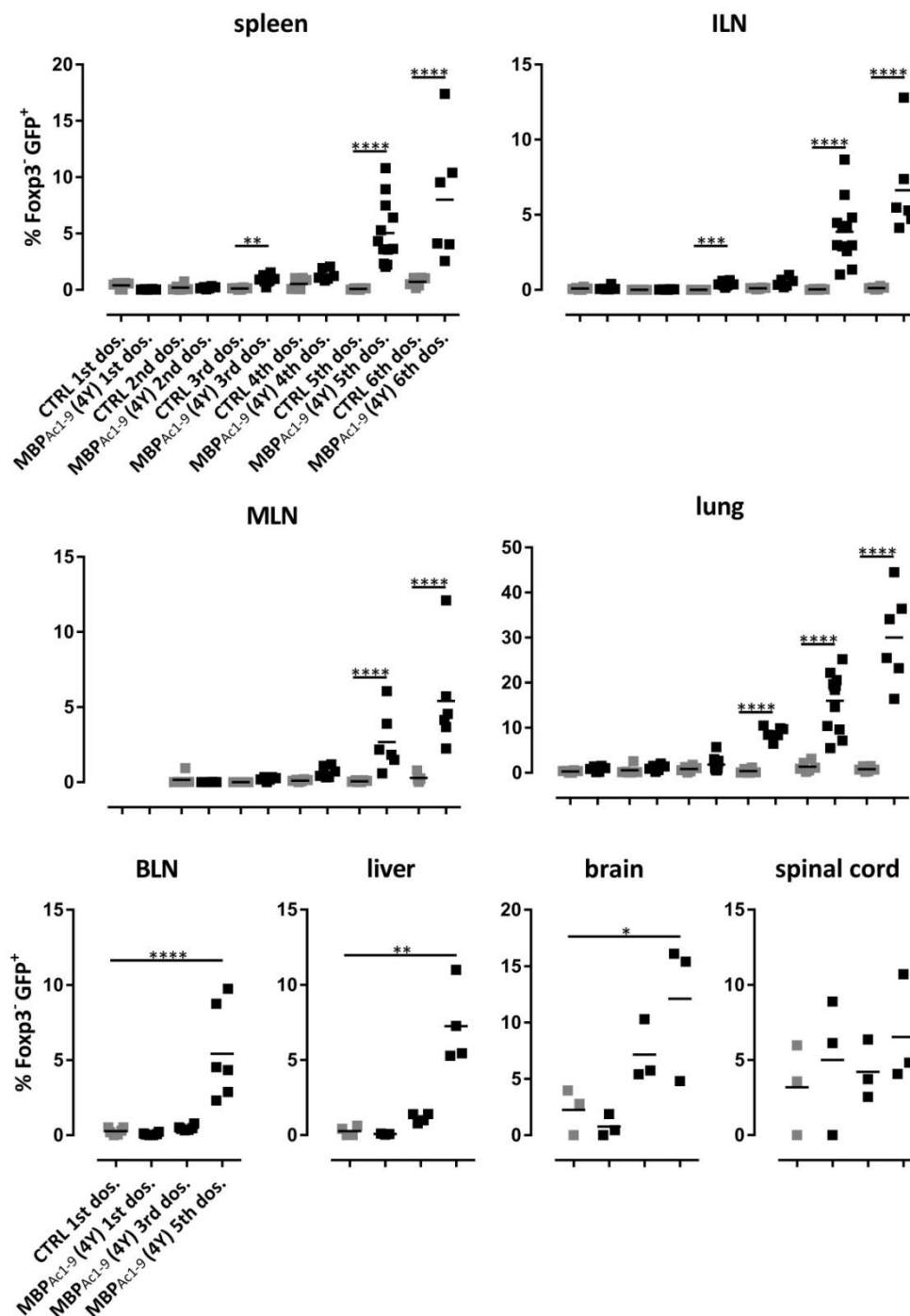
**Figure 4.11. Distribution of CD4$^+$ Foxp3$^-$ GFP$^+$ T cells during the course of tolerisation.** Tg4$^{IL-10/GFP}$ mice were treated with PBS or MBP$_{Ac1-9}$(4Y)-EDI. Two hours after the indicated dose animals were perfused with PBS and organs were isolated. After gating on viable, single CD4$^+$ T cells, Foxp3$^-$ IL-10$^+$ T cells were investigated by flow cytometry during the course of escalating dose immunotherapy. Horizontal lines indicate the mean. After checking for normality using the Shapiro-Wilk test either ANOVA followed by Sidak's multiple comparison

test was performed for normally distributed data or the Kruskal-Wallice test followed by Dunn's multiple comparison test for data that were not normally distributed (* = p ≤ 0.05, ** = p ≤ 0.01, *** = p ≤ 0.001, **** = p ≤ 0.0001). In the spleen, ILNs, MLNs, lung and BLNs each dot represents one individual. In the liver, in some cases cells from two animals were combined due to low cell numbers while in the CNS compartment each dot represents two individuals. Kruskal-Wallice test followed by Dunn's multiple comparison test was applied to liver, brain and spinal cord data. ANOVA followed by Sidak's multiple comparison test was applied to spleen, ILN, MLN, lung and BLN data. N=6-11, from two independent experiments.

### 4.1.5    IL-10 production increased gradually in the CD4+ T cell compartment during EDI

The overall IL-10 production of all CD4+ T cells increased gradually as a result of peptide treatment in all organs examined. Both in the spleen and lymph nodes, the percentage of CD4+ GFP+ T cells increased significantly after the 3rd dose and reached its peak with up to ~8% after the 6th dose compared to the PBS-treated group (Figure 4.12.). The percentage of CD4+ GFP+ T cells in the lung was upregulated even further after the 6th dose of peptide treatment with up to ~30%. Hepatic CD4+ T cells produced significantly more IL-10 after the 5th dose of EDI (p ≤ 0.01). The CNS compartment showed a major increase of CD4+ GFP+ T cells with ~50% CD4+ GFP+ T cells in the spinal cord after the 5th dose of peptide treatment compared to PBS-treated animals (p ≤ 0.05), whereas the same increment in the brain was not statistically significant due to low sample number and variance.
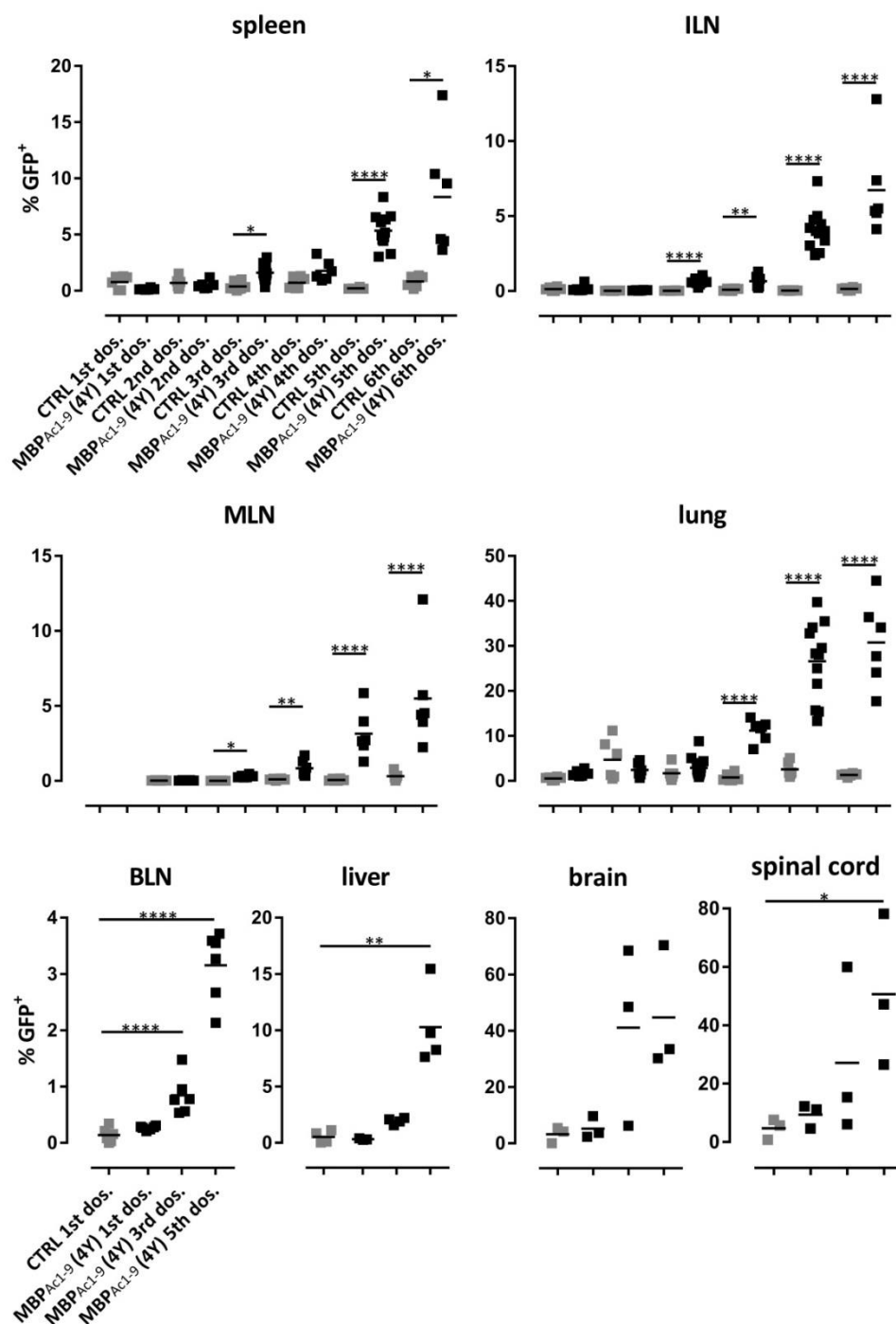
**Figure 4.12. Distribution of IL-10-producing CD4+ T cells during the course of tolerisation.** Tg4[IL-10/GFP] mice were treated with PBS or MBP$_{Ac1-9}$(4Y)-EDI. Two hours after the indicated dose animals were perfused with PBS and organs were isolated. After gating on viable, single CD4+ T cells, IL-10+ T cells were investigated by flow cytometry during the course of escalating dose immunotherapy. Horizontal lines indicate the mean. After checking for normality using the Shapiro-Wilk test either ANOVA followed by Sidak's multiple comparison

test was performed for normally distributed data or the Kruskal-Wallice test followed by Dunn's multiple comparison test for data that were not normally distributed (* = p ≤ 0.05, ** = p ≤ 0.01, *** = p ≤ 0.001, **** = p ≤ 0.0001). In the spleen, ILNs, MLNs, lung and BLNs each dot represents one individual. In the liver, in some cases cells from two animals were combined due to low cell numbers while in the CNS compartment each dot represents two individuals. Kruskal-Wallice test followed by Dunn's multiple comparison test was applied to liver, brain and spinal cord data. ANOVA followed by Sidak's multiple comparison test was applied to spleen, ILN, MLN, lung and BLN data. N=6-11, from two independent experiments.

### 4.1.5.1 Increased frequency of CD4$^+$ GFP$^+$ TIM-3$^+$ T cells during EDI

To further specifically characterise CD4$^+$ T cells actively producing IL-10 during dose escalation, the expression of the co-inhibitory molecules TIM-3, TIGIT and PD-1 on CD4$^+$ GFP$^+$ T cells was evaluated by flow cytometry. In the spleen, up to ~5% of CD4$^+$ T cells were GFP$^+$ TIM-3$^+$ after the 6th dose (both p ≤ 0.001) compared to PBS-treated animals (Figure 4.13.). In the lymph nodes, CD4$^+$ GFP$^+$ TIM-3$^+$ T cells represented around 1.5-3% of CD4$^+$ T cells on average after MBP$_{Ac1-9}$(4Y) treatment. CD4$^+$ GFP$^+$ TIM-3$^+$ T cells in the lung increased steadily between the 3$^{rd}$ dose and 6$^{th}$ dose with an increment of ~10% after every dose of MBP$_{Ac1-9}$(4Y) (p ≤ 0.01) compared to PBS-treated animals. Hepatic CD4$^+$ GFP$^+$ TIM-3$^+$ T cells increased significantly with ~7% after the 5$^{th}$ dose of MBP$_{Ac1-9}$(4Y) (p ≤ 0.05). We could not detect a significant difference in the percentage of CD4$^+$ GFP$^+$ TIM-3$^+$ T cells in the CNS compartment as a result of peptide treatment, possibly due to variance in results and a limited number of samples; however, there is a clear upward trend.

**Figure 4.13. Expression of TIM-3 on CD4$^+$ GFP$^+$ T cells during the course of tolerisation.** Tg4$^{IL-10/GFP}$ mice were treated with PBS or MBP$_{Ac1-9}$(4Y)-EDI. Two hours after the indicated dose animals were perfused with PBS and organs were isolated. After gating on viable, single CD4$^+$ T cells, GFP$^+$ TIM-3$^+$ T cells were investigated by flow cytometry during the course of escalating dose immunotherapy. Horizontal lines indicate the mean. After checking for normality using the Shapiro-Wilk test either ANOVA followed by Sidak's multiple comparison

test was performed for normally distributed data or the Kruskal-Wallice test followed by Dunn's multiple comparison test for data that were not normally distributed (* = p ≤ 0.05, ** = p ≤ 0.01, *** = p ≤ 0.001, **** = p ≤ 0.0001). In the spleen, ILNs, MLNs, lung and BLNs each dot represents one individual. In the liver, in some cases cells from two animals were combined due to low cell numbers while in the CNS compartment each dot represents two individuals. Kruskal-Wallice test followed by Dunn's multiple comparison test was applied to ILN, MLN, lung, liver, brain and spinal cord data. ANOVA followed by Sidak's multiple comparison test was applied to spleen and BLN data. N=6-11, from two independent experiments.

### 4.1.5.2   Increased frequency of CD4$^+$ GFP$^+$ TIGIT$^+$ T cells during EDI

In the spleen and lymph nodes, CD4$^+$ GFP$^+$ TIGIT$^+$ T cells were significantly upregulated with ~2-5% on average in MBP$_{Ac1-9}$(4Y)-treated animals compared to control animals (Figure 4.14.). A more pronounced increase of CD4$^+$ GFP$^+$ TIGIT$^+$ T cells was noticeable in the lung, where we detected ~15-20% of CD4$^+$ GFP$^+$ TIGIT$^+$ T cells after the 5$^{th}$ and 6$^{th}$ dose of peptide treatment (both p ≤ 0.001). In the liver, we noticed a significant increase of GFP$^+$ TIGIT$^+$ T cells with ~7.5% after 5 doses of MBP$_{Ac1-9}$(4Y) (p ≤ 0.01). The CNS compartment exhibited a significant difference in the percentage of CD4$^+$ GFP$^+$ TIGIT$^+$ as a result of peptide treatment only in the spinal cord after the 5$^{th}$ dose of MBP$_{Ac1-9}$(4Y)-treatment with up to ~50% (p ≤ 0.05) compared to PBS-treated animals with ~5% of CD4$^+$ GFP$^+$ TIGIT$^+$ T cells.
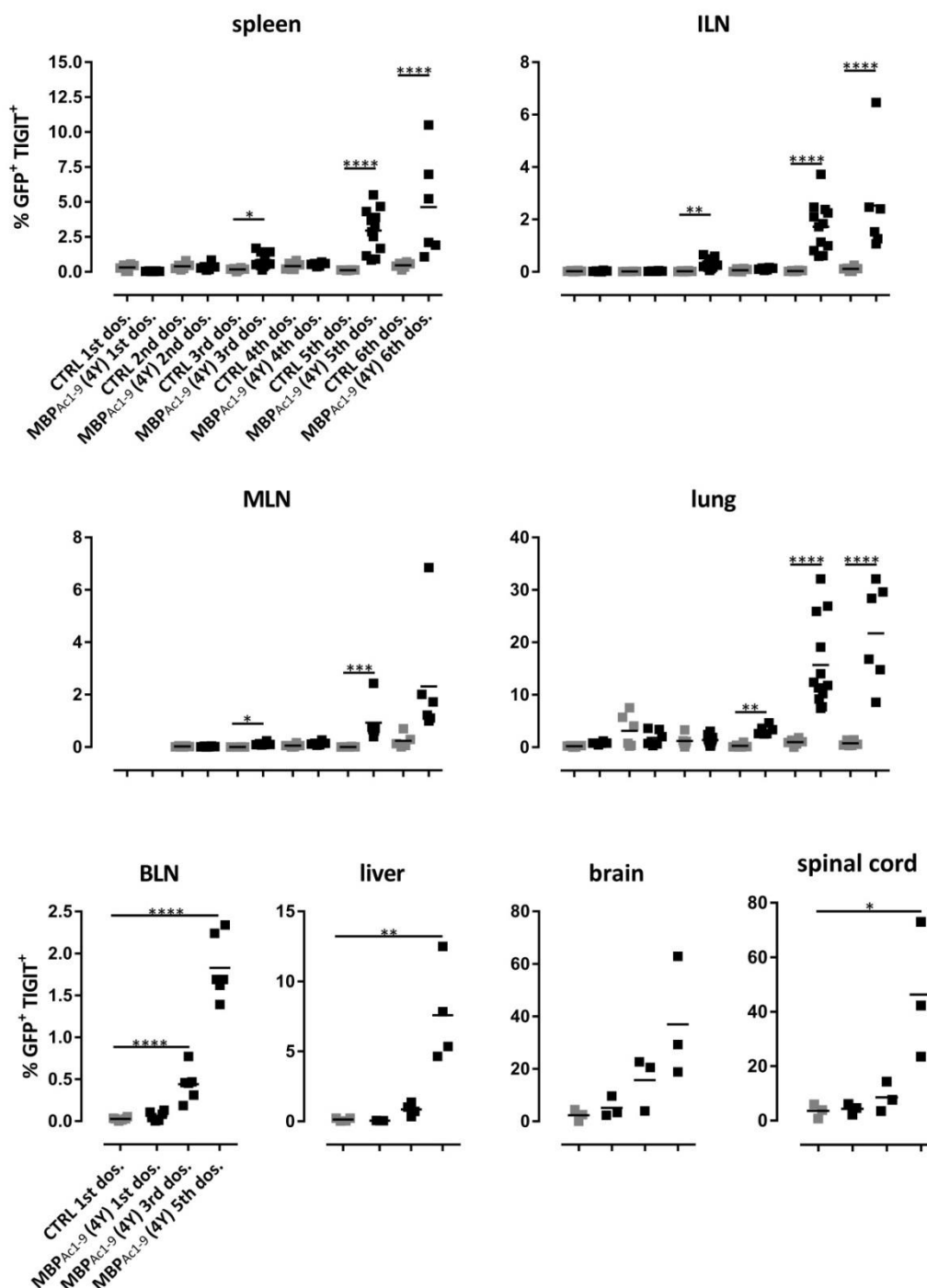
**Figure 4.14. Distribution of CD4^{+} GFP^{+} TIGIT^{+} T cells during the course of tolerisation.** Tg4[IL-10/GFP] mice were treated with PBS or MBP$_{Ac1-9}$(4Y)-EDI and two hours after the indicated dose animals were perfused with PBS and organs were isolated. After gating on viable, single CD4^{+} T cells, GFP^{+} TIGIT^{+} T cells were investigated by flow cytometry during the course of escalating dose immunotherapy. Horizontal lines indicate the mean. After checking for normality using the Shapiro-Wilk test either ANOVA followed by Sidak's multiple comparison

test was performed for normally distributed data or the Kruskal-Wallice test followed by Dunn's multiple comparison test for data that were not normally distributed (* = p ≤ 0.05, ** = p ≤ 0.01, *** = p ≤ 0.001, **** = p ≤ 0.0001). In the spleen, ILNs, MLNs, lung and BLNs each dot represents one individual. In the liver in some cases cells from two animals were combined due to low cell numbers while in the CNS compartment each dot represents two individuals. Kruskal-Wallice test followed by Dunn's multiple comparison test was applied to MLN, liver, brain and spinal cord data. ANOVA followed by Sidak's multiple comparison test was applied to spleen, ILN, lung and BLN data. N=6-11 from two independent experiments.

### 4.1.5.3  Increased frequency of CD4$^+$ GFP$^+$ PD-1$^+$ T cells during EDI

We found a significant increase in the percentage of CD4$^+$ GFP$^+$ PD-1$^+$ T cells mostly after the 5$^{th}$ dose of MBP$_{Ac1-9}$(4Y)-treatment although the percentage of CD4$^+$ GFP$^+$PD-1$^+$ T cells after the 6$^{th}$ dose were either the same or higher. In the spleen and lymph nodes, ~1.5-3% CD4$^+$ GFP$^+$ PD-1$^+$ T cells were found in MBP$_{Ac1-9}$(4Y)-treated animals after the 5$^{th}$ dose of treatment (all p ≤ 0.0001) (Figure 4.15.). CD4$^+$ GFP$^+$ PD-1$^+$ T cells in the lung reached a statistically significant difference compared to the PBS control group after the 5th dose with 25% on average (p ≤ 0.05). The percentage of hepatic CD4$^+$ GFP$^+$ PD-1$^+$ T cells was upregulated significantly with up to ~9% after the 5$^{th}$ dose of MBP$_{Ac1-9}$(4Y) (p ≤ 0.01). We could not detect a significant difference as a result of peptide treatment in the percentage of CD4$^+$ GFP$^+$ PD-1$^+$ T cells in the CNS compartment compared to PBS-treated mice, possibly due to low sample number and variance.
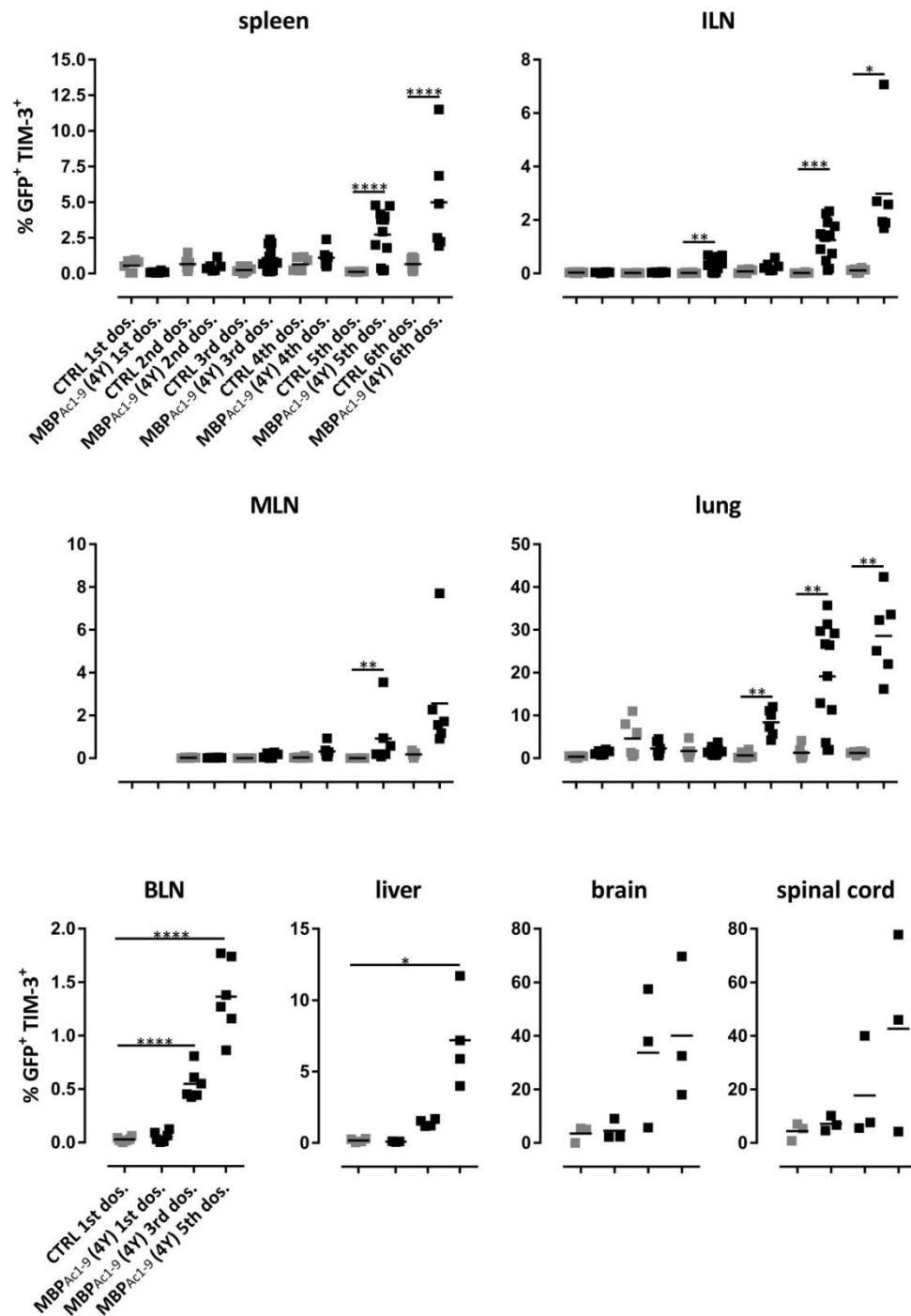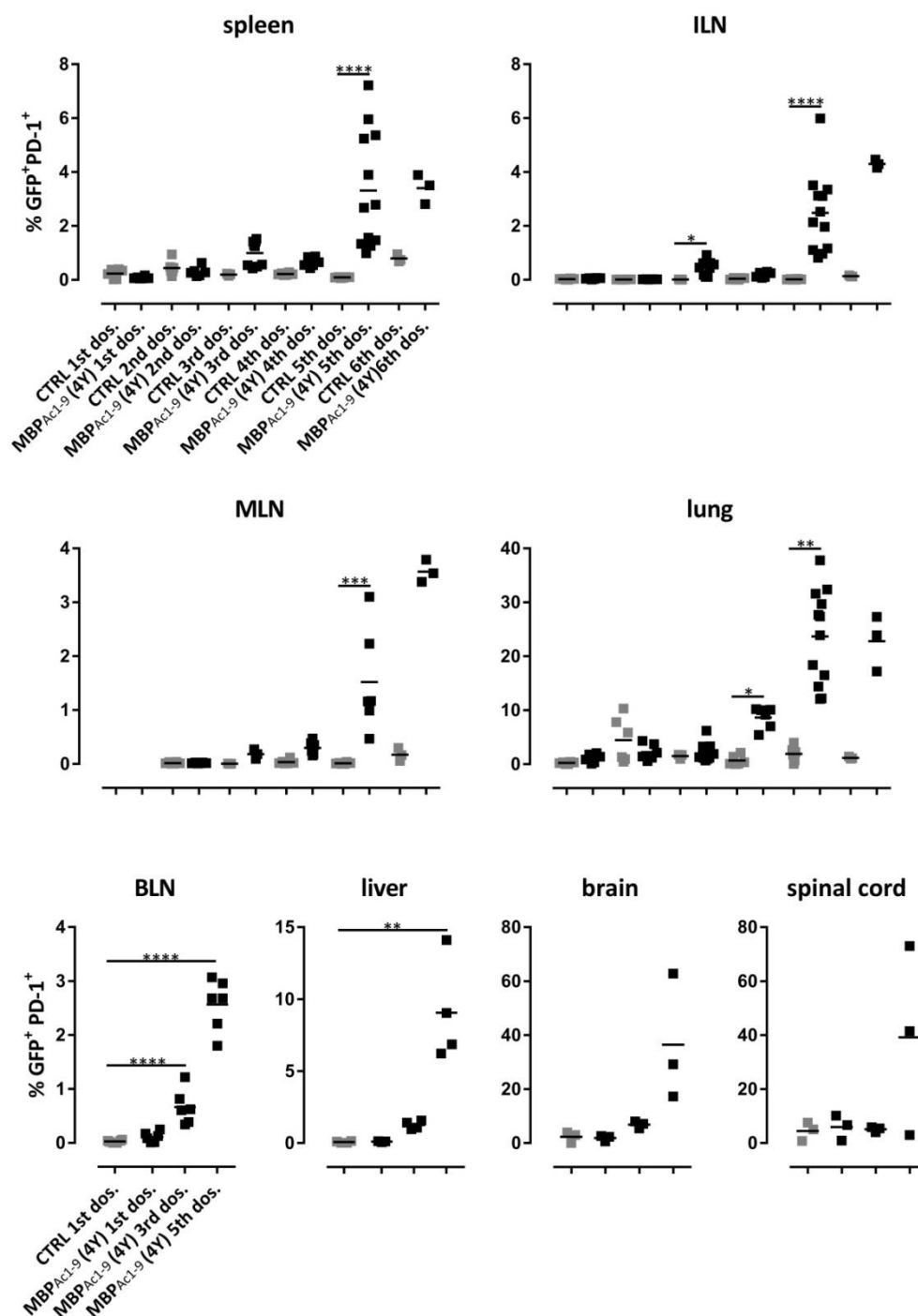
**Figure 4.15. Distribution of CD4+ GFP+ PD-1+ T cells during the course of tolerisation.** Tg4[IL-10/GFP] mice were treated with PBS or MBP_{Ac1-9}(4Y)-EDI and two hours after the indicated dose animals were perfused with PBS and organs were isolated. After gating on viable, single CD4+ T cells, GFP+ PD-1+ T cells were investigated by flow cytometry during the course of escalating dose immunotherapy. Horizontal lines indicate the mean. After checking for normality using the Shapiro-Wilk test either ANOVA followed by Sidak's multiple comparison

test was performed for normally distributed data or the Kruskal-Wallice test followed by Dunn's multiple comparison test for data that were not normally distributed (* = p ≤ 0.05, ** = p ≤ 0.01, *** = p ≤ 0.001, **** = p ≤ 0.0001). In the spleen, ILNs, MLNs, lung and BLNs each dot represents one individual. In the liver, in some cases cells from two animals were combined due to low cell numbers while in the CNS compartment each dot represents two individuals. Kruskal-Wallice test followed by Dunn's multiple comparison test was applied to spleen, ILN, MLN, lung, liver, brain and spinal cord data. ANOVA followed by Sidak's multiple comparison test was applied BLN data. N=6-11, from two independent experiments.

## 4.2    Histological assessment of spleen and LNs

In theory, either the IL-10-reporter construct itself or EDI could affect the structural make-up of secondary lymphoid organs in the mice, which in turn could affect the phenotype and functionality of CD4$^+$ T cells therein. In order to assess this possibility, histological examination of the spleen was conducted. In the spleen, no obvious alterations of the normal structure was apparent in H&E stained sections of Tg4$^{IL-10/GFP}$ mice (Figure 4.16. **A**, first row). Moreover, EDI treatment did not affect the gross structure of the organ compared to Tg4$^{IL-10/GFP}$ mice who received PBS-control treatment (Figure 4.16. **A**).

Additionally, spleen sections from tolerised Tg4$^{IL-10/GFP}$ PBS-treated controls and untreated Tg4 mice were stained with antibodies against CD4 and GFP to visualise the presence of CD4$^+$ T cells and IL-10-producing cells. The CD4 staining confirmed that the number and organisation of CD4$^+$ T cells in the spleen of Tg4$^{IL-10/GFP}$ cells was not affected by the construct. Moreover, comparison of the CD4$^+$ T cell density in PBS-treated or MBP$_{Ac1-9}$(4Y)-treated Tg4$^{IL-10/GFP}$ mice confirmed the reduction of CD4$^+$ T cell numbers in the spleen post EDI (Figure 4.16. **A**) as already observed by flow cytometry. Double staining of CD4 and GFP confirmed the increased production of IL-10 by CD4$^+$ T cells in Tg4$^{IL-10/GFP}$ mice (Figure 4.16. **A**, black arrows) compared to PBS-treated mice (Figure 4.16. **A**). The CD4$^+$ IL-10$^+$ T cells were not all found within the T cell zone but were dispersed throughout the organ (Figure 4.16. A, second row). CD4$^+$ IL-10$^+$ T cells in the T cell zone were primarily located at the rim of the T cell zone. Outside the T cell zone we noticed an increase of GFP production in non-CD4$^+$ T cells to the same extent as in CD4$^+$ T cells (Figure 4.16. **A**, bottom right). Control-treated Tg4$^{IL-10/GFP}$ mice also showed a small number of IL-10-secreting cells in the spleen, but these were not CD4$^+$ T cells (red arrows). As expected, the double staining of spleen from

untreated Tg4 mice did not provide a GFP signal, while the CD4 staining was comparable to PBS-treated Tg4$^{IL-10/GFP}$ mice (Figure 4.16. **A**). This confirms that the number of CD4$^+$ T cells was not affected by the IL-10 reporter construct and that the anti-GFP antibody was specific for its intended target. In the lung we noticed an increase of IL-10-producing CD4$^+$ T cells examined by flow cytometry as a result of MBP$_{Ac1-9}$(4Y)-treatment. Interestingly, immunohistochemistry revealed that CD4$^+$ GFP$^+$ T cells were primarily located in lymph nodes of the lung, rather than in the lung parenchyma, (Figure 4.16. **B**, black arrows), where we also found GFP$^+$ cells that were not CD4$^+$ (Figure 4.16. **B**, red arrows).
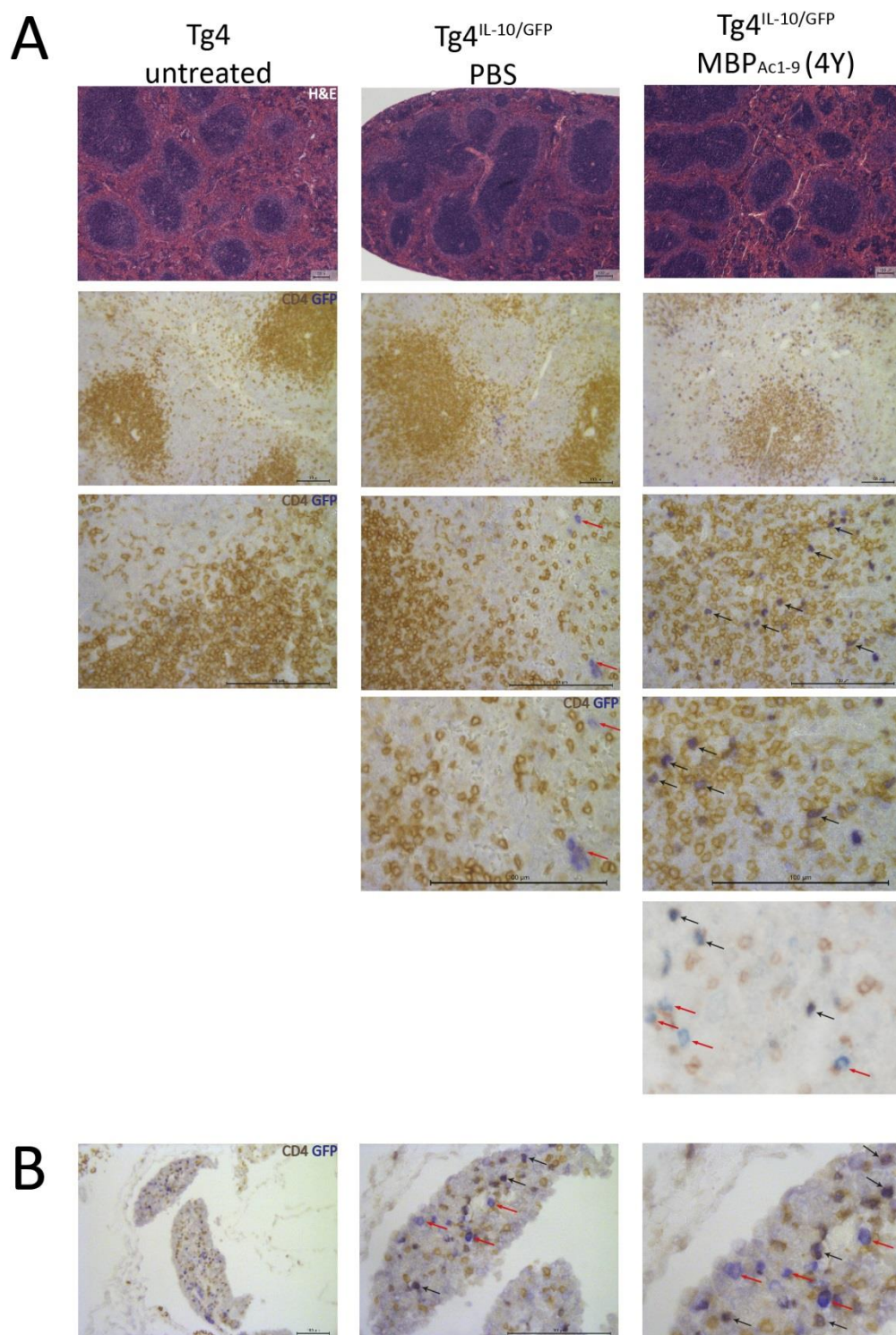
**Figure 4.16. Histological assessment of spleen and lung lymph nodes. A**) 5 μm paraffin sections of Tg4[IL-10/GFP] mice treated with MBP[Ac1-9](4Y), of Tg4[IL-10/GFP] mice treated with PBS and untreated Tg4 mice stained for H&E (top), or double-stained for CD4 (DAB - brown) and GFP staining (Fast blue - blue). Red arrows point to CD4⁻ GFP⁺ cells and black arrows point to CD4⁺ GFP⁺ T cells. **B**) Lymph nodes of the lung of MBP[Ac1-9](4Y)-treated Tg4[IL-10/GFP] mice are stained as in A. Representative images of organs from one mouse per group.

### 4.3 Spatiotemporal distribution of tolerised CD4$^+$ T cells in lymphoid and non-lymphoid tissue in EAE

To characterise CD4$^+$ T cells in EAE after tolerisation Tg4 or Tg4$^{IL-10/GFP}$ mice were treated either with PBS or MBP$_{Ac1-9}$(4Y) before the induction of EAE with their cognate peptide in CFA and pertussis toxin. Animals were analysed at the peak of disease when mice treated with PBS showed complete hind limb paralysis and EDI-treated animals showed no signs of disease at the time of the analysis.

### 4.3.1 MBP$_{Ac1-9}$(4Y)-treatment prevents CD4$^+$ T cells from migrating into the brain in EAE

We observed a significant reduction of CD4$^+$ T cells in the CNS compartment of tolerised versus PBS-treated mice, while the percentage of CD4$^+$ T cells was unchanged in the periphery (Figure 4.17.). In the brain ~2.5% CD4$^+$ T cells were detected in MBP$_{Ac1-9}$(4Y)-treated animals compared to PBS-treated animals that had ~10% viable CD4$^+$ T cells of single cells in the brain (p ≤ 0.05).

**Figure 4.17. Distribution of CD4+ T cells in EAE animals after tolerisation.** Tg4 mice were treated with PBS or MBP$_{Ac1-9}$(4Y)-EDI before the induction of EAE with their cognate peptide in CFA, and pertussis toxin given on days 0 and 2 post prime. Animals were analysed at the peak of disease when mice treated with PBS showed complete hind limb paralysis (grade 3) and EDI-treated animals showed no sign of disease. Gated on single cells. Horizontal lines indicate mean. After checking for normality using the Shapiro-Wilk test the unpaired t test was performed for normally distributed brain data (* = p ≤ 0.05, ** = p ≤ 0.01, *** = p ≤ 0.001, **** = p ≤ 0.0001). Each dot represents one individual. Unpaired t test was applied to results from the brain. N=7-11, from three independent experiments.

### 4.3.1.1 Dichotomy in the expression of TIM-3 on tolerised CD4+ T cells in animals protected from EAE

TIM-3 expression on tolerised CD4+ T cells was significantly increased in spleen, lung and liver of peptide-treated animals compared to PBS-treated animals with up to 20% on average (Figure 4.18.). In contrast, we noticed a markedly lower expression of TIM-3 on CD4+ T cells in the spinal cord, with ~40% in peptide-treated animals compared to 65% in control mice (p ≤ 0.05).

**Figure 4.18. Expression of TIM-3 on CD4$^+$ T cells in EAE after tolerisation.** Tg4 mice were treated with PBS or MBP$_{Ac1-9}$(4Y)-EDI before the induction of EAE with their cognate peptide in CFA, and pertussis toxin given on days 0 and 2 post prime. Animals were analysed at the peak of disease when mice treated with PBS showed complete hind limb paralysis (grade 3) and EDI-treated animals showed no sign of disease. After gating on viable, single CD4$^+$ T cells, TIM-3 expression was investigated by flow cytometry. Horizontal lines indicate mean. After the check for normality using the Shapiro-Wilk test either unpaired t test was performed for normal distributed data or the Mann-Whitney U test for data who were not normally distributed was performed (* = p ≤ 0.05, ** = p ≤ 0.01, *** = p ≤ 0.001, **** = p ≤ 0.0001). Each dot represents one individual. Unpaired t test was applied to lung and liver data while Mann-Whitney U test was applied to spleen and spinal cord data. N=7-11, from three independent experiments.

### 4.3.1.2 Lower PD-1 expression on tolerised CD4+ T cells in the CNS compartment in tolerised mice than in mice with EAE

PD-1 expression on CD4+ T cells was mostly unchanged in the periphery (Figure 4.19.). However, we detected a significant decrease of CD4+ PD-1+ T cells in the CNS compartment of EDI-treated mice with ~80% on average in brain and spinal cord compared to PBS-treated animals with ~60% CD4+ PD1+ T cells on average (p ≤ 0.01).



**Figure 4.19. Distribution of CD4+ PD-1+ T cells in EAE animals after tolerisation.** Tg4 mice were treated with PBS or MBP$_{Ac1-9}$(4Y)-EDI before the induction of EAE with their cognate peptide in CFA, and pertussis toxin given on days 0 and 2 post prime. Animals were analysed at the peak of disease when mice treated with PBS showed complete hind limb paralysis (grade 3) and EDI-treated animals showed no sign of disease. After gating on viable, single CD4+ T cells, PD-1 expression was investigated by flow cytometry. Horizontal lines indicate mean. After checking for normality using the Shapiro-Wilk test either unpaired t test was performed for normally distributed data or the Mann-Whitney U test for data that were not normally distributed (* = p ≤ 0.05, ** = p ≤ 0.01, *** = p ≤ 0.001, **** = p ≤ 0.0001). Each dot represents one individual. Mann-Whitney U test was applied to brain and spinal cord data. N=7-11, from three independent experiments.

### 4.3.2 Expression of CD4$^+$ Foxp3$^+$ T cells was lower in the periphery, but higher in the spinal cord of tolerised versus EAE mice

The percentage of CD4$^+$ T cells that express Foxp3 trended toward a minor reduction in most peripheral organs in tolerised versus EAE mice, but this reached statistical significance only in the ILNs (p ≤ 0.0001) (Figure 4.20.). In the CNS, we did not detect any significant differences, although two out of 7 tolerised animals showed a markedly higher percentage of Foxp3 expression than was detected in EAE mice.
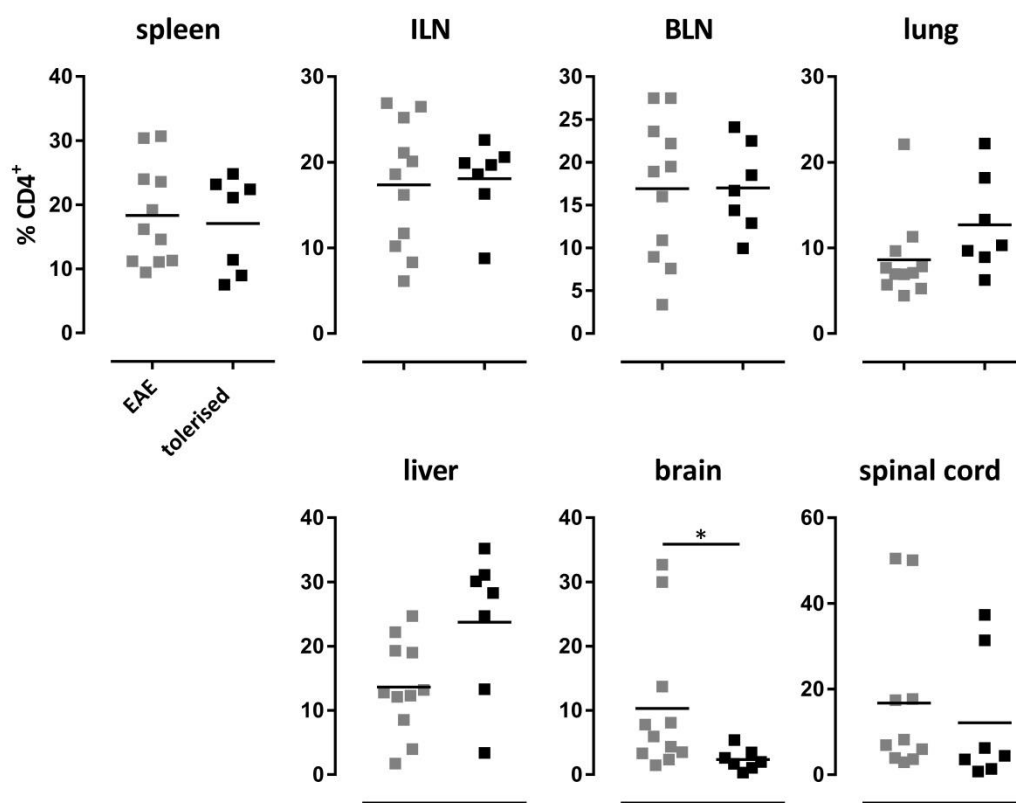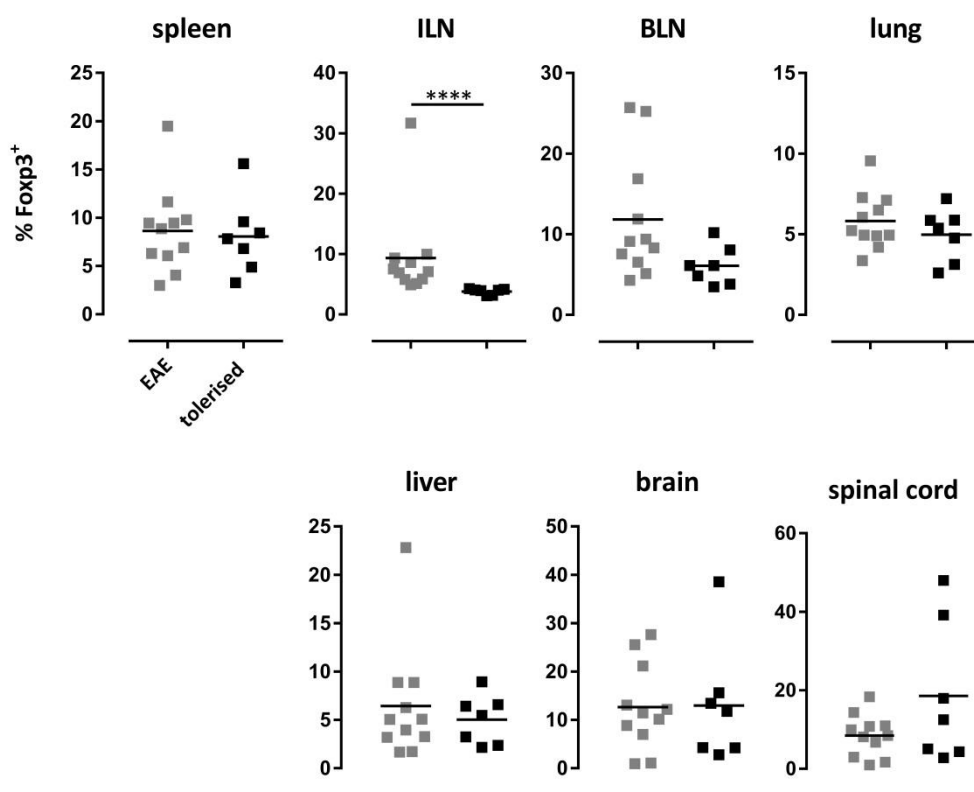


**Figure 4.20. Distribution of CD4$^+$ Foxp3$^+$ T cells in EAE after tolerisation.** Tg4 mice were treated with PBS or MBP$_{Ac1-9}$(4Y)-EDI before the induction of EAE with their cognate peptide in CFA, and pertussis toxin given on days 0 and 2 post prime. Animals were analysed at the peak of disease when mice treated with PBS showed complete hind limb paralysis (grade 3) and EDI-treated animals showed no sign of disease. After gating on viable, single CD4$^+$ T cells, Foxp3 expression was investigated by flow cytometry. Horizontal lines indicate mean. After checking for normality using the Shapiro-Wilk test either unpaired t test was performed for normally distributed data or the Mann-Whitney U test for data that were not normally distributed (* = p ≤ 0.05, ** = p ≤ 0.01, *** = p ≤ 0.001, **** = p ≤ 0.0001). Each dot represents one individual. Mann-Whitney U test was applied to ILN data. N=7-11, from three independent experiments.

### 4.3.2.1 Dichotomy in the expression of TIM-3 on tolerised CD4$^+$ Foxp3$^+$ T cells in animals protected from EAE

Similar to TIM-3 expression on all CD4$^+$ T cells, CD4$^+$ Foxp3$^+$ T cells exhibited the same dichotomy in the expression of TIM-3. CD4$^+$ Foxp3$^+$ TIM-3$^+$ T cells were significantly increased in the spleen, lung and liver as a result of peptide treatment with up to ~3% compared to PBS-treated animals with ~1.5%, while the percentages of CD4$^+$ Foxp3$^+$ TIM-3$^+$ T cells in the lymph nodes were unchanged (Figure 4.21.). In contrast, we noticed a markedly lower expression of TIM-3 on CD4$^+$ Foxp3$^+$ T cells in the brain, with ~1% in peptide-treated animals compared to 5% in control mice (p ≤ 0.01).
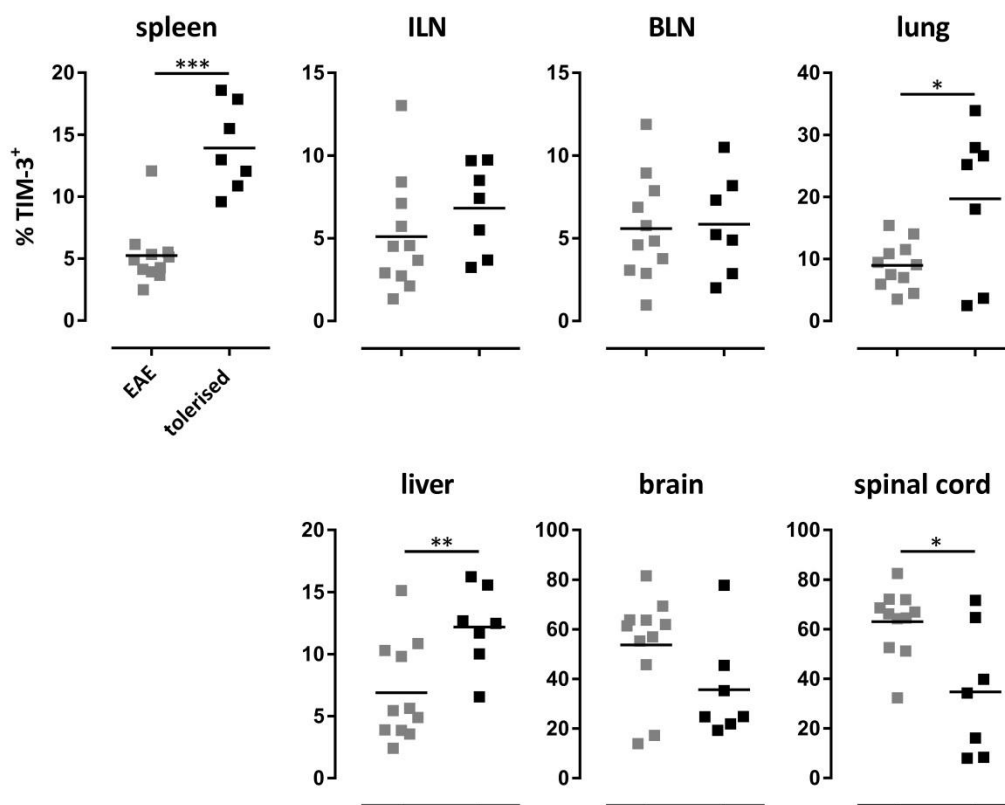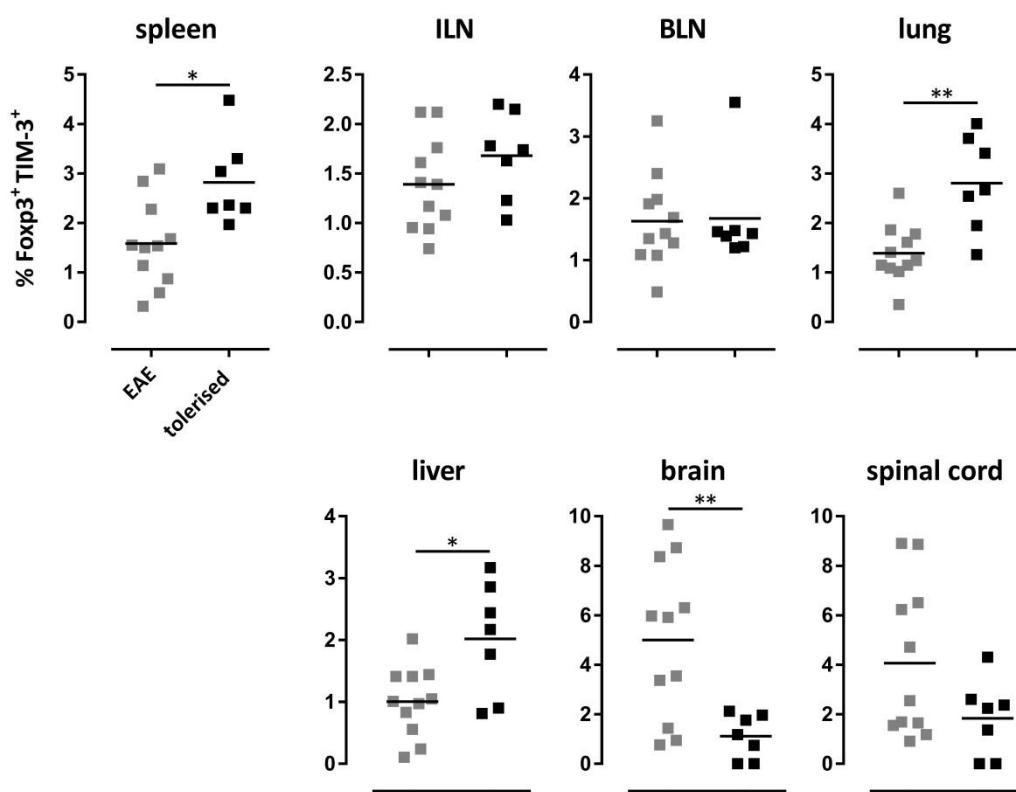


**Figure 4.21. Distribution of CD4$^+$ Foxp3$^+$ TIM3$^+$ T cells in EAE after tolerisation.** Tg4 mice were treated with PBS or MBP$_{Ac1-9}$(4Y)-EDI before the induction of EAE with their cognate peptide in CFA, and pertussis toxin given on days 0 and 2 post prime. Animals were analysed at the peak of disease when mice treated with PBS showed complete hind limb paralysis (grade 3) and EDI-treated animals showed no sign of disease. After gating on viable, single CD4$^+$ T cells, Foxp3$^+$ TIM-3$^+$ T cells were investigated by flow cytometry. Horizontal lines

indicate mean. After checking for normality using the Shapiro-Wilk test either unpaired t test was performed for normally distributed data or the Mann-Whitney U test for data that were not normally distributed (* = p ≤ 0.05, ** = p ≤ 0.01, *** = p ≤ 0.001, **** = p ≤ 0.0001). Each dot represents one individual. Unpaired t test was applied to spleen, lung, liver and brain data. N=7-11, from three independent experiments.

### 4.3.2.2 CD4⁺ T cells in the brain of tolerised mice produce more IL-10 than in EAE mice.

IL-10 is an important immunoregulatory cytokine and is known to be protective e.g. in allergy and autoimmunity and previous studies from our lab showed that the dose escalation protocol increases IL-10-producing CD4⁺ T cells (61). Hence, we examined the percentages of IL-10 producing CD4⁺ T cells in tolerised and EAE mice. We noticed that in most of the organs examined, percentages of CD4⁺ GFP⁺ T cells are unchanged whereas in the brain CD4⁺ T cells from tolerised animals tend to produce more IL-10 compared to EAE mice (Figure 4.22.). We detected around 9% CD4⁺ GFP⁺ T cells on average in tolerised mice and ~3% CD4⁺ GFP⁺ T cells in EAE mice but the difference did not reach statistical significance.
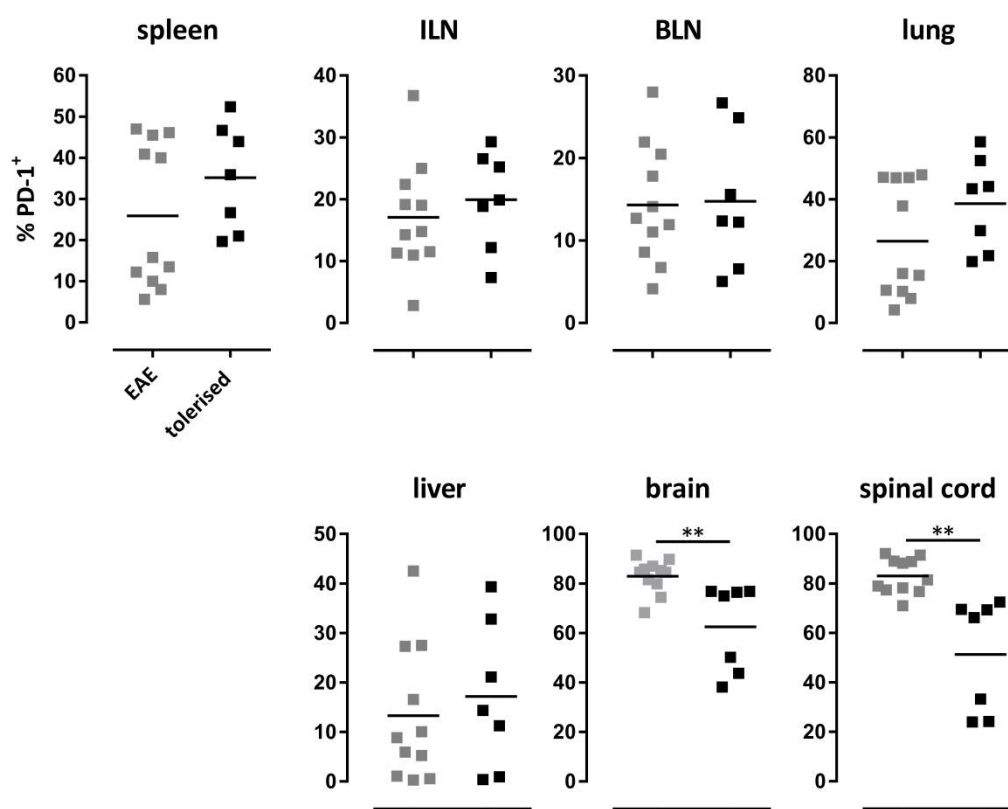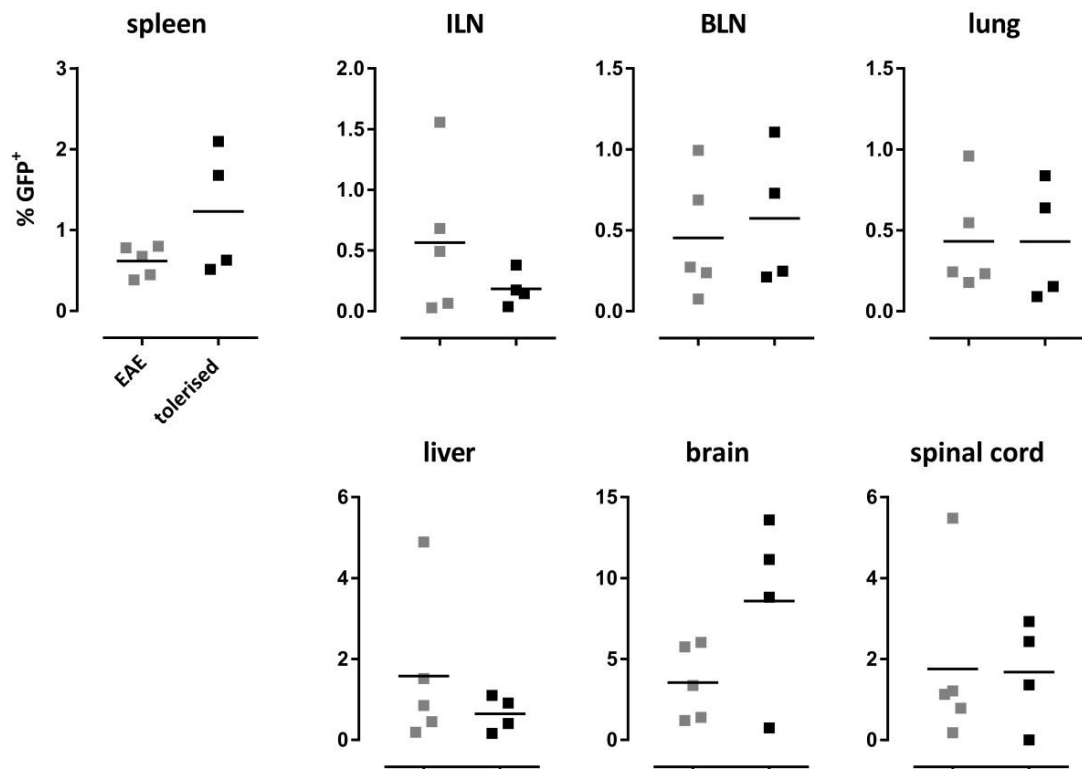
**Figure 4.22. Distribution of CD4⁺ GFP⁺ T cells in EAE animals after tolerisation.** Tg4$^{IL-10/GFP}$ mice were treated with PBS or MBP$_{Ac1-9}$(4Y)-EDI before the induction of EAE with their cognate peptide in CFA, and pertussis toxin given on days 0 and 2 post prime. Animals were analysed at the peak of disease when mice treated with PBS showed complete hind limb paralysis (grade 3) and EDI-treated animals showed no sign of disease. After gating on viable, single CD4⁺ T cells, GFP⁺ T cells were investigated by flow cytometry. Horizontal lines indicate mean. Mann-Whitney U test for data that were not normally distributed was performed (* = p ≤ 0.05, ** = p ≤ 0.01, *** = p ≤ 0.001, **** = p ≤ 0.0001). Each dot represents one individual. N=4-5, from two independent experiments.

## 4.4 Bystander suppression by tolerised CD4$^+$ T cells

### 4.4.1 Bystander suppression *in vitro*

Multiple sclerosis often involves CD4$^+$ T cell responses to more than one myelin antigen in the same individual. For tolerisation with peptide(s) from just one antigen to provide full protection from disease, the tolerised CD4$^+$ T cells that specific for one myelin protein will need to be able to suppress responses to other myelin antigens. To investigate if CD4$^+$ T cells from MBP$_{Ac1-9}$(4Y)-treated Tg4 mice, where tolerance is already established, are able to suppress responses to a second peptide we developed a novel *in vitro* assay. First, we crossed B10.PL mice with C57BL/6 mice to obtain mice that express both I-A$^u$ and I-A$^b$, which renders them susceptible to CD4$^+$ T cell responses against both MBP$_{Ac1-9}$(4K) and MOG$_{35-55}$. Splenic CD4$^+$ T cells from tolerised TG4 CD45.1$^+$ mice (T$_{tol}$) were co-cultured with CD4$^+$ T cells from (B10.PL x C57BL/6)F1 (T$_{conv}$) mice, primed with a combination of both peptides (100 µg each) in CFA. The latter population of CD4$^+$ T cells was labelled with cell proliferation dye (cpd-eFl450), which is distributed between daughter cells upon division. T$_{tol}$ cells (CD45.1$^+$) could easily be distinguished from T$_{conv}$ cells (CD45.2$^+$) in the co-culture. The cells in these co-cultures were then stimulated with 10 µg/ml MBP$_{Ac1-9}$ and/or 10 µg/ml MOG$_{35-55}$ in the presence of either immature or mature BMDCs generated from (B10.PL x C57BL/6)F1 mice. Ki-67 was included in the staining as a cellular marker for activated proliferating T cells. T$_{tol}$ cells reduced the proliferative response of T$_{conv}$ in response to MBP$_{Ac1-9}$(4K), as assessed by evaluation of cpd-eFl450$^+$ Ki-67$^+$ cells, by approximately half in both cultures with immature and mature BMDCs (Figure 4.23.). In response to MOG$_{35-55}$, the MBP-specific T$_{tol}$ had only a very minor effect on the proliferation of T$_{conv}$ and only when immature but not mature BMDCs were used. It should be noted here that more of the T$_{conv}$ cells in the absence of T$_{tol}$ responded to MOG$_{35-55}$ than to MBP$_{Ac1-9}$(4K). Importantly, in cultures where cells were stimulated with both antigens, the addition of the MBP$_{Ac1-9}$-specific T$_{tol}$ cells led to a dramatic reduction in the proliferative response of the T$_{conv}$ cells, thus abrogating the activation by both MBP$_{Ac1-9}$(4K) and MOG$_{33-55}$. This would suggest that T$_{tol}$ cells can supress the activation of CD4$^+$ T cells specific for other antigens, as long as they are presented within the same environment. Based on these encouraging results we decided to proceed to analyse this in detail *in vivo*.
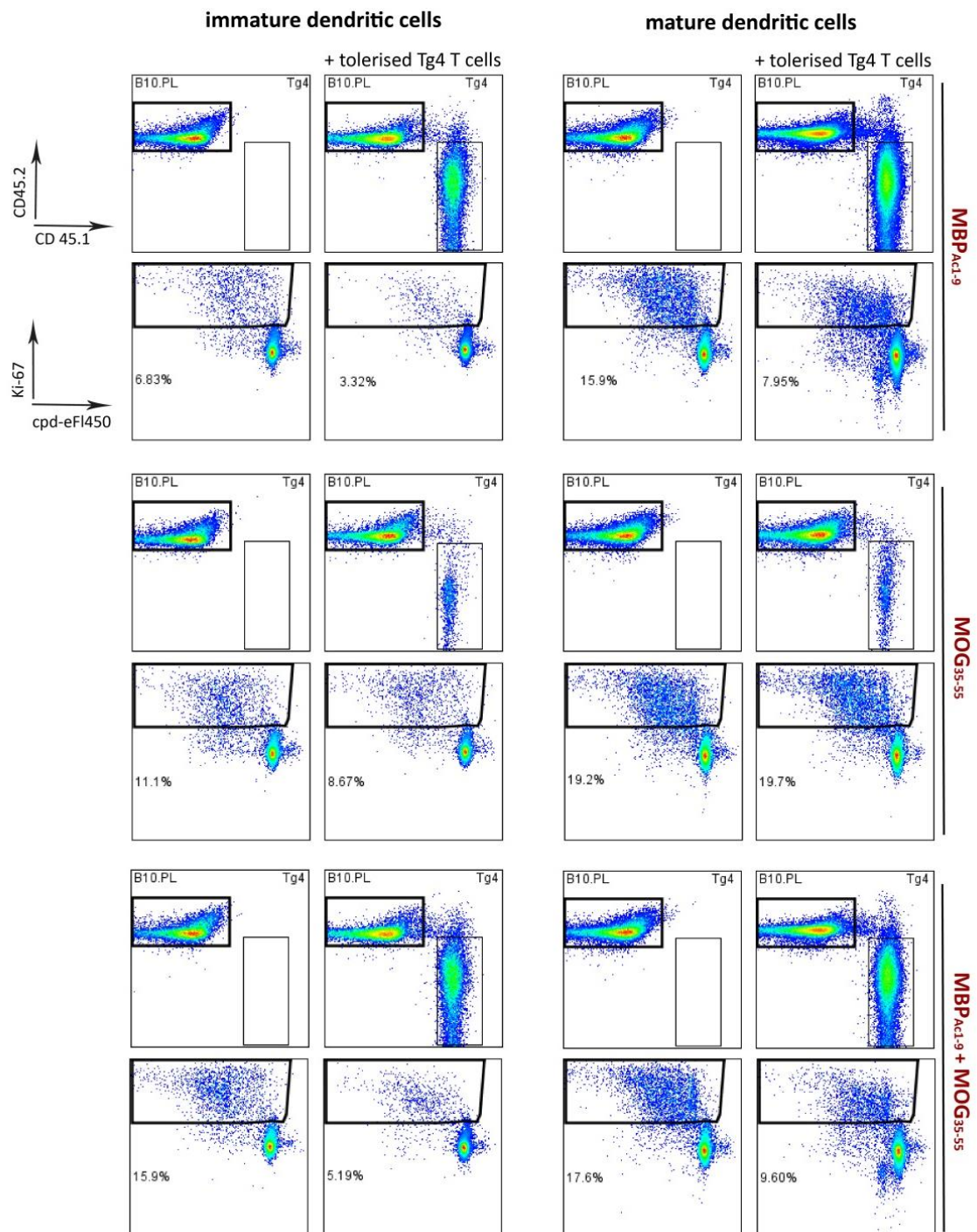
**Figure 4.23. *In vitro* bystander suppression by tolerised CD4+ T cells.** Representative FACS dot plots of antigen-experienced B10.PL x C57BL/6 ($T_{conv}$) cells labelled with cpd-eFl450 cultured without or with tolerised TG4 CD45.1+ T cells ($T_{tol}$) and stimulated with 10 μg/ml $MBP_{Ac1-9}(4K)$, 10 μg/ml $MOG_{35-55}$ or a mixture of both in the presence of immature or mature DCs. Gated on viable single CD4+ T cells. Proliferative cells are cpd-eFl450+ Ki76+. Shown is one representative experiment out of two.

**Table 4.1. *In vitro* bystander suppression by tolerised CD4⁺ T cells.** Antigen-experienced B10.PL x C57BL/6 ($T_{conv}$) cells labelled with cpd-eFl450 cultured without or with tolerised TG4 CD45.1⁺ T cells ($T_{tol}$) and stimulated with 10 µg/ml $MBP_{Ac1-9}(4K)$, 10 µg/ml $MOG_{35-55}$ or a mixture of both in the presence of immature or mature DCs. Gated on viable, single CD4⁺ T cells. Proliferative cells are cpd-eFl450⁺ Ki67⁺. Shown are the results of two experiments.

| | immature DC | | | | | | mature DC | | | | | |
|---|---|---|---|---|---|---|---|---|---|---|---|---|
| | MBP | MBP + $T_{tol}$ | MOG | MOG + $T_{tol}$ | MBP + MOG | MBP + MOG + $T_{tol}$ | MBP | MBP + $T_{tol}$ | MOG | MOG + $T_{tol}$ | MBP + MOG | MBP + MOG + $T_{tol}$ |
| % cpd-eFl450⁺ Ki67⁺ | 6.83 | 3.32 | 11.1 | 8.67 | 15.9 | 5.19 | 15.9 | 7.95 | 19.2 | 19.7 | 17.6 | 9.6 |
| | 7.92 | 3.89 | 14.2 | 8.69 | 12.8 | 7.09 | 9.84 | 4.07 | 12.2 | 11.2 | 14.5 | 9.56 |

#### 4.4.1.1 *Ex vivo* response to linked peptides in B10.PL x C57BL/6 mice

In order to be able to assess bystander suppression *in vivo*, we first had to determine if we could get an antigen-specific response in (B10.PL x C57BL/6)F1 mice to both $MBP_{Ac1-9}(4K)$ and $MOG_{35-55}$ (Figure 4.24. A). *Ex vivo*, splenocytes of (B10.PL x C57BL/6)F1 mice immunised with a mixture of both peptides each 0.04 mmol in CFA (which corresponds to 100 µg of $MOG_{35-55}$ and 43 ug of $MBP_{Ac1-9}(4K)$) showed a dose-dependent proliferative response in a ³H-Thymidine incorporation assay when stimulated with either $MBP_{Ac1-9}(4K)$ or $MOG_{35-55}$, while there was no proliferative response to the peptides in splenocytes from mice challenged with CFA only (Figure 4.24. **A**). We wanted to test the assumption that for bystander suppression to work the second antigen should be presented by the same APC as the antigen against which tolerance was established. To achieve this, we used the linker sequence HFFK to fuse both $MBP_{Ac1-9}(4K)$ and $MOG_{35-55}$ peptides together. We tested the functionality of these linked peptides *in vivo* compared to the priming effect of the separate peptides (Figure 4.24. **B**). Upon *ex vivo* restimulation, splenocytes isolated from mice primed with the linked peptide in CFA elicited to the same extent a proliferation response to $MOG_{35-55}$ as mice primed with a combination of their unlinked counterparts. The response to $MBP_{Ac1-9}(4K)$ was reduced when mice were antigen-challenged with the linked fusion peptide compared to mice primed with the individual peptides (Figure 4.24 **B**). To control for

the functionality of the MBP$_{Ac1-9}$(4K) sequence in the linked peptide, we use a control peptide where the MBP$_{Ac1-9}$(4K) sequence was scrambled randomly, whereas the MOG$_{35-55}$ sequence was unaltered. As expected, this scrambled linked peptide was non-functional in eliciting a response to MBP$_{Ac1-9}$(4K), whereas the response to MOG$_{35-55}$ was similar to that elicited by the functional linked peptide or the equal mixture of the individual peptides (Figure 4.24. **B**).
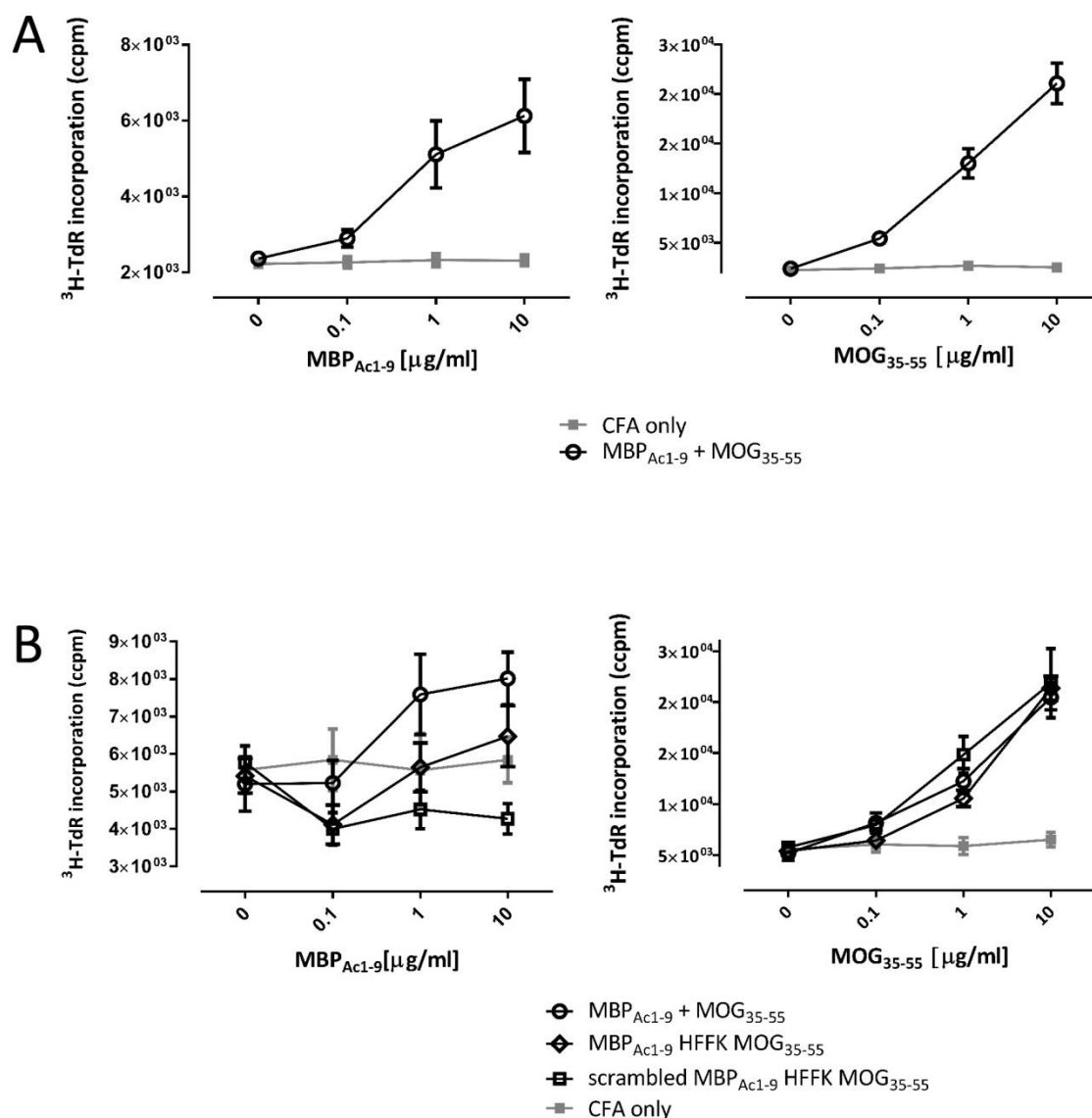


**Figure 4.24.** *Ex vivo* **response after priming with unlinked and linked peptides in B10.PL x C57BL/6 mice. A)** (B.10PL x C57BL/6)F1 mice were primed with a mixture of MBP$_{Ac1-9}$(4K) and MOG$_{35-55}$ in CFA. Splenocytes were isolated after 10 days and a $^3$H-Thymidine incorporation assay (mean ± SEM) was set up with titrated doses of the peptides MBP$_{Ac1-9}$(4K) and MOG$_{35-55}$. Line graph shows mean ± SEM (n = 6 per group). **B)** Splenocytes of B.10 PL x C57BL/6 mice

primed with a mixture of $MBP_{Ac1-9}$(4K) + $MOG_{35-55}$, the linked peptide $MBP_{Ac1-9}$(4K)-HFFK-$MOG_{35-55}$, a version of the linked peptide where the $MBP_{Ac1-9}$(4K) sequence was scrambled, or CFA only were restimulated *ex vivo* with $MBP_{Ac1-9}$(4K) or $MOG_{35-55}$ at titrated doses. Proliferation assessed by $^3$H thymidine incorporation after 72h. Line graph shows mean ± SEM (n = 4 per group).

### 4.4.2  *In vivo* bystander suppression

After we made sure that the linked peptides function as desired *in vivo*, we transferred CD4$^+$ T cells from $MBP_{Ac1-9}$(4Y)-tolerised Tg4 mice into (B10.PL x C57BL/6)F1 recipients i.p. and primed them with adjuvant with either linked peptides or the mixture of the individual peptides. Tg4 CD4$^+$ $T_{tol}$ were able to reduce the proliferative response to $MBP_{Ac1-9}$ *ex vivo* when mice were primed with a mixture of $MBP_{Ac1-9}$(4K) and $MOG_{35-55}$ in CFA compared to mice receiving no CD4$^+$ $T_{tol}$ transfer (Figure 4.25. **A**). The same trend was apparent when mice received CD4$^+$ $T_{tol}$ and were primed with the original sequence linked peptide. Priming with the linked peptide containing the scrambled version of $MBP_{Ac1-9}$(4K), with or without CD4$^+$ $T_{tol}$ transfer, did not induce a proliferative response to $MBP_{Ac1-9}$(4K). Tg4 CD4$^+$ $T_{tol}$ cells were only able to reduce the proliferation of (B10.PL x C57Bl/6)F1 splenocytes in response to $MOG_{35-55}$ at the highest concentration when mice were primed with a mixture of the individual peptides compared to mice receiving no cell transfer (Figure 4.25. **B**). When both peptides were presented by the same APC, as in the case of priming with the linked $MBP_{Ac1-9}$(4K)-HFFK-$MOG_{35-55}$ peptide, $MBP_{Ac1-9}$-specific CD4$^+$ $T_{tol}$ significantly reduced the proliferative response to $MOG_{35-55}$ at all concentrations tested. Tg4 $T_{tol}$ did not suppress the proliferative response to $MOG_{35-55}$ *ex vivo* when mice were primed with the linked peptide containing the scrambled version of $MBP_{Ac1-9}$. These findings corroborate the *in vitro* finding that MBP-specific CD4$^+$ Ttol cells can suppress CD4$^+$ T cell responses not only to their own cognate antigen, but also to related antigens if they are present in the same microenvironment.
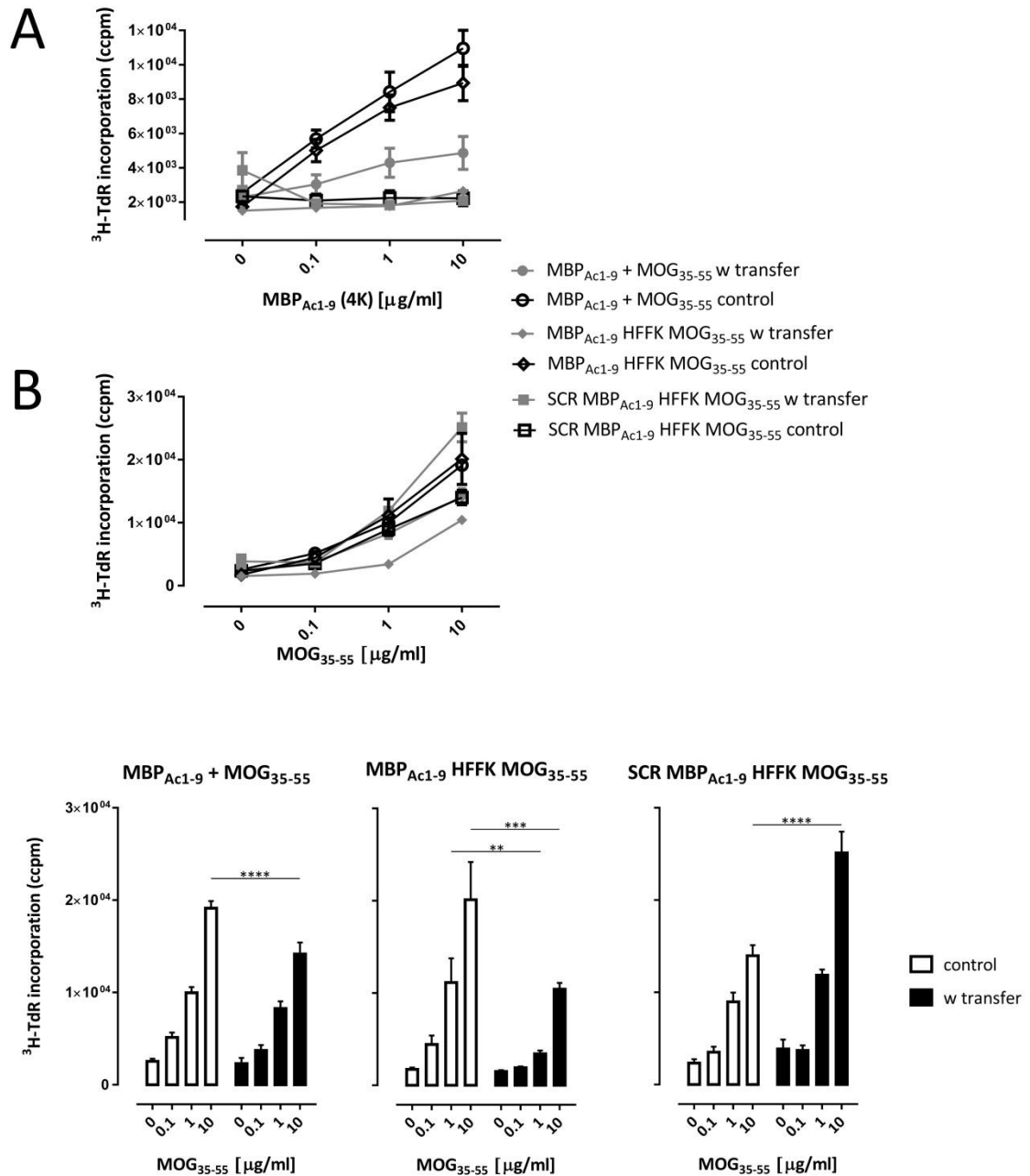
**Figure 4.25.** *In vivo* **bystander suppression.** Shown is the proliferative response ($^3$H-thymidine incorporation) of B10.PL x C57BL/6 splenocytes from mice primed with various peptides in CFA, with or without a transfer of 5 x 10$^6$ CD4$^+$ T$_{tol}$ cells from MBP$_{Ac1-9}$(4Y)-tolerised Tg4 in response to MBP (**A**) and MOG (**B**) Data shown as mean ± SEM. The MOG-response is also shown as a bar graph (mean + SEM) to facilitate easy comparison. After checking for normality using the Shapiro-Wilk test ANOVA followed by Sidak's multiple comparison test was performed (* = p ≤ 0.05, ** = p ≤ 0.01, *** = p ≤ 0.001, **** = p ≤ 0.0001) (n = 3 per group).

### 4.5 The role of myeloid-derived suppressor cells during antigen-specific peptide immunotherapy of autoimmune disease

This following body of work has demonstrated for the first time that myeloid-derived suppressor cells (MDSCs) accumulate during the course of peptide immunotherapy. Two subpopulations of MDSCs are currently known in mice; monocytic MDSCs (M-MDSCs) characterised by a $CD11b^+$ $Ly6G^-$ $Ly6C^{high}$ phenotype and polymorphonuclear MDSCs (PMN-MDSCs) that have a $CD11b^+$ $Ly6G^+$ $Ly6C^{low}$ phenotype. During the course of escalation-dose immunotherapy with $MBP_{Ac1-9}$(4Y), we noticed a more pronounced increase of PMN-MDSCs than M-MDSCs in spleen, ILN, BLN, liver, lung, brain and spinal cord (Figure 4.26. **A+B**). In the spleen, PMN-MDSCs were increased from 14% in the PBS control group to 37.6% post EDI compared to an increase in M-MDSC from 3.3% to 4.8%. In the lymph nodes, both subsets of MDSCs were nearly absent in control mice, as expected from the literature (Figure 4.26. **A**), whereas we did observe a small increase to about ~3% in the frequency of M-MDSCs in $MBP_{Ac1-9}$(4Y)-treated animals (Figure 4.26. **B**). The ample increase of PMN-MDSCs in the lymph nodes was more pronounced and we detected an increase of ~30 to 40% as a result of peptide treatment. In the liver we did not detect any changes in the percentages of M-MDSCs whereas PMN-MDSCs were increased from 13.7% to 32.6% during the course of EDI. The lung was the only organ where we observed an increase in the frequency of both MDSC subsets. Here, results showed an increase up to ~30% after $MBP_{Ac1-9}$(4Y)-treatment for both MDSC populations. Considering these results, we decided to concentrate on PMN-MDSCs for further experiments.
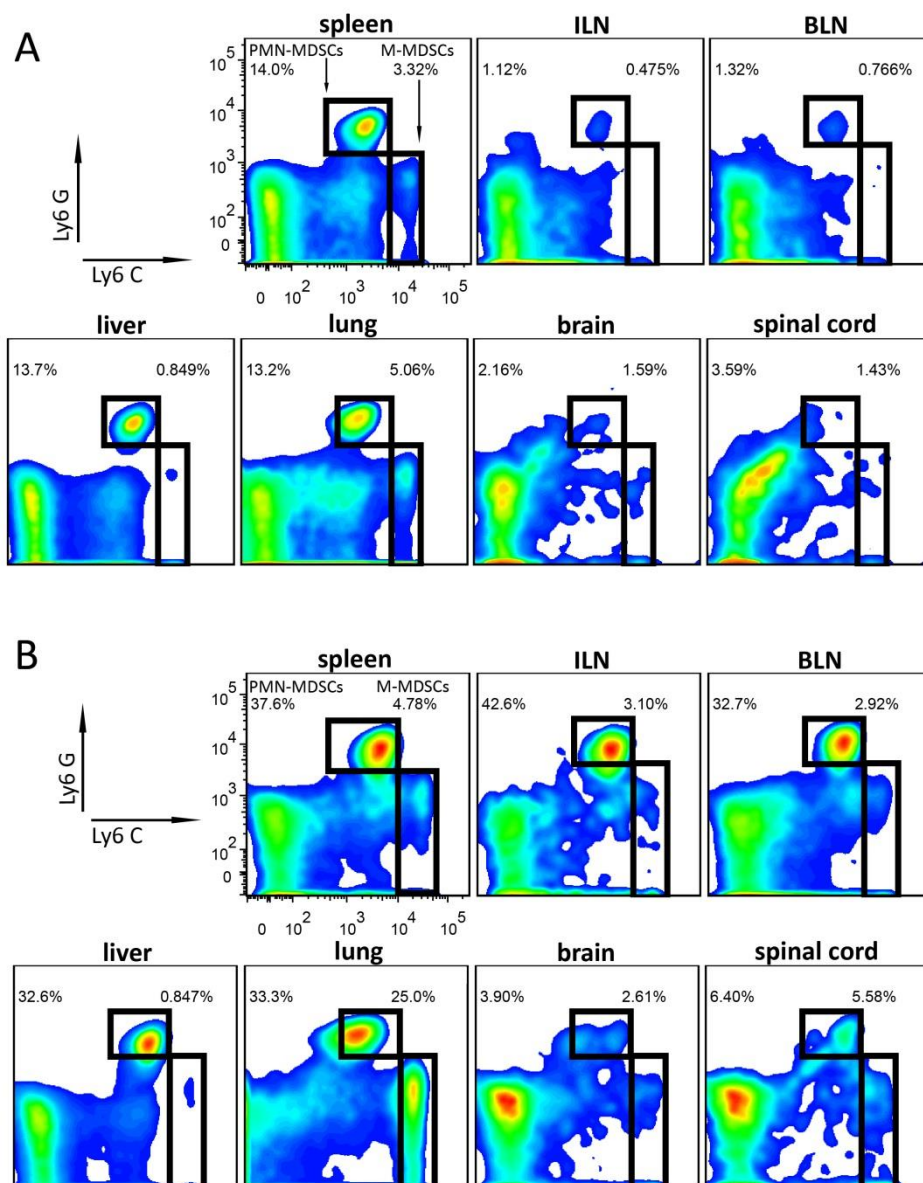
**Figure 4.26. Changes in the expression of M-MDSCs and PMN-MDSCs during EDI.** Shown are representative FACS plots from different organs from PBS-treated and MBP$_{Ac1-9}$(4Y)-treated TG4$^{IL-10/GFP}$ animals, gated on single, viable CD11b$^+$ cells. Organs from PBS controls (**A**) or MBP$_{Ac1-9}$(4Y)-animals (**B**) were isolated and stained with a panel of antibodies and two subpopulations of MDSCs were identified by flow cytometry. Representative of three individual experiments.

### 4.5.1 PMN-MDSC dynamics during EDI

During the course of MBP$_{Ac1-9}$(4Y)-dose escalation we noticed that percentages of PMN-MDSCs were significantly increased after the 3$^{rd}$ dose rather than the 5$^{th}$ dose in the spleen, with up to ~4%, and ILNs, with ~2% on average (Figure 4.27. **A**). In the BLNs and lungs we also observed a significant increase of PMN-MDSCs after the 5$^{th}$ dose (p ≤ 0.05) but the significance after the 3$^{rd}$ dose was higher (p ≤ 0.01) compared to PBS as a control. PMN-MDSCs in the liver were upregulated significantly after the 5$^{th}$ dose (p ≤ 0.01) while there was no change after the 3$^{rd}$ dose of peptide treatment. In the brain, PMN-MDSCs frequencies of tolerised mice were significantly increased after the 3$^{rd}$ dose (p ≤ 0.05) rather than the 5$^{th}$ dose, compared to control mice while we could not detect differences in PMN-MDSCs percentages in the spinal cord. In addition to the frequency of MDSCs, we also assessed absolute cell numbers for the different organs (Figure 4.27. **B**). These revealed a very similar pattern to the changes in the percentages. In the spleen, the absolute cell numbers were significantly upregulated with 4 x 10$^6$ PMN-MDSCs on average after the 3$^{rd}$ and 5$^{th}$ doses of peptide treatment (p ≤ 0.01), up from ~1 x 10$^6$ pre-treatment. The cell numbers in the lymph nodes and lung were significantly increased after the 3$^{rd}$ dose (p ≤ 0.001) with 3 x 10$^5$ cells on average in the lymph nodes and 9 x 10$^6$ cells on average in the lung compared to control mice. Hepatic PMN-MDSCs cell numbers were increased significantly after the 5$^{th}$ dose of MBP$_{Ac1-9}$(4Y) (p ≤ 0.05), whereas there was no change in cell numbers in the CNS compartment compared to control mice.
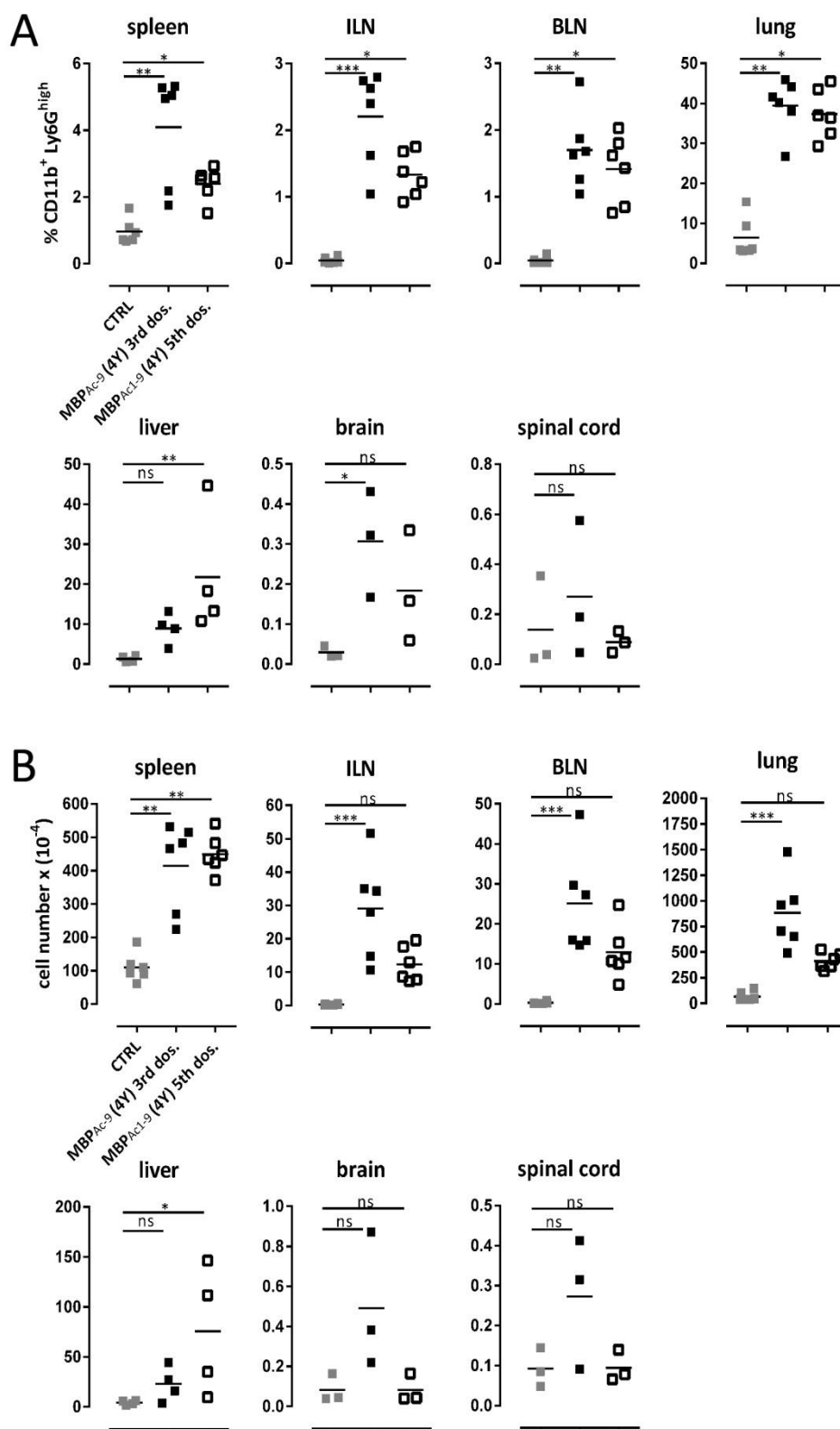
**Figure 4.27. PMN-MDSC dynamics in percentages and absolute cell numbers during EDI.** Shown is the frequency (**A**) and absolute cell numbers (**B**) of PMN-MDSCs during EDI after the 3rd and 5th dose of MBP$_{Ac1-9}$(4Y) in the spleen, ILNs, BLNs, lung ,liver, brain and spinal

cord compared to control mice receiving one dose of PBS. The gating strategy excluded dead cells and doublets. Horizontal lines indicate mean. After checking for normality using the Shapiro-Wilk test the Kruskal-Wallice test followed by Dunn's multiple comparison test for data that were not normally distributed was used (* = p ≤ 0.05, ** = p ≤ 0.01, *** = p ≤ 0.001, **** = p ≤ 0.0001). ). In the spleen, ILNs, BLNs and lung each dot represents one individual. In the liver in some cases cells from two animals were combined due to low cell numbers while in the CNS compartment each dot represents two individuals. N=6, from two independent experiments.

### 4.5.2 PMN-MDSC signature induced by dose escalation immunotherapy after the 3$^{rd}$ dose

The more significant accumulation of PMN-MDSCs and the coinciding increase of CD4$^+$ Foxp3$^+$ T cells after the 3$^{rd}$ dose of peptide treatment led us to further investigate PMN-MDSC phenotype and function at this point. We hypothesised that PMN-MDSCs-T cell-interaction could have provoked the increased accumulation of CD4$^+$ Foxp3$^+$ T cells *in vivo* as a result of peptide treatment because published work from other groups showed that MDSCs can induce CD4$^+$ Foxp3$^+$ T cell *in vitro*. It partially precedes and also coincides with the changes in CD4$^+$ T cell phenotype that characterise the EDI protocol, namely the reduction in effector cytokines and the switch on of IL-10-production in CD4$^+$ T cells. To further characterise the phenotype of PMN-MDSCs and find ways in which they influence the function of CD4$^+$ T cells during the course of EDI, we investigated several markers that can influence CD4$^+$ T cell activation, including Galectin-9, PD-L1, CD40, CD80 and CD86. Representative staining of splenic PMN-MDSCs is shown in Figure 4.28. **A**. After gating on viable single cells, co-staining of CD11b and Ly6G was used to identify PMN-MDSC in Tg4 mice. Thereafter, expression of the various markers on PMN-MDSC was evaluated. The extent to which expression of these markers on PMN-MDSCs was altered by EDI varied greatly depending on the location of cells. For example, Galectin-9 expression was increased up to ~70% on splenic PMN-MDSC (p ≤ 0.001) and a more minor increase up to 15% on average was detected on lung PMN-MDSC (p ≤ 0.05) compared to mice receiving PBS, in which the expression of Galectin-9 was only ~5% (Figure 4.28 **B**). In other organs there was no statistically significant difference in Galectin-9 expression. Furthermore, PD-L1 expression was significantly increased on splenic PMN-MDSCs (p ≤ 0.0001) but was decreased significantly on lung PMN-MDSCs (p ≤ 0.001). There was no difference in CD40 expression in any of the organs evaluated. CD80 expression on PMN-MDSCs trended towards a reduction

in MBP$_{Ac1-9}$(4Y)-treated animals but this was significant only in the ILNs (p ≤ 0.01). In contrast, the expression of CD86 generally showed the reverse trend of CD80, although the increased expression after MBP$_{Ac1-9}$(4Y)-treatment only reached significance in the spleen (p ≤ 0.05).
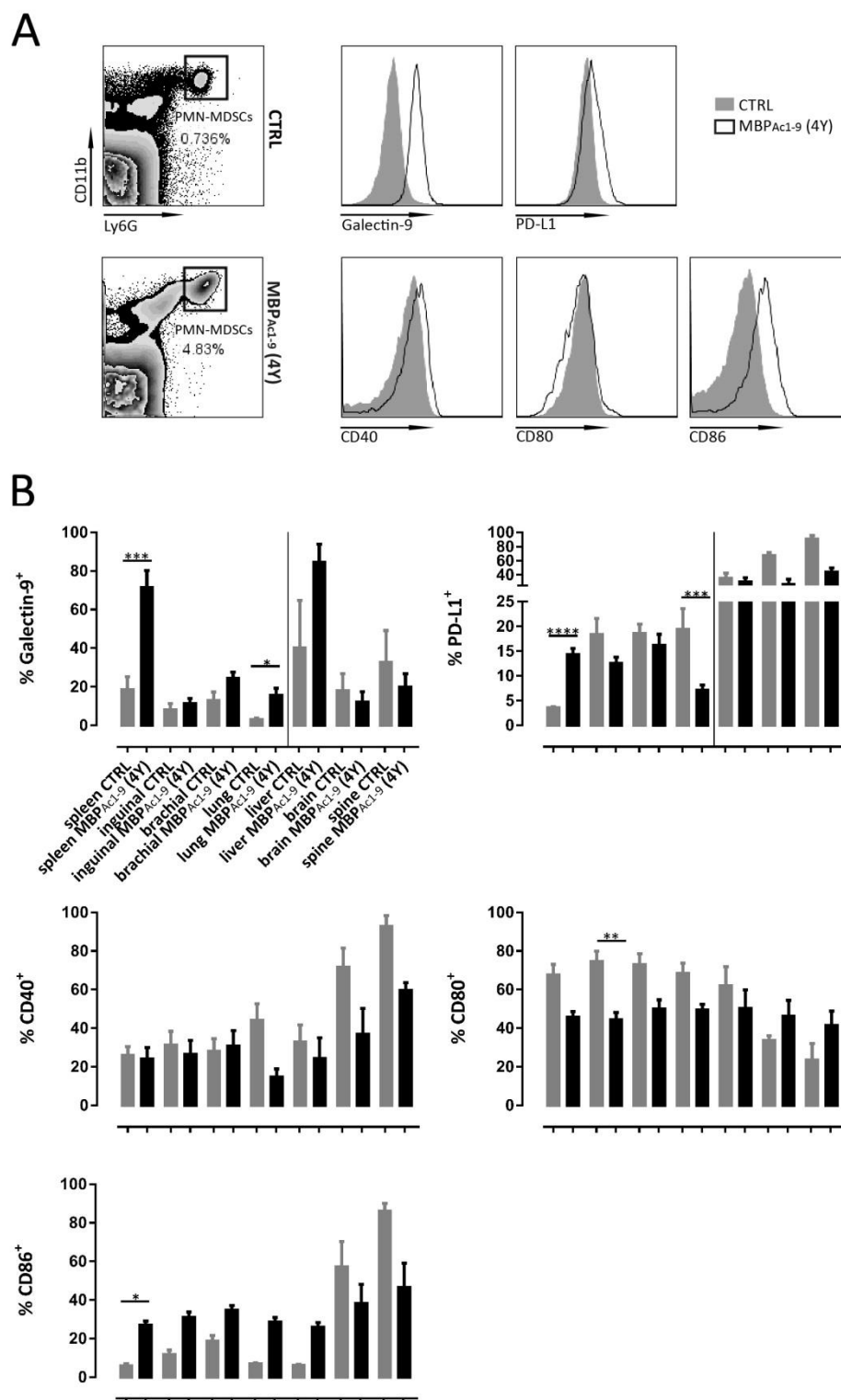
**Figure 4.28. Phenotypic analysis of PMN-MDSCs after dose escalation immunotherapy. A**) Representative flow cytometry plot of splenic PMN-MDSCs from MBP$_{Ac1-9}$(4Y)- and PBS-treated animals after gating on viable CD11b$^+$ Ly6G$^+$ cells and comparison of Galectin-9, PD-L1, CD40, CD80 and CD86 expression shown as histogram overlays. **B**) Bar graph shows mean

[+] SEM. After checking for normality using the Shapiro-Wilk test either ANOVA followed by Sidak's multiple comparison test was performed for normally distributed data or the Kruskal-Wallice test followed by Dunn's multiple comparison test for data that were not normally distributed (* = p ≤ 0.05, ** = p ≤ 0.01, *** = p ≤ 0.001, **** = p ≤ 0.0001). Data on the left hand side of the vertical line had a normal distribution. In the spleen, ILNs, BLNs and lung each bar graph represents six individuals. In the liver in some cases cells from two animals were combined due to low cell numbers (n = 4) while in the CNS compartment each measurement contained cells from two animals. Kruskal-Wallice test followed by Dunn's multiple comparison test was applied to CD40, CD80 and CD86 data. N=6, from two independent experiments.

### 4.5.3   Frequencies of PMN-MDSCs in peripheral organs in health and disease

As explained in the introduction, the accumulation of MDSCs has previously been associated with both the pathogenesis of autoimmune disease and the maintenance of peripheral tolerance. To assess the dynamics of PMN-MDSCs during EAE in the TG4 model, mice were either treated with $MBP_{Ac1-9}$(4Y) to confer protection or with PBS only as a control, prior to the induction of EAE by priming with $MBP_{Ac1-9}$(4K) in CFA and pertussis toxin. Animals were harvested at the peak of disease when PBS-treated animals had an average disease score of 3 with complete hind limb paralysis (typically around day 14 post prime). $MBP_{Ac1-9}$(4Y)-treated animals, which displayed no EAE symptoms, were taken at the same time of analysis. This confirmed that indeed the frequency of PMN-MDSCs was increased in animals in which EAE was induced compared to animals that were not primed for disease (Figure 4.29. compared to Figure 4.27. **A**). In fact, the frequency of PMN-MDSC in mice with EAE was significantly higher in many of the organs examined compared to mice that had been tolerised using EDI. This then prompted the question whether the PMN-MDSC that arise during the development of EAE are phenotypically different from the ones that are generated during tolerisation and therefore fail to offer protection.
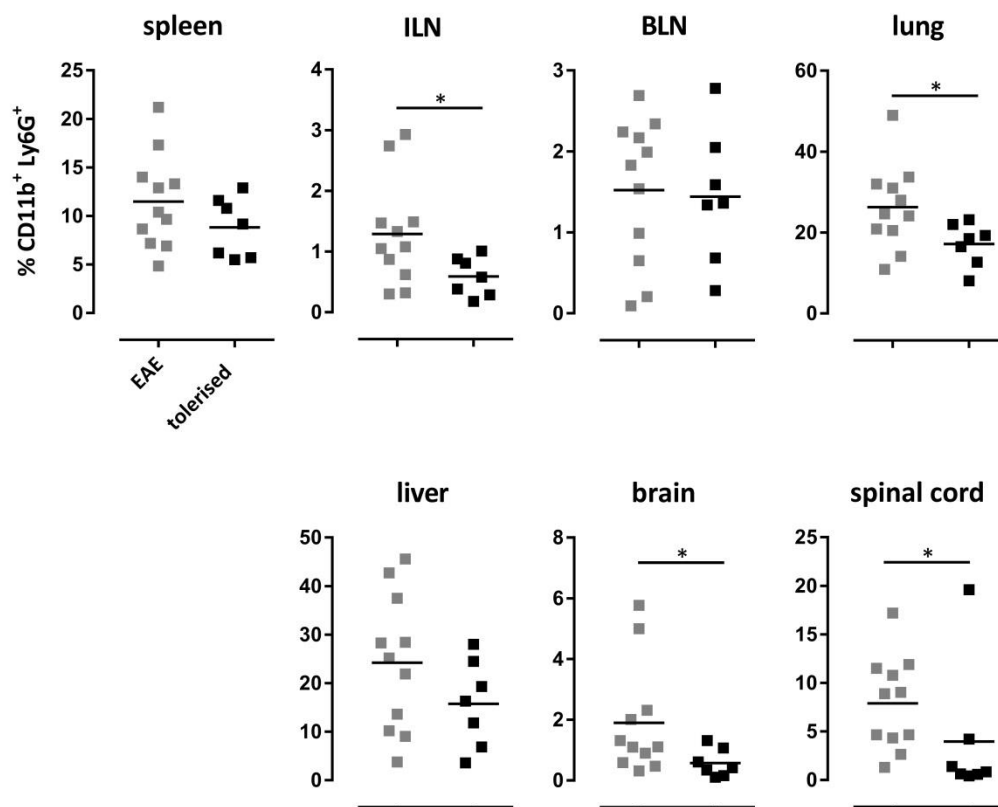
**Figure 4.29. Frequencies of PMN-MDSCs in peripheral organs in health and disease.** Tg4 mice were treated with PBS or $MBP_{Ac1-9}$(4Y)-EDI before the induction of EAE with their cognate peptide in CFA, and pertussis toxin given on days 0 and 2 post prime. Animals were analysed at the peak of disease when mice treated with PBS showed complete hind limb paralysis (grade 3) and EDI-treated animals showed no sign of disease. Shown are single, viable $CD11b^+$ $Ly6G^+$ cells. Horizontal lines indicate mean. After checking for normality using the Shapiro-Wilk test the unpaired t test was performed for normally distributed data (* = p ≤ 0.05, ** = p ≤ 0.01, *** = p ≤ 0.001, **** = p ≤ 0.0001). Each dot represents one individual, n=7-11. Pooled data from three independent experiments.

#### 4.5.3.1 Phenotype of PMN-MDSCs in diseased versus tolerised mice

Following the assessment of PMN-MDSC numbers during EAE, we further characterised those myeloid cells and noticed a significant two-fold lower CD40 expression on PMN-MDSCs in the spinal cord of mice with EAE compared to tolerised animals (p ≤ 0.05), whereas the expression of CD40 was not different in spleen, lymph nodes, lung, liver and brain (Figure 4.30. **A**). Furthermore, we detected a significantly lower expression of CD80 in the CNS compartment both in the brain and spinal cord, in tolerised animals compared to animals

with EAE (p ≤ 0.01) (Figure 4.30. **B**). In contrast to the decreased expression of CD40 and CD80 in the CNS compartment in tolerised mice, we noticed an increased expression of Galectin-9 and PD-L1 in the spleen and lymph nodes in tolerised mice (Figure 4.31. **A+B**). No change in the expression of Galectin-9 and PD-L1 in the CNS compartment could be detected. These findings hint at the possibility that phenotypic differences between the PMN-MDSCs that develop after EAE development or after tolerisation play a role in their functional dichotomy. Following the assessment of PMN-MDSC numbers during EAE, we further characterised those myeloid cells and noticed a significant two-fold lower CD40 expression on PMN-MDSCs in the spinal cord of mice with EAE compared to tolerised animals (p ≤ 0.05), whereas the expression of CD40 was not different in spleen, lymph nodes, lung, liver and brain (Figure 4.30. A). Furthermore, we detected a significantly lower expression of CD80 in the CNS compartment both in the brain and spinal cord, in tolerised animals compared to animals with EAE (p ≤ 0.01) (Figure 4.30. B). In contrast to the decreased expression of CD40 and CD80 in the CNS compartment in tolerised mice, we noticed an increased expression of Galectin-9 and PD-L1 in the spleen and lymph nodes in tolerised mice (Figure 4.31. A+B). No change in the expression of Galectin-9 and PD-L1 in the CNS compartment could be detected. These findings hint at the possibility that phenotypic differences between the PMN-MDSCs that develop after EAE development or after tolerisation play a role in their functional dichotomy.

**Figure 4.30. Phenotype of PMN-MDSCs in diseased versus tolerised mice.** Tg4 mice were treated with PBS or MBP$_{Ac1-9}$(4Y)-EDI before the induction of EAE with their cognate peptide in CFA, and pertussis toxin given on days 0 and 2 post prime. Animals were analysed at the peak of disease when mice treated with PBS showed complete hind limb paralysis (grade 3) and EDI-treated animals showed no sign of disease. Single, viable PMN-MDSCs were analysed for the expression of CD40 (**A**) and CD80 (**B**). Horizontal lines indicate mean. After

checking for normality using the Shapiro-Wilk test either unpaired t test was performed for normally distributed data or the Mann-Whitney U test  for data that were not normally distributed (* = p ≤ 0.05, ** = p ≤ 0.01, *** = p ≤ 0.001, **** = p ≤ 0.0001). Each dot represents one individual, n=7-11. Pooled data from three independent experiments. Unpaired t test was applied to CNS data.
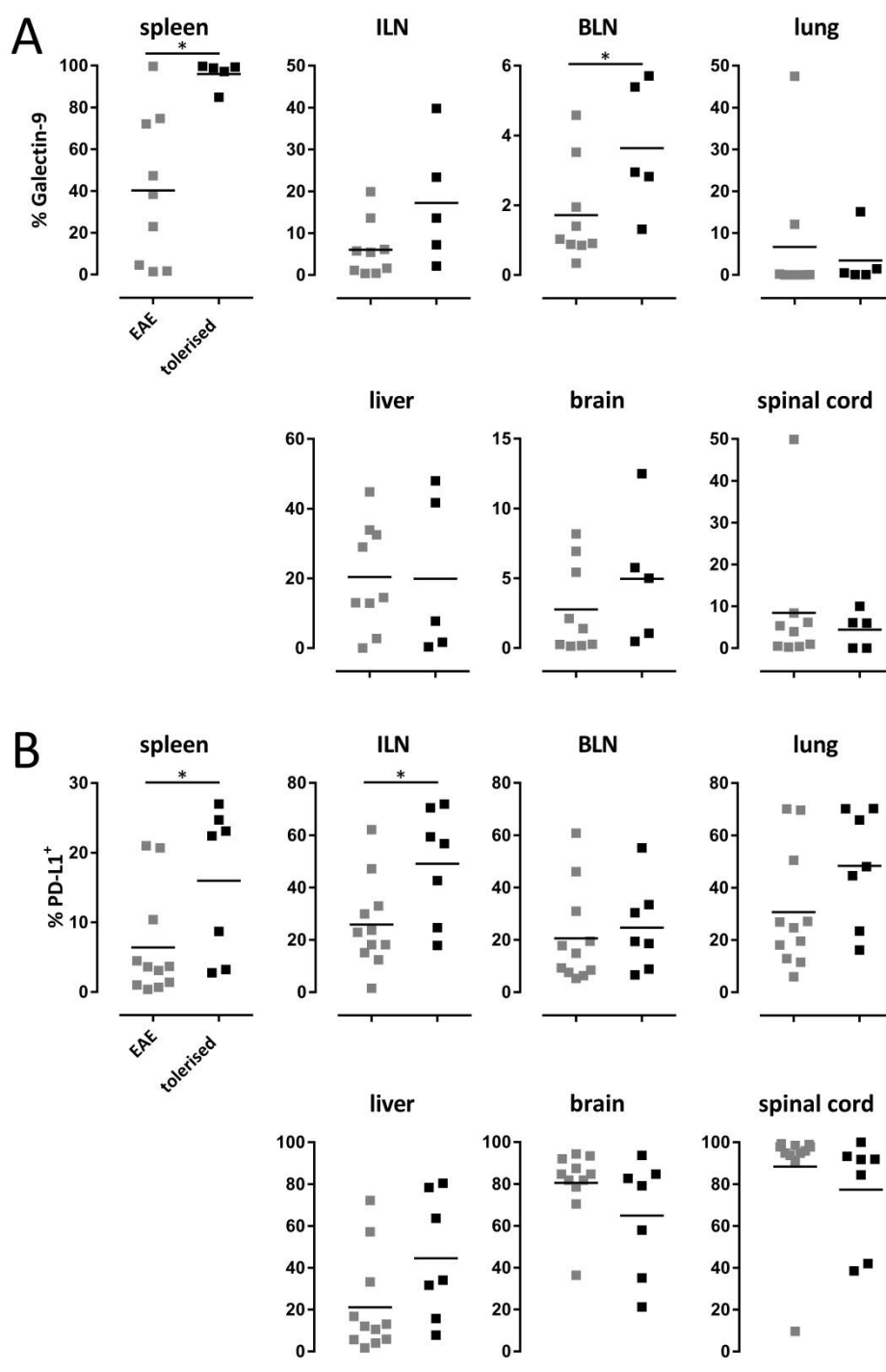
**Figure 4.31. Phenotype of PMN-MDSCs in diseased versus tolerised mice.** Tg4 mice were treated with PBS or MBP$_{Ac1-9}$(4Y)-EDI before the induction of EAE with their cognate peptide in CFA, and pertussis toxin given on days 0 and 2 post prime. Animals were analysed at the peak of disease when mice treated with PBS showed complete hind limb paralysis (grade 3) and EDI-treated animals showed no sign of disease. Single, viable PMN-MDSCs were analysed for the expression of Galectin-9 (**A**) and PD-L1 (**B**). Horizontal lines indicate mean.

After checking for normality using the Shapiro-Wilk test either unpaired t test was performed for normally distributed data or the Mann-Whitney U test for data that were not normally distributed (* = p ≤ 0.05, ** = p ≤ 0.01, *** = p ≤ 0.001, **** = p ≤ 0.0001). Each dot represents one individual, n=7-11. Pooled data from three independent experiments. Unpaired t test was applied to Galectin-9 BLN data and PD-L1 data whereas the Mann-Whitney U test was applied to spleen Galectin-9 data.

### 4.5.4 Splenic PMN-MDSC suppress the proliferation of naïve CD4$^+$ T cells *in vitro* in an antigen-specific manner

In order to establish whether the PMN-MDSCs that developed during EDI do indeed have immune regulatory properties, we assessed their effect on CD4$^+$ T cell proliferation *in vitro*. Naïve Tg4 CD4$^+$ T cells (T$_{naiv}$) and antigen-experienced CD4$^+$ T cells (T$_{ag}$) labelled with cell proliferation dye eFluor 450 (cpd-efl450) were co-cultured with CD11c$^+$ APCs and 10 µg/ml of cognate peptide, in the presence or absence of PMN-MDSCs from tolerised mice. After the co-culture for four days we measured CD4$^+$ T cell proliferation by flow cytometry and calculated the proliferation and division indexes. The former reflects the number of times that each responding cell has divided because it only takes cells into account that underwent at least one division. The latter is an average number of cell divisions that a cell in the original population has undergone, including cells that have not divided at all. These experiments revealed that addition of PMN-MDSCs to the T cell cultures reduced the division index of proliferating naïve CD4$^+$ T cell, but to our surprise, PMN-MDSCs were unable to reduce the proliferation of CD4$^+$ T$_{ag}$ cells (Figure 4.32. **A**). Importantly, addition of PMN-MDSCs led to the selective expansion of pre-existing CD4$^+$ Foxp3$^+$ regulatory T cells within the CD4$^+$ T cell population, although this only reached statistical significance in co-cultures containing CD4$^+$ T$_{ag}$ and not CD4$^+$ T$_{naiv}$ cells (Figure 4.32. **B**). This could potentially be explained by the additional requirement of IL-2 for optimal CD4$^+$ Treg cell expansion. This cytokine is secreted abundantly by CD4$^+$ T$_{ag}$ cells and not by CD4$^+$ T$_{naiv}$ cells.
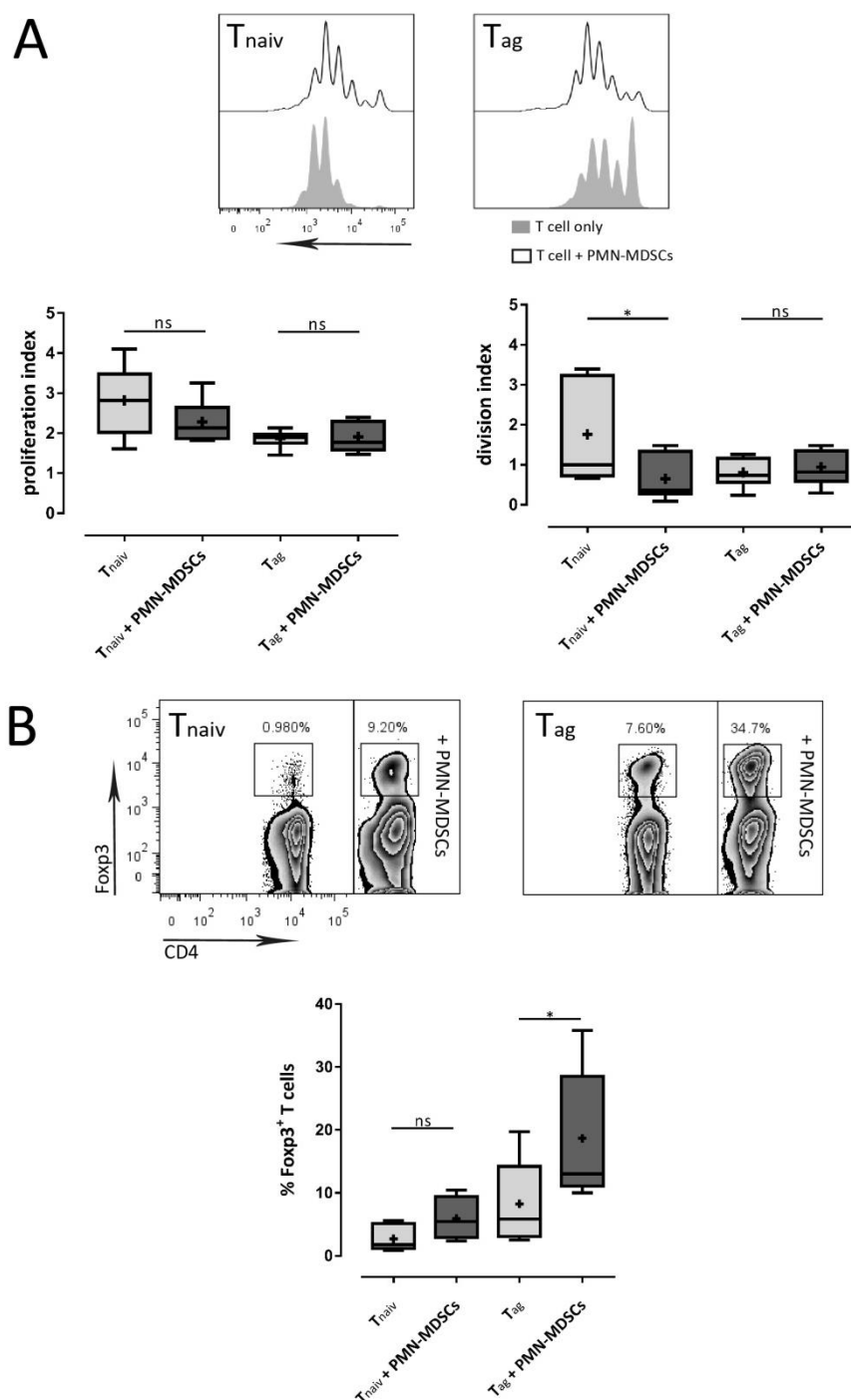
**Figure 4.32. Splenic PMN-MDSCs suppress the proliferation of naive CD4+ T cells *in vitro* in an antigen-specific manner.** PMN-MDSCs were co-cultured for four days together with naïve and antigen-experienced T cells labelled with cell proliferation dye at a ratio of 1:3 with their cognate peptide and CD11c+ cells used as APCs. Gated on single, viable CD4+ T cells. **A**) Proliferation of naïve (Tnaiv) and antigen-experienced CD4+ T cells (Tag) after culture with or without PMN-MDSCs (n=5). Box shows 25th to 75th percentiles. The horizontal line is plotted at the median. Whiskers show Min to Max. Mean is shown as a '+'. **B**) Foxp3 expression in CD4+ Tnaiv and CD4+ Tag after culture with or without PMN-MDSCc (n=5). Box

shows 25th to 75th percentiles. The horizontal line is plotted at the median. Whiskers show Min to Max. Mean is shown as a '+'. After checking for normality using the Shapiro-Wilk test ANOVA followed by Sidak's multiple comparison test was performed for normally distributed data (* = $p \leq 0.05$, ** = $p \leq 0.01$, *** = $p \leq 0.001$, **** = $p \leq 0.0001$).

### 4.5.5 Splenic PMN-MDSC suppress the proliferation of antigen-experienced CD4+ T cells activated by a non-specific stimulus *in vitro*

Next we sought to determine if, in addition to suppression in an antigen-specific manner, PMN-MDSC in the Tg4 model can act as non-specific repressors of CD4+ T cell proliferation *in vitro*. Either naïve CD4+ T cells ($T_{naiv}$) or antigen-experienced CD4+ T cells ($T_{ag}$), labelled with proliferation dye, were cultured together with PMN-MDSCs from tolerised mice on an anti-CD3+anti-CD28-coated plate at a ratio of 1:1 for four days. The suppressive activity of PMN-MDSCs is the main characteristic of MDSC but to make sure that this suppressive ability is the result of tolerance induction through EDI, we also isolated PMN-MDSCs from PBS-treated mice as a control and included those in our proliferation assays. PMN-MDSCs from tolerised mice were found to be potent non-specific immune suppressors because they reduced the division index of naïve CD4+ T cells significantly ($p \leq 0.01$, n=6) (Figure 4.33. **A**). On the other hand, PMN-MDSCs from control mice were not able to reduce the proliferation (n=3). The same phenomenon detected for CD4+ $T_{naiv}$ cells holds true for CD4+ $T_{ag}$ cells, as PMN-MDSCs from tolerised mice could suppress the proliferation and division index significantly, ($p \leq 0.05$) whereas control PMN-MDSCs could not suppress the proliferation of CD4+ $T_{ag}$ cells (Figure 4.33. **B**). In an attempt to unravel the mechanism though which the PMN-MDSCs from tolerised but not control mice exerted the suppressive effect on non-specific CD4+ T cell proliferation, we examined the production of ROS and NO. Supernatants were taken at day four of the co-culture and ROS and NO production were measured by Acridan Lumigen PS-3 assay for the first and Griess assay for the latter but no statistical differences were found although NO-production was increased in CD4+ T cell cultures with PMN-MDSCs compared to cultured CD4+ T cells alone (data not shown).
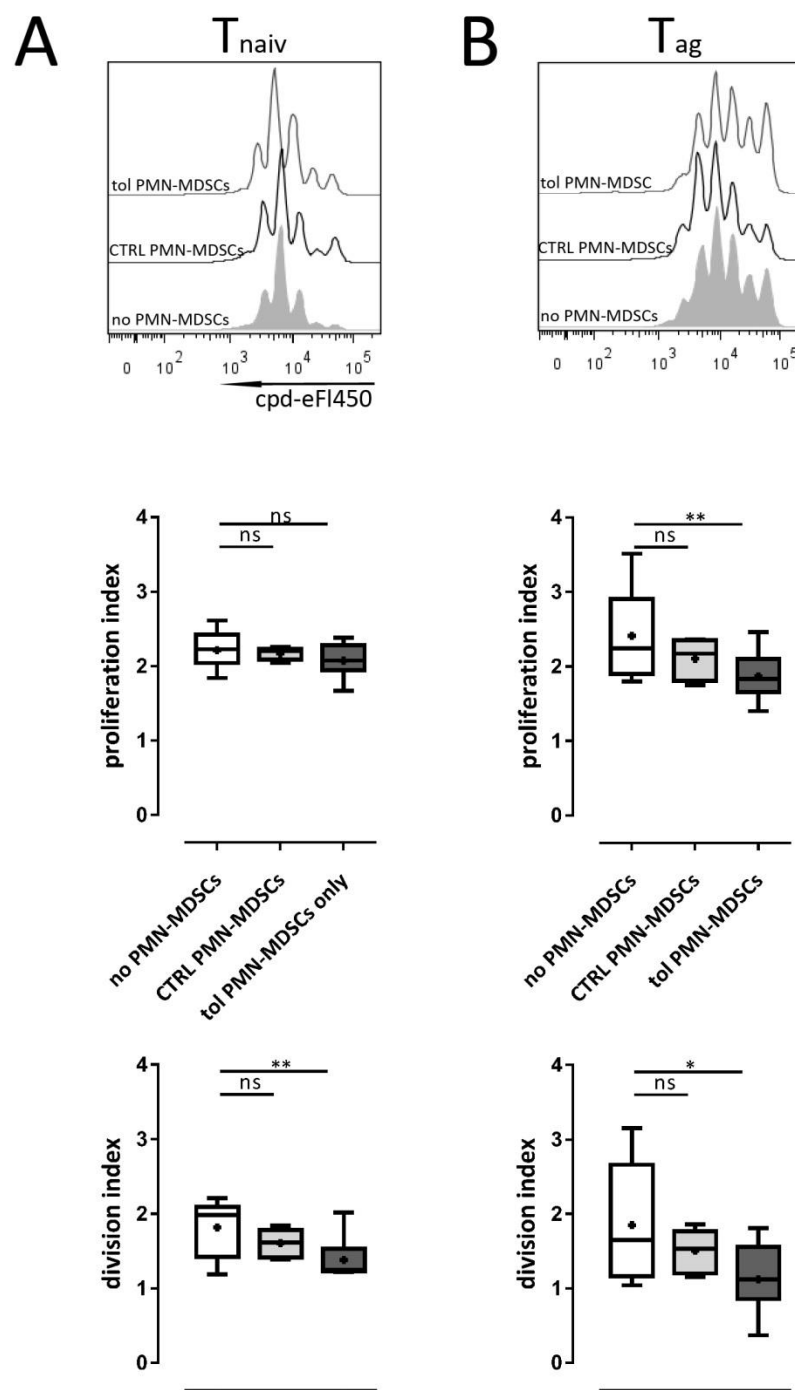
**Figure 4.33. Splenic PMN-MDSCs suppress CD4$^+$ T cell proliferation *in vitro* in response to plate-bound anti-CD3 and anti-CD28**. Naïve (**A**) or antigen-experienced CD4$^+$ T cells (**B**) labelled with cell proliferation dye, were cultured with PMN-MDSCs from either tolerised (n=6) or PBS-treated mice (n=3) on an anti-CD3+antiCD28-coated plate at a ratio of 1:1. Gated on single, viable CD4$^+$ T cells. Box shows 25th to 75th percentiles. The horizontal line is plotted at the median. Whiskers show Min to Max. Mean is shown as a '+'. Te Kruskal-Wallice test followed by Dunn's multiple comparison test was performed for data that were not normally distributed (* = p ≤ 0.05, ** = p ≤ 0.01, *** = p ≤ 0.001, **** = p ≤ 0.0001).

### 4.5.6 Splenic PMN-MDSCs suppress CD4^{+} T cell proliferation in a cell-contact dependent manner

In order to determine if the suppressive activity seen before is cell contact-dependent, Transwell experiments were performed. In these experiments, CD4^{+} $T_{ag}$ cells were cultured on an anti-CD3+anti-CD28-coated plate, separated by a membrane from splenic, FACS-sorted PMN-MDSC from tolerised Tg4 mice (ratio of 1:1). The suppression of CD4^{+} T cell proliferation by PMN-MDSCs described above was no longer apparent when the PMN-MDSCs and responder cells were physically separated (n=3) (Figure 4.34.). This result indicates that the PMN-MDSC-mediated suppression of CD4^{+} T cell proliferation is cell contact-dependent.
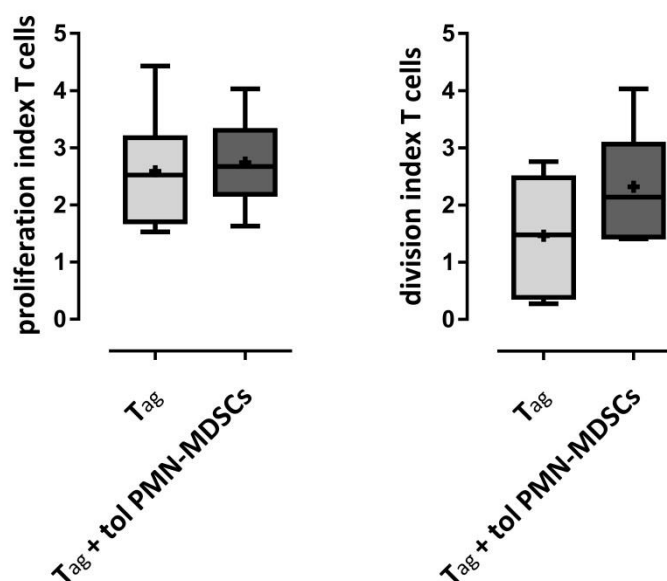


**Figure 4.34. Suppressive activity of PMN-MDSCs is contact dependent.** Splenic, FACS-sorted PMN-MDSC from tolerised mice and CD4^{+} $T_{ag}$ cells were cultured together at a ratio of 1:1 in on anti-CD3+anti-CD28-coated plate, separated by a membrane (n=3). Gated on single, viable CD4^{+} T cells. Box shows 25th to 75th percentiles. The horizontal line is plotted at the median. Whiskers show Min to Max. Mean is shown as a '+'.

### 4.5.7 Blockade of suggested mediators in cell contact-dependent suppression abrogate the suppressive effect of PMN-MDSCs *in vitro*

Several molecules have previously been suggested to mediate cell contact-dependent suppression by PMN-MDSCs. To investigate the molecules that may be involved in the suppressive effect of PMN-MDSCs, blocking antibodies targeting molecules expressed on the surface of PMN-MDSCs, namely Galectin-9, PD-L1, CD40, CD80 and CD86, or anti-IL-10R were added to the co-culture. In most of these conditions was the suppressive activity of PMN-MDSCs abrogated (Figure 4.35. **A**). The addition of anti-Galectin-9 or PD-L1 alone did not abrogate the suppressive activity of PMN-MDSCs while the co-blockade of both ligands restored CD4$^+$ T cell proliferation indicating a synergistic effect of Galectin-9 and PD-L1 in CD4$^+$ T cell suppression. IL-10 receptor signalling is not essential for the suppressive activity of PMN-MDSCs because in our *in vitro* suppression assay blockade of IL-10R signalling by an antibody (Figure 4.35 **A**) did not alleviate CD4$^+$ T cell suppression. The addition of the blocking antibodies targeting the surface molecules CD40, CD80 and CD86 restored CD4$^+$ T cell proliferation as well. Soluble factors may still be involved in mediating suppression of cells which are in close proximity. Therefore, the possible role of iNOS and arginase-1 in mediating the suppression of CD4$^+$ T cell proliferation by the PMN-MDSCs was investigated further by the addition of an inhibitor of iNOS, (NG-monomethyl-L-arginine (L-NMMA) or the inhibitor of arginase-1, (S-(2-boronoethyl)-L-cysteine (BEC) to the suppression assay at 500 µM (Figure 4.35. **B**). The addition of the arginase-1 inhibitor BEC abrogated the suppressive effect of PMN-MDSCs indicating that PMN-MDSCs use arginase-1 rather than iNOS for their suppressive activity. More recently, other mechanisms of suppression deployed by MDSCs were discovered, including the production of the enzyme indoleamine 2,3-dioxygenase (IDO). However, the addition of 1-methyl analogue of tryptophan (1-MT) to block IDO in our *in vitro* MDSC-T cell-co-cultures did not lead to abrogation of MDSC-mediated inhibition of T cell proliferation (data not shown). We were therefore able to determine the mechanism through which PMN-MDSCs from tolerised Tg4 mice exert their suppressive effect *in vitro*.
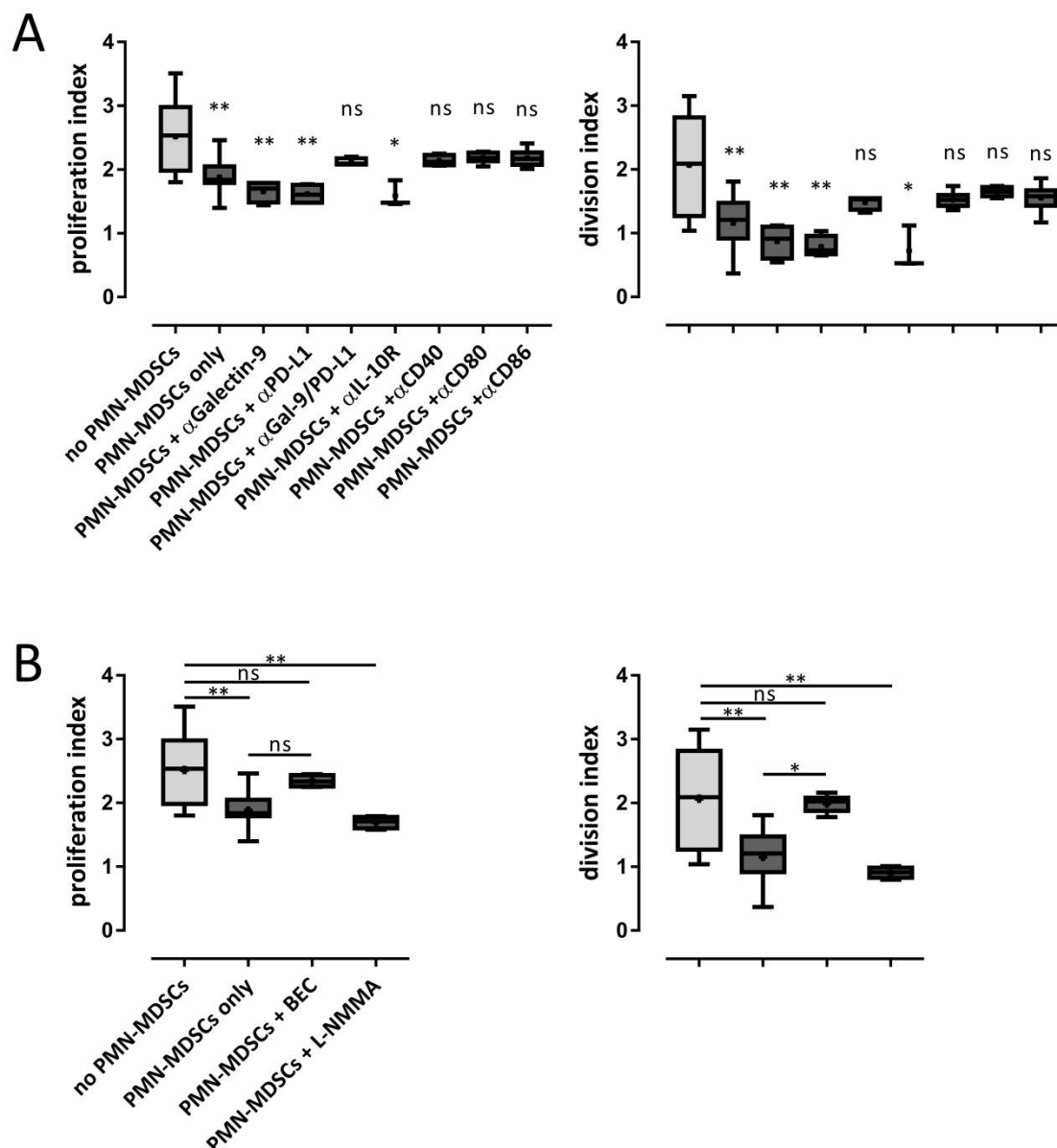
**Figure 4.35. Determination of the mechanism of PMN-MDSCs mediated CD4+ T cell suppression *in vitro*.** Splenic, FACS-sorted PMN-MDSC from tolerised mice and CD4+ Tag cells were cultured together at a ratio of 1:1 on an anti-CD3+anti-CD28-coated plate. **A**) Antibodies to Galectin-9, PD-L1, CD40, CD80, CD86 and IL-10R (10 μg/ml) or **B**) chemical inhibitors of NOS (L-NMMA) or arginase-1 (BEC) (both at 500 μM) were added for the duration of the culture (n = 3 each). Gated on single, viable CD4+ T cells. Box shows 25th to 75th percentiles. The horizontal line is plotted at the median. Whiskers show Min to Max. Mean is shown as a '+'. Kruskal-Wallice test followed by Dunn's multiple comparison test was performed (* = p ≤ 0.05, ** = p ≤ 0.01, *** = p ≤ 0.001, **** = p ≤ 0.0001).

### 4.5.8    PMN-MDSCs reduce CD4+ T cell proliferation after Ag challenge *in vivo*

In order to test if, in addition to their inhibitory effect *in vitro*, PMN-MDSCs are able to reduce the proliferation of CD4+ T cells *in vivo*, Tg4 mice received a cell transfer of $1.5 \times 10^6$ FACS sorted PMN-MDSC from tolerised mice i.p. three days before priming with $MBP_{Ac1-9}(4K)$ peptide in CFA at the base of the tail. Ten days later, spleen and ILNs were harvested and a $^3$H-Thymidine assay was set up. The proliferative response after restimulation *in vitro* with cognate peptide was significantly reduced in cells from the spleen but not the ILNs from mice that had received a transfer of PMN-MDSCs compared to mice that did not receive PMN-MDSCs (Figure 4.36. **A**). Next, to exclude the possibility that transferred PMN-MDSCs still present in the whole splenocyte suspensions mediate suppression of CD4+ T cell proliferation at the time of restimulation *in vitro*, CD4+ T cells were magnetically isolated from the spleen and a separate $^3$H-Thymidine assay was set up with titrated doses of $MBP_{Ac1-9}(4K)$ and irradiated APCs. Again, the proliferation of CD4+ T cells isolated from mice that had received a transfer of PMN-MDSCs was significantly reduced over a range of $MBP_{Ac1-9}(4K)$ peptide concentration compared to cells from mice who did not receive the transfer (Figure 4.36. **B**). In addition, intracellular cytokine staining demonstrated  a small but not significant reduction in the production of the proinflammatory cytokines IFN-γ or IL-17 by CD4+ T cells from animals that had received a PMN-MDSC transfer, upon restimulation with cognate antigen (Figure 4.36. **C**).
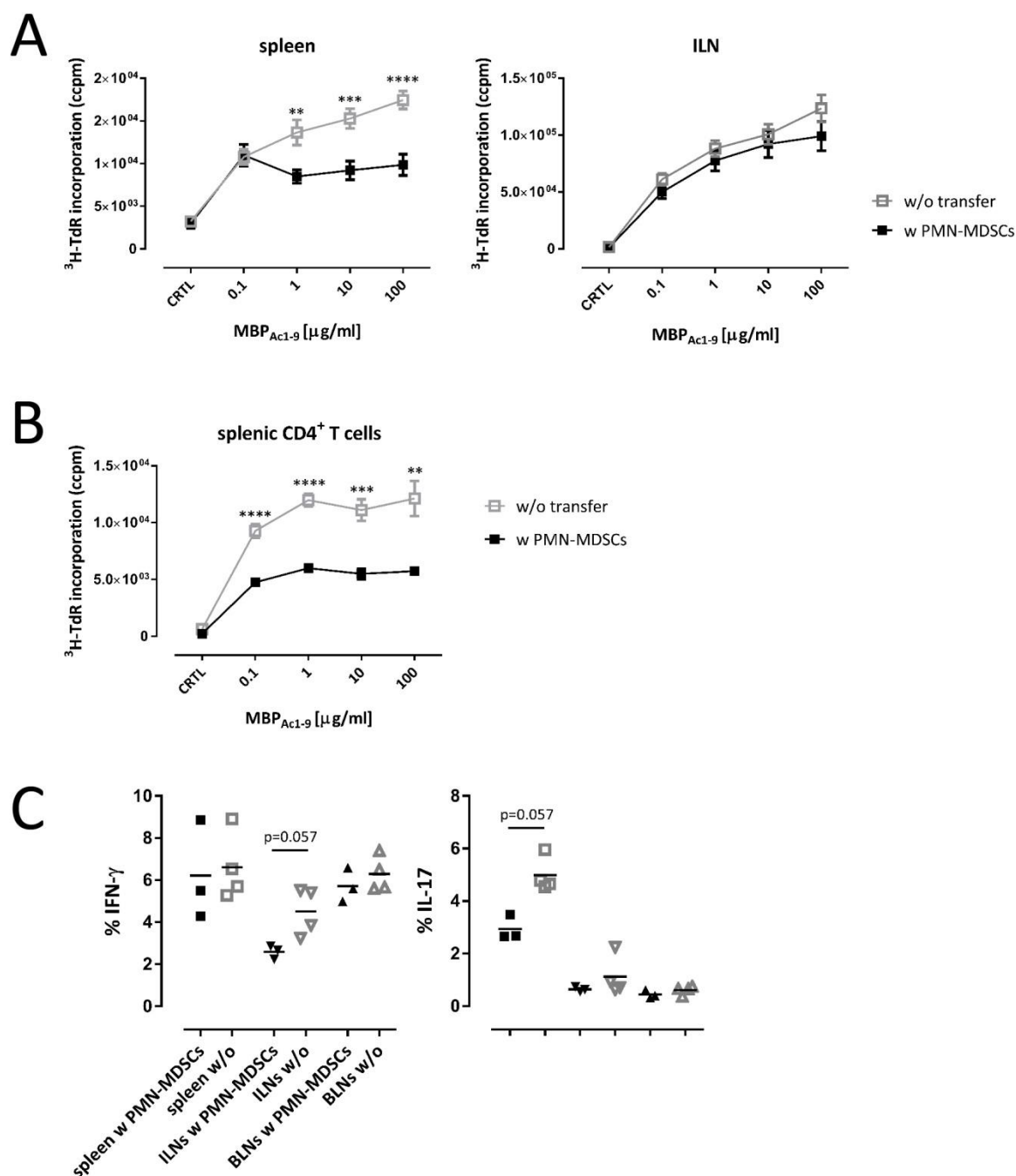
**Figure 4.36. Adoptive transfer of PMN-MDSCs reduces CD4+ T cell proliferation after antigen prime *ex vivo*.** Tg4 mice received either a cell transfer of 1.5 x 106 FACS sorted PMN-MDSC i.p. or no transfer three days before priming with MBP$_{Ac1-9}$(4K) peptide in CFA at the base of the tail. Ten days later, spleen and ILNs were harvested and a 3H-Thymidine assay was set up. **A**) Proliferative response of whole cell isolates from the spleen and ILN, after restimulation *in vitro* with titrated doses of MBP$_{Ac1-9}$(4K) (n = 6 - 8, pooled data from two independent experiments). After checking for normality using the Shapiro-Wilk test the unpaired t test was performed for normally distributed data (* = p ≤ 0.05, ** = p ≤ 0.01, *** = p ≤ 0.001, **** = p ≤ 0.0001). **B**) Proliferative response of magnetically isolated CD4+ T cells from the spleen and ILN, after restimulation *in vitro* with titrated doses of MBP $_{Ac1-9}$ in the

presence of irradiated APCs (n = 3). Mann-Whitney U test (* = p ≤ 0.05, ** = p ≤ 0.01, *** = p ≤ 0.001, **** = p ≤ 0.0001) **C)** ICCS of isolated single, viable CD4$^+$ T cells from spleen and lymph nodes. Each dot represents one individual (n=3). Horizontal lines indicate mean. (Mann-Whitney U test)

## 4.6  The spleen is essential for peptide-mediated tolerance induction

Our previous data have shown that immune regulation in the spleen can prevent the migration of activated myelin-reactive CD4$^+$ T cells into the brain. Moreover, we demonstrated an increase in the number of splenic PMN-MDSCs, with a marker profile distinct from PMN-MDSCs residing in the lymph nodes. Therefore, we wanted to further investigate the role of the spleen in tolerance induction. To achieve this, we performed splenectomies or sham control operations prior to tolerance induction in Tg4 mice. When we subsequently induced EAE in these mice, we found that an intact spleen was essential for successful tolerance induction with MBP$_{Ac1-9}$(4Y) (Figure 4.37. **A+B**). Animals without a spleen that received PBS as a control for tolerisation developed EAE to the same extent as animals that underwent sham surgery (and thus retained their spleen), reaching a mean maximum disease score of 3±SEM (Figure 4.37. **A**). However, animals receiving MBP$_{Ac1-9}$(4Y)-treatment after a sham operation were largely protected and develop only a mild grade of EAE with a mean disease score of 1±SEM. In contrast, their splenectomised counterparts all developed severe EAE with complete hind limb paralysis (grade 3), just like the PBS-treated control mice, albeit with perhaps a minor delay in the day of disease onset. In order to allow for statistical analysis of the EAE scores, the disease burden was calculated for each mouse as a sum of the daily disease scores over the course of the experiments and this demonstrated the same trend (Figure 4.37. **B**).
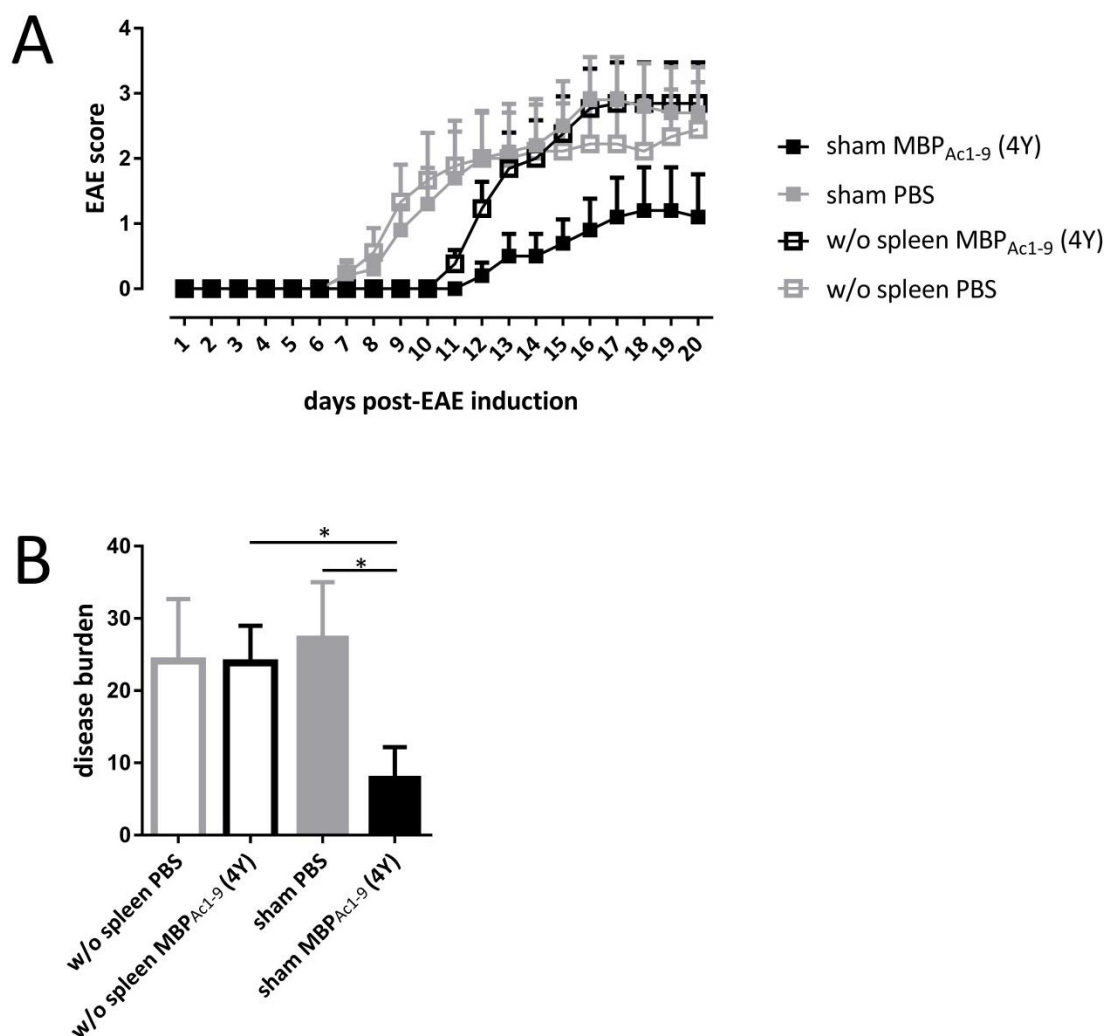
**Figure 4.37. The spleen is essential for peptide-mediated tolerance induction.** Tg4 mice underwent either sham operation or splenectomy 14 days before EDI to induce tolerance or were treated with PBS as a control. Subsequently, EAE was induced and animals were monitored daily for 20 days for signs of disease. **A**) Line graph shows disease scores over time (mean+SEM). **B**) Bar graph shows disease burden (sum of disease scores over time, mean+SEM). Mann-Whitney U test, p ≤ 0.05, n=9-12 for each group, pooled data from three independent experiments, mean+SEM).

### 4.6.1 Splenectomy affects Foxp3 expression but not IL-10 production and anergy in CD4+ T cells after EDI

The observation that tolerance induction requires an intact spleen, led us to investigate if this results from a reduced production of IL-10 by CD4+ T cells or changes in CD4+ regulatory T cells and PMN-MDSC composition. To address this question, Tg4IL-10/GFP mice underwent either sham surgery or splenectomy before undergoing EDI or receiving PBS-only control treatment. Two hours after the final treatment, ILNs, BLNs, lungs and liver were removed and analysed by flow cytometry. After gating on single, viable cells CD4+ T cells, the percentage of IL-10 producing (GFP+) T cells post EDI was unaffected by splenectomy in all organs examined (Figure 4.38. **A**). The percentage of CD4+ T cells that express Foxp3 was increased after EDI, but akin to what we observed for IL-10, this was not affected by splenectomy prior to tolerisation in CD4 + T cells isolated from the lymph nodes (Figure 4.38. **B**). In CD4+ T cells from the lungs, the percentage of Foxp3 expression was significantly lower in tolerised mice after splenectomy, although the expression of Foxp3 was still higher than in mice that had not been tolerised (Figure 4.38. **B**). In the liver, the increase in the percentage of Foxp3 expression on CD4+ T cells that results from EDI was abrogated completely by splenectomy (Figure 4.38. **B**). This demonstrates that the spleen is an important organ for the induction of Foxp3 expression, the expansion of Foxp3+ cells or the apoptosis of activated Foxp3- and controls the level of Treg cells not only within itself but also in other peripheral organs. In addition to the phenotypic analysis by FACS, we also set up a tritiated Thymidine incorporation assay to investigate if CD4+ T cells from splenectomised animals still show an anergic phenotype in response to their cognate peptide post EDI. As shown in Figure 4.38. **C**, CD4+ T cell anergy in ILNs was unaffected by the removal of the spleen. Thymidine incorporation was reduced to the same degree compared to their PBS controls in both sham operated and splenectomised mice after EDI.
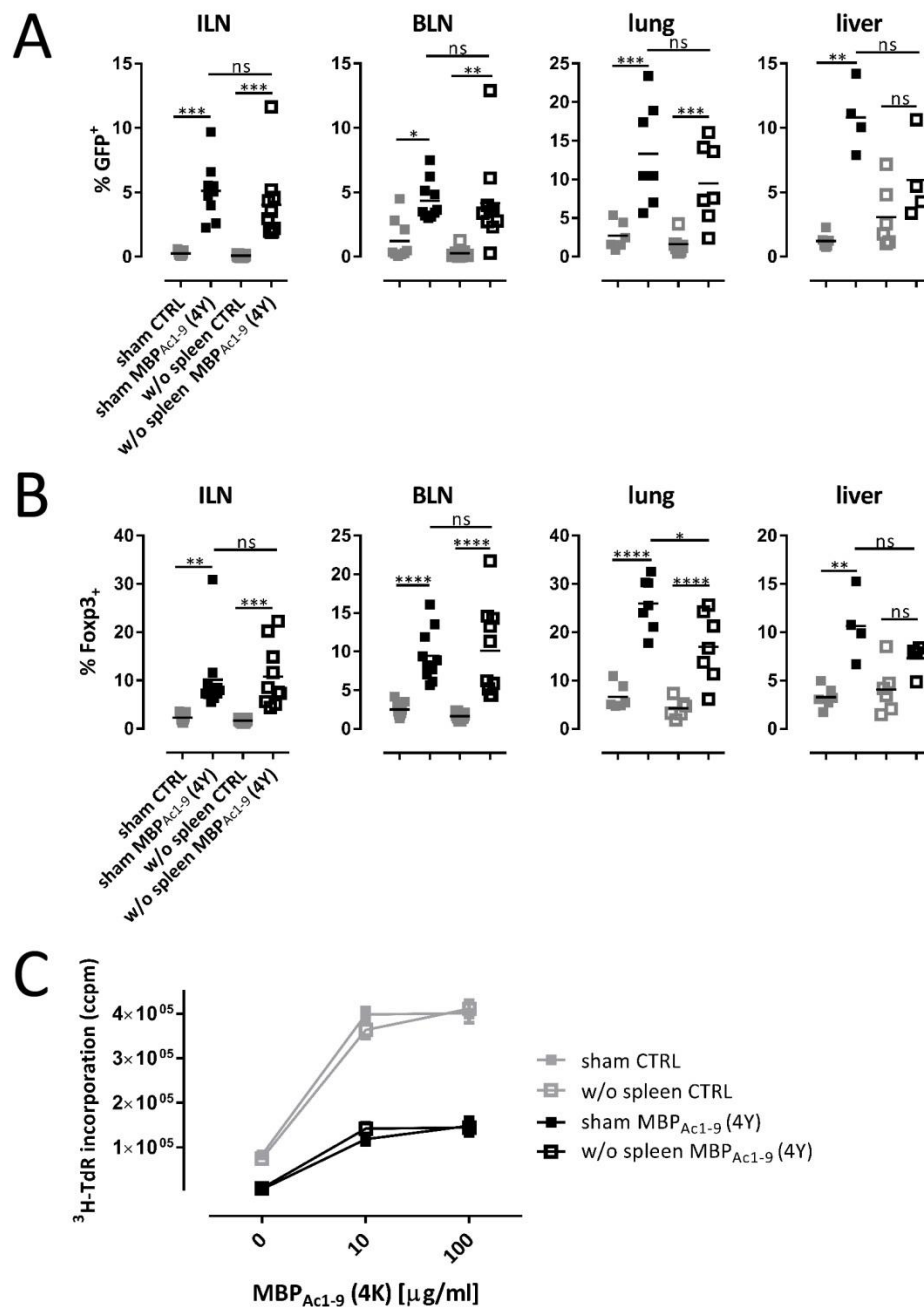
**Figure 4.38. Splenectomy affects Foxp3 expression but not IL-10 production and anergy in CD4+ T cells after EDI.** Tg4[IL-10/GFP] mice underwent either sham operation or splenectomy 14 days before EDI to induce tolerance or were treated with PBS as a control. Thereafter, ILNs, BLNs, lungs and liver were removed and analysed by flow cytometry. **A)** Expression of GFP (IL-10) in the single, viable CD4+ T cell population (each dot represents one individual). Kruskal-Wallice test followed by Dunn's multiple comparison test was applied to ILN, BLN data (n=9-10, pooled data from 3 independent experiments) and liver data (n = 4-6, pooled data from 2 independent experiments). ANOVA followed by Sidak's multiple comparison test was applied to lung data (n=6-7, pooled data from three independent experiments). **B)** Expression of Foxp3 in the single, live CD4+ T cell population (each dot represents one

individual). Kruskal-Wallice test followed by Dunn's multiple comparison was applied to ILN data (n=9-10, pooled data from 3 independent experiments) and liver data (n=4-6, pooled data from 2 independent experiments). ANOVA followed by Sidak's multiple comparison test was applied to BLN (n=9-10, pooled data from 3 independent experiments) and lung data (n=6-7, pooled data from 3 independent experiments). **C**) Tritiated Thymidine incorporation assay of whole lymphocytes from ILN stimulated with 0, 10 or 100 µg/ml MBP$_{Ac1-9}$ (4K) for 72 hours. (Mean ± SEM, n=9 in triplicates, pooled data from 3 independent experiments). After checking for normality using the Shapiro-Wilk test either ANOVA followed by Sidak's multiple comparison test was performed for normally distributed data or the Kruskal-Wallice test followed by Dunn's multiple comparison test for data that were not normally distributed (* = p ≤ 0.05, ** = p ≤ 0.01, *** = p ≤ 0.001, **** = p ≤ 0.0001).

### 4.6.2 Splenectomy impairs the increase in the number of PMN-MDSCs in the inguinal lymph nodes post EDI

Although we did not detect an effect of splenectomy on the phenotype or proliferative response *ex vivo* of CD4$^+$ T cells isolated from the lymph nodes of tolerised mice, we proceeded to examine if the number of PMN-MDSCs in the lymph nodes, lung or liver could be affected by splenectomy. As shown in Figure 4.39 **A**, splenectomy resulted in a statistically significant abrogation of the increase in the percentage of PMN-MDSCs after EDI only in the ILNs, although a similar trend was observed in the BLNs and, in particular, the liver. In absolute numbers of PMN-MDSCs, the effect of splenectomy did not reach statistical significance (Figure 4.39 **B**). However, the consistent effect of splenectomy on PMN-MDSCs in the ILNs and liver in particular would suggest that if more samples could have been analysed, these differences may prove to be true.
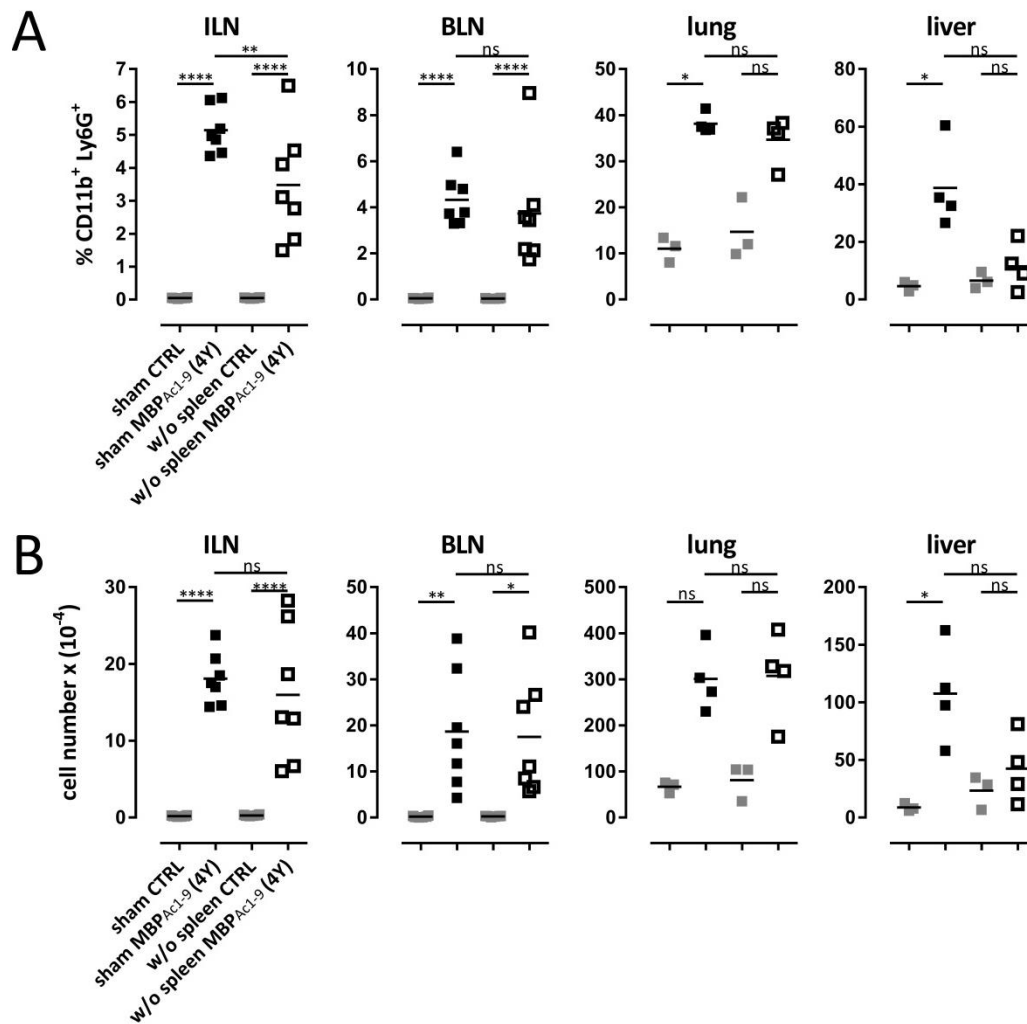
**Figure 4.39. Splenectomy impairs the increase in the number of PMN-MDSCs in the inguinal lymph nodes post EDI.** Tg4$^{IL-10/GFP}$ mice underwent either sham operation or splenectomy 14 days before EDI to induce tolerance or were treated with PBS as a control. Thereafter, ILNs, BLNs, lungs and liver were removed and analysed by flow cytometry (each dot represents an animal), gated on single, viable cells. Horizontal lines indicate mean. After checking for normality using the Shapiro-Wilk test either ANOVA followed by Sidak's multiple comparison test was performed for normally distributed data or the Kruskal-Wallice test followed by Dunn's multiple comparison test for data that were not normally distributed (* = p ≤ 0.05, ** = p ≤ 0.01, *** = p ≤ 0.001, **** = p ≤ 0.0001). **A)** Percentage of CD11b$^+$ Ly6G$^+$ PMN-MDSCs in the ILN, BLN, lung and liver in splenectomised or sham-operated mice that have either been tolerised with MBP$_{Ac1-9}$(4Y) or received control treatment with PBS only. ANOVA followed by Sidak's multiple comparison test was applied to ILN (n=6-7, pooled data from 2 independent experiments) and BLN data (n=6-7, pooled data from 2 independent experiments). Kruskal-Wallice test followed by Dunn's multiple comparison test was applied to lung and liver data (n=3-4, one experiment). **B)** Absolute numbers of CD11b$^+$ Ly6G$^+$ PMN-MDSCs in the ILN, BLN, lung and liver in splenectomised or sham-operated mice that have either been tolerised with MBP$_{Ac1-9}$(4Y) or received control treatment with PBS only. ANOVA followed by Sidak's multiple comparison test was applied to ILN (n=6-7, pooled data from 2

independent experiments) and BLN data (n=6 -7, pooled data from two independent experiments). Kruskal-Wallice test followed by Dunn's multiple comparison test was applied to lung and liver data (n=3-4, one experiment).

## 4.7 Signalling through the IL-10 receptor controls PMN-MDSC accumulation and phenotype

Our previous data showed that IL-10 receptor signalling is not essential for the suppressive activity of PMN-MDSCs because in our *in vitro* suppression assay blockade of IL-10R signalling by an antibody (Figure 4.35. **A**) did not alleviate CD4$^+$ T cell suppression. However, we were still interested to know if IL-10 signalling affects the quantity and phenotype of PMN-MDSCs. First, we treated Tg4IL-10-KO mice with either PBS or MBP$_{Ac1-9}$(4Y) according to the EDI protocol until the 3$^{rd}$ dose before isolating the spleen and lymph nodes to determine the quantity of PMN-MDSCs. The significant increase of PMN-MDSCs that results from peptide treatment in IL-10 sufficient animals was impaired in spleen and lymph nodes of Tg4IL-10$^{-/-}$ mice (Figure 4.40. **A**). This was true for both the increase in the percentage and absolute number of PMN-MDSCs in the lymph nodes (Figure 4.40. **B**). The fact that we saw less PMN-MDSCs in IL-10KO animals could be either a direct effect because MDSCs can express IL-10R (192) or an indirect effect of excess CD4$^+$ T cell activation in response to antigenic challenge in IL-10KO mice.
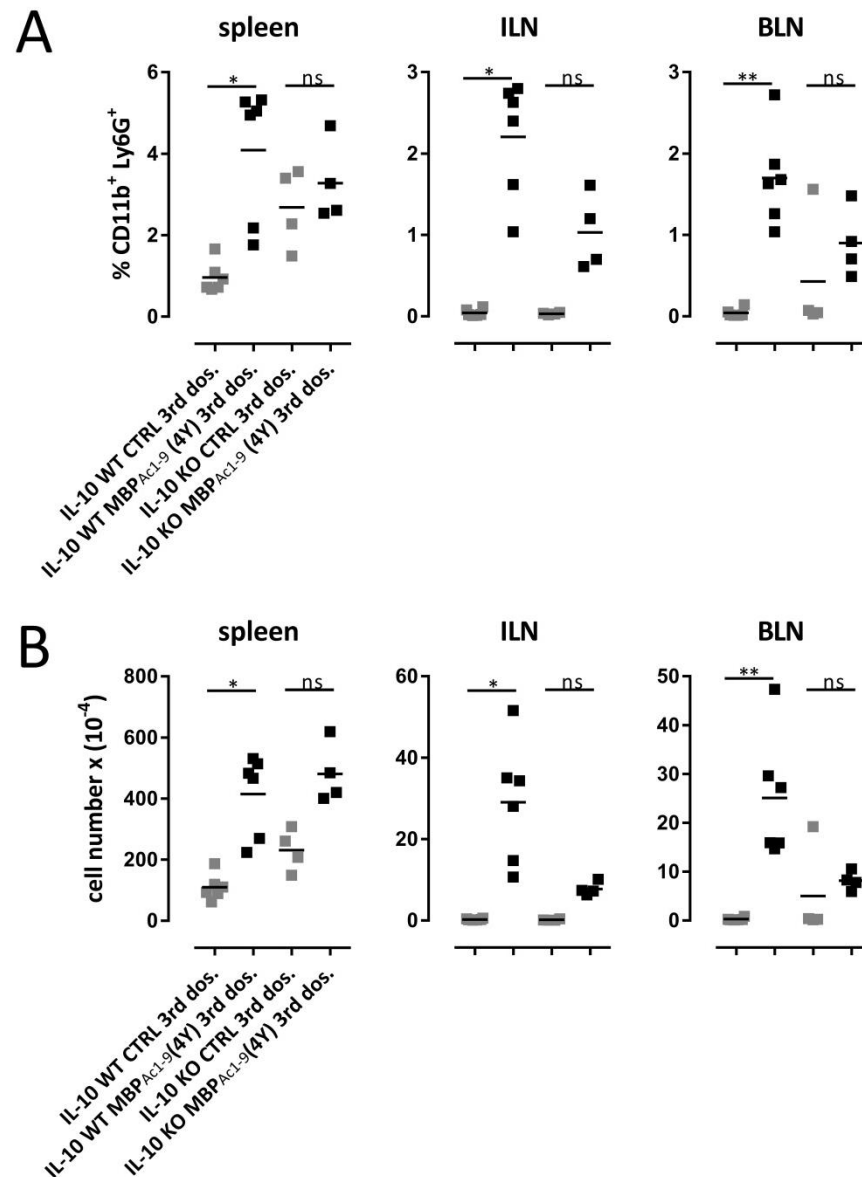
**Figure 4.40. Signalling through the IL-10 receptor is required for PMN-MDSCs accumulation.** Tg4IL-10$^{-/-}$ mice or Tg4$^{WT}$ mice were either treated with PBS as a control or MBP$_{Ac1-9}$(4Y) according to the EDI protocol until the 3$^{rd}$ dose before isolating the spleen and lymph nodes to define quantity of PMN-MDSCs. Horizontal lines indicate mean. Each dot represents one individual, n=4-6, pooled data from three independent experiments. Kruskal-Wallice test followed by Dunn's multiple comparison test was performed for data that were not normally distributed (* = p ≤ 0.05, ** = p ≤ 0.01, *** = p ≤ 0.001, **** = p ≤ 0.0001). **A)** Percentages of CD11b$^+$ Ly6G$^+$ PMN-MDSCs in spleen and lymph nodes of PBS or MBP$_{Ac1-9}$ (4Y)-treated Tg4$^{WT}$ and Tg4IL-10$^{-/-}$ mice, gated on single, viable cells. **B)** Absolute numbers of CD11b$^+$ Ly6G$^+$ PMN-MDSCs in spleen and lymph nodes of PBS or MBP$_{Ac1-9}$(4Y)-treated Tg4$^{WT}$ and Tg4IL-10$^{-/-}$ mice.

The reduction in the number of PMN-MDSCs in Tg4IL-10$^{-/-}$ animals led us to further characterise the phenotype of PMN-MDSC in this model. MHCII expression on PMN-MDSCs in BLNs after peptide treatment was increased in Tg4IL-10$^{-/-}$ mice compared to wild type Tg4 mice (Figure 4.41. **A**). Furthermore, the reduction of CD80 expression commonly observed in Tg4$^{WT}$ mice after MBP$_{Ac1-9}$(4Y)-treatment is abrogated in IL-10$^{-/-}$ mice (only statistically significant in the ILNs) (Figure 4.41. **B**). Moreover, the substantial increase of CD86 expression on PMN-MDSCs from Tg4$^{WT}$ mice in the spleen post EDI was impaired in Tg4IL-10$^{-/-}$ mice (Figure 4.41. **C**).
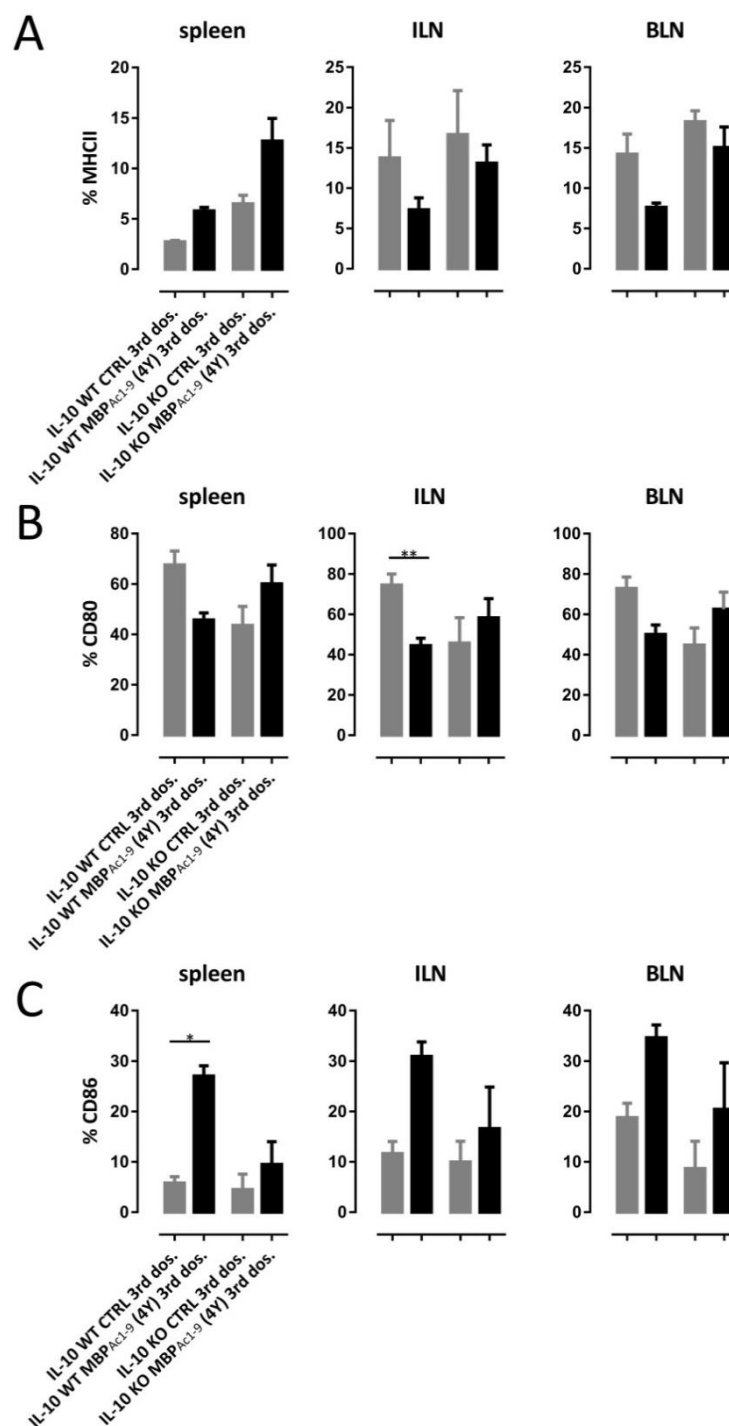
**Figure 4.41. Signalling through the IL-10 receptor determines the phenotype of PMN-MDSCs.** Tg4IL-10$^{-/-}$ mice or Tg4$^{WT}$ mice were either treated with PBS as a control or MBP$_{Ac1-9}$(4Y) according to the EDI protocol until the 3$^{rd}$ dose before isolating the spleen and lymph nodes to define the phenotype of PMN-MDSCs, gated on single, viable CD11b$^+$ Ly6G$^+$ PMN-MDSCs. n=4-6, pooled data from two to three independent experiments. Kruskal-Wallice test followed by Dunn's multiple comparison test was performed for data that were not normally distributed (* = p ≤ 0.05, ** = p ≤ 0.01, *** = p ≤ 0.001, **** = p ≤ 0.0001). Bar graph shows mean + SEM. **A)** MHCII expression on CD11b$^+$ Ly6G$^+$ PMN-MDSCs in spleen and

lymph nodes of PBS or MBP$_{Ac1-9}$ (4Y)-treated Tg4$^{WT}$ and Tg4IL-10$^{-/-}$ mice. **B**) CD80 expression on CD11b$^+$ Ly6G$^+$ PMN-MDSCs in spleen and lymph nodes of PBS or MBP$_{Ac1-9}$(4Y)-treated Tg4$^{WT}$ and Tg4IL-10$^{-/-}$ mice. **C**) CD86 expression on CD11b$^+$ Ly6G$^+$ PMN-MDSCs in spleen and lymph nodes of PBS or MBP$_{Ac1-9}$(4Y)-treated Tg4$^{WT}$ and Tg4IL-10$^{-/-}$ mice.

## 4.8 Adoptive transfer of splenic PMN-MDSCs from tolerised mice did not protect against EAE

A direct way to prove that PMN-MDSCs can mediate antigen-speccific tolerance *in vivo*, would be to demonstrate that adoptive transfer of PMN-MDSCs from tolerised mice can suppress the development of EAE in untreated recipient Tg4 mice. As shown in Figure 4.42. **A+B**, adoptive transfer of 1.5 x 10$^6$ PMN-MDSCs from tolerised Tg4 mice into untreated Tg4 mice three days prior to priming for disease with MBP $_{Ac1-9}$(4K) in CFA, plus two doses of pertussis toxin on day one and two post-priming, did not confer EAE protection in the recipients. There was no difference if mice were used with the spleen (n=3) (Figure 4.42. **A**) or after removal of the spleen (n=4) (Figure 4.42. **A**).
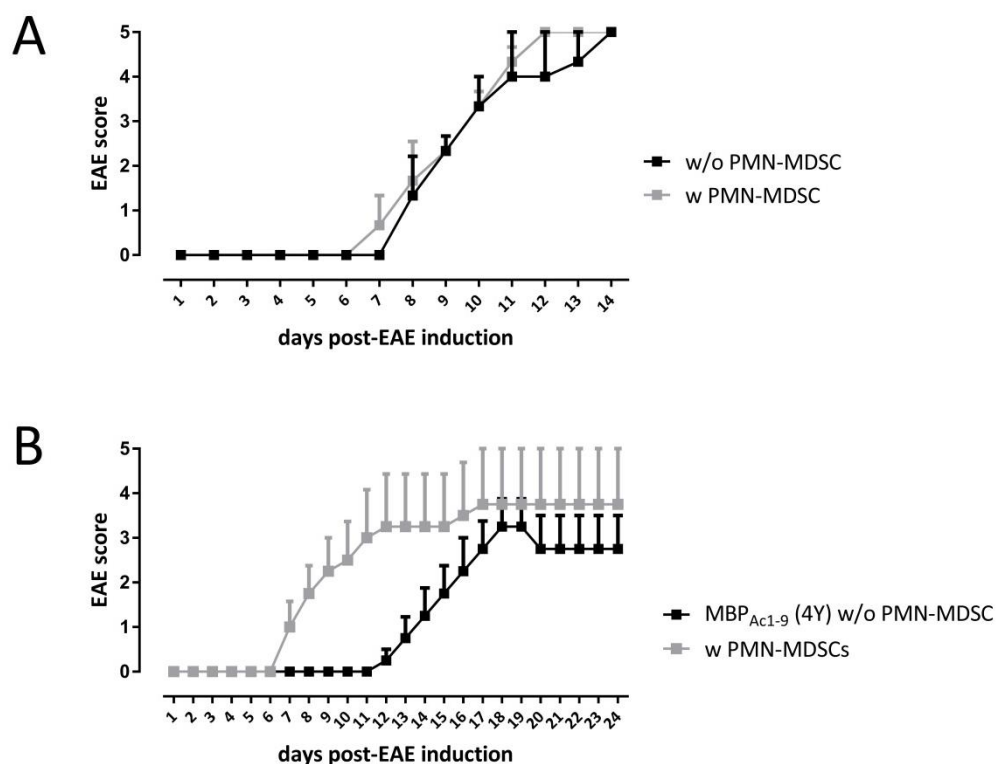
**Figure 4.42. Adoptive transfer of splenic PMN-MDSCs from tolerised mice did not protect against EAE.** Untreated Tg4 mice received an adoptive transfer of $1.5 \times 10^6$ PMN-MDSCs from tolerised Tg4 mice three days prior to priming for disease with MBP$_{Ac1-9}$(4K) in CFA, plus two doses of pertussis toxin on days one and two post-prime. Mice were monitored daily for signs of EAE. **A**) Mice that did not undergo splenectomy (n=3 per group). **B**) Mice with splenectomy (n=4 per group). Line graphs show mean + SEM.

**Table 4.2. Adoptive transfer of splenic PMN-MDSCs from tolerised mice did not protect against EAE.** Untreated or MBP$_{Ac1-9}$(4Y)-treated Tg4 mice received an adoptive transfer of 1.5 x 10$^6$ PMN-MDSCs from tolerised Tg4 mice three days prior to priming for disease with MBP$_{Ac1-9}$(4K) in CFA, plus 2 doses of Pertussis toxin on days one and two post-prime. Mice were monitored daily for sign of EAE. Mice that did not undergo splenectomy (n=3 per group) and mice with splenectomy (n=4 per group). * Day of onset is the first day mice showed signs of EAE after immunization. † Incidence is the number of sick mice/number of mice immunized for each group. ‡ Cumulative score is the sum of each mouse clinical score.

| treatment | day of onset* mean ± SEM | incidence† | maximum score mean ± SEM | cumulative score‡ mean ± SEM |
|---|---|---|---|---|
| **with spleen (Figure x A)** | | | | |
| w/o MDSCs | 8.3 ± 0.3 | 3/3 | 3.6 ± 0.6 | 24.3 ± 4.2 |
| w MDSCs | 7.6 ± 0.3 | 3/3 | 4.0 ± 0 | 27.3 ± 2.4 |
| **without spleen (Figure x B)** | | | | |
| MBP$_{Ac1-9}$ (4Y) w/o MDSCs | 14 ± 1.1 | 4/4 | 3 ± 0.4 | 29.3 ± 7.6 |
| w MDSCs | 5.5 ± 1.9 | 3/4 | 3 ± 1 | 57 ± 22.2 |

## 5   DISCUSSION

Antigen-specific peptide immunotherapy of autoimmune diseases to restore tolerance is a promising approach to combat MS as a disease-modifying strategy. In this thesis, we contribute to the understanding of this process on three levels. First, successful tolerance induction is accompanied by the upregulation of IL-10-production in CD4$^+$ T cells. We found that the cell surface receptors TIM-3, TIGIT and PD-1 were significantly upregulated on IL-10-secreting CD4$^+$ T cells and on CD4$^+$ Foxp3$^+$ T cells throughout the body but no single one or combination of these markers were expressed exclusively on these cells and could serve as a biomarker. Second, we studied linked bystander suppression and demonstrated that tolerised MBP-specific CD4$^+$ T cells could suppress CD4$^+$ T cell responses *in vivo* in (B.10PL x C57BL/.6)F1 mice when MOG$_{35-55}$ was presented together with MBP$_{Ac1-9}$(4K) on the same APC. Finally, we revealed for the first time an involvement of PMN-MDSCs in the process of tolerance induction. PMN-MDSCs inhibited CD4$^+$ T cell proliferation *in vitro* in a cell contact-dependent manner, the suppression being mediated by arginase-1. Furthermore, adoptive transfer of PMN-MDSCs reduced the T cell proliferative response upon restimulation *ex vivo*.

It was already known that EDI leads to the upregulation of IL-10 production in CD4$^+$ T cells in the spleen and that effective tolerance induction results in changes in the CD4$^+$ T cell signature, including the upregulation of co-inhibitory molecules (61). However, it was not yet clear if these changes are systemic and if Foxp3$^+$ regulatory T cells are affected by the peptide treatment. In this study, we observed a systemic and gradual upregulation of IL-10 production in CD4$^+$ T cells over the course of peptide treatment. The first clinical evidence that IL-10-secreting CD4$^+$ T cells are responsible for tolerance was adduced by the Roncarolo group who conducted a study where patients with severe combined immunodeficiency received HLA-mismatched hematopoietic stem cells to restore a healthy and balanced immune system (81). This demonstrated that, in this setting, donor T lymphocytes produced large amounts of IL-10 and were responsible for tolerance. This study and many others that followed in the fields of transplant rejection, allergy and autoimmune disease emphasised the importance of characterising IL-10-secreting T cells and defining biomarkers that can be used to assessed the success of tolerance induction protocols.

The majority of the induced IL-10-secreting CD4$^+$ T cells during EDI in our EAE model expressed the co-inhibitory molecules TIM-3, TIGIT and PD-1. The role of TIM-3 in tolerance induction was previously examined *in vivo* in several mouse models using either anti-TIM-3 monoclonal antibody or TIM-3-Ig fusion protein to block its function. The administration of either reagent prevented the induction of transplantation tolerance induced by donor-specific transfusion (DST) plus anti-CD40L-treatment in an MHC-mismatched islet allograft model (108). In addition, the treatment with DST and anti-CD40L to induce tolerance to islet allografts failed in TIM-3 knockout mice. Furthermore, in a model of Th1-mediated autoimmune diabetes the administration of either anti-TIM-3 monoclonal antibody or TIM-3-Ig fusion protein accelerated the onset of diabetes. These data suggest that TIM-3 promotes tolerance by directly inhibiting Th1 cells (103). It was shown that TIGIT expression on CD4$^+$ T cells exerts its inhibitory effect by driving DCs towards a more tolerogenic phenotype (131). Ligation of the surface receptor TIGIT on CD4$^+$ T cells to CD155 expressed on DCs was shown to enhance production of IL-10 and decrease production of IL-12 by these DCs, which in turn inhibited CD4$^+$ T cell responses. These data suggest that expression of TIGIT on tolerised CD4$^+$ T cells targets a very important arm of the immune system and might convert the DCs in our tolerised Tg4 model into immunoregulatory DCs that help protect mice from developing EAE. PD-1 is another important marker involved in tolerance. PD-1 blockade by an anti–PD-1 mAb in a model of autoimmune diabetes accelerated disease development (193). Furthermore, using the same animal model antigen-specific tolerance induction using insulin-coupled antigen-presenting cells was prevented by antibody-mediated PD-1 blockade and correlated with enhanced antigen-specific proliferation and the production of the pro-inflammatory cytokines IFN-γ and IL-2 by CD4$^+$ T cells (130). Altogether, these findings suggest that the expression of TIM-3, TIGIT and PD-1 on tolerised CD4$^+$ T cells can have a beneficial, disease-regulating effect either by directly inhibiting the pathogenicity of these autoreactive T cells themselves, or by potentiating the tolerogenicity of antigen-presenting cells. Unfortunately, none of these molecules were exclusively expressed by IL-10-secreting CD4$^+$ T cells which would allow them to serve as a surrogate marker to define this subset. CD4$^+$ GFP$^-$ (IL-10$^-$) T cells from Tg4$^{IL-10/GFP}$ (IL-10-GFP reporter) mice upregulate these markers as a result of peptide treatment as well which renders them unsuitable to study the *in vivo* differentiation and function of tolerised IL-10-secreting CD4$^+$ T

cells. Our results in tissues throughout the body corroborated published data generated from splenic CD4$^+$ T cells by our group (61). The complex and very diverse phenotype of tolerised CD4$^+$ T cells does not allow them to be defined by a limited set of biomarkers. In contrast, other groups have previously claimed to have identified such markers in mouse and man (82, 194-196). For example, in 2013 Gagliani et al. postulated that the coexpression of CD49b and LAG-3 would identify a population of IL-10-secreting T regulatory cells in both mouse and man (197) but both their own and our data demonstrate that these markers are expressed not only by a small percentage of IL-10$^+$ CD4$^+$ T cells but also by IL-10$^-$ CD4$^+$ T cells after tolerance induction.

An increase in the number of CD4$^+$ Foxp3$^+$ T cells as a result of EDI became apparent after the 3$^{rd}$ dose of MBP$_{Ac1-9}$(4Y)-treatment, which is in line with studies showing that Foxp3$^+$ Tregs develop in response to low levels of antigen (198, 199). The lack of exclusive markers that distinguish peripherally-induced Foxp3$^+$ Treg (pTreg) cells from thymus-derived Foxp3$^+$ Treg (tTreg) cells did not allow us to establish with any certainty which subset in particular was expanded or induced (191) and which subset was more important for disease protection post EDI. That said, an earlier study from our group using a GFP-Foxp3 reporter model where the development of pTregs but not tTregs was impaired, demonstrated that pTregs are not crucial in preventing EAE onset (200). As mentioned in the introduction, the ablation of Foxp3$^+$ Treg cells in mice shortly after birth results in lymphoproliferation and multiorgan autoimmune disease (70, 201). On the other hand, the enrichment of CD4$^+$ Foxp3$^+$ from normal mice and the transfer into nude mice, inoculated with CD25$^-$ lymphocytes, established tolerance to allogeneic skin organ grafts (202). It is therefore likely that, in addition to the *de novo* generation of IL-10-secreting CD4$^+$ T cells, CD4$^+$ Foxp3$^+$ T cells play a role in tolerance induction in our EAE model.

The vast majority of these Foxp3$^+$ Tregs that accumulate after peptide treatment express PD-1 while around 50% of Tregs express TIGIT and TIM3 on their cell surface, which is much higher than in control-treated mice. The expression of these markers can affect the functionality of Foxp3$^+$ Treg cells. CD4$^+$ Foxp3$^+$ T cells that are TIM-3$^+$ have previously been shown to display increased IL-10 and lower IL-2 messenger RNA (mRNA) expression and inhibited the proliferation of responder T cells to a greater extent than their TIM-3$^-$

counterparts (203). Similar to the situation of TIM-3, Foxp3$^+$ Treg cells expressing the coinhibitory molecule TIGIT showed enhanced competence to inhibit effector T cell proliferation and produced more IL-10 than their TIGIT$^-$ counterparts (135).

Either CD4$^+$ IL-10$^+$ T cells or Foxp3$^+$ T cells can prevent the onset of EAE or ameliorate EAE development in naïve recipients by indirectly modifying the maturation of DC (58). This was demonstrated by the fact that the co-culture of splenic DC from untreated B10.PL mice with splenic CD4$^+$ T cells from tolerised Tg4 animals in the presence of antigen inhibited DC maturation as assessed by the downregulation of the markers CD80 and CD86. Furthermore, when DC from either naïve or tolerised Tg4 mice were isolated and co-cultured with naïve Tg4 CD4$^+$ T cells in presence of cognate antigen, tolerised DC inhibited CD4$^+$ T cell proliferation and reduced the production of IL-2 and IFN-γ by CD4$^+$ T cells in comparison to their naïve DC counterparts.

The temporary reduction in the number CD4$^+$ T cells two hours after MBP$_{Ac1-9}$(4Y)-treatment, seen during EDI by flow cytometry and by immunohistochemistry on paraffin sections, can be the result of peptide-specific T cell deletion or the downregulation of CD4 expression on the surface of T cells (187). Our laboratory has previously shown that a single dose of 100 μg of MBP$_{Ac1-9}$(4Y) leads to cell death in the thymus and in the cervical lymph nodes 16 hours after peptide administration (59). More importantly, this cell death is only a transient effect of peptide treatment because CD4$^+$ T cell frequencies returned to their original levels in lymphoid organs within 48 h. In line with this study, our data generated from EAE experiments showed that CD4$^+$ T cell numbers are unchanged in the spleen and lymph nodes in tolerised healthy mice compared to control mice that have disease. Therefore, the protective effect of reduced migration of pathogenic CD4$^+$ T cell into the brain of tolerised mice after EAE induction is the result of qualitative changes and not of peptide-specific CD4$^+$ T cell deletion. This is demonstrated by the fact that CD4$^+$ T cells from tolerised disease-free-mice in the CNS compartment express lower levels of PD-1 and TIM-3, markers associated not only with co-inhibition but also with T cell activation (104, 124, 204). In contrast, CD4$^+$ T cells in the spleen had an increased expression of both markers as a result of the persistent antigenic stimulation during EDI. These findings suggest that activated T cells may be held in the spleen, which prevents them from migrating into the CNS. This hypothesis is further

supported by our finding that removal of the spleen prior to EDI and subsequent induction of EAE led to the development of severe disease in MBP$_{Ac1-9}$(4Y)-treated animals that would otherwise be protected.

EDI in protected animals led to a decrease in the infiltration of conventional T cells into the CNS, but concurrently we noticed an increase in the number of CD4$^+$ Foxp3$^+$ T cells in the spinal cord post EDI and subsequent EAE induction. A very elegant study showed that Tregs limit the proliferation and motility of myelin-specific T cells directly in the CNS during the effector phase of EAE in addition to their regulatory effect in the periphery (205). The authors combined timed selective depletion of Tregs with 2-photon microscopy using DEREG mice which express the diphtheria toxin (DT) receptor under the control of the Foxp3 locus (206). After the immunisation of DEREG mice with MOG$_{35-55}$ in CFA, they were able to deplete CD4$^+$ Foxp3$^+$ T cells by DT treatment four days post EAE onset, which resulted in enhanced proliferation of myelin-specific T cells and exacerbation of EAE.

As also seen in CD4$^+$ T cells overall, TIM-3 expression on CD4$^+$ Foxp3$^+$ T cells in particular exhibited a dichotomy in tolerised animals. We noticed an increase in the expression of TIM-3 on CD4$^+$ Foxp3$^+$ T cells in the spleen but a decrease in the brain. Considering the potentiating effect of TIM-3, this could imply that CD4$^+$ Foxp3$^+$ T cells with a higher suppressive potential might not optimally exert their regulation in the brain but preferentially in the spleen.

Both IL-10-secreting CD4$^+$ T cells and CD4$^+$ Foxp3$^+$ Treg cells can mediate tolerance in our EAE model but currently we are unable to define which of the two regulatory T cell subsets are more important since previous publications from our group showed that both subsets on are able to confer tolerance (77, 207). Peptide-induced IL-10-secreting CD4$^+$ T cells generated in Tg4 RAG-deficient mice, lacking Foxp3$^+$ T cells, suppressed the proliferation of transferred naïve Tg4 CD4$^+$ T cells after receiving a single dose of MBP$_{Ac1-9}$(4Y) (207). Similarly, the adoptive transfer of Tg4 iTreg cells into Tg4 RAG$^{-/-}$ mice prior to EAE induction with MBP$_{Ac1-9}$(4K) in CFA delayed disease progression. The latter study demonstrated that iTreg cells were still dependent on IL-10 for their function since the transfer of iTregs generated from Tg4IL-10$^{-/-}$ mice led to the development of EAE to the same degree as in mice receiving no cell transfer (77).

The clinical application of antigen-specific peptide immunotherapy in the treatment of MS may be hindered by the involvement of T cells specific for various myelin antigen (208). Hence, it would be beneficial if we could induce regulatory T cells that are able to inhibit not only autoreactive T cells specific for the tolerising antigen, but also those specific for other myelin antigens. Immunotherapy of EAE using recombinant T-cell receptor ligands (RTLs) can ameliorate EAE in an antigen-specific manner (209). These MHC class II/peptide complexes ligate specific TCRs expressed by pathogenic T cells without delivering costimulatory signals necessary for the activation of the pathogenic T cell, thus inducing T cell anergy (210). It was shown that treatment with a single RTL (with bound $PLP_{139-151}$ peptide) could supress EAE in SJL/J mice immunized with either spinal cord homogenate, or a combination of either $PLP_{139-151}$ + $PLP_{178-191}$ or $PLP_{139-151}$ + $MBP_{84-104}$ in CFA  (211). Stimulation of whole splenocytes from RTL-treated mice with their cognate peptide led to the downregulation of IL-17 production by $CD4^+$ T cells and to an increased IL-10 production by both $CD4^+$ T-cells and APCs. Another study showed that bystander suppression was partially mediated through $CD4^+$ $CD25^+$ Treg cells *in vitro* (212). In this study, when $CD4^+CD25^-$ T cells from TCR-transgenic mice that recognise the peptide MHC complex HA110–119/I-Ed were stimulated with both HA and PCC peptide in the presence of $CD4^+CD25^+$ T from PCC TCR-transgenic mice (PCC88–104/I-Ek), the HA-T cell response was suppressed. Both studies showed the importance of $CD4^+$ IL-10-secreting and $CD4^+$ $Foxp3^+$ T cells in bystander suppression, cell types we are inducing with our dose escalation regime in peptide-immunotherapy.

Our work reveals for the first time that the transfer of tolerised $CD4^+$ T cells specific for $MBP_{Ac1-9}$ can indeed mediate suppression of $MOG_{35-55}$ responses *in vivo* in (B.10 PL x C57BL/6)F1 mice. We also delivered evidence that this effect was better executed when the first antigen, to which tolerance was already established, was presented together with the second antigen by the same APC by coupling the two antigens with a HFFK linker sequence. To further investigate linked bystander suppression and the potential mechanism in detail we would need a new transgenic mouse model. The pitfall of the polyclonal (B10.PL x C57BL/6)F1 mouse model is the difficulty in detecting with any certainty the low numbers of antigen-specific cells that exist *in vivo*. A double transgenic adoptive transfer mouse model where a significant number of $CD4^+$ T cells would recognise either $MBP_{Ac1-9}$ or $MOG_{35-55}$ would help us to overcome this issue. For this purpose, we would isolate and label $CD4^+$ T

cells from our well-established transgenic Tg4 model as well as the 2D2 model, where nearly all CD4$^+$ T cells express a transgenic TCR specific for MOG$_{35-55}$ (45), and transfer them to (B10.PL x C57BL/6)F1-recipients. In this case, we would be able to determine with certainty if tolerisation of MBP-reactive T cells (pre- or post-transfer) can suppress the activation of MOG-reactive T cells and vice versa, *in vivo*. The same linked peptide that we have already validated could be instrumental in this model. Unfortunately, however, the establishment of this model was beyond the scope of the work in this thesis, but a follow-up project to demonstrate this principle would be highly informative and important.

We have shown here, for the first time that MDSCs, and PMN-MDSCs in particular, accumulate during the course of EDI in various organs from the CNS to the periphery. The preferential expansion of PMN-MDSCs over M-MDSCs does not come as a complete surprise because PMN-MDSCs represent the major pool of circulating and expanding MDSCs in both mice and humans in the tumour environment (213) revealing a 3:1 ratio of PMN-MDSCs to M-MDSCs (162). However, the higher abundancy of PMN-MDSCs does not necessarily imply that they are more important for suppression as it has been proposed previously that M-MDSCs might be more immunosuppressive (168, 214). The more pronounced accumulation of PMN-MDSC after the 3$^{rd}$ dose of EDI is possibly due the fact that Tg4 mice showed a peak in the amount of IL-6 and IL-17 after this dose (Bronwen R. Burton, doctoral thesis). These cytokines are known to mediate the accumulation of MDSCs and their immunosuppressive function (215-218). The PMN-MDSCs that we induced during antigen-specific peptide immunotherapy were able to reduce the proliferation of CD4$^+$ T cells and expand CD4$^+$ Foxp3$^+$ T cell *in vitro*. Adoptive transfer of PMN-MDSCs prior to priming of Tg4 mice with MBP$_{Ac1-9}$(4K) in CFA reduced the CD4$^+$ T cell proliferative response upon restimulation *ex vivo*.

We found that PMN-MDSCs were able to suppress naïve CD4$^+$ T cell proliferation induced by either an antigen-specific or non-specific stimulus. Surprisingly, PMN-MDSCs reduced the proliferative response of antigen-experienced T cells only when stimulated non-specifically with anti-CD3+anti-CD28. A study showed previously that MDSCs from the tumour site and spleen of the same mouse can differ in their ability to suppress CD8$^+$ T cell proliferation although they had the same phenotype (219). Both MDSC-populations were able to suppress

CD8^{+} T cell proliferation in an antigen-specific manner. However, the main difference was that splenic MDSCs did not suppress CD8^{+} T cell proliferation in response to anti-CD3+anti-CD28. These differences in suppression could be explained by the tumour environment where suppressive factors are present which are absent in the spleen. But the PMN-MDSCs we studied were isolated from the spleen and only the method of CD4^{+} T cell stimulation differed. So far, we have no definitive explanation as to why in our experiments antigen-experienced cells could be suppressed when stimulated with antibody and not when stimulated with antigen, but it could have to do with either the affinity of the interaction or the involvement of other co-stimulatory or co-inhibitory molecules.

The next question we asked was: What are the mechanisms that PMN-MDSCs use to exert their suppressive activity? Most of the published studies, and our study, have shown that MDSCs need direct cell-cell contact to exert their immunosuppressive function, which suggests that they either act through cell surface receptor-ligand interactions or that they use the release of soluble mediators that act only in close proximity. MDSCs have previously been shown to use multiple mechanisms to suppress T cell proliferation, as reviewed by Gabrilovich & Nagaraj (220). The majority of studies have found an involvement of the enzymes arginase-1 and iNOS in MDSC-mediated suppression of T cells (221, 222). However, the addition of the inhibitor of NOS, NG-monomethyl-L-arginine (L-NMMA) did not ablate the suppressive activity of PMN-MDSCs in our hands, while the arginase-1 inhibitor (BEC) restored CD4^{+} T cell proliferation indicating that PMN-MDSCs use arginase-1 to exert their suppressive activity in our model system.

More recently, other mechanisms of suppression deployed by MDSCs were discovered, including the production of the enzyme indoleamine 2,3-dioxygenase (IDO) (223). IDO degrades the essential amino acid L-tryptophan, depleting it from the microenvironment and thereby preventing the proliferation of nearby T cells (224). It has been shown that IDO expressing-macrophages are able to suppress T cell proliferation and that blockade of this enzyme with the 1-methyl analogue of tryptophan (1-MT) prevented macrophage-mediated suppression (225). MDSCs induced in patients with breast cancer have been shown to express IDO and again blockade of this enzyme with 1-MT, led to the loss of their T cell-

suppressive activity (223). However, the addition of 1-MT in our *in vitro* MDSC-T cell-co-cultures did not lead to abrogation of MDSC-mediated inhibition of CD4+ T cell proliferation.

In addition to these soluble factors, molecules expressed on the cell surface of MDSCs have been suggested to mediate the T cell suppressive effect, namely PD-L1 and Galectin-9 (158, 226). However, the blockade of PD-L1 does not decrease MDSC suppressive activity in all cases, which suggests that this molecule is not indispensable (162). In this published study, the functional role of PD-L1 was tested *in vitro* and *in vivo* and it was found that the blockade of PD-L1 did not reduce or eliminated MDSC-mediated T cell suppression. In our study the blockade of either cell surface receptor, by adding anti-Galectin-9 or anti-PD-L1 during the *in vitro* co-culture of PMN-MDSCs and CD4+ T cells, did not restore T cell proliferation while the co-blockade of both molecules led to the abrogation of PMN-MDSC-suppression indicating a synergistic effect of Galectin-9 and PD-L1. Huang et al. previously demonstrated that the anti-inflammatory cytokine IL-10 is produced by MDSCs and that the suppressive activity of MDSCs is dependent on IL-10 because it was shown that the administration of an anti-IL-10 antibody in tumour-bearing mice abrogated T cell suppression by MDSCs (166). This finding is not universally supported, however, as another group found that *in vitro* suppression by MDSC did not require IL-10-production (227). But, IL-10-signalling through the IL-10-receptor was found to be required to establish the phenotypic characteristics of MDSC, which would support our findings in this study that although addition of a blocking anti-IL-10R antibody did not restore CD4+ T cell hypoproliferation, tolerisation of IL-10-deficient animals showed a change in the phenotype of PMN-MDSCs compared to IL-10-sufficient mice.

After priming Tg4 mice with MBP$_{Ac1-9}$(4K) in CFA and pertussis toxin, the frequency of PMN-MDSC in mice with EAE was significantly higher in many of the organs examined compared to mice that had been protected by EDI beforehand. It was previously published that MDSC accumulate in the spleen after exposure to mycobacterial products, such as those present in CFA (228). This raises the question why animals are not protected from disease even though these potentially immunosuppressive PMN-MDSCs arise. Our findings hint at the possibility that phenotypic differences between those PMN-MDSCs that develop after EAE development and those that arise after tolerisation contribute to their functional dichotomy.

Compared to the PMN-MDSCs of mice with EAE, we detected the upregulation of Galectin-9 and PD-L1 expression on PMN-MDSCs in the spleen and lymph nodes while we noticed an increase of CD40 and a decrease of CD80 in the CNS compartment of tolerised animals. CD40 is expressed mainly by antigen-presenting cells (229, 230) whereas its ligand CD40L is expressed on activated but not resting T cells (231). The exact role of CD40 in MDSC-mediated suppression remains unclear but Pan et al. showed that CD40 expressed on MDSCs is essential for their suppressive function and Treg cell induction (179). They demonstrated that MDSCs from tumour-bearing CD40$^{-/-}$ mice lost the ability to suppress the proliferation of naïve T cells and the expansion of Foxp3$^{+}$ T cell, when either activated by a non-specific stimulus or by their antigen, *in vitro*. Furthermore, the administration of anti-CD40 i.p. into tumour-bearing mice led to a reduction in proliferation of tumour-specific T cells recovered from the spleen and prevented the expansion of Treg cells. These results may suggest that, in our model, the increased expression of CD40 on PMN-MDSCs in the CNS of tolerised animals contributes to enhance their suppressive activity and allow them to confer protection. This proposal is supported by our *in vitro* co-culture experiments, where blockade of CD40 abrogated PMN-MDSC-suppression and restored CD4$^{+}$ T cell proliferation.

In recent years, the expression of CD80 on MDSCs has been associated with immune suppression (232). It was shown that MDSCs in a murine model of ovarian carcinoma expressed high levels of CD80 and were better able to suppress antigen-specific T cell responses than their CD80-negative counterparts isolated from tumour-free mice. This is supported by our findings that the addition of anti-CD80 to our *in vitro* MDSC-T cell-co-cultures led to abrogation of MDSC-mediated inhibition of CD4$^{+}$ T cell proliferation. Furthermore, the transfection of ovarian carcinoma–associated MDSCs with CD80-targeted siRNA significantly decreased the suppressive potential of MDSCs. This, however, is in direct contrast to our hypothesis that peptide treatment promotes a more suppressive PMN-MDSC phenotype in the CNS, as we found a reduced expression of CD80 on PMN-MDSCs in the CNS of tolerised animals. Our theory is supported by Dugast et al. who showed that, in a rat model of kidney allograft tolerance, blood-derived CD80-positive MDSCs have the same suppressive capacity as their CD80-negative counterparts (233). The contradictory results in the literature, therefore, mean that the effect of CD80 expression on the function of PMN-MDSCs in the CNS of tolerised mice remains to be elucidated. Overall, it is unclear how

important the phenotype of PMN-MDSCs in the CNS is for the prevention of EAE as the maintenance of tolerance and prevention of disease development might be controlled in the periphery rather than the CNS. This hypothesis is supported by our finding that removal of the spleen prevents successful tolerance induction and hence protection from disease. This was also shown previously in a model of experimental autoimmune uveoretinitis (EAU) where splenectomy likewise abrogated the induction of tolerance (234).

PD-L1 expression on PMN-MDSCs was increased only in the spleen and no other organs of tolerised animals. PD-L1$^+$ PMN-MDSCs could potentially interact with PD-1-expressing CD4$^+$ T cells in the spleen. Tumour-infiltrating MDSCs from tumour-bearing mice have previously been shown to express high levels of PD-L1 and were able to suppress the proliferation of CD8$^+$ T cells (226). Anti-PD-L1-treatment of tumour-bearing mice resulted in a systemic decrease in the number of MDSCs and was associated with enhanced T cell functional activity and a reduction in tumour growth. Altogether these findings support the notion that MDSC-T cell interaction and suppression may be mediated by the PD-L1-PD-1 axis and that this interaction takes place in the spleen.

Another important negative regulator of T cell activity, TIM-3, was significantly upregulated on CD4$^+$ T cells in the spleen of tolerised animals that were successfully protected from EAE in our study. An earlier study described a potential role for the Tim-3/Galectin-9 pathway in MDSC proliferation (158). The treatment of T cell lymphoma-bearing mice with anti-TIM-3 antibody resulted in a delayed tumour progression that correlated with lower frequencies of MDSCs. Given the increased expression of Galectin-9 on splenic PMN-MDSCs in tolerised mice, the Galectin-9/TIM-3 axis could potentially contribute to the protection from induced EAE that results from peptide immunotherapy.

Our results suggest that the interaction of MDSCs with T cells in the spleen, and not just the differentiation of Treg cells could be very important and might, at least in part, be responsible for the protective effect of EDI. After all, our splenectomy experiments showed that animals without a spleen receiving EDI showed no reduction in the number of IL-10-producing CD4$^+$ T cells or CD4$^+$ Foxp3$^+$ Treg cells or in the level of anergy of conventional T cells in the lymph nodes, but were still more susceptible to EAE than mice that retained their spleen. Our findings are supported by a study where splenectomy prior to tolerance

induction to OVA did not result in a reduction in the number of CD4$^+$ Treg cells in the mesenteric LN or peripheral LN yet the establishment of skin tolerance and prevention of a DTH response could not be achieved (235). It was also very striking that we detected in most cases a very distinctive marker expression on both CD4$^+$ T cells and PMN-MDSCs in the spleen of tolerised mice. Previous work implied that T cells need to migrate through the spleen to become encephalitogenic and cause disease (151). It may be possible that PMN-MDSCs in the spleen prevent T cell licensing, meaning that they may inhibit the adjustment process of CD4$^+$ T cells in the spleen that allows them to cross the blood-brain-barrier, enter the brain and cause disease.

The presence of secondary lymphoid tissues is believed to be essential for the initiation of adaptive immunity and that during subcutaneous immunisation local APCs take up the antigen and transport it to lymph nodes (236). However, one study showed that the initiation of EAE after immunisation with MOG$_{35-55}$ was still possible even in the absence of secondary lymphoid tissues (237). They found that, in the absence of draining lymph nodes, subcutaneously delivered antigens are actively transported by local APCs to the liver. Histological analysis revealed extra-lymphoid aggregates in the liver that allowed the initiation of antigen-specific CD4$^+$ T cell proliferation, thus supporting an important role for the liver in initiating T cell responses. Furthermore, it is known that the liver can be a site of induced immune tolerance through to the induction of CD4$^+$ Foxp3$^+$ Treg cells by liver sinusoidal endothelial cells (LSECs) (238). In addition, the specific delivery of the autoantigen MBP by nanoparticles (NP) to LSECs has been shown to prevent the development of EAE in B.10PL mice (239). However, NP-induced tolerance to MBP in the liver was lost in splenectomised B10.PL mice, indicating that the spleen is crucial for tolerance maintenance initiated in the liver. The control of tolerance in this model was the result of the induction of CD4$^+$ CD25$^+$ Treg cells as Treg cell depletion by an anti-CD25 antibody abrogated the tolerogenic effect of MBP-NP. Interestingly, this supported our finding that splenectomy seemed to reduce the population of Foxp3$^+$ Tregs and IL-10$^+$ CD4$^+$ T cells in the liver in our Tg4 tolerance model.

Unfortunately, we have not been able to demonstrate that PMN-MDSCs can protect mice from EAE, although a previous study suggested that these cells do have the potential to

ameliorate EAE (185). One reason can be that in our study we were limited to only one dose of 1.5 x $10^6$ PMN-MDSCs whereas in the study mentioned they adoptively transferred $2 \times 10^6$ PMN-MDSCs intravenously on day four and again on day seven post prime. Another study showed that MDSCs could prevent type I diabetes by transferring 5 x $10^6$ MDSCs on both day one and day four after disease induction (182). Therefore, each mouse received a transfer of a total of 4 x $10^6$ MDSCs in the first study and 10 x $10^6$ MDSCs in the second, compared to 1.5 x $10^6$ PMN-MDSCs in our experiments. Transfer of greater numbers of PMN-MDSCs was not feasible in our study, because the huge number of donor mice required would have been prohibitive, not only due to limited resources but also for ethical reasons. Although we could not demonstrate the protective effect of PMN-MDSCs ourselves in our EAE model, we feel that the studies mentioned, as well our other findings, clearly support this concept.

The usual method to examine whether a treatment is dependent on a certain population of cells is to deplete the cells prior to or after the treatment. We considered several published methods that result in PMN-MDSC depletion: the administration of chemotherapeutic agents, liposome-encapsulated dichloromethylene disphosphonate (clodronate liposome) or neutralising/depleting antibodies against PMN-MDSC-associated surface molecules including CD11b, Gr-1 and Ly6G. Chemotherapeutic anti-cancer drugs have been found to decrease the number of MDSCs in tumour-bearing mice (240, 241) but unfortunately these agents target all dividing cells and their effect is therefore by no means limited to MDSCs. The second option is the administration of clodronate using liposomes as vehicles. This method has been widely used to specifically eliminate phagocytic cells like macrophages or microglia in vivo (242). Once ingested by phagocytic cells, lysosomal phospholipases destroy the phospholipid bilayers of the liposomes and the clodronate is released, eliminating the phagocyte by apoptosis. However, as previously shown, administration of clodronate liposomes also eliminates dendritic cells located in the spleen (243) which can negatively affect CD4$^+$ T cell activation and proliferation. So again the effect is not specific to PMN-MDSCs. We also considered depleting PMN-MDSCs using antibodies as an alternative method. However, as PMN-MDSCs and neutrophils have several surface markers in common, using neutralising antibodies such as anti-CD11b, anti-Gr-1 or anti-Ly6G to deplete PMN-MDSC would most likely be compromised by the unintended depletion of neutrophils (244-246), which would compromise EAE development (247-249).

In the commonly held view, myeloid progenitor cells from the bone marrow migrate into peripheral tissues and differentiate locally into MDSCs (220). This view now seems obsolete and may need to be modified because recent studies have pointed to the spleen as a source of MDSCs (250-252). In a murine model of cervical cancer they found that the removal of the spleen significantly reduced the number of PMN-MDSC and enhanced the efficacy of platinum-based chemotherapy (252). Another study, supporting the hypothesis of a splenic reservoir, examined the effects of splenectomy on the growth of non-small cell lung cancer (NSCLC) tumours in mice and found that removal of the spleen led to a decrease of M-MDSCs in the blood and in the tumour, which resulted in decreased tumour growth (251). Altogether, those studies corroborate our finding that splenectomy prior to tolerance induction reduced the number of PMN-MDSCs in the ILNs and liver, verifying that the spleen can act as a reservoir for myeloid progenitor cells that give rise to MDSCs depending on the environmental cues (Figure 5.1.).

This thesis provides new insights into the phenotypic characteristics of tolerised CD4$^+$ T cells over the course of EDI systematically throughout the whole body and corroborates published data from our group generated from splenic CD4$^+$ T cells. It also demonstrates that tolerised MBP-specific CD4$^+$ T cells can mediate linked bystander suppression of CD4$^+$ T cells specific for a MOG peptide. This implies that not all possible disease-mediating epitopes need to be covered for the successful clinical application of peptide immunotherapy but that a limited number of immunodominant epitopes can provide all-round protection. Furthermore, the results in this thesis underscore a previously unknown role for PMN-MDSCs in limiting immune responses in antigen-specific peptide immunotherapy. This indicates that the differentiation of tolerogenic PMN-MDSCs should be a target for antigen-specific immunotherapy.
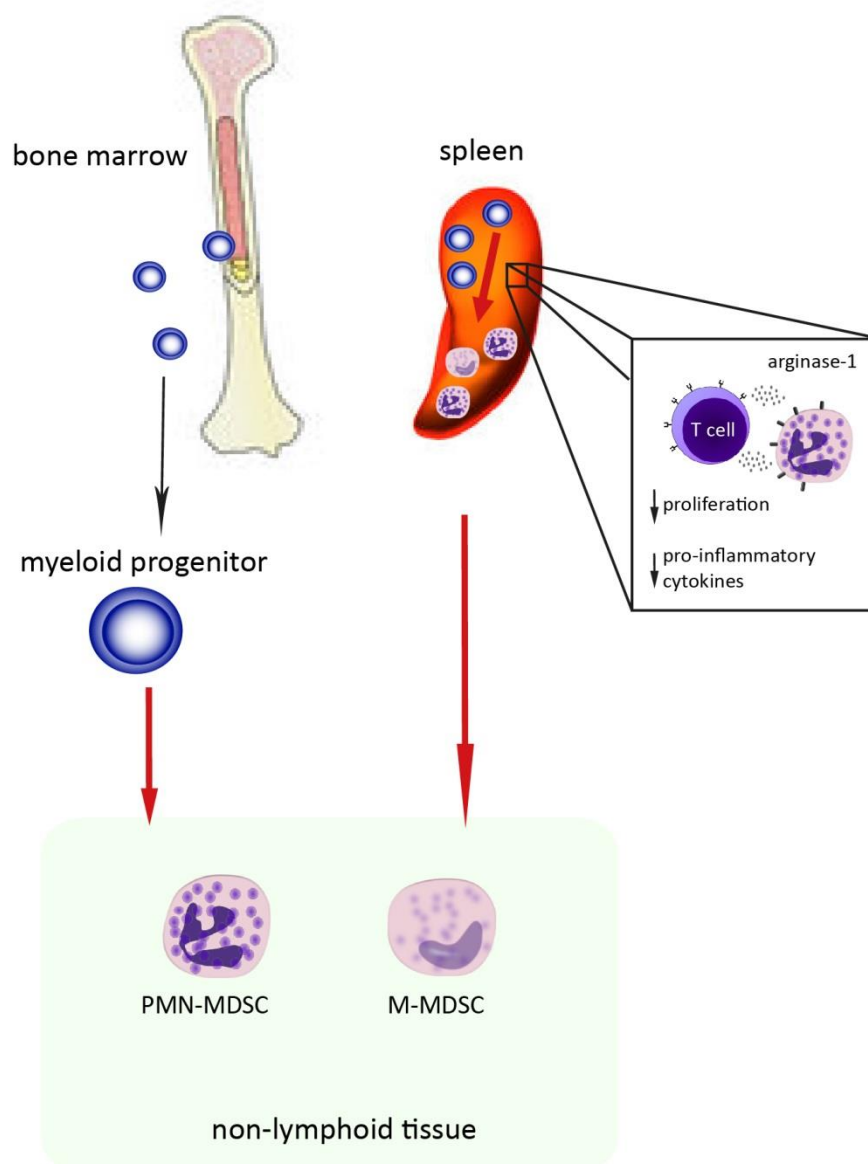
**Figure 5.1: MDSC differentiation during antigen-specific EDI**. MDSCs in non-lymphoid tissues, such as the liver, can either differentiate directly from bone marrow-derived myeloid progenitor cells in situ or can migrate there after differentiating from a pool of myeloid progenitors in the spleen. In addition to acting as a reservoir for MDSCs, the spleen is an important site for interactions between PMN-MDSCs and CD4^{+} T cells, which contributes to the protective effect of antigen-specific peptide immunotherapy.

# 6 REFERENCES

1. Janeway CA, Jr. & Medzhitov R (2002) Innate immune recognition. *Annual review of immunology* 20:197-216.

2. Munz C, Steinman RM, & Fujii S (2005) Dendritic cell maturation by innate lymphocytes: coordinated stimulation of innate and adaptive immunity. *The Journal of experimental medicine* 202(2):203-207.

3. Steinman RM & Banchereau J (2007) Taking dendritic cells into medicine. *Nature* 449(7161):419-426.

4. Miller JF (1961) Immunological function of the thymus. *Lancet* 2(7205):748-749.

5. Cantor H & Weissman I (1976) Development and function of subpopulations of thymocytes and T lymphocytes. *Progress in allergy* 20:1-64.

6. Stutman O (1978) Intrathymic and extrathymic T cell maturation. *Immunological reviews* 42:138-184.

7. Derbinski J, Schulte A, Kyewski B, & Klein L (2001) Promiscuous gene expression in medullary thymic epithelial cells mirrors the peripheral self. *Nature immunology* 2(11):1032-1039.

8. Anderson MS & Su MA (2011) Aire and T cell development. *Current opinion in immunology* 23(2):198-206.

9. Sainte-Marie G & Leblond CP (1964) Cytologic Features and Cellular Migration in the Cortex and Medulla of Thymus in the Young Adult Rat. *Blood* 23:275-299.

10. Bhan AK, Reinherz EL, Poppema S, McCluskey RT, & Schlossman SF (1980) Location of T cell and major histocompatibility complex antigens in the human thymus. *The Journal of experimental medicine* 152(4):771-782.

11. Zinkernagel RM*, et al.* (1978) On the thymus in the differentiation of "H-2 self-recognition" by T cells: evidence for dual recognition? *The Journal of experimental medicine* 147(3):882-896.

12. Abbas AK*, et al.* (2013) Regulatory T cells: recommendations to simplify the nomenclature. *Nature immunology* 14(4):307-308.

13. Mosmann TR, Cherwinski H, Bond MW, Giedlin MA, & Coffman RL (1986) Two types of murine helper T cell clone. I. Definition according to profiles of lymphokine activities and secreted proteins. *Journal of immunology* 136(7):2348-2357.

14. Killar L, MacDonald G, West J, Woods A, & Bottomly K (1987) Cloned, Ia-restricted T cells that do not produce interleukin 4(IL 4)/B cell stimulatory factor 1(BSF-1) fail to help antigen-specific B cells. *Journal of immunology* 138(6):1674-1679.

15. Zheng W & Flavell RA (1997) The transcription factor GATA-3 is necessary and sufficient for Th2 cytokine gene expression in CD4 T cells. *Cell* 89(4):587-596.

16. Zhang DH, Cohn L, Ray P, Bottomly K, & Ray A (1997) Transcription factor GATA-3 is differentially expressed in murine Th1 and Th2 cells and controls Th2-specific expression of the interleukin-5 gene. *The Journal of biological chemistry* 272(34):21597-21603.

17. Zhu J, Cote-Sierra J, Guo L, & Paul WE (2003) Stat5 activation plays a critical role in Th2 differentiation. *Immunity* 19(5):739-748.

18. Luckheeram RV, Zhou R, Verma AD, & Xia B (2012) CD4(+)T cells: differentiation and functions. *Clinical & developmental immunology* 2012:925135.

19. Szabo SJ*, et al.* (2000) A novel transcription factor, T-bet, directs Th1 lineage commitment. *Cell* 100(6):655-669.

20. Afkarian M*, et al.* (2002) T-bet is a STAT1-induced regulator of IL-12R expression in naive CD4+ T cells. *Nature immunology* 3(6):549-557.

21. Park H*, et al.* (2005) A distinct lineage of CD4 T cells regulates tissue inflammation by producing interleukin 17. *Nature immunology* 6(11):1133-1141.

22. Zhou L*, et al.* (2007) IL-6 programs T(H)-17 cell differentiation by promoting sequential engagement of the IL-21 and IL-23 pathways. *Nature immunology* 8(9):967-974.

23. Nurieva R*, et al.* (2007) Essential autocrine regulation by IL-21 in the generation of inflammatory T cells. *Nature* 448(7152):480-483.

24. Harris TJ*, et al.* (2007) Cutting edge: An in vivo requirement for STAT3 signaling in TH17 development and TH17-dependent autoimmunity. *Journal of immunology* 179(7):4313-4317.

25. Huang W, Na L, Fidel PL, & Schwarzenberger P (2004) Requirement of interleukin-17A for systemic anti-Candida albicans host defense in mice. *The Journal of infectious diseases* 190(3):624-631.

26. Bradley BL*, et al.* (1991) Eosinophils, T-lymphocytes, mast cells, neutrophils, and macrophages in bronchial biopsy specimens from atopic subjects with asthma: comparison with biopsy specimens from atopic subjects without asthma and normal control subjects and relationship to bronchial hyperresponsiveness. *The Journal of allergy and clinical immunology* 88(4):661-674.

27. Renno T*, et al.* (1994) Selective enrichment of Th1 CD45RBlow CD4+ T cells in autoimmune infiltrates in experimental allergic encephalomyelitis. *International immunology* 6(3):347-354.

28. Renno T, Krakowski M, Piccirillo C, Lin JY, & Owens T (1995) TNF-alpha expression by resident microglia and infiltrating leukocytes in the central nervous system of mice with experimental allergic encephalomyelitis. Regulation by Th1 cytokines. *Journal of immunology* 154(2):944-953.

29. Hirota K*, et al.* (2011) Fate mapping of IL-17-producing T cells in inflammatory responses. *Nature immunology* 12(3):255-263.

30. Kurschus FC*, et al.* (2010) Genetic proof for the transient nature of the Th17 phenotype. *European journal of immunology* 40(12):3336-3346.

31. Haak S*, et al.* (2009) IL-17A and IL-17F do not contribute vitally to autoimmune neuro-inflammation in mice. *The Journal of clinical investigation* 119(1):61-69.

32. Noseworthy JH, Lucchinetti C, Rodriguez M, & Weinshenker BG (2000) Multiple sclerosis. *The New England journal of medicine* 343(13):938-952.

33. Sherman DL & Brophy PJ (2005) Mechanisms of axon ensheathment and myelin growth. *Nature reviews. Neuroscience* 6(9):683-690.

34. Nave KA (2010) Myelination and the trophic support of long axons. *Nature reviews. Neuroscience* 11(4):275-283.

35. Steinman L (1996) Multiple sclerosis: a coordinated immunological attack against myelin in the central nervous system. *Cell* 85(3):299-302.

36. Mallucci G, Peruzzotti-Jametti L, Bernstock JD, & Pluchino S (2015) The role of immune cells, glia and neurons in white and gray matter pathology in multiple sclerosis. *Progress in neurobiology* 127-128:1-22.

37. de Rosbo NK & Ben-Nun A (1998) T-cell responses to myelin antigens in multiple sclerosis; relevance of the predominant autoimmune reactivity to myelin oligodendrocyte glycoprotein. *Journal of autoimmunity* 11(4):287-299.

38. Olsson T*, et al.* (1990) Autoreactive T lymphocytes in multiple sclerosis determined by antigen-induced secretion of interferon-gamma. *The Journal of clinical investigation* 86(3):981-985.

39. Chaudhuri A & Behan PO (2004) Multiple sclerosis is not an autoimmune disease. *Archives of neurology* 61(10):1610-1612.

40. Cifelli A*, et al.* (2002) Thalamic neurodegeneration in multiple sclerosis. *Annals of neurology* 52(5):650-653.

41. Matthews PM*, et al.* (1998) Putting magnetic resonance spectroscopy studies in context: axonal damage and disability in multiple sclerosis. *Seminars in neurology* 18(3):327-336.

42. Baxter AG (2007) The origin and application of experimental autoimmune encephalomyelitis. *Nature reviews. Immunology* 7(11):904-912.

43. Waldner H, Whitters MJ, Sobel RA, Collins M, & Kuchroo VK (2000) Fulminant spontaneous autoimmunity of the central nervous system in mice transgenic for the myelin proteolipid protein-specific T cell receptor. *Proceedings of the National Academy of Sciences of the United States of America* 97(7):3412-3417.

44. Goverman J*, et al.* (1993) Transgenic mice that express a myelin basic protein-specific T cell receptor develop spontaneous autoimmunity. *Cell* 72(4):551-560.

45. Bettelli E*, et al.* (2003) Myelin oligodendrocyte glycoprotein-specific T cell receptor transgenic mice develop spontaneous autoimmune optic neuritis. *The Journal of experimental medicine* 197(9):1073-1081.

46. Gold R, Linington C, & Lassmann H (2006) Understanding pathogenesis and therapy of multiple sclerosis via animal models: 70 years of merits and culprits in experimental autoimmune encephalomyelitis research. *Brain : a journal of neurology* 129(Pt 8):1953-1971.

47. Holland NJ, Schneider DM, Rapp R, & Kalb RC (2011) Meeting the needs of people with primary progressive multiple sclerosis, their families, and the health-care community. *International journal of MS care* 13(2):65-74.

48. Berkovich R (2013) Treatment of acute relapses in multiple sclerosis. *Neurotherapeutics : the journal of the American Society for Experimental NeuroTherapeutics* 10(1):97-105.

49. Abramsky O, Teitelbaum D, & Arnon R (1977) Effect of a synthetic polypeptide (COP 1) on patients with multiple sclerosis and with acute disseminated encephalomeylitis. Preliminary report. *Journal of the neurological sciences* 31(3):433-438.

50. Goodin DS*, et al.* (2003) The use of mitoxantrone (Novantrone) for the treatment of multiple sclerosis: report of the Therapeutics and Technology Assessment Subcommittee of the American Academy of Neurology. *Neurology* 61(10):1332-1338.

51. Vieira PL, Heystek HC, Wormmeester J, Wierenga EA, & Kapsenberg ML (2003) Glatiramer acetate (copolymer-1, copaxone) promotes Th2 cell development and increased IL-10 production through modulation of dendritic cells. *Journal of immunology* 170(9):4483-4488.

52. Kieseier BC (2011) The mechanism of action of interferon-beta in relapsing multiple sclerosis. *CNS drugs* 25(6):491-502.

53. Rice GP, Hartung HP, & Calabresi PA (2005) Anti-alpha4 integrin therapy for multiple sclerosis: mechanisms and rationale. *Neurology* 64(8):1336-1342.

54. Carlos TM*, et al.* (1990) Vascular cell adhesion molecule-1 mediates lymphocyte adherence to cytokine-activated cultured human endothelial cells. *Blood* 76(5):965-970.

55. Hauser SL*, et al.* (2008) B-cell depletion with rituximab in relapsing-remitting multiple sclerosis. *The New England journal of medicine* 358(7):676-688.

56. Duddy M & Bar-Or A (2006) B-cells in multiple sclerosis. *International MS journal / MS Forum* 13(3):84-90.

57. Campbell JD*, et al.* (2009) Peptide immunotherapy in allergic asthma generates IL-10-dependent immunological tolerance associated with linked epitope suppression. *The Journal of experimental medicine* 206(7):1535-1547.

58. Gabrysova L*, et al.* (2009) Negative feedback control of the autoimmune response through antigen-induced differentiation of IL-10-secreting Th1 cells. *The Journal of experimental medicine* 206(8):1755-1767.

59. Burkhart C, Liu GY, Anderton SM, Metzler B, & Wraith DC (1999) Peptide-induced T cell regulation of experimental autoimmune encephalomyelitis: a role for IL-10. *International immunology* 11(10):1625-1634.

60. Streeter HB, Rigden R, Martin KF, Scolding NJ, & Wraith DC (2015) Preclinical development and first-in-human study of ATX-MS-1467 for immunotherapy of MS. *Neurology(R) neuroimmunology & neuroinflammation* 2(3):e93.

61. Burton BR*, et al.* (2014) Sequential transcriptional changes dictate safe and effective antigen-specific immunotherapy. *Nature communications* 5:4741.

62. Sabatos-Peyton CA, Verhagen J, & Wraith DC (2010) Antigen-specific immunotherapy of autoimmune and allergic diseases. *Current opinion in immunology* 22(5):609-615.

63. Akdis CA*, et al.* (1996) Epitope-specific T cell tolerance to phospholipase A2 in bee venom immunotherapy and recovery by IL-2 and IL-15 in vitro. *The Journal of clinical investigation* 98(7):1676-1683.

64. Sakaguchi S*, et al.* (2001) Immunologic tolerance maintained by CD25+ CD4+ regulatory T cells: their common role in controlling autoimmunity, tumor immunity, and transplantation tolerance. *Immunological reviews* 182:18-32.

65. Fontenot JD, Gavin MA, & Rudensky AY (2003) Foxp3 programs the development and function of CD4+CD25+ regulatory T cells. *Nature immunology* 4(4):330-336.

66. Hori S, Nomura T, & Sakaguchi S (2003) Control of regulatory T cell development by the transcription factor Foxp3. *Science* 299(5609):1057-1061.

67. Burchill MA, Yang J, Vogtenhuber C, Blazar BR, & Farrar MA (2007) IL-2 receptor beta-dependent STAT5 activation is required for the development of Foxp3+ regulatory T cells. *Journal of immunology* 178(1):280-290.

68. Chen W*, et al.* (2003) Conversion of peripheral CD4+CD25- naive T cells to CD4+CD25+ regulatory T cells by TGF-beta induction of transcription factor Foxp3. *The Journal of experimental medicine* 198(12):1875-1886.

69. Williams LM & Rudensky AY (2007) Maintenance of the Foxp3-dependent developmental program in mature regulatory T cells requires continued expression of Foxp3. *Nature immunology* 8(3):277-284.

70. Bennett CL*, et al.* (2001) The immune dysregulation, polyendocrinopathy, enteropathy, X-linked syndrome (IPEX) is caused by mutations of FOXP3. *Nature genetics* 27(1):20-21.

71. Brunkow ME*, et al.* (2001) Disruption of a new forkhead/winged-helix protein, scurfin, results in the fatal lymphoproliferative disorder of the scurfy mouse. *Nature genetics* 27(1):68-73.

72. Tran DQ, Ramsey H, & Shevach EM (2007) Induction of FOXP3 expression in naive human CD4+FOXP3 T cells by T-cell receptor stimulation is transforming growth factor-beta dependent but does not confer a regulatory phenotype. *Blood* 110(8):2983-2990.

73. Komatsu N*, et al.* (2014) Pathogenic conversion of Foxp3+ T cells into TH17 cells in autoimmune arthritis. *Nature medicine* 20(1):62-68.

74. Akdis M*, et al.* (2004) Immune responses in healthy and allergic individuals are characterized by a fine balance between allergen-specific T regulatory 1 and T helper 2 cells. *The Journal of experimental medicine* 199(11):1567-1575.

75. Meiler F*, et al.* (2008) In vivo switch to IL-10-secreting T regulatory cells in high dose allergen exposure. *The Journal of experimental medicine* 205(12):2887-2898.

76. Groux H*, et al.* (1997) A CD4+ T-cell subset inhibits antigen-specific T-cell responses and prevents colitis. *Nature* 389(6652):737-742.

77. Verhagen J, Gabrysova L, Shepard ER, & Wraith DC (2014) Ctla-4 modulates the differentiation of inducible Foxp3+ Treg cells but IL-10 mediates their function in experimental autoimmune encephalomyelitis. *PloS one* 9(9):e108023.

78. Asnagli H*, et al.* (2014) Type 1 regulatory T cells specific for collagen type II as an efficient cell-based therapy in arthritis. *Arthritis research & therapy* 16(3):R115.

79. Barrat FJ*, et al.* (2002) In vitro generation of interleukin 10-producing regulatory CD4(+) T cells is induced by immunosuppressive drugs and inhibited by T helper type 1 (Th1)- and Th2-inducing cytokines. *The Journal of experimental medicine* 195(5):603-616.

80. Nakamura K, Kitani A, & Strober W (2001) Cell contact-dependent immunosuppression by CD4(+)CD25(+) regulatory T cells is mediated by cell surface-bound transforming growth factor beta. *The Journal of experimental medicine* 194(5):629-644.

81. Bacchetta R*, et al.* (1994) High levels of interleukin 10 production in vivo are associated with tolerance in SCID patients transplanted with HLA mismatched hematopoietic stem cells. *The Journal of experimental medicine* 179(2):493-502.

82. Haringer B, Lozza L, Steckel B, & Geginat J (2009) Identification and characterization of IL-10/IFN-gamma-producing effector-like T cells with regulatory function in human blood. *The Journal of experimental medicine* 206(5):1009-1017.

83. Riedinger M, Karjalainen K, & Brocker T (1997) Targeted expression of MHC class II genes to dendritic cells in vivo. *Immunology letters* 57(1-3):155-158.

84. Anderson AC, Joller N, & Kuchroo VK (2016) Lag-3, Tim-3, and TIGIT: Co-inhibitory Receptors with Specialized Functions in Immune Regulation. *Immunity* 44(5):989-1004.

85. June CH, Ledbetter JA, Gillespie MM, Lindsten T, & Thompson CB (1987) T-cell proliferation involving the CD28 pathway is associated with cyclosporine-resistant interleukin 2 gene expression. *Molecular and cellular biology* 7(12):4472-4481.

86. Linsley PS, Clark EA, & Ledbetter JA (1990) T-cell antigen CD28 mediates adhesion with B cells by interacting with activation antigen B7/BB-1. *Proceedings of the National Academy of Sciences of the United States of America* 87(13):5031-5035.

87. Azuma M*, et al.* (1993) B70 antigen is a second ligand for CTLA-4 and CD28. *Nature* 366(6450):76-79.

88. Rudd CE, Taylor A, & Schneider H (2009) CD28 and CTLA-4 coreceptor expression and signal transduction. *Immunological reviews* 229(1):12-26.

89. Hathcock KS, Laszlo G, Pucillo C, Linsley P, & Hodes RJ (1994) Comparative analysis of B7-1 and B7-2 costimulatory ligands: expression and function. *The Journal of experimental medicine* 180(2):631-640.

90. Inaba K*, et al.* (1994) The tissue distribution of the B7-2 costimulator in mice: abundant expression on dendritic cells in situ and during maturation in vitro. *The Journal of experimental medicine* 180(5):1849-1860.

91. Hathcock KS*, et al.* (1993) Identification of an alternative CTLA-4 ligand costimulatory for T cell activation. *Science* 262(5135):905-907.

92. Gross JA, Callas E, & Allison JP (1992) Identification and distribution of the costimulatory receptor CD28 in the mouse. *Journal of immunology* 149(2):380-388.

93. Linsley PS*, et al.* (1996) Intracellular trafficking of CTLA-4 and focal localization towards sites of TCR engagement. *Immunity* 4(6):535-543.

94. Viola A & Lanzavecchia A (1996) T cell activation determined by T cell receptor number and tunable thresholds. *Science* 273(5271):104-106.

95. Thompson CB*, et al.* (1989) CD28 activation pathway regulates the production of multiple T-cell-derived lymphokines/cytokines. *Proceedings of the National Academy of Sciences of the United States of America* 86(4):1333-1337.

96. Engelhardt JJ, Sullivan TJ, & Allison JP (2006) CTLA-4 overexpression inhibits T cell responses through a CD28-B7-dependent mechanism. *Journal of immunology* 177(2):1052-1061.

97. van der Merwe PA & Davis SJ (2003) Molecular interactions mediating T cell antigen recognition. *Annual review of immunology* 21:659-684.

98. Waterhouse P*, et al.* (1995) Lymphoproliferative disorders with early lethality in mice deficient in Ctla-4. *Science* 270(5238):985-988.

99. Tivol EA*, et al.* (1995) Loss of CTLA-4 leads to massive lymphoproliferation and fatal multiorgan tissue destruction, revealing a critical negative regulatory role of CTLA-4. *Immunity* 3(5):541-547.

100. Mandelbrot DA, McAdam AJ, & Sharpe AH (1999) B7-1 or B7-2 is required to produce the lymphoproliferative phenotype in mice lacking cytotoxic T lymphocyte-associated antigen 4 (CTLA-4). *The Journal of experimental medicine* 189(2):435-440.

101. Perez VL*, et al.* (1997) Induction of peripheral T cell tolerance in vivo requires CTLA-4 engagement. *Immunity* 6(4):411-417.

102. Greenwald RJ, Boussiotis VA, Lorsbach RB, Abbas AK, & Sharpe AH (2001) CTLA-4 regulates induction of anergy in vivo. *Immunity* 14(2):145-155.

103. Sabatos CA*, et al.* (2003) Interaction of Tim-3 and Tim-3 ligand regulates T helper type 1 responses and induction of peripheral tolerance. *Nature immunology* 4(11):1102-1110.

104. Monney L*, et al.* (2002) Th1-specific cell surface protein Tim-3 regulates macrophage activation and severity of an autoimmune disease. *Nature* 415(6871):536-541.

105.   Nakayama M*, et al.* (2009) Tim-3 mediates phagocytosis of apoptotic cells and cross-presentation. *Blood* 113(16):3821-3830.

106.   Chiba S*, et al.* (2012) Tumor-infiltrating DCs suppress nucleic acid-mediated innate immune responses through interactions between the receptor TIM-3 and the alarmin HMGB1. *Nature immunology* 13(9):832-842.

107.   Huang YH*, et al.* (2015) CEACAM1 regulates TIM-3-mediated tolerance and exhaustion. *Nature* 517(7534):386-390.

108.   Sanchez-Fueyo A*, et al.* (2003) Tim-3 inhibits T helper type 1-mediated auto- and alloimmune responses and promotes immunological tolerance. *Nature immunology* 4(11):1093-1101.

109.   Zhu C*, et al.* (2005) The Tim-3 ligand galectin-9 negatively regulates T helper type 1 immunity. *Nature immunology* 6(12):1245-1252.

110.   Su EW, Bi S, & Kane LP (2011) Galectin-9 regulates T helper cell function independently of Tim-3. *Glycobiology* 21(10):1258-1265.

111.   Leitner J*, et al.* (2013) TIM-3 does not act as a receptor for galectin-9. *PLoS pathogens* 9(3):e1003253.

112.   Jones RB*, et al.* (2008) Tim-3 expression defines a novel population of dysfunctional T cells with highly elevated frequencies in progressive HIV-1 infection. *The Journal of experimental medicine* 205(12):2763-2779.

113.   Kassu A*, et al.* (2010) Regulation of virus-specific CD4+ T cell function by multiple costimulatory receptors during chronic HIV infection. *Journal of immunology* 185(5):3007-3018.

114.   Golden-Mason L*, et al.* (2009) Negative immune regulator Tim-3 is overexpressed on T cells in hepatitis C virus infection and its blockade rescues dysfunctional CD4+ and CD8+ T cells. *Journal of virology* 83(18):9122-9130.

115.   Sehrawat S*, et al.* (2010) Galectin-9/TIM-3 interaction regulates virus-specific primary and memory CD8 T cell response. *PLoS pathogens* 6(5):e1000882.

116.   Geng H*, et al.* (2006) Soluble form of T cell Ig mucin 3 is an inhibitory molecule in T cell-mediated immune response. *Journal of immunology* 176(3):1411-1420.

117.   Ishida Y, Agata Y, Shibahara K, & Honjo T (1992) Induced expression of PD-1, a novel member of the immunoglobulin gene superfamily, upon programmed cell death. *The EMBO journal* 11(11):3887-3895.

118.   Nishimura H, Nose M, Hiai H, Minato N, & Honjo T (1999) Development of lupus-like autoimmune diseases by disruption of the PD-1 gene encoding an ITIM motif-carrying immunoreceptor. *Immunity* 11(2):141-151.

119.   Appleman LJ, van Puijenbroek AA, Shu KM, Nadler LM, & Boussiotis VA (2002) CD28 costimulation mediates down-regulation of p27kip1 and cell cycle progression by activation of the PI3K/PKB signaling pathway in primary human T cells. *Journal of immunology* 168(6):2729-2736.

120.   Parry RV*, et al.* (2005) CTLA-4 and PD-1 receptors inhibit T-cell activation by distinct mechanisms. *Molecular and cellular biology* 25(21):9543-9553.

121.   Chemnitz JM, Parry RV, Nichols KE, June CH, & Riley JL (2004) SHP-1 and SHP-2 associate with immunoreceptor tyrosine-based switch motif of programmed death 1 upon primary human T cell stimulation, but only receptor ligation prevents T cell activation. *Journal of immunology* 173(2):945-954.

122. Boise LH*, et al.* (1995) CD28 costimulation can promote T cell survival by enhancing the expression of Bcl-XL. *Immunity* 3(1):87-98.

123. Keir ME, Butte MJ, Freeman GJ, & Sharpe AH (2008) PD-1 and its ligands in tolerance and immunity. *Annual review of immunology* 26:677-704.

124. Agata Y*, et al.* (1996) Expression of the PD-1 antigen on the surface of stimulated mouse T and B lymphocytes. *International immunology* 8(5):765-772.

125. Dong H, Zhu G, Tamada K, & Chen L (1999) B7-H1, a third member of the B7 family, co-stimulates T-cell proliferation and interleukin-10 secretion. *Nature medicine* 5(12):1365-1369.

126. Latchman Y*, et al.* (2001) PD-L2 is a second ligand for PD-1 and inhibits T cell activation. *Nature immunology* 2(3):261-268.

127. Tseng SY*, et al.* (2001) B7-DC, a new dendritic cell molecule with potent costimulatory properties for T cells. *The Journal of experimental medicine* 193(7):839-846.

128. Yamazaki T*, et al.* (2002) Expression of programmed death 1 ligands by murine T cells and APC. *Journal of immunology* 169(10):5538-5545.

129. Latchman YE*, et al.* (2004) PD-L1-deficient mice show that PD-L1 on T cells, antigen-presenting cells, and host tissues negatively regulates T cells. *Proceedings of the National Academy of Sciences of the United States of America* 101(29):10691-10696.

130. Fife BT*, et al.* (2006) Insulin-induced remission in new-onset NOD mice is maintained by the PD-1-PD-L1 pathway. *The Journal of experimental medicine* 203(12):2737-2747.

131. Yu X*, et al.* (2009) The surface protein TIGIT suppresses T cell activation by promoting the generation of mature immunoregulatory dendritic cells. *Nature immunology* 10(1):48-57.

132. Joller N*, et al.* (2011) Cutting edge: TIGIT has T cell-intrinsic inhibitory functions. *Journal of immunology* 186(3):1338-1342.

133. Levin SD*, et al.* (2011) Vstm3 is a member of the CD28 family and an important modulator of T-cell function. *European journal of immunology* 41(4):902-915.

134. Zhang Y*, et al.* (2013) Genome-wide DNA methylation analysis identifies hypomethylated genes regulated by FOXP3 in human regulatory T cells. *Blood* 122(16):2823-2836.

135. Joller N*, et al.* (2014) Treg cells expressing the coinhibitory molecule TIGIT selectively inhibit proinflammatory Th1 and Th17 cell responses. *Immunity* 40(4):569-581.

136. Fiorentino DF, Bond MW, & Mosmann TR (1989) Two types of mouse T helper cell. IV. Th2 clones secrete a factor that inhibits cytokine production by Th1 clones. *The Journal of experimental medicine* 170(6):2081-2095.

137. Sabat R*, et al.* (2010) Biology of interleukin-10. *Cytokine & growth factor reviews* 21(5):331-344.

138. Arif S*, et al.* (2004) Autoreactive T cell responses show proinflammatory polarization in diabetes but a regulatory phenotype in health. *The Journal of clinical investigation* 113(3):451-463.

139. Kuhn R, Lohler J, Rennick D, Rajewsky K, & Muller W (1993) Interleukin-10-deficient mice develop chronic enterocolitis. *Cell* 75(2):263-274.

140. Bettelli E, *et al.* (1998) IL-10 is critical in the regulation of autoimmune encephalomyelitis as demonstrated by studies of IL-10- and IL-4-deficient and transgenic mice. *Journal of immunology* 161(7):3299-3306.

141. van Boxel-Dezaire AH, *et al.* (1999) Decreased interleukin-10 and increased interleukin-12p40 mRNA are associated with disease activity and characterize different disease stages in multiple sclerosis. *Annals of neurology* 45(6):695-703.

142. Croxford AL & Buch T (2011) Cytokine reporter mice in immunological research: perspectives and lessons learned. *Immunology* 132(1):1-8.

143. Calado DP, Paixao T, Holmberg D, & Haury M (2006) Stochastic monoallelic expression of IL-10 in T cells. *Journal of immunology* 177(8):5358-5364.

144. Kamanaka M, *et al.* (2006) Expression of interleukin-10 in intestinal lymphocytes detected by an interleukin-10 reporter knockin tiger mouse. *Immunity* 25(6):941-952.

145. Neves P, *et al.* (2010) Signaling via the MyD88 adaptor protein in B cells suppresses protective immunity during Salmonella typhimurium infection. *Immunity* 33(5):777-790.

146. Bouabe H, Liu Y, Moser M, Bosl MR, & Heesemann J (2011) Novel highly sensitive IL-10-beta-lactamase reporter mouse reveals cells of the innate immune system as a substantial source of IL-10 in vivo. *Journal of immunology* 187(6):3165-3176.

147. Madan R, *et al.* (2009) Nonredundant roles for B cell-derived IL-10 in immune counter-regulation. *Journal of immunology* 183(4):2312-2320.

148. Atarashi K, *et al.* (2011) Induction of colonic regulatory T cells by indigenous Clostridium species. *Science* 331(6015):337-341.

149. Maynard CL, *et al.* (2007) Regulatory T cells expressing interleukin 10 develop from Foxp3+ and Foxp3- precursor cells in the absence of interleukin 10. *Nature immunology* 8(9):931-941.

150. Wekerle H, Kojima K, Lannes-Vieira J, Lassmann H, & Linington C (1994) Animal models. *Annals of neurology* 36 Suppl:S47-53.

151. Flugel A, *et al.* (2001) Migratory activity and functional changes of green fluorescent effector cells before and during experimental autoimmune encephalomyelitis. *Immunity* 14(5):547-560.

152. Odoardi F, *et al.* (2012) T cells become licensed in the lung to enter the central nervous system. *Nature* 488(7413):675-679.

153. Manouchehrinia A, *et al.* (2013) Tobacco smoking and disability progression in multiple sclerosis: United Kingdom cohort study. *Brain : a journal of neurology* 136(Pt 7):2298-2304.

154. Mastrangelo A, *et al.* (2015) The Role of Posttranslational Protein Modifications in Rheumatological Diseases: Focus on Rheumatoid Arthritis. *Journal of immunology research* 2015:712490.

155. Metzler B & Wraith DC (1996) Mucosal tolerance in a murine model of experimental autoimmune encephalomyelitis. *Annals of the New York Academy of Sciences* 778:228-242.

156. Anderton SM & Wraith DC (1998) Hierarchy in the ability of T cell epitopes to induce peripheral tolerance to antigens from myelin. *European journal of immunology* 28(4):1251-1261.

157. Jun S, Ochoa-Reparaz J, Zlotkowska D, Hoyt T, & Pascual DW (2012) Bystander-mediated stimulation of proteolipid protein-specific regulatory T (Treg) cells confers

protection against experimental autoimmune encephalomyelitis (EAE) via TGF-beta. *Journal of neuroimmunology* 245(1-2):39-47.

158. Dardalhon V*, et al.* (2010) Tim-3/galectin-9 pathway: regulation of Th1 immunity through promotion of CD11b+Ly-6G+ myeloid cells. *Journal of immunology* 185(3):1383-1392.

159. Buessow SC, Paul RD, & Lopez DM (1984) Influence of mammary tumor progression on phenotype and function of spleen and in situ lymphocytes in mice. *Journal of the National Cancer Institute* 73(1):249-255.

160. Almand B*, et al.* (2001) Increased production of immature myeloid cells in cancer patients: a mechanism of immunosuppression in cancer. *Journal of immunology* 166(1):678-689.

161. Kusmartsev S & Gabrilovich DI (2006) Role of immature myeloid cells in mechanisms of immune evasion in cancer. *Cancer immunology, immunotherapy : CII* 55(3):237-245.

162. Youn JI, Nagaraj S, Collazo M, & Gabrilovich DI (2008) Subsets of myeloid-derived suppressor cells in tumor-bearing mice. *Journal of immunology* 181(8):5791-5802.

163. Ribechini E, Greifenberg V, Sandwick S, & Lutz MB (2010) Subsets, expansion and activation of myeloid-derived suppressor cells. *Medical microbiology and immunology* 199(3):273-281.

164. Bronte V*, et al.* (1999) Unopposed production of granulocyte-macrophage colony-stimulating factor by tumors inhibits CD8+ T cell responses by dysregulating antigen-presenting cell maturation. *Journal of immunology* 162(10):5728-5737.

165. Gallina G*, et al.* (2006) Tumors induce a subset of inflammatory monocytes with immunosuppressive activity on CD8+ T cells. *The Journal of clinical investigation* 116(10):2777-2790.

166. Huang B*, et al.* (2006) Gr-1+CD115+ immature myeloid suppressor cells mediate the development of tumor-induced T regulatory cells and T-cell anergy in tumor-bearing host. *Cancer research* 66(2):1123-1131.

167. Rodriguez PC, Quiceno DG, & Ochoa AC (2007) L-arginine availability regulates T-lymphocyte cell-cycle progression. *Blood* 109(4):1568-1573.

168. Movahedi K*, et al.* (2008) Identification of discrete tumor-induced myeloid-derived suppressor cell subpopulations with distinct T cell-suppressive activity. *Blood* 111(8):4233-4244.

169. Harari O & Liao JK (2004) Inhibition of MHC II gene transcription by nitric oxide and antioxidants. *Current pharmaceutical design* 10(8):893-898.

170. Rivoltini L*, et al.* (2002) Immunity to cancer: attack and escape in T lymphocyte-tumor cell interaction. *Immunological reviews* 188:97-113.

171. Kusmartsev S, Nefedova Y, Yoder D, & Gabrilovich DI (2004) Antigen-specific inhibition of CD8+ T cell response by immature myeloid cells in cancer is mediated by reactive oxygen species. *Journal of immunology* 172(2):989-999.

172. Vickers SM, MacMillan-Crow LA, Green M, Ellis C, & Thompson JA (1999) Association of increased immunostaining for inducible nitric oxide synthase and nitrotyrosine with fibroblast growth factor transformation in pancreatic cancer. *Archives of surgery* 134(3):245-251.

173. Nagaraj S*, et al.* (2007) Altered recognition of antigen is a mechanism of CD8+ T cell tolerance in cancer. *Nature medicine* 13(7):828-835.

174. Gabrilovich DI, Velders MP, Sotomayor EM, & Kast WM (2001) Mechanism of immune dysfunction in cancer mediated by immature Gr-1+ myeloid cells. *Journal of immunology* 166(9):5398-5406.

175. Haile LA*, et al.* (2008) Myeloid-derived suppressor cells in inflammatory bowel disease: a new immunoregulatory pathway. *Gastroenterology* 135(3):871-881, 881 e871-875.

176. Willimsky G*, et al.* (2008) Immunogenicity of premalignant lesions is the primary cause of general cytotoxic T lymphocyte unresponsiveness. *The Journal of experimental medicine* 205(7):1687-1700.

177. Nagaraj S, Youn JI, & Gabrilovich DI (2013) Reciprocal relationship between myeloid-derived suppressor cells and T cells. *Journal of immunology* 191(1):17-23.

178. Nagaraj S*, et al.* (2012) Antigen-specific CD4(+) T cells regulate function of myeloid-derived suppressor cells in cancer via retrograde MHC class II signaling. *Cancer research* 72(4):928-938.

179. Pan PY*, et al.* (2010) Immune stimulatory receptor CD40 is required for T-cell suppression and T regulatory cell activation mediated by myeloid-derived suppressor cells in cancer. *Cancer research* 70(1):99-108.

180. Mildner A*, et al.* (2009) CCR2+Ly-6Chi monocytes are crucial for the effector phase of autoimmunity in the central nervous system. *Brain : a journal of neurology* 132(Pt 9):2487-2500.

181. Yi H, Guo C, Yu X, Zuo D, & Wang XY (2012) Mouse CD11b+Gr-1+ myeloid cells can promote Th17 cell differentiation and experimental autoimmune encephalomyelitis. *Journal of immunology* 189(9):4295-4304.

182. Yin B*, et al.* (2010) Myeloid-derived suppressor cells prevent type 1 diabetes in murine models. *Journal of immunology* 185(10):5828-5834.

183. Zhu B*, et al.* (2007) CD11b+Ly-6C(hi) suppressive monocytes in experimental autoimmune encephalomyelitis. *Journal of immunology* 179(8):5228-5237.

184. Kurko J*, et al.* (2014) Identification of myeloid-derived suppressor cells in the synovial fluid of patients with rheumatoid arthritis: a pilot study. *BMC musculoskeletal disorders* 15:281.

185. Ioannou M*, et al.* (2012) Crucial role of granulocytic myeloid-derived suppressor cells in the regulation of central nervous system autoimmune disease. *Journal of immunology* 188(3):1136-1146.

186. Whitfield-Larry F, Felton J, Buse J, & Su MA (2014) Myeloid-derived suppressor cells are increased in frequency but not maximally suppressive in peripheral blood of Type 1 Diabetes Mellitus patients. *Clinical immunology* 153(1):156-164.

187. Liu GY*, et al.* (1995) Low avidity recognition of self-antigen by T cells permits escape from central tolerance. *Immunity* 3(4):407-415.

188. Fairchild PJ, Wildgoose R, Atherton E, Webb S, & Wraith DC (1993) An autoantigenic T cell epitope forms unstable complexes with class II MHC: a novel route for escape from tolerance induction. *International immunology* 5(9):1151-1158.

189. Hewitt EW*, et al.* (1997) Natural processing sites for human cathepsin E and cathepsin D in tetanus toxin: implications for T cell epitope generation. *Journal of immunology* 159(10):4693-4699.

190. Brown AM (2005) A new software for carrying out one-way ANOVA post hoc tests. *Computer methods and programs in biomedicine* 79(1):89-95.

191. Verhagen J, Wegner A, & Wraith DC (2015) Extra-thymically induced T regulatory cell subsets: the optimal target for antigen-specific immunotherapy. *Immunology* 145(2):171-181.

192. Liu G*, et al.* (2014) SIRT1 limits the function and fate of myeloid-derived suppressor cells in tumors by orchestrating HIF-1alpha-dependent glycolysis. *Cancer research* 74(3):727-737.

193. Ansari MJ*, et al.* (2003) The programmed death-1 (PD-1) pathway regulates autoimmune diabetes in nonobese diabetic (NOD) mice. *The Journal of experimental medicine* 198(1):63-69.

194. Cobbold SP*, et al.* (2003) Regulatory T cells and dendritic cells in transplantation tolerance: molecular markers and mechanisms. *Immunological reviews* 196:109-124.

195. Rahmoun M*, et al.* (2006) Enhanced frequency of CD18- and CD49b-expressing T cells in peripheral blood of asthmatic patients correlates with disease severity. *International archives of allergy and immunology* 140(2):139-149.

196. Schuler PJ*, et al.* (2014) Human CD4+ CD39+ regulatory T cells produce adenosine upon co-expression of surface CD73 or contact with CD73+ exosomes or CD73+ cells. *Clinical and experimental immunology* 177(2):531-543.

197. Gagliani N*, et al.* (2013) Coexpression of CD49b and LAG-3 identifies human and mouse T regulatory type 1 cells. *Nature medicine* 19(6):739-746.

198. Kretschmer K*, et al.* (2005) Inducing and expanding regulatory T cell populations by foreign antigen. *Nature immunology* 6(12):1219-1227.

199. Apostolou I & von Boehmer H (2004) In vivo instruction of suppressor commitment in naive T cells. *The Journal of experimental medicine* 199(10):1401-1408.

200. Verhagen J*, et al.* (2013) Modification of the FoxP3 transcription factor principally affects inducible T regulatory cells in a model of experimental autoimmune encephalomyelitis. *PloS one* 8(4):e61334.

201. Lahl K*, et al.* (2007) Selective depletion of Foxp3+ regulatory T cells induces a scurfy-like disease. *The Journal of experimental medicine* 204(1):57-63.

202. Sakaguchi S, Sakaguchi N, Asano M, Itoh M, & Toda M (1995) Immunologic self-tolerance maintained by activated T cells expressing IL-2 receptor alpha-chains (CD25). Breakdown of a single mechanism of self-tolerance causes various autoimmune diseases. *Journal of immunology* 155(3):1151-1164.

203. Gautron AS, Dominguez-Villar M, de Marcken M, & Hafler DA (2014) Enhanced suppressor function of TIM-3+ FoxP3+ regulatory T cells. *European journal of immunology* 44(9):2703-2711.

204. Hastings WD*, et al.* (2009) TIM-3 is expressed on activated human CD4+ T cells and regulates Th1 and Th17 cytokines. *European journal of immunology* 39(9):2492-2501.

205. Koutrolos M, Berer K, Kawakami N, Wekerle H, & Krishnamoorthy G (2014) Treg cells mediate recovery from EAE by controlling effector T cell proliferation and motility in the CNS. *Acta neuropathologica communications* 2:163.

206. Lahl K & Sparwasser T (2011) In vivo depletion of FoxP3+ Tregs using the DEREG mouse model. *Methods in molecular biology* 707:157-172.

207. Nicolson KS*, et al.* (2006) Antigen-induced IL-10+ regulatory T cells are independent of CD25+ regulatory cells for their growth, differentiation, and function. *Journal of immunology* 176(9):5329-5337.

208. McFarland HF & Martin R (2007) Multiple sclerosis: a complicated picture of autoimmunity. *Nature immunology* 8(9):913-919.

209. Sinha S*, et al.* (2010) Binding of recombinant T cell receptor ligands (RTL) to antigen presenting cells prevents upregulation of CD11b and inhibits T cell activation and transfer of experimental autoimmune encephalomyelitis. *Journal of neuroimmunology* 225(1-2):52-61.

210. Offner H, Sinha S, Wang C, Burrows GG, & Vandenbark AA (2008) Recombinant T cell receptor ligands: immunomodulatory, neuroprotective and neuroregenerative effects suggest application as therapy for multiple sclerosis. *Reviews in the neurosciences* 19(4-5):327-339.

211. Sinha S*, et al.* (2009) Cytokine switch and bystander suppression of autoimmune responses to multiple antigens in experimental autoimmune encephalomyelitis by a single recombinant T-cell receptor ligand. *The Journal of neuroscience : the official journal of the Society for Neuroscience* 29(12):3816-3823.

212. Thornton AM & Shevach EM (2000) Suppressor effector function of CD4+CD25+ immunoregulatory T cells is antigen nonspecific. *Journal of immunology* 164(1):183-190.

213. Gabrilovich DI, Ostrand-Rosenberg S, & Bronte V (2012) Coordinated regulation of myeloid cells by tumours. *Nature reviews. Immunology* 12(4):253-268.

214. Dolcetti L*, et al.* (2010) Hierarchy of immunosuppressive strength among myeloid-derived suppressor cell subsets is determined by GM-CSF. *European journal of immunology* 40(1):22-35.

215. Bunt SK*, et al.* (2007) Reduced inflammation in the tumor microenvironment delays the accumulation of myeloid-derived suppressor cells and limits tumor progression. *Cancer research* 67(20):10019-10026.

216. Novitskiy SV*, et al.* (2011) TGF-beta receptor II loss promotes mammary carcinoma progression by Th17 dependent mechanisms. *Cancer discovery* 1(5):430-441.

217. Parker KH, Beury DW, & Ostrand-Rosenberg S (2015) Myeloid-Derived Suppressor Cells: Critical Cells Driving Immune Suppression in the Tumor Microenvironment. *Advances in cancer research* 128:95-139.

218. Yang Z*, et al.* (2010) Mast cells mobilize myeloid-derived suppressor cells and Treg cells in tumor microenvironment via IL-17 pathway in murine hepatocarcinoma model. *PloS one* 5(1):e8922.

219. Corzo CA*, et al.* (2010) HIF-1alpha regulates function and differentiation of myeloid-derived suppressor cells in the tumor microenvironment. *The Journal of experimental medicine* 207(11):2439-2453.

220. Gabrilovich DI & Nagaraj S (2009) Myeloid-derived suppressor cells as regulators of the immune system. *Nature reviews. Immunology* 9(3):162-174.

221. Bronte V & Zanovello P (2005) Regulation of immune responses by L-arginine metabolism. *Nature reviews. Immunology* 5(8):641-654.

222. Rodriguez PC & Ochoa AC (2008) Arginine regulation by myeloid derived suppressor cells and tolerance in cancer: mechanisms and therapeutic perspectives. *Immunological reviews* 222:180-191.

223. Yu J*, et al.* (2013) Myeloid-derived suppressor cells suppress antitumor immune responses through IDO expression and correlate with lymph node metastasis in patients with breast cancer. *Journal of immunology* 190(7):3783-3797.

224. Mellor AL & Munn DH (2004) IDO expression by dendritic cells: tolerance and tryptophan catabolism. *Nature reviews. Immunology* 4(10):762-774.

225. Munn DH*, et al.* (1999) Inhibition of T cell proliferation by macrophage tryptophan catabolism. *The Journal of experimental medicine* 189(9):1363-1372.

226. Deng L*, et al.* (2014) Irradiation and anti-PD-L1 treatment synergistically promote antitumor immunity in mice. *The Journal of clinical investigation* 124(2):687-695.

227. Hart KM, Byrne KT, Molloy MJ, Usherwood EM, & Berwin B (2011) IL-10 immunomodulation of myeloid cells regulates a murine model of ovarian cancer. *Frontiers in immunology* 2:29.

228. Dietlin TA*, et al.* (2007) Mycobacteria-induced Gr-1+ subsets from distinct myeloid lineages have opposite effects on T cell expansion. *Journal of leukocyte biology* 81(5):1205-1212.

229. van Kooten C & Banchereau J (1997) Functions of CD40 on B cells, dendritic cells and other cells. *Current opinion in immunology* 9(3):330-337.

230. Bourgeois C, Rocha B, & Tanchot C (2002) A role for CD40 expression on CD8+ T cells in the generation of CD8+ T cell memory. *Science* 297(5589):2060-2063.

231. Quezada SA, Jarvinen LZ, Lind EF, & Noelle RJ (2004) CD40/CD154 interactions at the interface of tolerance and immunity. *Annual review of immunology* 22:307-328.

232. Yang R*, et al.* (2006) CD80 in immune suppression by mouse ovarian carcinoma-associated Gr-1+CD11b+ myeloid cells. *Cancer research* 66(13):6807-6815.

233. Dugast AS*, et al.* (2008) Myeloid-derived suppressor cells accumulate in kidney allograft tolerance and specifically suppress effector T cell expansion. *Journal of immunology* 180(12):7898-7906.

234. Suh ED*, et al.* (1993) Splenectomy abrogates the induction of oral tolerance in experimental autoimmune uveoretinitis. *Current eye research* 12(9):833-839.

235. Buettner M, Bornemann M, & Bode U (2013) Skin tolerance is supported by the spleen. *Scandinavian journal of immunology* 77(4):238-245.

236. Zinkernagel RM*, et al.* (1997) Antigen localisation regulates immune responses in a dose- and time-dependent fashion: a geographical view of immune reactivity. *Immunological reviews* 156:199-209.

237. Greter M, Hofmann J, & Becher B (2009) Neo-lymphoid aggregates in the adult liver can initiate potent cell-mediated immunity. *PLoS biology* 7(5):e1000109.

238. Carambia A*, et al.* (2014) TGF-beta-dependent induction of CD4(+)CD25(+)Foxp3(+) Tregs by liver sinusoidal endothelial cells. *Journal of hepatology* 61(3):594-599.

239. Carambia A*, et al.* (2015) Nanoparticle-based autoantigen delivery to Treg-inducing liver sinusoidal endothelial cells enables control of autoimmunity in mice. *Journal of hepatology* 62(6):1349-1356.

240. Suzuki E, Kapoor V, Jassar AS, Kaiser LR, & Albelda SM (2005) Gemcitabine selectively eliminates splenic Gr-1+/CD11b+ myeloid suppressor cells in tumor-bearing animals and enhances antitumor immune activity. *Clinical cancer research : an official journal of the American Association for Cancer Research* 11(18):6713-6721.

241. Vincent J*, et al.* (2010) 5-Fluorouracil selectively kills tumor-associated myeloid-derived suppressor cells resulting in enhanced T cell-dependent antitumor immunity. *Cancer research* 70(8):3052-3061.

242. Claassen I, Van Rooijen N, & Claassen E (1990) A new method for removal of mononuclear phagocytes from heterogeneous cell populations in vitro, using the

liposome-mediated macrophage 'suicide' technique. *Journal of immunological methods* 134(2):153-161.

243.  Leenen PJ*, et al.* (1998) Heterogeneity of mouse spleen dendritic cells: in vivo phagocytic activity, expression of macrophage markers, and subpopulation turnover. *Journal of immunology* 160(5):2166-2173.

244.  Rose S, Misharin A, & Perlman H (2012) A novel Ly6C/Ly6G-based strategy to analyze the mouse splenic myeloid compartment. *Cytometry. Part A : the journal of the International Society for Analytical Cytology* 81(4):343-350.

245.  Liu ZX, Han D, Gunawan B, & Kaplowitz N (2006) Neutrophil depletion protects against murine acetaminophen hepatotoxicity. *Hepatology* 43(6):1220-1230.

246.  Jaeger BN*, et al.* (2012) Neutrophil depletion impairs natural killer cell maturation, function, and homeostasis. *The Journal of experimental medicine* 209(3):565-580.

247.  Pierson ER, Wagner CA, & Goverman JM (2016) The contribution of neutrophils to CNS autoimmunity. *Clinical immunology*.

248.  Steinbach K, Piedavent M, Bauer S, Neumann JT, & Friese MA (2013) Neutrophils amplify autoimmune central nervous system infiltrates by maturing local APCs. *Journal of immunology* 191(9):4531-4539.

249.  Rumble JM*, et al.* (2015) Neutrophil-related factors as biomarkers in EAE and MS. *The Journal of experimental medicine* 212(1):23-35.

250.  Cortez-Retamozo V*, et al.* (2012) Origins of tumor-associated macrophages and neutrophils. *Proceedings of the National Academy of Sciences of the United States of America* 109(7):2491-2496.

251.  Levy L*, et al.* (2015) Splenectomy inhibits non-small cell lung cancer growth by modulating anti-tumor adaptive and innate immune response. *Oncoimmunology* 4(4):e998469.

252.  Kawano M*, et al.* (2015) The significance of G-CSF expression and myeloid-derived suppressor cells in the chemoresistance of uterine cervical cancer. *Scientific reports* 5:18217.

# 7   ACKNOWLEDGEMENTS

## 8   SELBSTÄNDIGKEITSERKLÄRUNG

Hiermit erkläre ich, Anja Wegner, dass ich die vorliegende Dissertation mit dem Thema:

"**Cellular mechanism of antigen-specific immunotherapy of autoimmune disease**"

selbstständig und ohne fremde Hilfe verfasst und keine anderen Hilfsmittel als angegeben

verwendet habe. Insbesondere versichere ich, dass ich alle wörtlichen und sinngemäßen

Übernahmen aus anderen Werken als solche kenntlich gemacht habe.

Datum                                        Unterschrift

# 9    CURRICULUM VITAE